Improvement of therapeutic vaccination for the treatment of chronic hepatitis B in a preclinical model (woodchuck)

Inaugural-Dissertation

zur

Erlangung des Doktorgrades

Dr. rer. nat.

der Fakultät für

Biologie

an der

Universität Duisburg-Essen

vorgelegt von

Anna Dagmara Kosinska

aus Lodz (Polen)

April 2011

Die der vorliegenden Arbeit zugrunde liegenden Experimente wurden am Institut für Virologie der Universität Duisburg-Essen oder durchgeführt.

1. Gutachter: Herr Prof. Dr. med. Michael Roggendorf

2. Gutachter: Frau Prof. Dr. rer. nat. Astrid Westendorf

3. Gutachter:

Vorsitzender des Prüfungsausschusses: Herr Prof. Dr. rer. nat. Ralf Küppers

Tag der mündlichen Prüfung: 28.07.2011

Table of contents

1 Introduction

1.1 Hepadnaviridae

1.1.1 Classification

The family of *Hepadnaviridae* classifies the non-cythopatic hepatotropic DNA viruses which can cause transient and chronic liver infections in humans and animals. The common features of all hepadnaviruses are enveloped virions containing 3 to 3.3 kb partially double stranded DNA genome. Hepadnaviruses show narrow host ranges and infect species only closely related to the natural host [*Ganem et al., 2001*]. In the family of *Hepadnaviridae* two genera can be distinguished: *Orthohepadnavirus* and *Avihepadnavirus*. The genus *Orthohepadnavirus* compromises the members recovered from the mammalian hosts, including human hepatitis B virus (HBV) as the prototype virus for the family [*Dane et al., 1970*]. Viruses that are the most closely related to HBV (70% sequence homology of the genomes) have been found in woodchucks (woodchuck hepatitis virus; WHV) [*Summers et al., 1978*] and in ground squirrels [*Marion et al., 1980*]. More distantly related viruses, that share the same genome organization but almost no sequence homology are found in ducks and geese [*Mason et al., 1980; Sprengel et al., 1988*]. The avian hepadnaviruses are grouped in the genus *Avihepadnavirus*. The representative members of *Hepadnaviridae* family are presented in table 1.1.

Tab. 1.1 The representative members of *Hepadnaviridae* family

Genus/Virus		Host	Reference
Orthohepadnavirus			
Hepatitis B virus	HBV	*Homo sapiens*	Dane et al., 1970
Woodchuck hepatitis virus	WHV	*Marmota monax*	Summers et al., 1978
Ground squirrel hepatitis virus	GSHV	*Spermophilus beecheyi*	Marion et al., 1980
Arctic squirrel hepatitis virus	ASHV	*Spermophilus parryi kennicotti*	Testut et al., 1996
Woolly monkey hepatitis B virus	WMHBV	*Lagothrix lagothricha*	Lanford et al., 1998
Avihepadnavirus			
Duck hepatitis B virus	DHBV	*Anas domesticus*	Mason et al., 1980
Heron hepatitis B virus	HHBV	*Adrea cinera*	Sprengel et al., 1988

1.1.2 Morphology of the virion

The hepadnaviral virions are spherical enveloped particles approximately 40 to 47 nm in diameter (Fig. 1.1A). The outer envelope consists of host-derived lipids and is spiked with these viral glycoproteins: the preS1- (large surface antigen; L), preS2- (medium surface antigen; M) and S-protein (small surface antigen; S). The sphere contains the nucleocapsid with a diameter of 22 to 25nm that is built from the core protein. The capsid encloses the viral DNA genome together with the viral DNA polymerase that has reverse transciptase and RNase H activity [*Robinson et al., 1976*].

Except for fully developed virions (known as 'Dane particles', after their discoverer) two other morphological forms can be distinguished in the sera of hepatitis B patients. The most abundant are small, spherical particles 17 to 25 nm in diameter. Filamentous forms of 20 nm diameter and variable length that lack the nucleocapsid are also observed (Fig. 1.1B). Both particles are non-infectious and only consist of the lipids and the viral surface antigens [*Robinson et al., 1976*]. The number of those subviral particles can exceed that of infectious virions by factor 10^3 to 10^5 [*Ganem et al., 2001*].

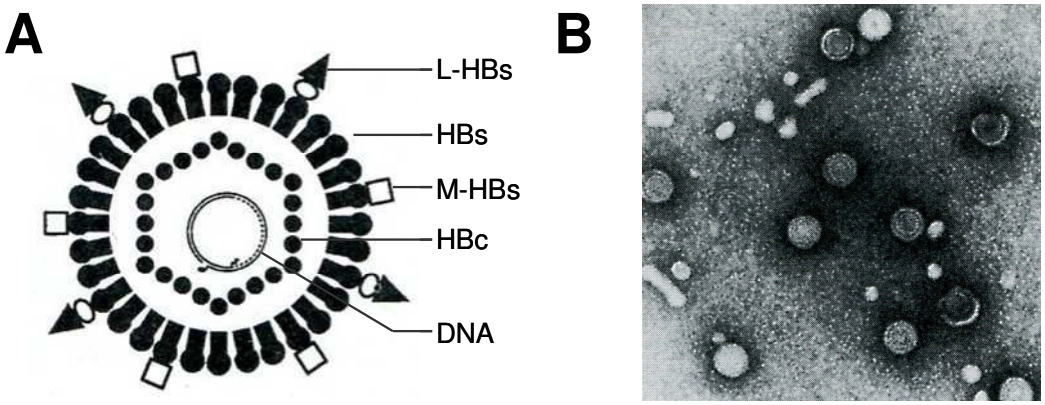

Fig. 1.1 The structure of hepadnaviral virions and subviral particles

A. Schematic illustration of the HBV virion. The outer envelope contains viral surface glycoproteins (L-, M- and HBs). The inner nucleocapsid is built from single capsid protein (HBc). The viral DNA contains a terminal protein (solid oval) domain of the viral polymerase attached to the negative strand and a short RNA (wavy line) attached to the positive strand. Dashes indicate single-stranded gap region on virion DNA [modified from *Ganem et al., 2001*].

B. Electron micrograph of hepatitis B particles including virions and subviral particles (spheres and filaments) [*Ganem et al., 2001*].

1.1.3 The genome organization and viral transcripts

Hepadnaviruses have small genomes of partially double-stranded relaxed circular DNA from 3 to 3.3 kb in length. The strands of DNA molecule are not perfectly symmetric and the circularity is maintained by 5'-cohesive ends [*Sattler et al.; 1979*]. The complete DNA strand has a negative sense-orientation. Its 5'-end is covalently linked to the terminal protein (TP) domain of the viral polymerase [*Gerlich et al., 1980; Ganem, 1982*]. The positive strand is shorter and bears a capped oligoribonucleotide at its 5'-end [*Lien et al., 1986*]. The regions of 11-nucleotides short direct repeats (DRs) are located at 5'-ends of both negative and positive strands (DR1 and DR2, respectively). These repeats are involved in priming the synthesis of their respective DNA strands [*Lien et al., 1986*; *Seeger et al., 1986*].

The genomes of hepadnaviruses show a highly compact coding organization. Approximately half of the sequence is translated in more than one open reading frame (ORF) and non-coding regions are not present in the genome [*Galibert et al., 1979; Miller et al., 1989*]. As shown in Fig. 1.2, four ORFs encoding seven viral proteins are present in the DNA:

1. ORF P: encodes the viral DNA polymerase that has reverse transciptase and RNase H activity as well as the terminal protein found on negative-stranded DNA [*Bosch et al., 1988*].
2. ORF preC/C: encodes the structural core protein and "e" antigen [*Galibert et al., 1982*].
3. ORF S/preS: contains three start codons for viral surface glycoproteins: L (preS1/preS2/S); M (preS2/S) and S [*Heermann et al., 1984; Ganem et al., 2001*].
4. ORF X: encodes the regulatory "x" protein, that is required for viral infectivity *in vivo* and regulates, directly or indirectly, the viral and host gene expression [*Galibert et al., 1982; Ganem et al., 2001*].

The negative strand DNA is the template for the synthesis of the viral mRNA transcripts. The viral RNAs include pregenomic RNA (pgRNA) that serves as a template for viral DNA synthesis and translation of ORFs preC/C and P, as well as three subgenomic mRNAs (two for *Avihepadnaviridae*, excluding "x" protein transcript) necessary for translation of the envelope proteins and "x" protein [*Seeger et al., 2000*].

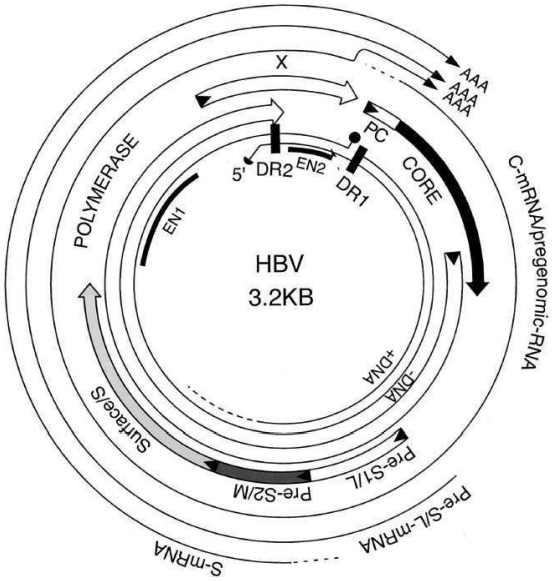

Fig. 1.2 Genome organization of HBV

The inner circle represents two strands of viral DNA (+DNA and –DNA), with terminal protein at the 5'-end of the negative strand (black sphere) and capped oligoribonucleotide at 5'-end of the positive strand (black half sphere). The locations of direct repeats DR1 and DR2, as well as two enhancers EN1 and EN2 are indicated. Boxes represent four viral protein-coding regions with arrows indicating direction of translation. Pre-core(PC)/core, polymerase, X and the envelope genes (L, M and S) open reading frames are shown. The outer circle represents three major viral RNAs: core(C)/pregenomic RNA, preS/L mRNA and the S mRNA (the "x" protein mRNA is not shown). The common 3'-ends of mRNAs are indicated by letter A [*Seeger et al., 2000*].

1.1.4 The replication cycle

Little is known about the early stages of hepadnaviral life cycle in hepatocytes. It is assumed, that the enveloped virion binds to the cell surface and is internalized into the cell by endocytosis. The specific cellular receptors for hepadnaviruses remain unknown. The virus–host membrane fusion process is probably mediated by a pH-independent mechanism [*Rigg et al., 1992; Kock et al., 1996*] and results in release of the viral nucleocapsid into the cytoplasm. The nucleocapsid is transported to the nucleus where the viral genome is delivered. The question whether the whole nucleocapsid or just the viral DNA is translocated into the nucleus remains without an answer.

In the nucleus, the partially duplex, relaxed circular DNA (RC DNA) is converted into episomal, covalently closed circular DNA (cccDNA) [*Tuttleman et al.,1986*]. This requires repair of the single-stranded gap, removal of the 5'-end terminal structures (RNA and TP) and covalent ligation of the strands. The cccDNA serves as a template for the transcription of the viral mRNAs and pgRNA. The viral transcripts are

polyadenylated and transported into the cytoplasm where they are translated into the proteins (core, polymerase, surface glycoproteins, “e” and “x” proteins). The pregenomic RNA is packaged together with viral polymerase into core particles where it acts as a template for reverse transcription of the negative-strand DNA [*Buscher et al., 1985; Moroy et al., 1985*]. Next, the synthesis of the positive-strand occurs. The particles are transported back to the nucleus where the DNA is converted back to cccDNA (process named “recycling”). This process leads to the increase of the cccDNA pool in the nucleus [*Tuttleman et al.,1986*]. Alternatively, the progeny nucleocapsids bud into the endoplasmic reticulum (ER) or proximal Golgi membranes to acquire their glycoprotein envelope [*Roingeard et al., 1990*]. The mature virions are secreted out of the cell through the vesicular transport pathway. The steps of hepadnaviral replication cycle are schematically illustrated on Fig. 1.3.

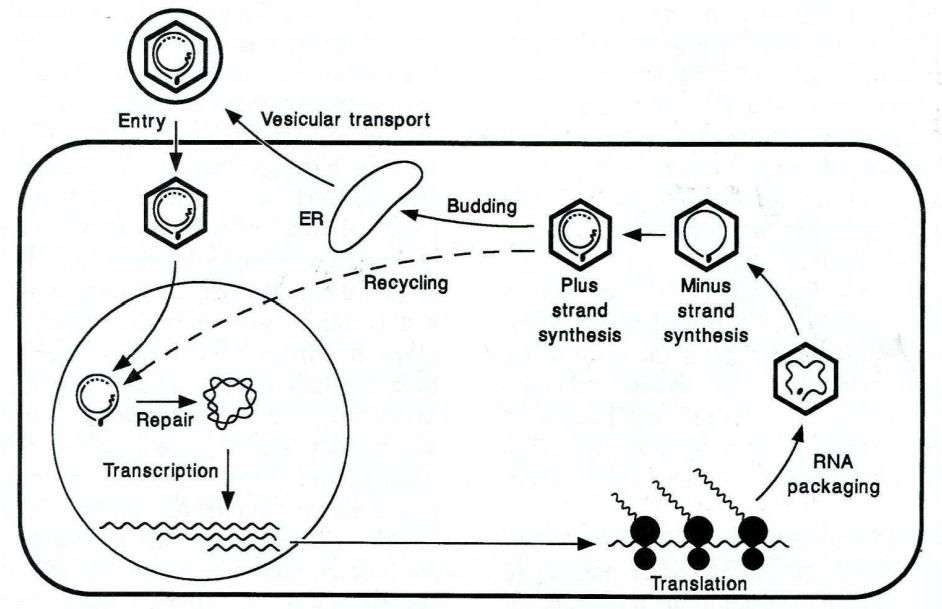

Fig. 1.3 Replication cycle of HBV

The HBV virion binds to the cell surface and is internalized into the cell by endocytosis. The nucleocapsid is transported to the nucleus where the viral genome is delivered. In the nucleus, the partially duplex, relaxed circular DNA is repaired into covalently closed circular DNA (cccDNA). The cccDNA serves as a template for the transcription of the viral mRNAs and pgRNA. The transcripts are transported into the cytoplasm where they are translated into the viral proteins. The pregenomic RNA is packaged together with viral polymerase into core particles where it acts as a template for reverse transcription of the negative-strand DNA. Next, the synthesis of the positive-strand occurs. The pool of the nucleocapsids is transported back to the nucleus (process named recycling). Alternatively, the progeny nucleocapsids bud into the ER or proximal Golgi membranes to acquire their glycoprotein envelope. Finally, the mature virions are secreted out of the cell through the vesicular transport pathway [*Ganem et al., 2001*].

1.2 Clinical outcomes of HBV infection

The outcome of HBV infection varies greatly from person to person (Fig. 1.4). HBV causes a spectrum of liver diseases ranging from self-limiting acute hepatitis to chronic hepatitis, cirrhosis, and hepatocellular carcinoma (HCC). HBV is transmitted through contact with infected body fluids such as: blood, blood products, sexual contact, or perinatally from an infected mother to the newborn [*Ganem, 1982*]. The average incubation period (time from exposure to the appearance of jaundice) of acute hepatitis B is 90 days [*Krugman et al., 1979*]. Over 90% of perinatal infections are asymptomatic, while the manifestations of the disease are noted in 30-50% of adolescents and adults [*McMahon et al., 1985*]. The symptoms of acute hepatitis B include nausea, fever, vomiting, abdominal pain, jaundice and hepatomegaly. Occasionally, acute HBV infection may lead to the extensive necrosis of the liver and to fulminant hepatitis that is fatal in 80% of the cases [*Berk et al., 1978*]. In most of the individuals acute HBV infection is cleared spontaneously, however, 5-10% of adults develop a chronic infection. By contrast, 40-90% of the children which are born to HBV infected mothers will progress to develop a persistent liver disease [*McMahon et al., 1985*]. Chronically HBV-infected patients may remain asymptomatic or encounter periodic flares-up of symptoms of acute hepatitis B. Approximately 15-25% of HBV chronic carriers will die prematurely from liver cirrhosis and hepatocellular carcinoma [*McMahon et al., 1990; Beasley et al., 1991*].

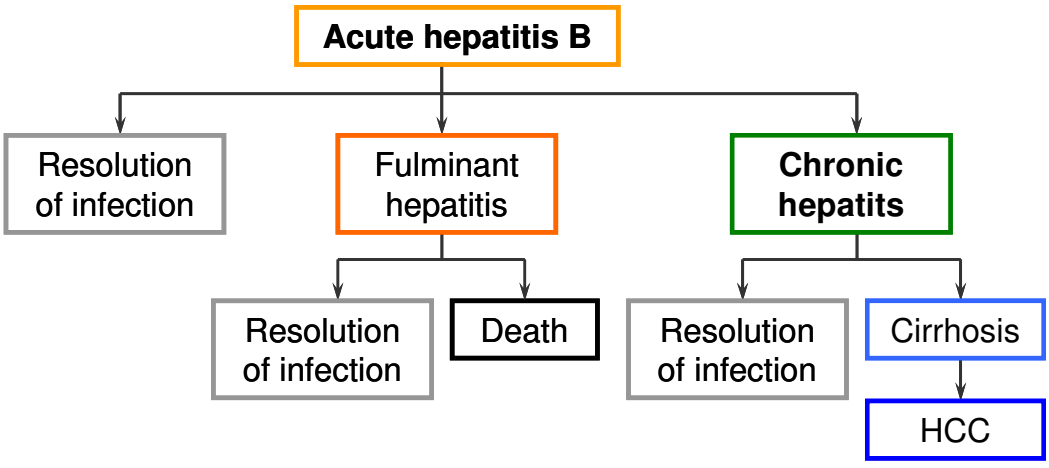

Fig. 1.4 Spectrum of liver diseases caused by HBV infection
HBV causes a spectrum of liver diseases ranging from transient acute infection, to fulminant hepatitis up to chronic infection, that may result in liver cirrhosis and hepatocellular carcinoma (HCC) development.

The World Health Organization (WHO; 2010) estimates that about 2 billion people worldwide have been infected with HBV. Over 360 million are persistently infected, of whom 1 million die each year from HBV associated liver cirrhosis or HCC.

1.2.1 Serologic markers of acute and chronic HBV infection

As presented in Fig. 1.5A, the first serologic marker of HBV infection is the hepatitis B surface antigen (HBsAg) that becomes detectable approximately 6 weeks after exposure. Subsequently, hepatitis B “e” antigen (HBeAg) can be detected. The first detectable antibodies in the sera of patients are immunoglobulin M (IgM) antibodies directed against the HBV core protein (anti-HBc). Elevated levels of IgM-specific antibodies correlate with the onset of serum transaminases level abnormalities. The increase in transaminases, mostly in alanine transaminase (ALT) during acute hepatitis B varies from 3 to over 100-fold above the “normal” levels. Approximately 6 months after infection, anti-HBc IgM antibodies become undetectable [*Cohen, 1987*]. Nevertheless, the IgG-specific antibodies to hepatitis B core antigen (HBcAg) persist lifelong and are found in individuals with chronic infection (Fig. 1.5B), as well as those who resolved the HBV infection (Fig. 1.5A). The seroconversion of HBeAg to anti-HBe antibodies indicates the reduction in viral replication and beginning of the resolution of the disease [*Hoofnagle, 1981*]. The termination of the infection occurs with disappearance of HBsAg and the appearance of neutralizing anti-HBs antibodies [*Chisari et al., 1995*]. Anti-HBs antibodies provide protection against re-infection with HBV.

Chronic HBV infection is defined as either the presence of HBsAg in the serum for at least 6 months or the presence of HBsAg in individuals who have undetectable IgM-specific anti-HBc antibodies. Chronic HBV carriers do not develop anti-HBs and HBsAg persists for decades [*Bortolotti et al., 1990*]. HBeAg is usually present in the early phases of chronic HBV infection. For a high proportion of patients HBeAg becomes undetectable years after the establishment of chronic HBV infection and may reappear during the flare-ups. In some patients the seroconversion of HBeAg to anti-HBe is observed [*Liaw et al., 1987*]. During the chronic HBV infection a persistent mild elevation in serum ALT is observed in up to 90% of the patients. The transaminases may become markedly elevated during the relapse of the disease [*Hollinger et al., 2001*].

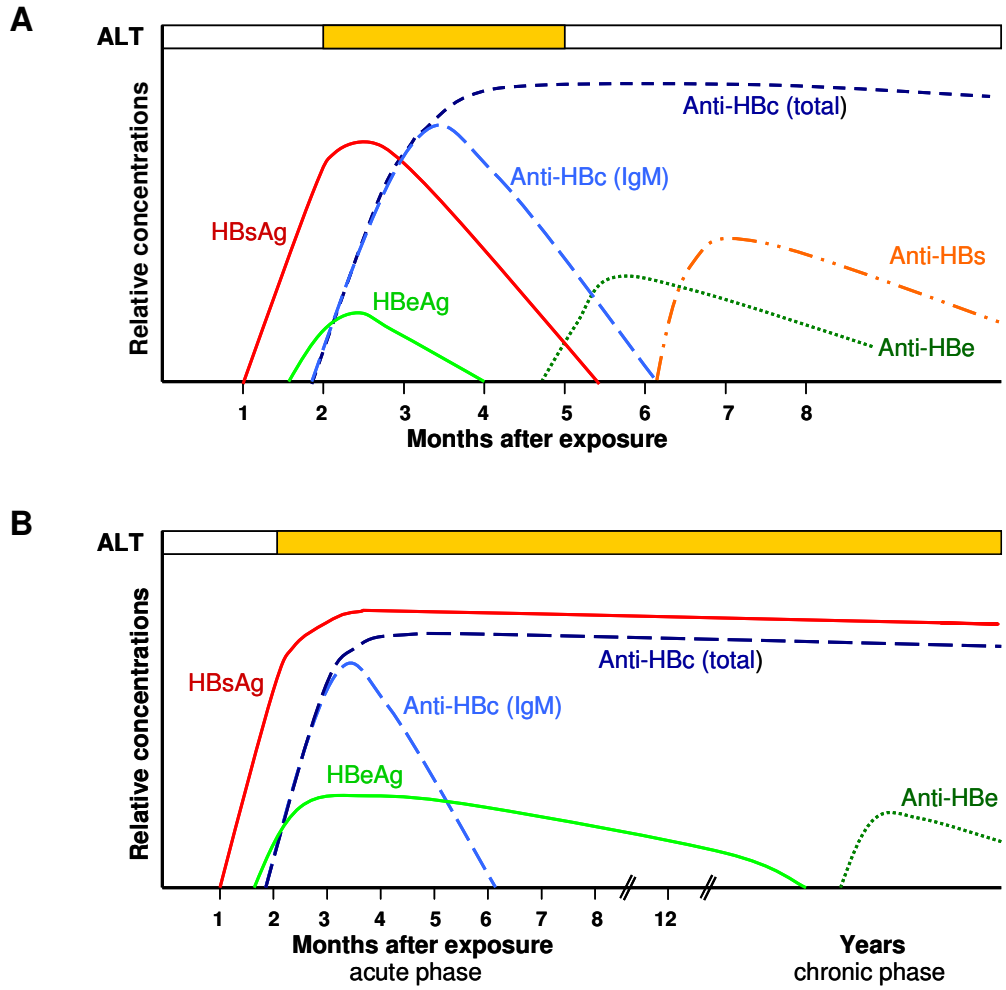

Fig. 1.5 Serologic patterns observed during acute (A) and chronic HBV infection (B)

The periodical appearance of HBV proteins: HBsAg and HBeAg, as well as HBV specific antibodies: anti-HBs, anti-HBc (IgM / total) and anti-HBe in the sera of patients during acute and chronic HBV infection is shown. The time period of serum ALT elevation is demonstrated as orange boxes above the graphs.

1.3 Prophylaxis and treatment of HBV infection

1.3.1 Hepatitis B vaccine

The currently available prophylactic hepatitis B vaccine is a yeast-derived recombinant vaccine that contains one of the viral surface antigens (small, HBsAg; or medium, M-HBsAg). A series of three intramuscular administrations is recommended, with the second injection at least one month after the first dose and the third injection given six months after the first dose. Following the course of the vaccination, the evaluation of protective anti-HBs antibodies titers should be performed. The full response to the vaccination occurs in about 85-90% of the vaccinees. The long-

lasting protection of at least 25 years has been proved in those who showed an adequate initial response to the primary course of vaccinations [*Vandamme et al., 2007*].

The hepatitis B vaccination is highly recommended in infants born to HBV-infected mothers, health-care workers, or immunocompromised individuals. In 1997, the World Health Organisation recommended the integration of hepatitis B vaccine into the national immunization programmes in all countries.

1.3.2 Treatment of chronic HBV infection

Currently, the two types of antiviral therapies are approved: treatment with pegylated interferon alpha 2a (PEG-IFNα) or nucleoside analogues, such as adefovir, entecavir (ETV), lamivudine, telbivudine and tenofovir [*Conjeevaram et al., 2003; Janssen et al., 2005; Lau et al., 2005; Dienstag, 2008*]. Nevertheless, the efficacy of those therapies in preventing liver cirrhosis and HCC is still limited. Treatment with PEG-IFNα leads to a sustained antiviral response in only one third of patients, regardless of combining the therapy with nucleoside analogues. On the other hand, the treatment with nucleoside analogues significantly suppresses HBV replication that leads to a decrease of necroinflammation in the liver. However, those antivirals can not completely eradicate the virus. After withdrawal of the drug, the rebound of viremia is observed in the majority of patients. Furthermore, the long-term treatment is subsequently associated with the appearance of drug-resistant HBV strains that is often the cause of therapy failure [*Raney et al., 2003; Locarnini et al., 2006*].

1.4 Immunological control of HBV infection

It is well documented that an appropriate adaptive immune response is required to efficiently control the HBV infection. The T cell-mediated immune response directed against hepatitis B virus antigens, predominantly core antigen (HBcAg), is crucial for the resolution of the infection [*Ferrari et al., 1990; Penna et al., 1996; 1997; Guidotti et al., 1999; Maini et al., 2000; Thimme et al., 2003*]. HBV-specific $CD8^+$ T cells are able to clear HBV-infected hepatocytes by secretion of T_{H1} (helper T cell response type 1) antiviral cytokines such as interferon gamma (IFNγ) and tumor necrosis factor alpha (TNFα) and direct cytotoxic mechanisms (perforin/granzyme, ligand-ligand induced cell death, e.g. Fas-Fas-L) [*Guidotti et al., 1996; McClary et al., 2000;*

Trapani et al., 2002]. An early, vigorous, polyclonal and multi-specific cellular immune response against the viral proteins is associated with the clearance of hepatitis B in acutely-infected patients. In contrast, chronic HBV carriers demonstrate weak, transient or often undetectable $CD8^+$ T cell response that correlates with HBV persistence [*Jung et al., 1991; Penna et al., 1991; Rehermann et al., 2005; Yang et al., 2010*]. Humoral immune response, especially neutralizing anti-envelope antibodies, play a key role in preventing HBV spread to non-infected hepatocytes [*Chisari et al., 1995; Rehermann et al., 2005*].

Recent studies indicate that several mechanisms may be involved in the loss of the function of HBV-specific T cells during chronic hepatitis B. It was shown that high-level viremia negatively influences the virus-specific immune responses. High viral replication in the liver with a viral load higher than 10^7 copies/ml is correlating with hyporesponsiveness of virus-specific $CD8^+$ T-cells in patients with chronic hepatitis B [*Webster et al., 2004*]. Moreover, the prolonged exposure to viral antigens occurring during the chronic viral infections can trigger the T cells to become tolerant and prone to apoptosis. The interaction between programmed death 1 (PD-1) receptor and its ligand PD-L1 (also known as B7-H1) plays an important role to prevent an overreaction of the immune system [*Okazaki et al., 2006*]. Recent studies revealed that inhibitory molecules such as PD-1 and CTLA-4 are markedly up-regulated on virus-specific T cells, resulting in exhaustion (e.g. lack of IFNγ production and proliferation) [*Wherry et al., 2007*]. Simultaneously, this mechanism can contribute to the development of the chronic infection by impairment of the effective anti-viral response. This hypothesis was previously proven for hepatitis C virus (HCV) [*Urbani et al., 2006*] and human immunodeficiency virus (HIV) infection in humans [*Trautmann et al., 2006*] and more recently for HBV [*Boni et al., 2007; Maier et al., 2007*]. Furthermore, several studies imply that functional defects of antigen presenting cells (APCs), mainly dendritic cells (DCs), may contribute to the impaired T cell response in chronic hepatitis B patients. *In vitro* studies showed that DCs isolated from HBV chronic carriers produce lower amount of antiviral cytokines, such as type I interferons and TNFα, in comparison to healthy controls. In addition, those DCs are less efficient in T cell activation and stimulation of T cell proliferation [*Van Der Molen et al., 2004*]. The novel report demonstrated that myeloid DCs from chronic HBV patients express an increased level of inhibitory PD-L1 molecule and

therefore may downregulate functions of HBV-specific T cells [*Chen et al., 2007*]. Several investigations underline the significance of $CD4^+$ $CD25^+$ regulatory T cells in pathogenesis of persistent viral infections [*Li et al., 2008*]. In HCV and HIV-infected patients it was shown that regulatory T cells may downregulate HCV- and HIV-specific $CD8^+$ and therefore influence the disease progression [*Weiss et al., 2004; Rushbrook et al., 2005*]. The role of regulatory T cells in HBV infection is still not clear. Nevertheless, the increased numbers of $CD4^+$ $CD25^+$ regulatory T cells were detected in the blood and the liver of patients with chronic severe hepatitis B [*Xu et al., 2006*]. In addition, the liver itself is an organ with tolerogenic properties that might contribute to the immunological tolerance during chronic HBV infection [*Bertolino et al., 2001; Bowen et al., 2004*]. Finally, viruses developed the strategies to efficiently evade the host immune response resulting in persistent infections. HBV immune escape due to the mutation of $CD4^+$, $CD8^+$ and B cell epitopes in a given HLA background have been observed in patients [*Liu et al., 2002; Ni et al., 2008*].

1.5 Clinical trials of therapeutic immunization

Over the last 20 years, continuous efforts have been undertaken to develop a therapeutic vaccine for chronic hepatitis B to enhance the virus-specific immune responses and overcome persistent HBV infection.

Numerous clinical trials of therapeutic immunization exploited the conventional prophylactic HBsAg-based protein vaccines. These studies demonstrated reductions in viremia, HBeAg/anti-HBe seroconversion and HBV-specific T cell responses in some patients. However, the anti-viral effect was only transient and did not lead to an effective control of the HBV [*Pol et al., 1994; 2001; Couillin et al., 1999; Jung et al., 2002; Dikici et al., 2003; Ren et al., 2003; Safadi et al., 2003; Yalcin et al., 2003*]. Combination of the HBsAg protein vaccines with antiviral treatment with lamivudine did not lead to a satisfactory improvement of the therapies [*Dahmen et al., 2002; Horiike et al., 2005; Vandepapelière et al., 2007*].

The strategies designed to specifically stimulate HBV-specific T cell response were also not successful. The lipopeptide-based vaccine containing a single cytotoxic T lymphocyte (CTL) epitope derived from HBV nucleocapsid was able to induce a vigorous primary HBV-specific T cell response in naïve subjects [*Vitiello et al., 1995*]. However, in HBV chronic carriers the vaccine initiated only poor CTL activity

and had no effect on viremia or HBeAg/anti-HBe seroconversion [*Heathcote et al., 1999*]. The DNA vaccine expressing small and middle envelope proteins proved to elicit the HBV-specific cellular immune response in chronic HBV carriers. However, this effect was only transient [*Mancini-Bourgine et al., 2004*].

Yang et al. presented the novel DNA vaccine for treatment of chronic hepatitis and combined the immunizations with lamivudine treatment [*Yang et al., 2006*]. The multigene vaccine contains five different plasmids encoding most of HBV antigens and human IL-12 gene as a genetic adjuvant. The combination therapy led to a sustained antiviral response in 6 out of 12 HBV chronically-infected patients. The responders were able to clear HBeAg and had undetectable viral loads at the end of a 52-week follow-up. Those effects were correlating with a detectable T cell response to at least one of the HBV antigens. Nevertheless, further studies are needed to evaluate this strategy on a larger cohort of HBV chronic carriers.

The therapeutic vaccine based HBsAg complexed with human anti-HBs was proposed by the group of Wen et al. [*Wen et al., 1995*]. Immunogenic complexes (IC) stimulate robust T cell response by increasing uptake of HBsAg through Fc receptors on APCs and, therefore, modulate HBsAg processing and presentation. It was demonstrated that this vaccine administered to HBeAg-positive patients led to a decrease of HBV DNA in the serum, HBeAg seroconversion and development of anti-HBs in part of the subjects [*Yao et al., 2007*]. Currently, the IC-based vaccine is the only one that entered phase III of clinical trials in chronic hepatitis B patients [*Xu et al., 2008*]. Even though the IC-based vaccine led to antiviral effects, clearance of HBV was not observed in treated patients. It seems that the vaccine alone is not sufficient to achieve the full control over HBV. Therefore, some steps have been undertaken to combine the IC-based vaccine with nucleoside analogues treatment [*Yu-mei Wen*, *personal communication*]. The ongoing clinical trial will show, whether IC are effective as a therapeutic vaccine in chronic hepatitis B.

1.6 The woodchuck as a preclinical model for pathogenesis and therapy of chronic hepatitis B

The Eastern woodchuck (*Marmota monax*) is naturally infected by woodchuck hepatitis virus. WHV and HBV show a marked similarity in the virion structure, genomic organization and the mechanism of replication (section 1.1), but differ in

several aspects e.g. regulation of transcription [*Di et al., 1997*]. WHV causes acute self-limiting and chronic infection similar to HBV infection in the pathogenesis and profiles of the virus-specific immune response [*Menne et al., 2007*]. This feature of the woodchuck model makes it so significant for investigation of the new therapeutic approaches in chronic hepatitis B.

Experimental infection of neonates or adult woodchucks with WHV reflects the outcome of HBV infection in humans (Tab. 1.2). In adult woodchucks infection with WHV usually leads to the resolution of infection and only 5-10% of animals will develop the chronic hepatitis. The exposure of woodchuck neonates to WHV results in development of chronic WHV infection in 60-75% of the cases [*Cotte et al., 2000*]. The continuous replication of WHV in the liver during the chronic infection is nearly always associated with the development of HCC in the woodchucks [*Popper et al.,1987; Tennant et al., 2004*]. After diagnosis of HCC the survival prognosis of the animals is estimated on about 6 months, like in humans. The common features of HBV- and WHV-induced carcinogenesis give the opportunity to examine the new anti-HCC therapies in the woodchucks [*Gerin et al., 1991*].

Tab. 1.2 Clinical features of HBV and WHV infection

	HBV	**WHV**
Course of infection		
Epidemic	360 million people infected worldwide	Endemic in some woodchuck population in North America
Vertical transmission	The most common: from mother to newborn chronicity rate: 45-90%	Neonatal woodchucks infected by WHV inoculum chronicity rate: 60%-75%
Horizontal transmission	Transmitted by body fluids, 90% of individuals recover	Adult woodchucks infected by WHV inoculum, 90-95% of animals recover
Clinical features of chronic infection	Variable HBV DNA levels: 10^4-10^{12} copies/ml HBsAg levels: 50-300 µg/ml liver transaminases elevation	WHV DNA levels: 10^9-10^{11} copies/ml WHsAg levels: 100-300 µg/ml liver transaminases elevation
Disease progression		
Liver cirrhosis	2-5% in HBeAg-positive patients (genotype dependent)	Not common
Hepatocellular carcinoma	5-year cumulative HCC incidence in patients with cirrhosis: 16% (data in Asia)	Nearly 100% of chronic infected animals have HCC after 3 years

according to: *Chisari et al., 1995; Cote et al., 2000; Rehermann et al., 2005*

1.6.1 Evaluation of WHV-specific T cell response

For many years, the studies on immunopathogenesis of WHV infection in woodchucks were restricted to the determination of humoral immune response [*Roggendorf et al., 1995*]. The lack of appropriate methods to evaluate antigen-specific T cell response was a serious limitation of this model.

The proliferation assay for peripheral blood mononuclear cells (PBMCs) based on incorporation of [^{3}H]-thymidine by cellular DNA, routinely used for human and mouse system, has been ineffective in the woodchuck PBMCs [*Korba et al., 1988; Cotte et al., 1995*]. The failure of this approach is consistent with the fact that woodchuck lymphocytes do not express the thymidine kinase gene [*Menne et al., unpublished results*]. This obstacle had been overcome by usage of the alternative radioactively-labeled nucleotide 2[^{3}H]-adenine. The development of 2[^{3}H]-adenine-based proliferation assay enabled to detect the T helper lymphocyte responses after stimulation of woodchuck PBMCs with WHV core, surface and "x" antigens (WHcAg, WHsAg and WHxAg, respectively) In addition, using the 2[^{3}H]-adenine-based proliferation assay in PBMCs from acutely infected animals, several T helper epitopes within WHcAg [*Menne et al., 1998*] and WHsAg were identified (Fig. 1.6) [*Menne et al., unpublished results*].

Recently established, a novel CD107a degranulation assay for woodchuck PBMCs and splenocytes made a significant breakthrough in studying pathogenesis of hapadnaviral infections in the woodchuck model [*Frank et al., 2007*]. Several studies demonstrated that detection of CD107a, as a degranulation marker, is a suitable method for the determination of antigen-specific cytotoxic T lymphocytes [*Betts et al., 2003; Rubio et al., 2003*]. The assay enables detection of WHV-specific CTLs basing on their granule-dependent effector function. The recognition of the infected cells by CTLs results in the exposure of CD107a molecule on the CTL surface. In the woodchuck system, CD107a molecule can be stained by cross-reactive anti-mouse CD107a antibody, what enables the flow cytometric analysis of the woodchuck CTLs.

The introduction of those immunological tools for studying the T cell response in woodchucks revealed a significant similarity between the pathogenesis of WHV infection in woodchucks and HBV in humans. It was demonstrated that acute self-limiting and resolved WHV infections correlate with robust multifunctional T helper and cytotoxic T cell responses [*Menne et al., 1998; Frank et al., 2007*]. Moreover, this

efficient cellular immune response to viral antigens results in the liver injury and is necessary for viral clearance. With the novel CD107a degranulation assay one immunodominant CTL epitope within WHcAg (aa 96-110) [*Frank et al., 2007*], and one CTL epitope within the WHsAg (aa 220-234) [*Frank et al., unpublished results*] were characterized. In contrast to self-limiting infection, WHV chronic carriers demonstrate weak or no virus-specific T cell response against the identified epitopes [*Menne et al., 1998; Frank et al., 2007*].

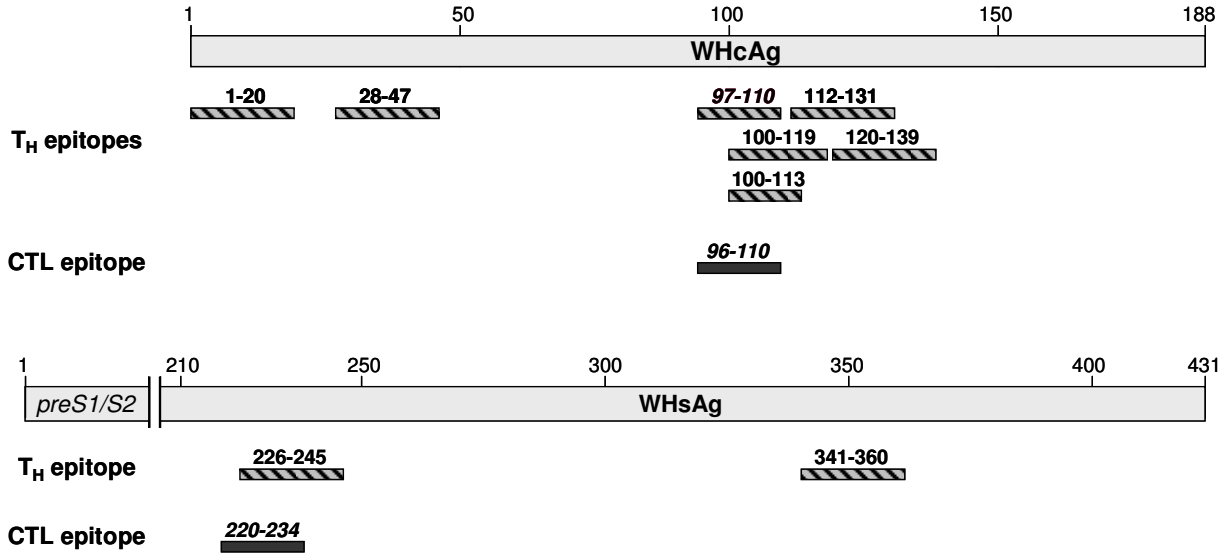

Fig. 1.6 Position of woodchuck CD4⁺ and CD8⁺ epitopes in WHcAg and WHsAg
Woodchuck helper T cell epitopes (T_H) are demonstrated as stripped boxes and CTL epitopes are shown as solid boxes. The aa position of the epitopes within WHcAg and WHsAg is given above the boxes. Immunodominant epitopes' sequences are labelled in italics.

1.7 Therapeutic immunization approaches in the woodchuck model

Up to date, several studies of diverse therapeutic vaccinations have been carried out in woodchucks. The pioneer investigations of the therapeutic vaccines based on WHV core [*Roggendorf et al., 1995*] or surface antigens in combination with a helper peptide FIS [*Hervas-Stubbs et al., 1997*], or with potent T_{H1} adjuvants like monophosphoryl lipid A [*Lu et al., 2003*] did not lead to satisfactory results. Those experiments proved that vaccinations could induce specific B- and/or T-cell responses in chronic WHV carriers. However, this alone was not sufficient to achieve the control of virus replication.

It is assumed that high level viremia, during chronic hepatitis B, can inhibit the induction of HBV-specific T cell immune response by therapeutic vaccination. Therefore, reduction of viral load by the nucleoside analogues pre-treatment might support the efficacy of immunization to enhance the virus-specific immune responses. This hypothesis was tested in three experimental trials of the combination therapies in chronic WHV carriers.

The first study performed by Hervas-Stubbs *et al.* was based on lamivudine therapy [*Hervas-Stubbs et al., 2001*]. Five chronically WHV-infected woodchucks were treated orally with the drug for 23 weeks. At week 10, after decline of WHV DNA by 3-5 logs, three animals were vaccinated with 3 doses of serum-purified WHsAg combined with T helper FIS peptide derived from sperm whale myoglobin. The vaccination induced T helper responses against WHV antigens, shifting the cytokine profile from T_{H2} to T_{H0}/T_{H1}. However, no beneficial effect on WHV viral load and WHsAg levels was observed in comparison to non-immunized animals. After withdrawal of the lamivudine treatment the values of viremia returned to the pre-treatment levels.

The second trial evaluated the therapy with a very potent antiviral drug: clevudine [1-(2-fluoro-5-methyl-β-*L*-arabinofuranosyl)-uracil] combined with a WHsAg-based immunization [*Menne et al., 2000; 2002*]. A large cohort of thirty 1-2 years-old chronically WHV-infected woodchucks was enrolled in the study. Half of the animals were orally treated with clevudine (10 mg/kg/day) for 32 weeks; the other 15 woodchucks received placebo. After withdrawal of clevudine treatment, 8 animals from each group were vaccinated with the four doses of formalin inactivated alum-adsorbed WHsAg and 7 were injected with the saline as a control. Combination of the drug and vaccine therapy resulted in marked reductions WHV DNA (6-8 logs) and WHsAg in serum during the 60-week monitoring period, in contrast to the vaccine only and placebo groups, where both markers remained at high levels. Combination therapy did not enhance anti-WHs response beyond those measured for vaccine alone. However, treatment with clevudine and vaccine together led to more sustained and robust lymphoproliferative responses to WHsAg and additionally to WHcAg, WHeAg (woodchuck hepatitis “e” antigen) and WHxAg. Moreover, combination therapy delayed the onset of the liver disease and prevented HCC development in up

to 38% of treated chronic WHV carriers in the long-term follow up study [*Korba et al., 2004*].

Recently, a novel therapeutic approach for treatment of chronic hepatitis B in a woodchuck model was described. The therapy combined the antiviral treatment with immunization by plasmid DNA and antigen-antibody immunogenic complex vaccines together [*Lu et al., 2008*]. DNA vaccines are considered to stimulate both humoral and cellular immune response, polarizing T cells in the direction of T_{H1} response [*Michel et al., 2001*]. Immunization of the naïve woodchucks with the plasmids encoding WHV core and preS2/S genes (pWHcIm and pWHsIm, respectively) induced the lymphoproliferative responses against the antigens and provided a protection against WHV challenge [*Lu et al., 1999*]. In addition, the DNA vaccine expressing HBsAg proved to elicit the vigorous T cell response in chronic HBV carriers, however, this effect was only transient [*Mancini-Bourgine et al., 2004*]. The HBsAg/anti-HBs IC vaccine is currently under investigation in chronic HBV patients [*Wen et al., 1995; Yao et al., 2007; Xu et al. 2008*].

To evaluate the efficacy of the above mentioned immunotherapy in woodchucks, firstly 10 chronic WHV carriers were treated with 15mg of lamivudine, daily for 21 weeks. At week 10, four animals were pretreated with cardiotoxin and then received three immunizations with DNA vaccine containing three plasmids expressing WHsAg, WHcAg and woodchuck IFNγ (pWHsIm, pWHcIm and pwIFN, respectively). Simultaneously, the other four woodchucks received three doses of the combination of DNA vaccine and WHsAg/anti-WHs immunogenic complex. Two chronic WHV carriers served as lamivudine monotherapy control. Lamivudine treatment resulted in only a slight decrease of WHV DNA levels in the woodchucks serum (0,7 and 0,32 log, respectively). Surprisingly, the DNA vaccination did not lead to any additional therapeutic effect beyond that observed for lamivudine treatment alone. In contrast, the triple combination of antiviral treatment, plasmid DNA encoding WHcAg, WHsAg and wIFNγ and IC vaccines was able to decrease WHV viral load up to 2,9 log and the serum WHsAg up to 92%. Moreover, three of the four treated animals developed anti-WHs antibodies. Nevertheless, these effects were not sustained and all parameters reached the baseline levels shortly after withdrawal of lamivudine treatment. In addition, the vaccination did not induce WHV-specific T cell responses in the majority of woodchucks, even in animals which exhibited virological response.

Significant lymphoproliferative response against WHV antigens were detected only in one animal after three immunizations with DNA vaccine [*Lu et al. 2008*]. The study demonstrated the benefit of using the combinatory therapy in chronically WHV-infected woodchucks. However, the transient therapeutic effects, suggest that this strategy needs further optimization.

A new strategy evaluated the potency of an entecavir treatment and increased number of immunizations [*Lu et al.*, unpublished results]. Chronically WHV-infected woodchucks were pretreated with the entecavir for 21 weeks; 10 weeks in a daily and 11 weeks in a weekly manner. During the weekly administration of the drug, one group of animals received 6 immunizations with two-plasmid DNA vaccine (pWHsIm and pWHcIm), the second group received a combination of DNA vaccine together with purified WHV core and surface antigens, and the third group remained untreated. The entecavir therapy resulted in rapid and significant decease of the viral load and WHsAg levels in serum of the animals. The effect was especially pronounced in animals that additionally received vaccines. In woodchucks treated only with entecavir the increase of viremia was observed already during the weekly administration or immediately after withdrawal of the drug. By contrast, in both groups of animals, that were immunized with DNA or DNA/proteins vaccines, the delay before the rebound of WHV replication was significantly prolonged. In addition, entecavir treatment was effective to suppress WHV replication and enhanced the induction of WHV-specific T cell responses. An increased CTL activity was detected in individual woodchucks after DNA or DNA/proteins vaccinations. Moreover, two animals completely eliminated the virus from the blood and were WHV DNA negative in the liver [*Lu et al.*, unpublished results].

The results of therapeutic immunization trials in the woodchuck model are summarized in table 1.3.

Tab. 1.3 Studies on therapeutic vaccinations in the woodchuck model

Vaccines	Application	Adjuvant	Outcome	Reference
WHcAg	intramuscular	Ø	Viral elimination in 1 of 6 animals	Roggendorf et al., 1995
WHsAg and T_H-peptide	intramuscular	T_H-peptide	Transient anti-WHs antibody response Two woodchucks died	Hervas-Stubbs et al., 1997
WHsAg and T_H-peptide in combination with lamivudine	intramuscular	T_H-peptide	No induction of anti-WHs antibodies Detectable T-cell responses to WHV proteins	Hervas-Stubbs et al., 2001
WHsAg in combination with clevudine	intramuscular	alum	Reduction of serum viral loads and viral replication in liver Induction of anti-WHs and detection of T-cell responses to WHV proteins Delayed occurrence of HCC	Menne et al., 2000, 2002
WHsAg	intramuscular	monophosphoryl lipid A	No reduction of serum viral load, Development of antibodies to the preS region of WHsAg	Lu et al., 2003
Plasmid DNA expressing WHsAg, WHcAg, and woodchuck IFN-γ in combination with lamivudine	intramuscular	Ø	Transient reduction of serum viral loads	Lu et al., 2008
WHsAg/anti-WHs immunogenic complex and DNA vaccines in combination with lamivudine	intramuscular	Ø	Transient reduction of serum viral loads Transient appearance of anti-WHs antibodies and WHcAg-specific T cell response	Lu et al., 2008
Plasmid DNA encoding WHsAg and WHcAg in combination with entecavir	intramuscular	Ø	Transient reduction of serum viral loads Viral elimination in 2 of 6 animals	Lu et al., [*unpublished results*]
Plasmid DNA encoding WHsAg and WHcAg in combination with protein WHsAg/WHcAg vaccine in combination with entecavir	intramuscular	Ø		

Ø – no adjuvant

1.8 Adenoviridae

1.8.1 Classification

Adenoviridae is a family of non-enveloped viruses containing 34-44 kb linear double-stranded DNA as genome. Up to date over 100 members of the *Adenoviridae* family have been identified which infect a wide range of mammalian hosts, including human (genus *Mastadovirius*), reptiles (genus *Atadenovirus*), amphibians (genus *Siadenovirus*) and birds (genus *Aviadenovirus*) [*Buchen-Osmond, 1997*].

So far, 51 human adnenovirus serotypes have been distinguished. The serotypes have been classified into six subgroups (A – F) on the basis of their ability to agglutinate the red blood cells, oncogenicity in rodents, and the sequence homolology of their genomes (Tab. 1.4).

Tab. 1.4 Classification of human adenoviruses [modified from: *Shenk, 2001*]

Subgroup	Hemagglutination groups		Representative serotypes	Tumours in animals
A	IV	little or no agglutination	12, 18, 31	high
B	I	complete agglutination of monkey erythrocytes	3, 7, 11, 14, 16, 21, 34, 35	moderate
C	III	partial agglutination of rat erythrocytes	1, 2, 5, 6	low or none
D	II	complete agglutination of rat erythrocytes	8-10, 13, 17, 19, 22-30, 32, 33, 36-39, 42-47	low or none
E	III	partial agglutination of rat erythrocytes	4	low or none
F	III	partial agglutination of rat erythrocytes	40, 41	unknown

Adenoviruses can infect and replicate at various sites of the respiratory tract, as well as in the eye, gastrointestinal tract, urinary bladder, and liver. Approximately one-third of human adenovirus serotypes is associated with various human diseases. Adenoviruses are known to induce respiratory infections (serotypes form groups B, C and E), infections of the eye (groups B and D), infections of urinary tract (group B) and gastroenteritis (group F) [*Horwitz, 2001*].

1.8.2 Morphology of the viron

Adenoviruses are icosahedral particles that are 70-100 nm in diameter. The virion contains a protein shell (capsid) surrounding a DNA-containing core. The capsid is composed of 252 subunits (capsomeres) of which 240 are hexons and 12 are pentons (Fig. 1.7A). Each penton contains a base that is projecting the fiber whose length and number varies among the serotypes [*Vayda et al., 1983; Signas et al., 1985*]. The capsid is a complex structure built of seven known viral proteins: polypeptide II (hexon), III (penton), IIIa, IV (fiber), VI, VIII and IX.

The core of the virion contains four proteins that interact with the viral DNA. Polypeptides V, VII and X maintain the structure of the viral genome and its proper position within the capsid. The fourth protein present in the core is the terminal protein (TP), which is covalently bound to the 5'-ends of the viral DNA (Fig. 1.7B). The terminal protein serves as a primer for DNA replication and mediates interaction of the viral DNA with the nuclear matrix [*Rux et al., 2004*].

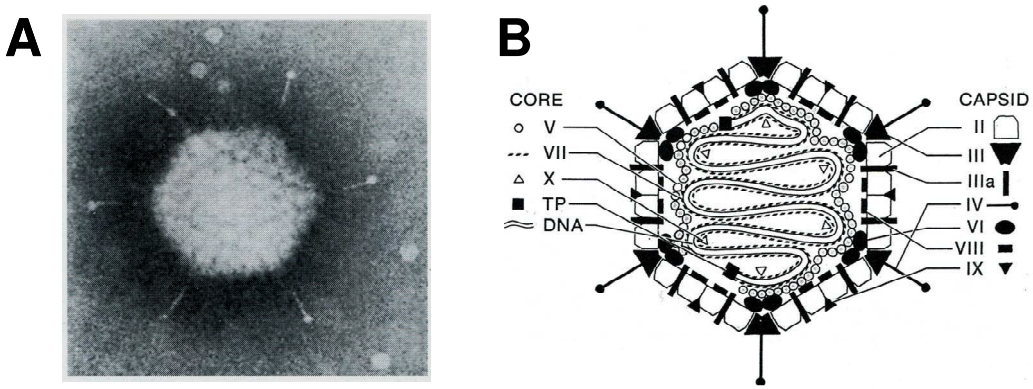

Fig. 1.7 The structure of adenoviral virion

A. Electron micrograph of adenovirus serotype 5. Icosahedral capsid and six of twelve fibers that are present on each viral particle are shown [*Shenk, 2001*].

B. Schematic illustration of the virion. The respective viral polyproteins that build the capsid layer and the inner core of the virion are indicated. Terminal protein (TP) is covalently attached to the 5'-ends of viral DNA [*Shenk, 2001*].

1.8.3 Genome organization, replication mechanism and viral transcripts

The adenoviral genome consists of a 34-44 kb single linear, double-stranded DNA molecule with short inverted terminal repeats (ITRs) on its ends which play an important role in genome replication. The viral genome carries five early transcription units (E1A, E1B, E2, E3 and E4), two delayed early units (IX and IVa2), one late unit

transcribed by RNA polymerase II. The transcription of those genes leads to generation of multiple mRNAs that are differentiated by alternative splicing [*Pettersson et al., 1986*]. The viral chromosome also carries one or two (depending on the serotype) VA genes transcribed by RNA polymerase III. The products of early genes are necessary for late viral gene expression and replication of viral DNA. In addition, they induce cell cycle progression, block apoptosis and antagonize with a variety of host antiviral mechanisms. The late viral genes encode the structural proteins that build the progeny virions [*Shenk, 2001*].

The ITRs of the viral chromosome serve as replication origins. The replication is initiated at one of the termini of the genome, and one strand serves as a template for the synthesis of the daughter strand. The other displaced strand circularizes and serves as a template for the generation of the second duplex DNA molecule [*Lechner et al., 1977*]. This mechanism allows for the most effective usage of once initiated replication machinery.

1.8.4 The replication cycle

The attachment of the adenoviruses to the cell is mediated by the fiber protein. The carboxy-terminal domain of the fiber protein forms a knob that binds to the cellular receptor. Most of the known human adenovirus serotypes (except of group B) interact with coxsackie and adedenovirus receptor (CAR). The serotypes from group B, such as human adenovirus serotype 35 (Ad35), bind to CD46 [*Bergelson, 1999*]. The internalization of the virion via clathrin-mediated endocytosis is mediated by interaction of the viral penton base with $\alpha_V\beta_3$ and $\alpha_V\beta_5$ integrins [*Wickham et al., 1993*]. In the acidified environment of the endosome the partial disassembly of the particle occurs. The interaction of the viral capsid protein pVI with endosome membrane results in the release of the uncoated particle into the cytoplasm. The particles are transported along the microtubules to the nucleus by means of motor proteins e.g. dynein [*Suomalainen et al., 1999*]. The viral DNA is translocated into the nucleus through the nuclear pore complex. The cell entry process of adenoviruses is presented in Fig. 1.8.

In the nucleus, the replication of the genome and expression of the viral proteins occurs. After their production, the viral proteins accumulate in the nucleus where the

assembly of the virions occurs. The release of the progeny virions is associated with the host cell lysis [*Shenk, 2001*].

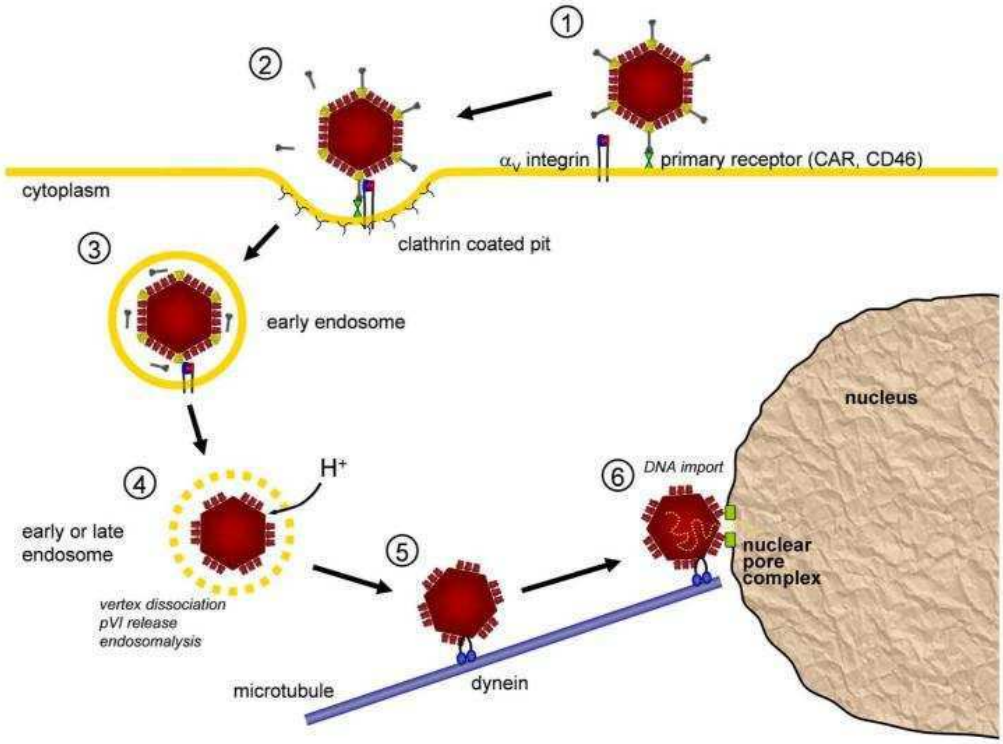

Fig. 1.8 The cell entry pathway of adenovirus

The fiber of adenovirus attaches to the primary receptor (CAR or CD46, step1). Subsequently, the virion is internalized via clathrin-mediated endocytosis, which is mediated by interaction of the viral penton base with αv integrins (step 2). In the low pH of the endosome the virion begins to disassemble (step 3) and uncoated particle is released to the cytoplasm by disruption of the endosomal membrane (step 4). The virion is transported by the microtubule motor dynein along microtubules to the nuclear pore complex (step 5). At the nuclear pore the viral DNA is imported into the nucleus (step 6) [*Nemerow et al., 2009*].

1.8.5 Recombinant adenoviruses as vaccines

Recombinant adenoviruses have been one of the intensively investigated viral vectors for therapeutic purposes. The development of novel methods for the manipulation of the viral genome resulted in the three generations of recombinant adenoviral vectors (Fig. 1.9). Various deletions in the genome led to an increased capacity, allowing the insertion of multiple transgenes [*Danthinne et al., 2000*]. Several trials imply the usefulness of these vectors in gene therapy of genetic diseases and cancer [*Khalighinejad et al., 2008; Kuhlmann et al., 2008; Matthews et al., 2009; Wirth et al., 2009*]. For many years, the first generation replication-deficient E1 or E1/E3-deleted adenoviral vectors have been explored as the prophylactic vaccines against many human pathogens such as Ebola virus, HIV, severe acute

respiratory syndrome (SARS) virus and *Bacillus antracis* (antrax) [*Xiang et al., 1996; Shiver et al., 2002; Fitzgerald et al., 2003; Tatsis et al., 2004; Zakhartchouk et al., 2005; Richardson et al., 2009*].

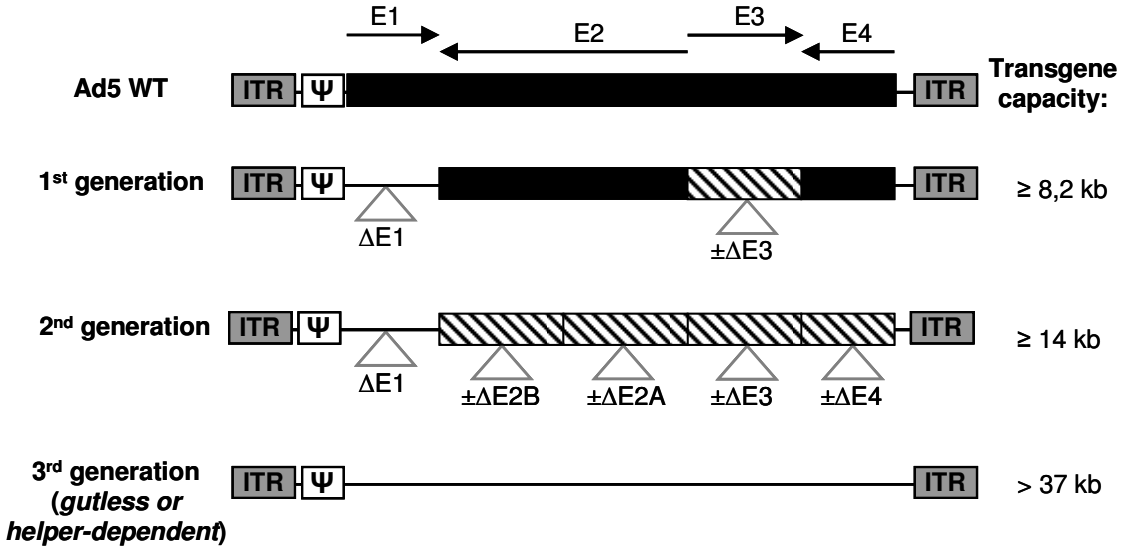

Fig. 1.9 Genome structures of the first, second, and third generation of adenoviral vectors

Wild-type adenoviral sequences are labelled in black. The localization of the early genes (E1-E4) is represented by arrows. Deletion sites are shown as a thin line or as striped boxes for alternative deletions. ITR: inverted terminal repeats; Ψ: packaging signal [modified from: *Danthinne et al., 2000*].

Adenoviral vectors have several advantages that can be beneficial for potent therapeutic vaccines. First of all, adenoviruses are relatively susceptible for genetic modifications and can be easily produced in high titers. After transduction of the cells, the adenoviral genome is not integrated into the host DNA and stays in the episomal form. As a result, the risk of the possible activation of the cellular oncogenes is minimal. Adenovirus-based vaccines proved to elicit vigorous and sustained humoral and T cell responses to the incorporated antigen that is considered to be crucial in clearance of persistent viral diseases [*Shiver et al., 2002; Fitzgerald et al., 2003; Tatsis et al., 2004; Zakhartchouk et al., 2005*]. The benefit of adenoviral vectors as a vaccine carrier is not only limited to a stable delivery of proteins of interest. Several findings on additional immunostimulatory effects, e.g. induction of the innate immune response, that originate from the nature of adenoviruses itself, may enhance the vaccine efficacy. The capsid of adenoviruses demonstrates immunostimulatory properties, that is why the co-administration of the adjuvant is usually unnecessary. Those vectors can directly transduce DCs causing their maturation and upregulation

of MHC and costimulatory molecules on their surface, thus lead to enhanced antigen presentation. Moreover, it was shown that AdV-transduced DCs are secreting antiviral cytokines, such as IFNα, TNFα and IL-6 [*Morelli et al., 2002*]. Interleukin-6 is one of the most important factors that suppress the function of the regulatory T cells [*Wan et al., 2007*].

Nevertheless, apart from the above-mentioned advantages modified adenoviruses have one serious limitation. Thus far, vectors that were so comprehensively examined as the vaccines have been based on the human adenovirus serotype 5 (Ad5) [*Tatsis et al., 2004*]. This serotype is the most common in the human population. Anti-Ad5 neutralizing antibodies are detectable in 45-90% of adults [*Farina et al., 2001*]. The pre-existing immunity directed against Ad5 is considered as a main reason of failure in the phase I clinical trial of a protective HIV-1 vaccine. The STEP study guided by Merck pharmaceutical concern, based on 3-dose regimen of a trivalent Ad5 vaccine, suggested that the immunization might increase the risk of HIV-1 infection in the subjects with high neutralizing anti-Ad5 titers [*Buchbinder et al., 2008; McElrath et al., 2008*]. Moreover, even single immunization may induce immunity to the vector in seronegative individuals.

The negative effect of the pre-existing or Ad5-induced immunity against the vaccine, mostly when the therapy requires multiple dosages, may be overcome by heterologous prime-boost regimen. The utility of the rare human serotypes (e.g. serotype 35) [*Gao et al., 2003; Barouch et al., 2004*] or recombinant adenoviruses of non-human origin has been recently tested [*Bangari et al., 2006*]. In particular, subsequent priming immunizations with plasmid DNA vaccine followed by a booster vaccination with AdV seem to be a very promising strategy. DNA prime – adenovirus boost regimen proved to induce more robust and potent immune response in comparison to plasmid DNA alone and provided protection against the pathogen infection in several animal models of infectious diseases [*Sullivan et al., 2000; Gao et al., 2003; Casimiro et al., 2005; Xin et al., 2005*]. Furthermore, a clinical trial of multiclade HIV-1 DNA plasmid-Ad5 boost vaccine, HIV-uninfected individuals demonstrated high immunogenicity even in the presence of high anti-Ad5 antibody titer. In addition, the vaccine proved to be well tolerated in the participants of the study [*Kibuuka et al., 2010*].

2 Aim of the study

The currently available treatment of chronic hepatitis B with IFNα and/or nucleoside analogues does not lead to a satisfactory result. On the one hand, therapy with IFNα results in sustained antiviral response in only one third of the patients. On the other hand, the treatment with nucleoside analogues can significantly suppresses HBV replication in the majority of patients, however it cannot completely eradicate the virus and needs a lifelong therapy. Therefore, there is a need to develop new therapeutic strategies for the treatment of chronic HBV infection.

The natural occurrence of chronic infection with WHV in woodchucks, that is closely related to HBV, allows to evaluate new therapeutic strategies in this preclinical model. It is well known that in the chronic hepadnaviral infections an appropriate virus-specific T cell-mediated immune response, predominantly against core antigen, is absent. Therefore, the therapeutic vaccination strategy which is able to boost an antiviral T cell response may be a promising option to terminate the viral persistence. It was shown that vaccines based on viral proteins (surface or core antigen) are not successful in chronic hepadnaviral infection in woodchucks and in patients. Plasmid DNA vaccines inducing a strong T cell response against CTL epitopes in the core or surface antigens prevented hepadnaviral infection. However, they were also not effective as therapeutic vaccines in chronic carriers. Nevertheless, the application of DNA vaccine expressing WHcAg in combination with antivirals in chronic WHV carriers led at least to a prolonged control of the viral replication. A significantly better induction of WHcAg-specific T cells using more potent vaccines, such as recombinant viral vectors, may be required to achieve sustained antiviral response.

The aim of the study was to evaluate the innovative therapeutic vaccination based on improved DNA vaccine and recombinant adenoviral vectors expressing WHcAg in chronic WHV carriers. The application of the new vectors, an optimized vaccination regimen, and the addition of a potent antiviral treatment (entecavir) may be an effective strategy to achieve: (1) improved WHV-specific immune responses, (2) long term viral control, and (3) resolution of chronic WHV infection.

To achieve this goal, several steps had to be accomplished:

1. Generation of a new DNA plasmid vaccine and recombinant adenoviral vectors with increased WHcAg expression.

2. Investigation on the magnitude of $CD8^+$ T cell response using the improved vaccines in comparison to previously used constructs *in vivo*. As more potent immunological tools to efficiently evaluate the immunization strategies are available for the mouse model, the preliminary experiments were performed in mice. To effectively characterize $CD8^+$ T cell response in C57BL/6 and WHV transgenic mice, the identification of $CD8^+$ T cell H-2^b-restricted epitopes within WHcAg was required.
3. Evaluation whether heterologous DNA prime – AdV boost immunization elicits a more robust, multifunctional and effective $CD8^+$ T cell response in C57BL/6 mice, as compared to DNA vaccination.
4. Evaluation whether heterologous DNA prime – AdV boost immunization elicits effective humoral and cellular immune responses that lead to suppression of WHV replication in WHV transgenic mice.
5. Investigation whether immunization of naïve woodchucks using optimized recombinant adenoviral vectors induces CTL response and provides protective immunity against WHV infection.
6. Finally, evaluation whether heterologous DNA prime – AdV boost in combination with entecavir treatment leads to a more sustained antiviral response in chronic WHV carriers than previously performed studies.

3 Materials

3.1 Laboratory animals

3.1.1 Wild-type mice

Ten weeks old C57BL/6 female mice (genotype H-$2^{b/b}$) were purchased from Harlan Winkelmann Laboratories (Borchen, Germany). The mice were kept under specific pathogen-free (SPF) conditions and had free access to drinking water and standard food.

3.1.2 WHV transgenic mice, strain 1217

WHV transgenic mice (Tg) were created on C57BL/6 background (genotype H-$2^{b/b}$) by Prof. Bill Mason's group (Fox Chase Cancer Center, Philadelphia, Pennsylvania, USA) and further bred at the animal facility of the University Hospital Essen.

The 1217 strain mice carry a wild-type WHV transgene integrated into Chromosome 10. Those mice are characterized by WHV replication and presence of viral transcripts in the liver, as well as secretion of WHV particles into the bloodstream.

All 1217 WHV Tg mice used were sex-matched and 10-12 weeks of age at the beginning of experiments. The mice were kept under SPF conditions and had free access to drinking water and standard food.

3.1.3 Woodchucks (*Marmota Monax*)

Naïve and chronically WHV infected woodchucks were trapped in the state of New York and Delaware. Woodchucks were purchased from North Eastern Wildlife (Itaca, New York, United States of America) and maintained according to the guidelines of the animal facility of the University Hospital Essen.

3.2 Anesthetics

Isofluran	Delta Select, Germany
Ketamine 10%	Ceva Tiergesundheit, Germany
Xylazine 2%	Ceva Tiergesundheit, Germany
T61	Intervet, Germany

3.3 Virus stock

WHV stock used for the experiments was obtained from the serum of chronically WHV infected woodchucks and stored at -80°C.

3.4 Bacteria strains

Eschrichia coli Top10 ..... (Invitrogen, Germany)	*F'mcr*A Δ(*mrr-hsd*RMS*mcr*BC) φ80*lac*ZΔM15Δ*lac*X74 *nup*G *rec*A1 *ara*D139 Δ(*ara-leu*)7697 *gal*E15 *gal*K16 *rps*L(Str^R) *end*A1-λ
Escherichia coli BJ5183 ..... (Stratagene, Germany)	*end*A1 *sbc*BC *rec*BC *gal*K *met thi*-1 *bio*T *hsd*R (Str^R)
Escherichia coli DH5α ..... (New England Biolabs, Germany)	*supE*44 Δ*lac*U169 (φ80*lac*ZΔM15) *hsd*R17 *recA*1 *endA*1 *gyrA*96*thi*-1 *relA*1

3.5 Eukaryotic cell lines

BHK-21

Baby Hamster Kidney fibroblast cell line; was used in transfection experiments.

HEK-293A

Human kidney epithelial cell line; expresses adenoviral E1 gene products; was used in generation and propagation of recombinant adenoviruses.

3.6 Chemicals and reagents

Acetic acid, Cesium chloride, EDTA solution pH 8.0, Saccharose, Salmon sperm DNA, SDS (sodium dodecyl sulphate), Tween 20……..	AppliChem
FACS Clean, FACS Flow, FACS Rinse, Yeast extract……..	Becton Dickinson
Ficoll……	Biochrom AG
Entecavir…….	Bristol-Myers Squibb, USA
Ionomycin, PMA (phorbol-12-myristat-13-acetate)…….	CalBiochem
Polyethylenimin (PEI)……...	CellnTec, Switzerland
D-PBS, TBE ultrapure 10x, Trypan Blue, Trypsin EDTA……	Gibco Invitrogen
Percoll…….	GE Healthcare, UK

2[^{3}H]adenine, [^{32}P]-dCTP……..... Hartmann Analytic
SSC ultrapure 20x, SSPE ultrapure 20x..... Invitrogen
Boric acid..... JT Baker, Netherlands
Cardiotoxin……. Latoxan, France
Potassium chloride, Potassium dihydrogenphosphate, Sodium acetate, Sodium azide, Sodium carbonate, Sodium chloride, Sodium dihydrogenphosphate, Sodium hydrogencarbonate, Sodium oxide..... Merck
Glicine, Tris-Base…….. MP Biomedicals
Microscint 20…….. Perkin Elmer, USA
Murine IL-2 Roche
Acrylamide solution, Ethidium bromide, Hydrogen peroxide, LB-Agar (Luria/Miller), LB-Medium (Luria/Miller), Milk powder, Phenol..... Roth
BSA (bovine serum albumin) fraction V..... Serva
β-mercaptoethanol, Agarose, APS (ammonium persulfate), Brefedin A, Bromophenol blue, Chlorophorm, Concavalin A, DMSO (Dimethyl sulfoxide), DTT (Dithiothreitol), Ethanol, Glycerol, Hydrochloric acid, Isopropanol, Methanol, OPD tablettes (o-Phenylenediamine), Orange G, TEMED..... Sigma

3.7 Antibiotics

Ampicillin	AppliChem, Germany
Kanamycin	AppliChem, Germany
Penicillin/Streptomycin	PAA Laboratories, Austria

3.8 Cell culture media

The media for cell culturing were provided by Gibco Invitrogen, Germany and PAA Laboratories, Austria. Fetal Calf Serum (FCS) was provided by Biochrom AG, Germany.

Murine splenocytes ……	RPMI 1640 medium
	10% FCS
	1% Penicillin/Streptomycin

Woodchuck PBMCs ……	AIM-V medium
	10% FCS
	1% Penicillin/Streptomycin
BHK cell line ……	MEM medium
	10% FCS
	1% Penicillin/Streptomycin
HEK-293A cell line ……	DMEM medium
	10% FCS
	1% Penicillin/Streptomycin

3.9 Bacterial culture media

SOC medium……..	Invitrogen (Germany)
LB-Medium…….……	1% (w/v) Trypton
	0.5% (w/v) Yeast extract
	…..170 mM NaCl
	pH 7,2 -7,5
LB-Agar.....	1,5% (w/v) Agar in LB-Medium

Media were sterilized by autoclaving for 10 minutes at 121°C and 202,7kPa. Ampicillin was added at a final concentration of 100 µg/ml and kanamycin was added at a final concentration of 50 µg/ml.

3.10 Buffers and solutions

PBS (pH 7,4) ..……	8 g NaCl
	0,2 g KCl
	1,44 g Na_2HPO_4; KH_2HPO_4
	1 L H_2O
Carbonate buffer (pH 9,6) ……..	3,18 g Na_2CO_3
	5,88 g $NaHCO_3$
	0,2 g NaN_3
	1 L H_2O
Blocking solution (ELISA) ……..	PBS
	5% (v/v) FCS

T-PBS washing buffer (ELISA / Western blot)....	PBS
	0,5% (v/v) Tween 20
OPD-substrate solution (ELISA) ……..	o-Phenylenediamine (1 pill)
	10 ml PBS
	10 µl H_2O_2
STOP solution (ELISA) ……..	0,5 N H_2SO_4
FACS buffer I ……...	PBS
	0,1% (m/v) BSA
	0,02% (m/v) NaN_3
FACS buffer II (mice) ……..	PBS
	1x PermWashBuffer
	0,1% (m/v) BSA
	0,02% (m/v) NaN_3
FACS buffer III (woodchucks) ……...	PBS
	1x PermWashBuffer
	5% (m/v) BSA
	0,02% (m/v) NaN_3
DNA loading buffer ……..	5.5 mM Orange G
	1.2 M saccharose
1x TBE buffer (pH 8,4) ……..…….	100 mM Tris Base
	90 mM boric acid
	1 M EDTA
Buffer P1, pH 8,0 (plasmid preparation)	50mM Tris Base
	12mM Na_2EDTA H_2O
	100 mg RNAse
	1L H_2O
Lysis buffer P2 (plasmid preparation)	200 mM NaOH
	35 mM SDS
Neutralisation buffer p3 (plasmid preparation) ...	3 M potassium acetate
	150 ml acetic acid
	1 L H_2O
TE buffer (pH 8,0) …….	1 % (v/v) 1 M Tris-HCl
	1 mM EDTA

1x SDS sample lysis buffer …….	62.5 mM Tris-HCl, pH 6.8
	2% (m/v) SDS
	10% (v/v) glycerol
	50 mM DTT
	0.01% (w/v) bromophenol blue
Blocking solution (Western blot) …..……	PBS
	5% (m/v) milk powder
10x SDS running buffer ..……...	Rotiphorese 10xSDS PAGE
	Roth, Germany
Transfer buffer (Western blot) ……..	72 g glycine
	15 g Tris Base
	25 ml 20% SDS
	1L H_2O
Denaturation buffer (Dot blot / Southern blot)…..	0,5 M NaOH
	1,5 M NaCl
Neutralization buffer (Dot blot / Southern blot)....	0,5 M Tris-HCl
	1,5 M NaCl
20xSSPE buffer (pH 7,4) ……..	3 M NaCl
	0,2 M NaH_2PO_4
	0,02 M EDTA
20xSSC buffer (pH 7,0) ……..	3 M NaCl,
	0,3 M sodium citrate
Hybridization buffer (Dot blot / Southern blot)….	RapidHyb buffer
	(GE Healthcare, UK)
Washing buffer I (Dot blot / Southern blot)…..…..	H_2O
	2x SSC
	0,1% (v/v) SDS
Washing buffer II (Dot blot / Southern blot)……..	H_2O
	0,1x SSC
	0,1% (v/v) SDS

3.11 Enzymes and commercial Kits

CombiZyme DNA Polymerase Mix	Invitek, Germany
Cytofix / Cytoperm Kit	BD Pharmingen, Germany
DecaLabel DNA Labelling Kit	Fermentas, Germany
Effectene Transfection Reagent Kit	Qiagen, Germany
ELC Western Blotting Detection Kit	GE Healthcare, UK
GoTaq Polymerase (+ 5× reaction buffer)	Promega, Germany
Lipofectamine Transfection Reagent Kit	Invitrogen, Germany
Platinum SYBR Green Kit	Invitrogen, Germany
QIAamp DNA Mini Kit	Qiagen, Germany
QIAprep Mini-, Midi-, Maxi-, Gigaprep Kit	Qiagen, Germany
QIAquick Gel Extraction Kit	Qiagen, Germany
Rapid Ligation Kit (containing T4 ligase)	Fermentas, Germany
Restore PLUS Western Blot Stripping Buffer	Thermo Scientific, USA
Restriction endonucleases	NEB, Germany
Vivaspin AdenoPACK 100 Kit	Sartorius, Germany

3.12 Standards

Smart Ladder	Eurogentec, Belgium
GeneRuler 1kb Ladder Plus	Fermentas, Germany
Roti-Mark Prestained	Roth, Germany

3.13 Plasmids

pWHcIm and pWHsIm

The expression plasmids encode WHcAg (pWHsIm) and WHcIm (pWHsIm) under control of a CMV-IE promoter. Both plasmids were constructed on the basis of pcDNA3 vector (Invitrogen). Both plasmids pWHcIm and pWHsIm were used as DNA vaccines in immunization trials. Plasmids were kindly provided by Prof. Mengji Lu (Institut für Virologie, Universitätsklinikum, Essen). The vector map is included in the Appendix section (10.3; Fig. 10.1)

pCG

The plasmid pCG is an expression plasmid that contains a β-globin intron sequence between CMV-IE promoter and the polyadenylation signal. The plasmid was kindly provided by Prof. Ulf Dittmer (Institut für Virologie, Universitätsklinikum, Essen). The sequence of WHcAg was cloned into the pCG vector and newly created pCGWHc plasmid was used as a DNA vaccine in immunization trials. The vector map of pCGWHc is included in the Appendix section (10.3; Fig. 10.2).

pShuttle

pShuttle is a cloning vector used for generation of recombinant adenoviruses using AdEasy system. The gene of interest (WHcAg) was subcloned into pShuttle and the pShuttle/WHc plasmid was used for homologous recombination with adenoviral backbone plasmids. The vector map of pShuttle/WHc is included in the Appendix section (10.3; Fig. 10.3)

pAdEasy-1 and pAdEasy-1/F35

Adenoviral backbone plasmids used for generation of recombinant adenoviral vectors using AdEasy system. The pAdEasy-1 plasmid contains the genome sequences of adenovirus serotype 5 and pAdEasy-1/F35 is a chimeric vector that encodes fiber shaft and knob domains of adenovirus serotype 35. Both plasmids are characterized by deletion in E1 and E3 region of AdV genome.

3.14 Antibodies

Antibodies used for the flow cytometric analysis of murine splenic lymphocytes and woodchuck PBMCs are listed in tables below (Tab. 3.1 and Tab. 3.2, respectively). Characteristics of the antibody-coupled fluorochromes used for flow cytometric purposes are presented in table 3.3. The other antibodies and conjugates are gathered in table 3.4.

Tab. 3.1 Monoclonal antibodies and dyes used for flow cytometric analysis of murine lymphocytes

Antibody	Clone	Manufacturer
7AAD	-	BD Pharmingen
CFSE	-	Invitrogen
CD4 PE rat anti-mouse antibody	L3T4 (RM4-5)	BD Pharmingen
CD4 PerCP rat anti-mouse antibody	L3T4 (RM4-5)	BD Pharmingen
CD4 AF700 rat anti-mouse antibody	L3T4 (RM4-5)	eBioscience
CD8a FITC rat anti-mouse antibody	53-6.7	BD Pharmingen
CD8a PE rat anti-mouse antibody	53-6.7	BD Pharmingen
CD8a eF450 rat anti-mouse antibody	53-6.7	eBioscience
CD43 PerCP rat anti-mouse antibody	1B11	eBioscience
CD107a FITC rat anti-mouse antibody	1D4B	BD Pharmingen
IFNγ FITC rat anti-mouse antibody	XMG1.2	eBioscience
IFNγ APC rat anti-mouse antibody	XMG1.2	BD Pharmingen
IL-2 PE rat anti-mouse antibody	JES6-5H4	eBioscience
TNFα APC rat anti-mouse antibody	MP6-XT22	eBioscience

Tab. 3.2 Antibodies and dyes used for flow cytometric analysis of woodchuck lymphocytes

Antibody	Clone	Manufacturer
7AAD	-	BD Pharmingen
CD3 polyclonal rabbit anti-human antibody	-	DakoCytomation (Denmark)
αIgG PE polyclonal donkey anti-rabbit antibody	-	Abcam (United Kingdom)
CD4 FITC monoclonal mouse anti-human antibody	L200	BD Pharmingen
CD4 PE monoclonal mouse anti-human antibody	L200	BD Pharmingen
CD4 PerCP monoclonal mouse anti-human antibody	L200	BD Pharmingen
CD107a FITC rat anti-mouse antibody	1D4B	BD Pharmingen

Tab. 3.3 Charasteristics of fluorochromes

Fluorochrome	Abbreviation	Absorption (nm)	Emission (nm)
7-aminoactinomycin D	7AAD	488	647
Alexa Fluor 700	AF700	633	723
Allophycocyanin	APC	633	660
Carboxyfluorescein succinimidyl ester	CFSE	488	520
eFluor 450	eF450	405	455
Fluorescein isothiocyanate	FITC	488	518
Peridinin-chlorophyll-protein complex	PerCP	488	675
Phycoerythrin	PE	488	575

Tab. 3.4 Other antibodies and conjugates

Antibody	Clone	Usage	Manufacturer
CD28 monoclonal hamster anti-mouse antibody	37.51	co-stimulation	BD Pharmingen
anti-mouse IgG (HRP conjugated)	-	ELISA	Sigma
anti-mouse IgG_1 (HRP conjugated)	X56	ELISA	BD Pharmingen
anti-mouse IgG_2 (HRP conjugated)	R19-15	ELISA	BD Pharmingen
Protein G (HRP conjugated)	-	ELISA	Sigma
mouse monoclonal anti-HBcAg (10E11): cross-reactive with WHcAg	-	Western blot	Santa Cruz Biotech., USA
mouse monoclonal anti-β-actin	-	Western blot	Sigma
anti-mouse IgG/IgM (HRP conjugated)		Western blot	Dianova

Monoclonal mouse anti-WHcAg antibodies 6C5C8E4, used for Western blotting analysis, were kindly provided by Prof. Mengji Lu (Institut für Virologie, Universitäts-klinikum, Essen).

3.15 Peptides

Peptides used for *in vitro* stimulation of murine and woodchuck lymphocytes were synthetized by EMC microcollections (Germany). The list of WHV core- and surface protein-derived peptides is included in the Appendix section 10.2. As negative control the peptide YILEETSVM derived from human cytomegalovirus (CMV) was used.

Lyophilisates of peptides were diluted in PBS containing 10% DMSO to the concentration 1mg/ml, aliquoted and stored at -20°C.

3.16 Membranes and films

Hybond N+ membrane	GE Healthcare, UK
PVDF membrane	Millipore, Germany
High performance chemiluminescence film	GE Healthcare, UK
Glass fibre filters	Perkin Elmer, USA

3.17 Oligonucleotides

All oligonucleotides used in the study were synthesized by Biomers (Germany). The nucleotide sequence, annealing temperature (T_{ann}) employed for PCR and usage of the oligonucleotides are presented in table 3.5.

Tab. 3.5 Oligonucleotides

Primer	Orientation	Sequence (5'→3')	T_{ann}[°C]	Usage
pCG *Kpn*I	sense	CATGGTACCTAATCGACTCACTATAGG GAGACC	60	cloning
pCG *Bgl*II	anti-sense	CATAGATCTAGCTCCTCGAGTTCATAA GAGAAG	60	cloning
WHc *Xba*I	sense	AGCTTCTAGACCATGGACATAGATCCC TATAAA	56	cloning
WHc *Sbf*I	anti-sense	AGCTCCTGCAGGAATTCGGCTTCATTG AAGATCAGCAGTT	56	cloning
wc1	sense	TGGGGCCATGGATATAGATCCTTA	50/60	real-time PCR
wc2	anti-sense	CATTGAATTCAGCAGTTGGCAGATGG	50	PCR
wc149s	anti-sense	AAGATCTCTAAATGACTGTATGTTCCG	60	real-time PCR
coreS	sense	GGAACATACAGTCATTAGG	50	sequencing
coreAS	anti-sense	GCAGTAGCAGTGTCCACCA	55	sequencing
pShuttleS	sense	TAACGCCAATAGGGACTTTC	55	sequencing
pShuttleAS	anti-sense	TTGTGATGCTATTGCTTTATTTG	55	sequencing
pShuIn2S	sense	GCAAGTGTGGCGGAACACATG	55	sequencing
pShuInAS	anti-sense	CAGGACCCTCAACGACCGAG	55	sequencing

3.18 Materials and equipment

Beakers	Schott, Germany
Capillaries (heparinised)	Hirschmann Laborgeräte, Germany
Cell culture flasks (T25; T75; T175, T300)	Greiner bio-one, Germany
Cell culture plates (6- and 24-well)	Greiner bio-one, Germany
Cell strainers (70µm)	Falcon BD, Germany
Chamberslides (8-well)	NUNC, Denmark
Cryo-tubes (2ml; 5ml)	Greiner bio-one, Germany
Combitips (0,5ml; 2,5ml; 5ml)	Eppendorf, Germany
Dishes	Greiner bio-one, Germany
Disposable scalpels	HMD Healthcare, UK
Disposable syringes (1ml)	TERUMO, Belgium
Disposable syringes (2ml; 5ml; 10ml)	B.Braun, Germany
Erlenmeyer flasks	Schott, Germany
FACS tubes	Becton Dickinson, Germany
Flat-bottom 96-well microplates	Falcon BD, Germany
Forceps (pointed and curved)	Oehmen, Germany
Leucosept tubes	Falcon BD, Germany
Light cycler capillaires 20µl	Roche, Germany
Hybridization Tubes	Amersham Bioscience, USA
Microcon colums YM10	Millipore, Germany
MicroSpin colums S-200	GE Healthcare, UK
Needles (0,4x19mm ; 0,9x40mm)	Becton Dickinson, Germany
NUNC Immunoplates (96-well)	NUNC, Denmark
Parafilm	American National Can, USA
Pipette tips (10µl ; 200µl ; 1000µl)	STARLAB, Germany
Plastic sterile pipettes (5ml; 10ml; 25ml)	Greiner bio-one, Germany
Reaction tubes (1,5ml; 2ml)	Eppendorf, Germany
Scissors	Oehmen, Germany
Screw-cap tubes (15ml; 50 ml)	Falcon BD, Germany
S-Monovette tubes (K3E and Z, 9ml)	Sarstedt, Germany
TopSeal-A: 96-well microplates	Perkin Elmer, USA
U-bottom 96-well microplates	Falcon BD, Germany

Balance Vibra AJ-2200CE	Shinko Denshi, Japan
Bio-imaging system (Gene Genius)	Syngene, USA
Centrifuge Megafuge 1.0R	Heraeus, Germany
Centrifuge Avanti J-26XPi	Beckman Coulter, Germany
Centrifuge : Ultracentrifuge Optima L-70K	Beckman Coulter, Germany
Cyclone (Storage Phosphor Screen)	Packard, USA
CO_2 incubator	Thermo, Deutschland
ELISA Expert Plus Microplate Reader	Biochrom, UK
Electrophoresis chambers	BioRad, Germany
Electroporator Gene Pulser	BioRad, Germany
FACSCalibur flow cytometer	Becton Dickinson, Germany
Fridge / Freezer (-20^{o}C)	AEG, Germany
Freezer (-80^{o}C)	Thermo Forma, Germany
Laminar flow	KOJAIR, Germany
LightCycler 2.0	Roche, Germany
LSRII flow cytometer	Becton Dickinson, Germany
Harvester	Packard, USA
Heating block (Thermo Stat Plus)	Eppendorf, Germany
Hybridization oven	BINDER, USA
Microcentrifuges	Eppendorf, Germany
Microscope (inverted)	ZEISS, Germany
Microscope (confocal, Leica DM IRE2)	Leica Microsystems, Germany
Osmotic pumps (ALZET 2ML4)	Durect, USA
Single-, multichannel pipettes, multipettes	Eppendorf, Germany
Shaker (Duomax 1030)	Heidolph, Germany
Spectrophotometer (Gene Quant pro)	Amersham Bioscience, USA
Thermocycler	Biometra, Germany
Thoma cell counting chamber	Marienfeld, Germany
Top Count NXT	Packard, USA
Transblot SemiDry transfer cell	BioRad, Germany
UV transiluminator FLX-20M	MWG-BioTech, Germany
Vaccum blotter 785	BioRad, Germany
Vortex Genie 2	Bender & Hobein AG, Switzerland

4 Methods

4.1 Molecular biology methods

4.1.1 Amplification of DNA inserts using Polymerase Chain Reaction (PCR)

The amplification of the DNA inserts was performed using CombiZyme DNA Polymerase Mix (Invitek). CombiZyme is a cocktail of recombinant Taq DNA polymerase with a thermostable DNA polymerase providing a 3'-5' proofreading activity. Insert-specific primers introducing restriction sites necessary for further cloning were used. The reaction mixture components and the PCR conditions are presented in tables 4.1 and 4.2, respectively.

Tab. 4.1 The PCR reaction using CombiZyme Mix

Reagent	Concentration	Volume [µl]
10× OptiPerform Buffer III	1×	5
$MgCl_2$	2,5 mM	2,5
dNTP-Mix	0,25 mM	1
5× OptiZyme Enhancer	1×	10
sense / antisense primers	0,4 µM	each: 2
CombiZyme DNA polymerase	3 U	0,75
H_2O	-	22,25
DNA		0,5
		total: 50

Tab. 4.2 The PCR conditions

PCR step	Temperature [oC]	Time [min]	Number of cycles
Denaturation	94	4	1
Denaturation	94	1	30
Annealing	60 / 56*	1	
Elongation	72	2	
Final elongation	72	8	1

*The annealing temperature for pair of primers pCG *Kpn*I + pCG *Bgl*II was 60°C and for pair of primers WHc *Xba*I + WHc *Sbf*I was 56°C.

4.1.2 Agarose gel electrophoresis

DNA fragments were separated in a horizontal 1-2% agarose gel containing 0.5 µg/ml of ethidium bromide. The electrophoresis was carried out in 1× TBE buffer at 130 V for approximately one hour. The visualization of the separated DNA fragments was performed using a UV-Bioimaging System (Syngene).

4.1.3 DNA extraction from agarose gel

Restricted plasmids or amplified DNA fragments were separated by agarose gel electrophoresis. The fragments of interest were cut out of the gel and purified with the QIAquick Gel Extraction Kit (Qiagen) according to the manufacturer's protocol. The elution of purified fragments was performed in 30 µl of H_2O.

4.1.4 DNA restriction digestion

Plasmids and PCR-products were restricted either with a single endonuclease or with a combination of two enzymes. In that case, the set of restriction enzymes that work optimally in the same reaction buffer and temperature (usually 37°C) was chosen. The PCR products used for restriction were previously purified by extraction from the agarose gel. For preparative purposes 100 µl of restriction reaction was prepared and incubated overnight at the optimal temperature. The control digestion of successful cloning was carried out in 10 µl reaction for 1 h (Tab. 4.3).

Tab. 4.3 Restriction of plasmids and PCR-products

Reagent	Preparative digestion	Control digestion
DNA	5-10 µg of plasmid 30 µl of purified PCR product	1 µg of plasmid
Enzyme I	2 µl	0,5 µl
Enzyme II	2 µl / -	0,5 µl / -
10× buffer	10 µl	1 µl
10×BSA (if required)	10 µl	1 µl
nuclease-free H_2O	added to: 100 µl	added to: 10 µl

The products of the restriction reaction were separated by agarose gel electrophoresis and purified using the QIAquick Gel Extraction Kit (Qiagen). The linearized plasmids were precipitated by phenol-chloroform method.

4.1.5 Phenol – chloroform precipitation

For phenol–chloroform precipitation of the linearized plasmids two 100 µl restriction reactions were performed. After the digestion, the reactions were mixed by vortexing with 400 µl of phenol, incubated on ice for 5 minutes, and centrifuged (16 000× g, 3 min). The upper phase containing DNA was transferred to a fresh tube, mixed by vortexing with 400 µl of chloroform, and centrifuged (16 000× g, 3 min). Again the upper phase containing DNA was transferred to a fresh tube and mixed with 40µl of 3 M sodium acetate (pH 7) and 1200 µl of absolute ethanol. The mixture was incubated overnight at -20^{o}C. The next day, the tube was centrifuged (16 000× g, 30 min), the supernatant was discarded and pellet was washed with 100 µl of 70% ethanol (16 000× g, 10 min). The pellet was left to dry and afterwards suspended in 20 µl of nuclease-free H_2O.

4.1.6 Ligation of DNA fragments

Purified, linearized plasmid and insert DNA were ligated using T4 DNA ligase. For reaction, 2 µl of linearized plasmid, 6 µl of purified insert, 1 µl of T4 ligase and 1 µl of 10× optimal ligation buffer (Rapid Ligation Kit, Fermentas) were used. The mixture was incubated 20 min at room temperature and used for transformation of competent *E.coli* cells.

4.1.7 Transformation of *E.coli*

4.1.7.1 Transformation of chemically competent *E.coli* strains

Transformation of chemically competent *E.coli* strains (Top10, DH5α) was performed according to manufacturer's instructions. Briefly, 50 µl aliquots of bacteria were thawed on ice, mixed gently with 2-3 µl of ligation mixture and incubated on ice for 30 min. To improve DNA absorption by bacteria, a heat shock for 30 s at 42^{o}C followed by a subsequent incubation on ice for 2 minutes was performed. Afterwards 200 µl of SOC medium (Invitrogen) was added to the cells and the mixture was incubated on a shaker for 2 hours at 37^{o}C. Using a sterile spatula the complete mixture was spread over an LB-agar plate containing a selective antibiotic (100µg/ml of ampicillin or 50µg/ml kanamycin). The plates were incubated overnight at 37^{o}C.

4.1.7.2 Transformation of *E.coli* strains using electroporation

Homologous recombination between pShuttle plasmid (carrying the gene of interest) and adenoviral genome was carried out in electrocompetent *E.coli* strain BJ5183. The strain used in the experiments was previously transformed with pAdEasy-1 plasmids. The pShuttle plasmid was linearized using *Pme*I restriction endonuclease and desalted on a Microcon YM10 column (Millipore) according to manufacturer's protocol. For transformation 5 µl of linearized pShuttle plasmid and 50 µl of bacteria were mixed and transferred to an ice-cold 2-mm electroporation cuvette. The electric pulse (2500 V, 200 Ω, 25 µF) was delivered in a Gene Pulser Electroporator (BioRad). The mixture was suspended in 200 µl of SOC medium (Invitrogen) and spread over a kanamycin LB-agar plate. The plates were incubated overnight at 37°C. The correct recombinant plasmids were selected by *Hind*III restriction digestion.

4.1.8 Plasmid DNA purification using commercial kits

One bacterial colony was picked up from the LB agar plate, using a sterile pipette tip and transferred into the flask with LB-medium containing selective antibiotic. The volume of 2 ml of the culture was used for Mini, 50 ml for Midi, 250 ml for Maxi and 2500 ml for Giga preparations. After overnight incubation on the shaker at 37°C the plasmid DNA was extracted using QIAprep Kits (Qiagen) according to manufacturer's protocol. The DNA concentration was quantified by spectrophotometric OD_{260nm} measurement as follows:

$$Concentration\ [\mu g/ml] = OD_{260nm} \times dilution\ factor \times 50$$

Purified plasmid DNA was checked by control restriction digestion (section 4.1.4).

4.1.9 Plasmid DNA purification using CsCl gradient ultracentrifugation

Preparative purification (MaxiPrep) of recombinant adenoviral plasmids was performed using CsCl gradient ultracentrifugation. The correct recombinant plasmids were retransformed to DH5α *E.coli* strain and the cultures of 300 ml were prepared. After overnight incubation at 32°C, the cultures were centrifuged (6 000× g, 10 min) and the pellet was suspended in 10 ml of buffer P1. Next,15 ml of lysis buffer P2 was added and mixed. After 5 minutes incubation 25 ml of neutralization P3 buffer was added, mixed and the tube was centrifuged (5 000× g, 10 min). The supernatant was

filtrated into a fresh tube, mixed with 0,7 volume of isopropanol and centrifuged at 4°C (12 000× g, 30 min). The pellet was resuspended in 4,1 ml of buffer P1 containing 4,6 g of CsCl and 40 µl of ethidium bromide. The solution was transferred into an ultracentrifuge tube and centrifuged for 4 h at 70 000× rpm (Rotor NVT100). Afterwards, the band stained with ethidium bromide was collected using a syringe and washed with 90% buthanol in 10% TE buffer until the dye was removed. The DNA phase was mixed with 0,7 volumes of isopropanol and centrifuged (12 000× g, 30 min). The pellet was washed with 70% ethanol, dried and resuspended in 200-500 µl of TE buffer. Recombinant adenoviral plasmids were linearized using *Pac*I restriction endonuclease and used for transfection of HEK-293A cells (section 4.2.7).

4.1.10 DNA sequencing

Sequencing was performed at the DNA-Sequencing Service (Universitätsklinikum Essen). Non-standard primers designed for sequencing are listed in the Materials section (Tab. 3.5).

4.2 Cell culture

4.2.1 Thawing and cryoconservation of cells

Cryotubes containing cells were taken out from the liquid nitrogen and thawed quickly in a warm water-bath. Cells were washed twice in 10 ml of the culture medium. Afterwards, cells were suspended in 10ml of fresh medium, placed in 25 cm^2 flask, and cultured at 37°C in humidified atmosphere containing 5% CO_2.

For cryoconservation, the cell suspension was centrifuged in 50 ml tubes (300× g, 5 min) and washed once with sterile PBS. The pellet was suspended in 1 ml of culture medium supplemented with 25% FCS and 10% DMSO. Cells were frozen slowly overnight in -80°C and then transferred to a liquid nitrogen tank.

4.2.2 Passaging of cells

The medium was removed and cells were washed twice with 10 ml of sterile PBS. Then 2 ml of Trypsin-EDTA was added to cover the bottom of the 75 cm^2 flask. After approximately 2 minutes when the cells started to detach from the bottom 8 ml of

fresh medium was added. Cells were placed in fresh flasks in 20 ml of culture medium in the given concentration.

4.2.3 Culture of BHK-21 cells

Adherent BHK-21 cells were grown in monolayers in MEM (*Minimum Essential Medium*) medium supplemented with 10% FCS and 10 U/ml penicillin-streptomycin. Cells were passaged twice a week at a dilution 1:10.

4.2.4 Culture of HEK-293A cells

Adherent BHK cells were grown in monolayers in DMEM (*Dulbecco's Modified Eagle Medium*) medium supplemented with 10% FCS and 10 U/ml penicillin-streptomycin. Cells were passaged twice a week at a dilution 1:5.

4.2.5 Counting of viable cells using Trypan blue exclusion microscopy

Trypan blue is a negatively charged dye that only interacts with the cell when the membrane is damaged. Therefore, all the cells which exclude the dye are viable. Aliquots of cell suspension were diluted with 0.4% Trypan blue stain and 10 µl of the diluted aliquot solution was transferred onto a Thoma hemocytometer. The viable cells were counted and the number of cells per ml was calculated as follows:

$$number\ of\ cells\ /\ ml = number\ of\ cells\ in\ the\ large\ square \times dilution\ factor \times 10^4$$

4.2.6 Transfection of BHK cells

4.2.6.1 Using Effectene reagent

Up to 5×10^4 BHK-21 cells per well were plated on a 24-well plate and incubated at 37°C till the cells reached confluence of 80%. Cells were washed with sterile PBS and 350 µl of the culture medium was added per well. Cells were transfected with 1 µg of plasmid using the Effectene reagent (Qiagen) according to manufacturer's protocol. As a negative control cells treated only with Effectene reagent were used.

For 8-well chamberslides up to 1×10^3 BHK-21 cells per well were plated and incubated at 37°C till the cells reached confluence of 80%. Cells were washed with sterile PBS and 200 µl of the culture medium was added per well. For one well a half volume of the transfection mixture prepared for a well of 24-well plate was used. Cells treated only with Effectene reagent served as the negative control.

4.2.6.2 Using Lipofectamine reagent

Up to 1×10^6 BHK-21 cells per well were plated on a 6-well plate and incubated at 37°C till the cells reached confluence of 80%. Cells were washed with sterile PBS and 1,5 ml of the Opti-MEM medium was added per well. Cells were transfected with 1 µg of plasmid using the Lipofectamine reagent (Invitrogen) according to manufacturer's protocol. As a negative control cells treated only with Lipofectamine reagent were used. After 5 h the Opti-MEM medium was replaced with fresh culture medium.

4.2.7 Transfection of HEK-293A cells with recombinant AdV plasmids

Transfection was performed using polyethyleneimine (PEI). The reagent is forming a complex with DNA which is absorbed by the cells through endocytosis process. Per one 25 cm^2 culture flask of HEK-293A cells the transfection mixture containing 6-8 µg of *Pac*I-linerized AdV plasmids (pAd5WHc or pAd5F35WHc), 10 µl of PEI and 500 µl of serum-free DMEM medium was prepared. The mixture was incubated for 10 min and added on the cells (90-95% confluent). The cells were cultured in DMEM medium supplemented with 2% FCS and after 6 h the medium was replaced for a standard culture medium.

4.2.8 Production and purification of recombinant adenoviral vectors

Approximately 14 days after the PEI transfection, the content of the 25 cm^2 culture flasks in which cells were completely lysed by replicating adenoviruses was collected and centrifuged (300× g, 5 min). The supernatant was collected in a fresh tube and the cell debris were subsequently frozen and thawed (liquid nitrogen – warm water bath) to release remaining particles. The supernatant was used to infect fresh HEK-293 cells cultured in 75 cm^2. In the next rounds of the production 175 cm^2 and finally 300 cm^2 culture flasks were used.

The recombinant adenoviral particles were purified from supernatant of five 300 cm^2 culture flasks using Vivaspin AdenoPACK 100 Kit (Sartorius) according to the manufacturer's protocol.

4.2.9 Determination of the infectious adenoviral particles titer

The titer of infectious adenoviral particles was determined using $TCID_{50}$ (*tissue culture infectious dose 50*) assay. For that purpose, HEK-293A cells were plated in

a flat-bottom 96-well plate (1×10^4 cells per well) and infected in every row with 100 µl of serial logarithmic dilutions of the purified virus stock. After 5-10 days the cytophatic effect (CPE) in every well was monitored. The ratio of CPE-positive wells for every dilution was determined and the $TCID_{50}$ per ml of the virus stock was calculated as follows:

$$TCID_{50}/ml = 10^{1+d\,(S-0,5)} \times 10$$

Where: d = Log 10 of the dilution; S = the sum of CPE ratios for every dilution

To transform $TCID_{50}$/ml value in PFU (*plaque forming units*) per ml the following formula was used:

$$PFU/ml = [TCID_{50}/ml]^{-0,7}$$

4.2.10 Infection of HEK-293A cells with recombinant adenoviral vectors

Up to 5×10^6 HEK-293A cells per well were plated on a 6-well plate and incubated at 37°C till the cells reached confluence of 80-90%. Cells were washed with sterile PBS and 1,5 ml of culture medium containing 5×10^7 PFU (MOI 10) of Ad5WHc or Ad35WHc was added. After 2 h the medium was replaced with 3 ml of fresh culture medium. Cells treated only with medium served as negative control.

4.3 Protein-biochemical methods

4.3.1 Immunoblot analysis (Western Blot)

4.3.1.1 Preparation of the cell lysates

The cell lysates were prepared 24 h after transfection with WHcAg-expressing plasmids (section 4.2.6) or 36 h after infection with recombinant adenoviral vectors (section 4.2.10). The medium was removed and cells were washed twice with PBS. The cells were suspended in lysing buffer (200 µl per well of 24-well plate; 350 µl per well of 6-well plate) and denaturated for 20 min at 95°C. The cell lysates were stored at -20°C.

4.3.1.2 SDS-PAGE

Proteins were separated using standard discontinuous, one-dimensional SDS-PAGE (*Sodiumdodecylsulfate Polyacrylamide Gel Electrophoresis*). The ingredients needed

for preparation of 15% separation gel and 5% stacking gel are presented in the Tab. 4.4.

Tab. 4.4 Reagents used for preparation of SDS gels

Reagent	Stacking gel (5%)	Separation gel (15%)
30% Acrylamid solution (29:1)	360 µl	2,5 ml
1,5M Tris-HCl (pH 8,8)	27 µl	1,3 ml
10% SDS	22,5 µl	50 µl
10 % APS	12,5 µl	50 µl
TEMED	2,5 µl	2 µl
H_2O	1,6 ml	1,1 ml

Up to 10 µl of the cell lysates were loaded per well and 5 µl of Roti-Mark Prestained (ROTH) as a molecular weight marker. Proteins were separated approximately 1,5 h at 130 V.

4.3.1.3 Immunoblotting

The proteins were transferred to PVDF (*polyvinylidene fluoride*) membrane using semi-dry transfer method. The membrane was pre-incubated in methanol and placed together with the SDS gel between three layers of Whatmann paper soaked in the transfer buffer. Transfer took place for 15 minutes at 7,5 V using SemiDry-transfer blotter (BioRad). The membrane was turned towards anode and the gel towards cathode. After the transfer, the binding sites on the membrane were blocked using 5% milk powder solution. After 1 h incubation at room temperature on the shaker the blocking solution was removed and the membrane was washed twice for 10 minutes with T-PBS. The WHcAg-specific mouse monoclonal antibodies: 6C58E4 or cross-reactive HBcAg 10E11 were diluted 1:2000 or 1:1000, respectively, in T-PBS and incubated with the membrane for 1 h incubation at room temperature on the shaker. After washing three times for 10 minutes wit T-PBS membrane was incubated with secondary peroxidase-conjugated anti-mouse IgG (dilution 1:20000 for 6C58E4; 1:2500 for 10E11) and washed three times for 10 minutes wit T-PBS. The presence of WHcAg was detected on radiographic film (High performance chemiluminescence film, GE Healthcare) by using ECL Western Blotting Detection Kit (GE Healthcare) according to manufacturer's protocol.

The membrane was kept overnight at 4°C in T-PBS solution and the next day the detection of β-actin as an internal control of the protein content in the lysates was performed. The membrane was stripped using Restore PLUS Western Blot Stripping Buffer (Thermo Scientific) according to manufacturer's protocol. The membrane was developed as described above. As the first antibody β-actin-specific mouse monoclonal antibodies diluted 1:5000 were used. The secondary antibody was peroxidase-conjugated anti-mouse IgG (dilution 1:15000).

4.3.2 Immunofluorescence staining

Immunofluorescence staining of WHcAg was performed 24h after transfection on a 8-well chamberslides (section 4.2.6.1). The medium was removed and the chamberslides were left to dry. The cells were fixed with ice-cold 50% methanol for 20 min at 4°C. Afterwards, methanol was removed and chamberslides were left to dry. The cells were incubated with 100 µl of polyclonal rabbit WHcAg-specific antibodies (diluted 1:80 in PBS) in humidified chamber for 1 h at 37°C and washed two times with PBS. Next, cells were incubated with 100 µl of secondary FITC-conjugated anti-rabbit IgG antibodies (diluted 1:80 in PBS) in humidified chamber for 1 h at 37°C and washed two times with PBS. The chambers were removed and the slide was left to dry for 10 min in the darkness. The slide was fixed using Dako Cytomation Mounting Medium. The pictures of the cells were taken using a confocal laser scanning microscope in magnifications 40× and 100×.

4.4 Animal experiments

All animal experiments were carried out in accordance with the "*Guide for the Care and Use of Laboratory Animals*" and were approved by the local Animal Care and Use Committee (Animal Care Center, University of Duisburg-Essen, Essen, Germany and the district government of Düsseldorf, Germany).

4.4.1 Anesthetization

For blood withdrawal and immunizations mice were anesthetized for several minutes with Isofluran vapors. Mice were placed in a glass jar filled with Isofluran-soaked kerchiefs until the animals got numb.

For blood withdrawal, immunizations and surgeries the woodchucks were deeply anesthetized by intramuscular injection of 4ml of 10% ketamine mixed with 1ml of 2% xylazine.

4.4.2 Blood withdrawal

Blood withdrawal from the anesthetized mice was performed by retroorbital punction using 3mm heparin-coated glass capillaries. The blood was collected in 1,5 ml Eppendorf tubes.

Blood withdrawal from the anesthetized woodchucks was performed from the hind limb veins (*Vena saphena)* using 0,9 × 40 mm needles. The blood samples were collected into S-Monovette Serum and EDTA-blood tubes.

Serum samples were obtained by centrifugation of blood (6000× g, 10 min) and collection of the supernatants. Sera were stored at -20^{o}C.

4.4.3 Immunization trials

Intramuscular (i.m.) injections of mice were performed into the *Tibialis anterior* muscle of the hind limbs using 0,4×19 mm needles. DNA plasmids and recombinant adenoviral vectors were diluted to the given concentration in 100 µl of sterile PBS and equal volume of 50 µl was injected into each muscle.

Intramuscular injections of woodchucks were performed into the *Tibialis anterior* muscle of the hind limbs using 0,9×40 mm needles. DNA plasmids and recombinant adenoviral vectors were diluted to the given concentration in 1 ml of sterile PBS and equal volume of 500 µl was injected into each muscle.

Seven days before the intramuscular DNA immunizations animals were pretreated with cardiotoxin (Latoxan; 10 µM in sterile PBS) to increase the effectiveness of the gene transfer [*Davis et al., 1994*]. Cardiotoxin solution was injected into the *Tibialis anterior* muscle of the hind limbs. Mice received 100 µl (50 µl per limb), whereas woodchucks received 1 ml (500 µl per limb) of the cardiotoxin solution.

4.4.3.1 Immunization of C57BL/6 with pCGWHc and pWHcIm plasmids

Ten weeks old female C57BL/6 mice were injected intramuscularly with cardiotoxin. One week later animals were intramuscularly vaccinated with 100 µg of pWHcIm or pCGWHc. Mice intramuscularly injected with 100 µl sterile PBS (50 µl per leg),

served as controls. Overall three vaccinations were performed in two weeks intervals. Mice were sacrificed two weeks after the last immunization.

4.4.3.2 Immunization of C57BL/6 in heterologous DNA prime – AdV boost regimen

Ten weeks old female C57BL/6 mice were intramuscularly injected with cardiotoxin. One week later animals were subsequently vaccinated twice in a two-week interval with 100 µg of pCGWHc plasmid. Four weeks after the second DNA immunization groups of mice were immunized with 2×10^9 PFU of Ad5WHc or 2×10^9 PFU Ad35WHc or 100 µg pCGWHc as a reference. Mice which were immunized twice with 100µg of "empty" pCG and boosted with 2×10^9 PFU Ad5 expressing GFP served as controls. Mice were sacrificed two weeks after the last immunization.

4.4.3.3 Immunization of 1217 WHV transgenic mice in heterologous DNA prime – AdV boost regimen

Ten to twelve weeks old sex-matched groups of 1217 WHV Tg mice were injected intramuscularly with cardiotoxin. One week later animals were subsequently vaccinated for two times in two-week interval with 100 µg of pCGWHc plasmid. Four weeks after the second DNA immunization groups of mice were immunized with 2×10^9 PFU of Ad5WHc or 100 µg pCGWHc as a reference. Mice which were immunized twice with 100 µg of "empty" pCG and boosted with 2×10^9 PFU Ad5 expressing GFP served as controls. Mice were sacrificed two weeks after the third immunization. The group of mice immunized twice with pCGWHc in combination with Ad5WHc was boosted for a second time with 2×10^9 PFU of Ad35WHc. The vaccination was performed four weeks after Ad5WHc immunization and mice were sacrificed two weeks later.

4.4.3.4 Immunization of naïve woodchucks with plasmid DNA or recombinant adenoviral vectors

Two naïve woodchucks (number: 58059 and 58063) were injected intramuscularly with cardiotoxin. One week later animals were subsequently immunized for three times with 1 mg of pCGWHc plasmid. The first two immunizations were performed in two-week interval, the third immunization was performed 4 weeks later. The experiment was repeated on naïve woodchuck number 70096. The animal was

pretreated with cardiotoxin solution and one week later the woodchuck was immunized for three times with 1 mg of pCGWHc in two weeks intervals.

Two naïve woodchucks (number: 46949 and 46957) were intramuscularly immunized with 5×10^9 PFU Ad5WHc and four weeks later boosted with 1×10^{10} PFU of Ad35WHc. Two weeks after the last immunization all vaccinated woodchucks were challenged with WHV (section 4.4.4). Two naïve woodchucks (number: 58055 and 58056) were only infected with WHV and served as controls.

4.4.3.5 Therapeutic vaccination in combination with ETV treatment of WHV chronically infected woodchucks

Seven chronically WHV infected woodchucks (number: 61786, 61787, 61789, 61791, 61792, 61793 and 61795) were treated for 23 weeks with the nucleoside analogue entecavir (ETV). Initially, the drug was administered for 12 weeks, by means of the osmotic pumps (DURECT) implanted surgically under the skin of the animals. The pump releases subcutaneously approximately 0,2mg of ETV per day. Pumps were exchanged every 4 weeks; overall 3 pumps were implanted. From week 8 to 23 of the therapy subcutaneous injections of 1 mg of ETV were performed twice a week. At week 7, five of the seven ETV-treated animals (number: 61786, 61787, 61789, 61792 and 61793) were injected intramuscularly with cardiotoxin. Starting from week 8 the animals received subsequently 9 intramuscular immunizations, as follows:

- week 8, 10 and 12: 0,5 mg of pCGWHc + 0,5 mg pWHsIm plasmids
- week 14: 1×10^{11} PFU Ad5WHc + 0,5 mg pWHsIm plasmid
- week 16: 1×10^{11} PFU Ad35WHc + 0,5 mg pWHsIm plasmid
- week 19: 1×10^{11} PFU Ad5WHc + 0,5 mg pWHsIm plasmid
- week 22: 1×10^{11} PFU Ad35WHc + 0,5 mg pWHsIm plasmid
- weeks 25 and 27: 0,5 mg of pCGWHc + 0,5 mg pWHsIm plasmids

4.4.4 WHV infection

Woodchucks were infected with 1×10^7 WHV strain 8 genome equivalents (GE) by intravenous injection (*Vena saphena*) using 0,9×40 mm needles. Virus aliquots for injections were prepared in 500 µl of sterile PBS.

4.4.5 Organs removal

Mice were anesthetized with Isofluran and euthanized by cervical dislocation. Then, the abdominal cavity was opened using sterile scissors and forceps. Spleens and lymph nodes were removed into the Petri-dishes filled with 5 ml of ice-cold PBS.

For removal of the livers, woodchucks were anesthetized with ketamine/xylazine and euthanized by intracardiac injection of T61. Liver samples were collected and frozen in the liquid nitrogen. Afterwards, the samples were stored at -80^{o}C.

4.5 Preparation of single-cell suspensions of murine splenocytes

Spleens were homogenized thoroughly with a syringe plunger, and single-cell suspensions were prepared using a 70 µm nylon cell strainer. Subsequently, cells were washed twice in 50 ml of sterile PBS and resuspended in 10 ml of RPMI 1640 medium supplemented with 10% FCS and 10U/ml penicillin-streptomycin. Cell counting was performed manually using a Thoma hemocytometer and Trypan blue exclusion microscopy (cell dilution 1:20) [section 4.2.5].

4.6 In vitro stimulation of murine splenocytes

4.6.1 *In vitro* stimulation of murine splenocytes for intracellular cytokine staining and CD107a degranulation assay (7 days incubation)

Up to 2×10^{6} of isolated splenocytes per well were plated in 96-well flat-bottom plates in 200 µl of RPMI 1640 medium supplemented with 10% FCS and 10U/ml penicillin-streptomycin. For stimulation, peptide pools or individual peptides were added to a final concentration of 2 µg/ml per peptide. The list of WHcAg-derived peptide amino acid sequences used for *in vitro* stimulation is included in the Appendix section (Tab. 10.1 and Tab. 10.2). Unstimulated cells and cells stimulated with CMV-derived peptide (YILEETSVM) served as a negative control. After 2 days of culturing, 10 U/ml of recombinant murine IL-2 was added.

Restimulation of splenocytes for intracellular cytokine staining (section 4.9.1) was performed after 7 days of *in vitro* stimulation. Cells were transferred to 96-well round-bottom plates and restimulated for 6 h with 200 µl of medium containing peptide

pools or individual peptides in a final concentration of 2 µg/ml per peptide. Cells were restimulated in the presence of 1 µg/ml of α-CD28 antibody as unspecific T cell receptor (TCR) costimulator, and 5 µg/ml of brefeldin A, that blocks secretion of extracellular proteins, such as cytokines. As a positive control cells stimulated with 400 ng/ml of PMA and 10 µg/ml of ionomycin were used.

For CD107a degranulation assay (section 4.9.1) cells were restimulated for 5 h in the presence of FITC labeled anti-mouse CD107a antibody (1:200) to detect degranulation, 1 µg/ml of α-CD28 antibody, and 5 µg/ml of brefeldin A for intracellular IFNγ detection.

4.6.2 *In vitro* stimulation of murine splenocytes for intracellular cytokine staining (6 hours incubation)

Up to 1×10^6 of isolated splenocytes per well were plated in 96-well round-bottom plates in 200µl of RPMI 1640 medium supplemented with 10% FCS and 10U/ml penicillin-streptomycin. For 6 h stimulation, peptides were added to a final concentration of 2 µg/ml. Unstimulated cells and cells stimulated with CMV-derived peptide (YILEETSVM) served as a negative control. For intracellular cytokine staining (section 4.9.1) cells were incubated in the presence of 1 µg/ml of α-CD28 antibody, and 5 µg/ml of brefeldin A. As a positive control cells stimulated with 400 ng/ml of PMA and 10 µg/ml of ionomycin were used.

4.7 Isolation of PBMCs from peripheral blood of woodchucks

Peripheral blood mononuclear cells (PBMCs) were separated by Ficoll density gradient centrifugation. For that, PBS-diluted blood was transferred into 50 ml Leucosept separation tubes, containing 15 ml of Ficoll. After centrifugation (1200× g, 10 min) the PBMCs-containing middle layer between Ficoll and plasma phases were transferred to a fresh tube. Subsequently, cells were washed twice in 50 ml of sterile PBS and resuspended in 10 ml of AIM-V medium supplemented with 10% FCS and 10 U/ml penicillin-streptomycin. Cell counting was performed manually using Trypan blue exclusion microscopy (cell dilution 1:10) [section 4.2.5].

4.8 In vitro stimulation of woodchuck PBMCs

4.8.1 *In vitro* stimulation of woodchuck PBMCs for CD107a degranulation assay

Up to 1×10^6 of isolated PBMCs per well were plated in 96-well flat-bottom plates in 200 µl of AIM-V medium supplemented with 10% FCS and 10 U/ml penicillin-streptomycin. For stimulation, WHcAg epitope c96-110 (KVRQSLWFHLSCLTF) and WHsAg epitope s220-234 (AGLQVVYFLWTKILT) were added to a final concentration of 2 µg/ml per peptide. Unstimulated cells and cells stimulated with CMV-derived peptide (YILEETSVM) served as a negative control.

Restimulation of PBMCs for CD107a degranulation assay (section 4.9.1) was performed after 3 days of *in vitro* stimulation. Cells were transferred to 96-well round-bottom plates and restimulated for 5 h with 200 µl of medium containing WHcAg and WHsAg epitopes in a final concentration of 2 µg/ml per peptide. Cells were restimulated in the presence of FITC labeled anti-mouse CD107a antibody (1:100) to detect degranulation.

4.8.2 *In vitro* stimulation of woodchuck PBMCs for proliferation assay

Up to 5×10^4 of isolated PBMCs per well were plated in triplicates in 96-well flat-bottom plates in 200 µl of AIM-V medium supplemented with 10% FCS and 10 U/ml penicillin-streptomycin. For stimulation, WHcAg- and WHsAg-derived peptides were added to a final concentration of 5 µg/ml per peptide. The list of the peptides used for *in vitro* stimulation was included in the Appendix section (Tab. 10.3 and Tab. 10.4). Unstimulated cells and cells stimulated with CMV-derived peptide (YILEETSVM) served as a negative control. As a positive control cells stimulated with 2 µg/ml of concavalin A were used.

After 5 days of *in vitro* stimulation proliferation assay with 2[^{3}H]-adenine was performed (section 4.10).

4.9 Flow cytometry

Flow cytometry is a technology that simultaneously measures multiple physical characteristics of cells such as relative size, relative granularity and relative fluorescence intensity. The cells are transported in the fluid stream to the measuring

cell where they are examined by the laser beam one after another. Using monoclonal antibodies conjugated with a fluorescent dye, flow cytometry enables to identify a particular cell type within complex cell populations based on their individual antigenic markers.

4.9.1 Staining of cells for flow cytometric analysis

For estimation of intracellular production of the cytokines, murine splenocytes were restimulated for 6 h in the presence of BFA and α-CD28 antibody as mentioned in sections 4.6.1 and 4.6.2. The degranulation capacity of murine splenocytes and woodchucks PBMCs was determined by detection of CD107a molecule on the cell surface. The staining of CD107a was performed by adding the specific antibody during the 5h restimulation period (sections 4.6.1 and 4.8.1). After the incubation time, cells were centrifuged (300× g, 5 min) and the culture medium was removed. Cells were washed with 200 µl FACS buffer I (PBS + 0,1% BSA + 0,02% NaN_3).

First, the molecules expressed extracellularly were stained for 15 minutes at 4°C using antibodies diluted in 100 µl FACS buffer I per sample. The exclusion of the dead cells and cellular debris was performed using the dye 7AAD (*7-amino-actinomycin*). The dye stably interacts with cellular DNA of cells in which the cell membrane was disrupted. Therefore, 7AAD-positive cells are marked as dead cells. The dye was added to the sets of antibodies during extracellular staining. Cells were washed with 200 µl FACS buffer I.

Second, the cells were fixed and permeabilized for 20 minutes at 4°C using 100 µl of Cytofix/Cytoperm Solution (BD Pharmingen). Cells were washed with 200 µl FACS buffer II (PBS + 1x PermWashBuffer + 0,1% BSA + 0,02% NaN_3).

The intracellular staining was performed for 25 minutes at 4°C using antibodies diluted in 100 µl FACS buffer II for murine cells and 100µl FACS buffer III (PBS + 1x PermWashBuffer + 5% BSA + 0,02% NaN_3) for woodchuck cells.

Finally, cells were washed twice with 200 µl FACS buffer II, suspended in 250 µl FACS flow and measured on FACSCalibur or LSRII Flow Cytometers. Approximately 200 000-250 000 events were acquired for murine splenocytes and 100 000-150 000 events for woodchuck PBMCs. The data were analyzed using FlowJo software.

Sets of antibodies and dyes, dilutions and the suspending buffers used during various stainings are gathered in tables 4.5-4.8.

Tab. 4.5 Intracellular IFNγ staining of murine splenocytes

Staining	Antibody	Fluorochrome	Dilution	Buffer
Extracellular	anti-mouse CD8	FITC	1:100	FACS buffer I
	anti-mouse CD4	PE	1:150	
	7AAD	-	2µl/sample	
Intracellular	anti-mouse IFNγ	APC	1:200	FACS buffer II

Tab. 4.6 Multifunctionality assay of murine splenocytes

Staining	Antibody	Fluorochrome	Dilution	Buffer
Extracellular	anti-mouse CD8	eF450	1:100	FACS buffer I
	anti-mouse CD4	AF700	1:150	
	7AAD	-	2µl/sample	
	or: CD43	PerCP	1:200	
Intracellular	anti-mouse IFNγ	FITC	1:200	FACS buffer II
	anti-mouse IL-2	PE	1:200	
	anti-mouse TNFα	APC	1:200	

Tab. 4.7 CD107a degranulation assay of murine splenocytes

Staining	Antibody	Fluorochrome	Dilution	Buffer
Extracellular	anti-mouse CD107a	FITC	1:200	RPMI 1640 medium
	anti-mouse CD8	PE	1:200	FACS buffer I
	7AAD	-	2µl/sample	
Intracellular	anti-mouse IFNγ	APC	1:200	FACS buffer II

Tab. 4.8 CD107a degranulation assay of woodchucks PBMCs

Staining	Antibody	Fluorochrome	Dilution	Buffer
Extracellular	anti-mouse CD107a	FITC	1:100	AIM-V medium
	anti-human CD4	APC	1:200	FACS buffer I
	7AAD	-	2µl/sample	
Intracellular	rabbit anti-human CD3	-	1:150	FACS buffer III
	anti-rabbit IgG	PE	1:250	

4.10 Proliferation assay of woodchuck PBMCs

After 5 days *in vitro* stimulation of woodchuck PBMCs with WHcAg- and WHsAg-derived peptides (section 4.8.2), cells were labelled with 1 µCi of 2[^{3}H]-adenine for 16 h and transferred to glass fibre filters (Packard) using a cell harvester. Membranes were placed into 96-well TopSeal-A microplates and 20 µl of scintillator was added to every well. The 2[^{3}H]-adenine absorption by dividing cells was measured by Top Count NXT counter. Results for triplicate cultures are presented as a mean stimulation index (SI). The SI value was calculated using the formula:

$$SI = \frac{mean\ total\ absorption\ for\ stimulated\ PBMCs}{mean\ total\ absorption\ for\ unstimulated\ control}$$

The SI ≥2,7 was considered significant.

4.11 In vivo cytotoxicity assay

The assay allows to evaluate the CTLs effector function *in vivo* in three groups of vaccinated mice: mice immunized for 3 times with pCGWHc plasmid, mice immunized twice with pCGWHc plasmid and boosted with Ad5WHc and mice immunized twice with “empty” pCG and boosted with Ad5GFP as controls. The immunization protocol is described in section 4.4.3.2. Eight days after the last immunization, the *in vivo* cytotoxicity assay was performed.

Lymphocytes were isolated from spleens and lymph nodes of naïve C57BL/6 mice. Single-cell suspensions were prepared using a 70 µm nylon cell strainer and the cells

were washed with 50 ml of sterile PBS. Mononuclear cells from the spleens were separated additionally by Percoll density gradient centrifugation. Splenocytes were suspended in 20 ml of RPMI 1640 medium supplemented with 10% FCS and 10U/ml penicillin-streptomycin and slowly overlaid on a 20 ml Percoll layer in 50 ml Falcon tube. After centrifugation (300× g, 10 min, without a brake) the lymphocytes-containing middle layer were transferred to the fresh tube. Subsequently, cells were washed twice in 50 ml of sterile PBS. Cell suspensions from the spleens and lymph nodes were mixed together and divided in equal volume of 15 ml of medium into two tubes. The cells in one tube were loaded with 1 µM of WHcAg-specific epitope c13-21 (YQLLNFLPL) for 2 h at 37°C and afterwards stained with 36 nM CFSE (*carboxyfluorescein succinimidyl ester*) dye for 10 min at 37°C (target cells). The unloaded cells were stained with 9 nM CFSE, and served as a reference. The difference in the CFSE concentration allows to distinguish between the target and reference cell populations as well as the recipient cells during the FACS analysis. Peptide loaded and unloaded cells were counted using Trypan blue exclusion microscopy and suspended in sterile PBS in 1:1 ratio. Cells (2×10^7 of each population per mouse) were injected intravenously into immunized mice and naïve mice as a reference. After 8 hours, recipient mice were sacrificed and single-cell suspensions of the splenocytes were prepared (section 4.5). Up to 1×10^8 cells were suspended in 500 µl of FACS buffer and analyzed by flow cytometry. The percent killing was calculated as follows:

$$killing = 100 - \frac{\frac{number\ of\ peptide\ loaded\ cells\ detected\ for\ immunized\ mice}{number\ of\ unloaded\ cells\ detected\ for\ immunized\ mice}}{\frac{number\ of\ peptide\ loaded\ cells\ detected\ for\ naive\ mice}{number\ of\ unloaded\ cells\ detected\ for\ naive\ mice}} \times 100$$

4.12 Detection of WHV-specific antibodies in mouse and woodchuck serum

WHV-specific antibodies were detected by enzyme-linked immunosorbent assay (ELISA). For that, 96-well immunoplates (NUNC) were coated with 10 µg/ml of WHcAg or 0,2 µg/ml of WHsAg diluted in carbonate buffer (50 µl of the antigen solution per well) and incubated for 1 h at 37°C. Plates were washed four times with 200 µl of T-PBS. Unspecific binding of the serum components was avoided by

blocking with 5%FCS in PBS. Plates were incubated for 1 h at 37°C and afterwards washed four times with 200 µl of T-PBS. Murine sera were diluted 1:250; 1:1000 or 1:5000 in 100 µl PBS and incubated on the plates for 1 h at 37°C. Alternatively, woodchuck sera were diluted 1:10 in 100 µl PBS. Plates were incubated for 1 h at 37°C and afterwards washed four times with 200 µl of T-PBS. Detection of the murine WHV-specific IgG, IgG_1 or IgG_{2a} antibodies was performed using peroxidase-conjugated anti-mouse IgG, IgG_1 or IgG_{2a} secondary antibodies diluted 1:1000 in 100 µl of PBS per well, respectively. Woodchuck WHcAg- or WHsAg-specific antibodies were detected using peroxidase-conjugated protein G diluted 1:500 in 100 µl of PBS per well. Plates were incubated for 1 h at 37°C and washed four times with 200 µl of T-PBS. After the final washing step, 100 µl of OPD substrate solution was added to each well. The plates were incubated in the dark for 15 min and the reaction was stopped by adding 100 µl of Stop solution (concentrated H_2SO_4). Finally the OD_{490nm} was measured using an Elisa Reader.

4.13 Detection of WHV DNA in the serum

4.13.1 Extraction of WHV DNA from the serum

Viral DNA from serum samples obtained from woodchucks and 1217 WHV Tg mice was extracted using QIAamp DNA Mini Kit (Qiagen) according to the manufacturer's protocol. Extraction was performed on 100 µl serum samples from woodchucks and 50-200 µl serum samples for 1217 WHV Tg mice.

4.13.2 Detection of WHV DNA in the serum by standard PCR

WHV DNA was detected by PCR using GoTaq polymerase (Promega) and the WHc-specific primers wc1 and wc2 (Materials section, Tab. 3.5). The compounds of the reaction mixture are presented in table 4.9. Conditions of the PCR reaction were as described previously (Tab. 4.2). The annealing of the primers was carried out at 50°C.

Tab. 4.9 The reaction mixture of WHV standard PCR

Reagent	Concentration	Volume [µl]
5x Reaction Buffer with $MgCl_2$	1×	10
dNTP-Mix	0,2 mM	1
wc1 / wc2 primers	1 µM	each: 5
GoTaq Polymerase	0,5 U	0,25
H_2O	-	23,75
DNA	-	5
		total: 50

4.13.3 Quantification of WHV DNA in the serum

WHV DNA was quantified by real-time PCR using a LightCycler 2.0 (Roche). The reaction was prepared using Platinum SYBR Green Kit (Invitrogen) and the WHc-specific primers wc1 and wc149s (Materials section, Tab. 3.5). The compounds of the reaction mixture and the PCR reaction conditions are presented in tables 4.10 and 4.11, respectively.

Tab. 4.10 The reaction mixture of WHV real-time PCR

Reagent	Concentration	Volume [µl]
Mastermix with $MgCl_2$	1×	10
$MgCl_2$	total: 5 mM	0,8
BSA (10×)	1×	1
wc1 / wc149s primers	32 nM	each: 0,4
H_2O	-	5,4
DNA	-	2
		total: 20

Tab. 4.11 The PCR conditions of WHV real-time PCR

PCR step	Temperature [°C]	Time [s]	Temperature changing rate [°C/s]	Number of cycles
Denaturation	50	120	20	1
	95	120	20	
PCR	94	15	20	40
	60	30	20	
	72	10	2	
Melting curve	95	0	20	1
	63	15	20	
	95	0	0,1	

Quantification of the C_T values and WHV copy number per reaction (according to the standard curve) was performed using LightCycler Software 3.5.3. A plasmid containing a full-length WHV genome served as a standard. The quantification of the viral load (WHV GE per ml of serum) was performed according to the formula:

$$viral\ load\ /\ ml = [\frac{viral\ load\ \ per\ reaction}{volume\,(ml)\,of\ \ DNA\ per\ reaction}] \times [\frac{volume\,(ml)\,of\ \ buffer\ used\ \ for\ elution}{volume\,(ml)\,of\ \ serum\ used\ \ for\ extraction}]$$

The detection limit of this assay is 10^3 WHV GE per ml of serum.

4.13.4 Detection of WHV DNA in the serum by a dot blot technique

The woodchuck sera (volume 5 µl) were spotted on Hybond-N+ nylon membrane. Serial dilutions of DNA sample with a known concentration were used as a standard (10^6 to 10^9 GE/ml). After drying, the DNA on the membrane was denaturated and fixed by incubation in denaturation, neutralization and 20× SSPE buffers (each 10 min, shaking) and UV crosslinking (150 J/cm^2). The WHV DNA was detected by hybridization with [^{32}P]-labelled plasmid containing the entire WHV strain 8 genome as a probe. The radioactive labelling of the probe was performed using DecaLabel DNA Labelling Kit (Fermentas), 50 ng of plasmid and [^{32}P]-dCTPs, according to the manufacturer's protocol. The probe was purified using MicroSpin columns and mixed with 100 µl of 10 mg/ml sonicated salmon sperm DNA. The membrane was incubated overnight at 65°C with [^{32}P]-labelled probe in RapidHyb Buffer (GE Healthcare). The membrane was washed twice for 15 min at room temperature with washing buffer I, once for 20 min at 65°C with washing buffer II (Materials, section 3.10) and left to dry. The membrane was exposed overnight on the phospho-screen

and the image was acquired using Cyclone phospho-imager. The detection limit of this assay is approximately 5×10^7 WHV GE per ml of serum.

4.14 Detection of WHV replication in the liver

4.14.1 Extraction of DNA

Viral DNA from the woodchucks' liver samples was extracted using QIAamp DNA Mini Kit (Qiagen) according to the manufacturer's protocol. Liver samples were homogenized in liquid nitrogen and extraction was performed from approximately 50 mg of the tissue (2 columns per sample). The DNA concentration was quantified by spectrophotometric OD_{260nm} measurement (section 4.1.8).

4.14.2 Southern blot

Approximately 10 µg of the DNA samples was separated by agarose gel electrophoresis. Next, the DNA was denaturated by incubation in: 0,25 M HCl, denaturation and neutralization buffers (each 30 min, shaking). The DNA was transferred to Hybond-N+ nylon membrane using Vaccum blotter 785 (BioRad) by 13 Hg pressure for 2 h in 20× SSC buffer and afterwards fixed by UV crosslinking (150 J/cm^2). The WHV DNA was detected by hybridization with [^{32}P]-labelled plasmid containing the entire WHV strain 8 genome as a probe as described in section 4.13.4.

4.15 Evaluation of serum GOT levels

The glutamic oxaloacetic transaminase (GOT; also known as *aspartate transaminase*, AST) levels in the woodchuck sera were quantified using the standard diagnostic procedure at Zentrallabor (Universitätsklinikum Essen).

4.16 Statistical analysis

Statistical analyses were performed using Graph Pad Prism software version 5. Statistical differences (*p*-value) were analyzed by unpaired Student *t* test and Wilcoxon signed rank test. The *p*-values < 0,05 were considered significant.

5 Results

5.1 Identification of CD8⁺ epitopes of WHcAg in C57BL/6 mice

The scope of this work was to choose, improve and optimize the best vaccination strategy to induce a potent T cell response in chronically WHV infected woodchucks. To this purpose, vaccines expressing WHcAg were used. The various immunization protocols of preliminary experiments were performed in C57BL/6 mice in order to obtain the effective and economically beneficial model. Before analyzing the $CD8^+$ T cell response, knowledge about $CD8^+$ T cell epitopes in the antigen is required to prove the effectiveness of any immunization strategy. The first step was to characterize H-2^b-restricted epitopes within the WHcAg since they had not been identified yet.

For this purpose, C57BL/6 mice were immunized two or three times with plasmid DNA vaccines encoding complete WHcAg sequence and sacrificed two weeks after the last immunization. Isolated splenocytes were stimulated *in vitro* in the presence of 6 peptide pools, containing 6 overlapping by 10 amino acid residues 15-mer synthetic peptides, spanning the whole WHcAg sequence of WHV strain 8 (Fig. 5.1). After 7 days of culture, cells were restimulated for 6h and intracellular staining for IFNγ was performed as mentioned in the Methods section (4.9.1).

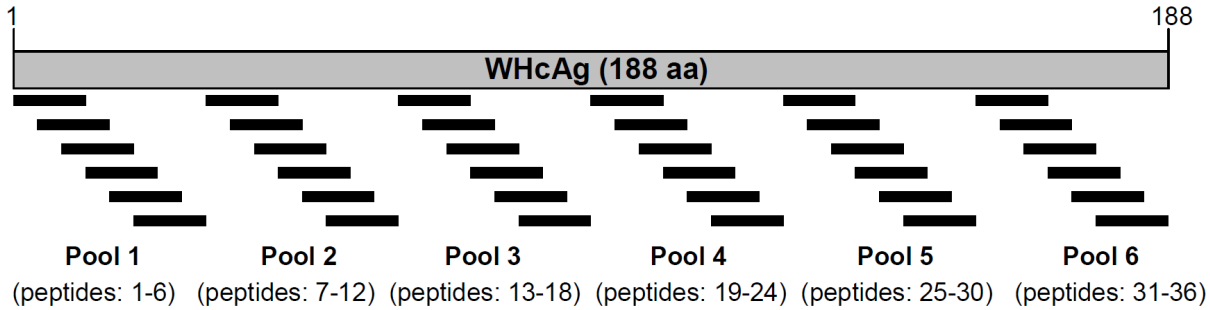

Fig. 5.1 Schematic illustration of WHcAg peptide pools used for stimulation of murine splenocytes

Thirty-six synthetic peptides covering the sequence of the WHcAg of WHV strain 8 were merged into six pools containing six peptides each.

Detection of intracellular IFNγ in splenocytes from C57BL/6 mice stimulated with WHcAg-derived peptide pools demonstrated $CD8^+$ T cell response directed against pool 1, containing peptides 1-6 (covering aa 1 to 40 of WHcAg) and pool 3, containing peptides 13-18 (aa: 61-100), as shown in Fig. 5.2.

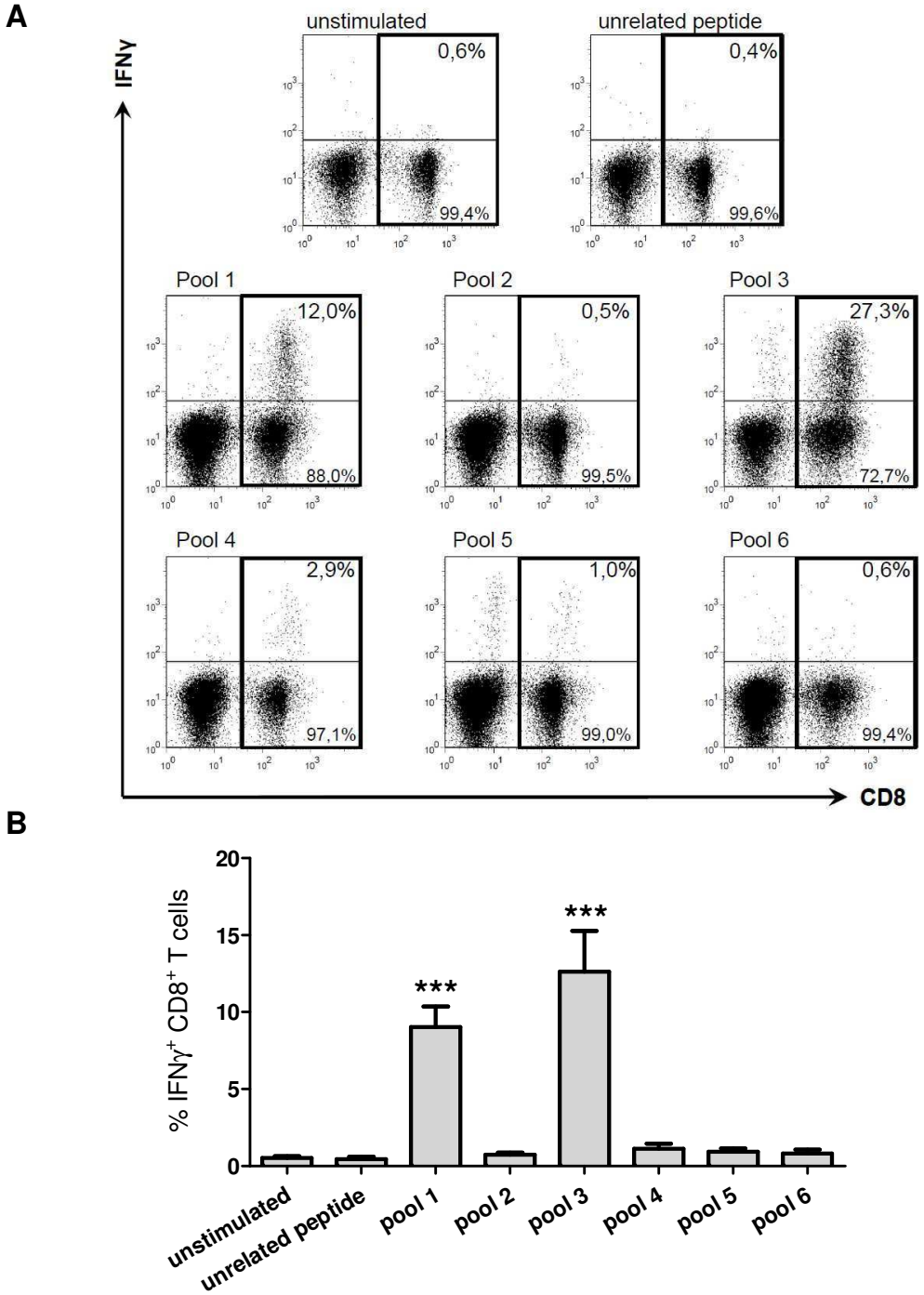

Fig. 5.2 Determination of CD8$^+$ T cell responses in mouse splenocytes after stimulation with WHcAg-derived peptide pools

A. Representative dotplots of splenocytes from C57BL/6 mouse immunized 3 times with DNA plasmid expressing WHcAg. Cells were expanded *in vitro* for 7 days in the presence of 6 WHcAg-derived peptide pools. CD8$^+$ T cell response was evaluated by intracellular IFNγ staining. Presented values indicate the percentage of IFNγ$^+$ CD8$^+$ T cells in the CD8$^+$ T cell population. Unstimulated cells and cells stimulated with unrelated CMV-derived peptide served as negative controls.

B. CD8$^+$ T cell response in murine splenocytes stimulated with WHcAg-derived peptide pools. Bars represent the mean value obtained from ten DNA-immunized C57BL/6 mice including SEM (standard error of the mean). The statistical analysis between the groups was performed using the unpaired Student *t* test. Asterisks mark the significant difference (*** < 0,0005)

The percentages of IFNγ$^+$ CD8$^+$ T cells detected in ten mice after stimulation with WHcAg-derived peptide pool 1 and 3 ranged between 5,7% – 17,9% (mean: 9,0%) and 4,0% – 27,3% (mean: 12,6%), respectively. CD8$^+$ T cell response detected against peptide pool 1 and 3 were significantly higher than the background values of 0,2% - 1,2% in unstimulated controls (P < 0,0005). Stimulation of splenocytes with WHcAg-derived peptide pools 2, 4, 5 and 6 did not lead to significant responses as compared to negative controls (Fig. 5.2B).

For identification of CD8$^+$ T cell epitopes within positive WHcAg-derived pools, splenocytes from DNA–immunized C57BL/6 mice were stimulated for 7 days with 12 individual 15-mer peptides contained by pools 1 and 3. Stimulation of splenocytes with WHcAg-derived peptides 1 to 6 (p1-p6, pool 1) showed that peptides accountable for the IFNγ response detected in pool 1 are peptides 2 (c6-20) and 3 (c11-25). Stimulation with the other peptides of this pool (c1-15 and c16-30 to c26-40) induced no response (Fig. 5.3A). In contrast, stimulation with individual peptides from WHcAg-derived peptide pool 3 (peptides 13 to 18) pointed to only one positive peptide – peptide 18 (c86-100) - whereas other peptides (c61-75 to c81-95) remained negative after 7 days of stimulation (Fig. 5.3B). As shown in Fig. 5.4, the mean frequency of IFNγ$^+$ CD8$^+$ T cells in the CD8$^+$ T cell population as measured in splenocytes of ten DNA–immunized mice was the highest after stimulation with peptide 2 (c6-20): 29,1%. The mean response detected for stimulation with peptide 3 (c11-25) was 8,9% and for peptide 18 (c86-100) 16,8%. CD8$^+$ T cell response detected against peptides 2, 3 and 18 were significantly higher than the background values in negative controls (P < 0,0005).

It is known that murine MHC class I molecules bind peptides that are from 8 to 9 amino acid long [*Falk et al., 1991*]. In these experiments 15-mer peptides which are overlapped by 10 aa residues were used for stimulation of splenocytes. Thus, the obtained results indicated the presence of two H-2^b-restricted epitopes within WHcAg: firstly within the overlapping sequence of peptides 2 and 3 (aa 6 to 25), and secondly within the sequence covered by peptide 18 (aa 86 to 100). To test this hypothesis splenocytes of mice that had been immunized with DNA plasmid encoding WHcAg, were stimulated for 7 days with peptide 2 or 18 and then restimulated for 6h with shorter, overlapping by 8aa residues 9-mer peptides covering

the sequence of WHcAg from aa 7 to 22 and 86 to 100, as described in the Methods section (4.6.1 and 4.6.2).

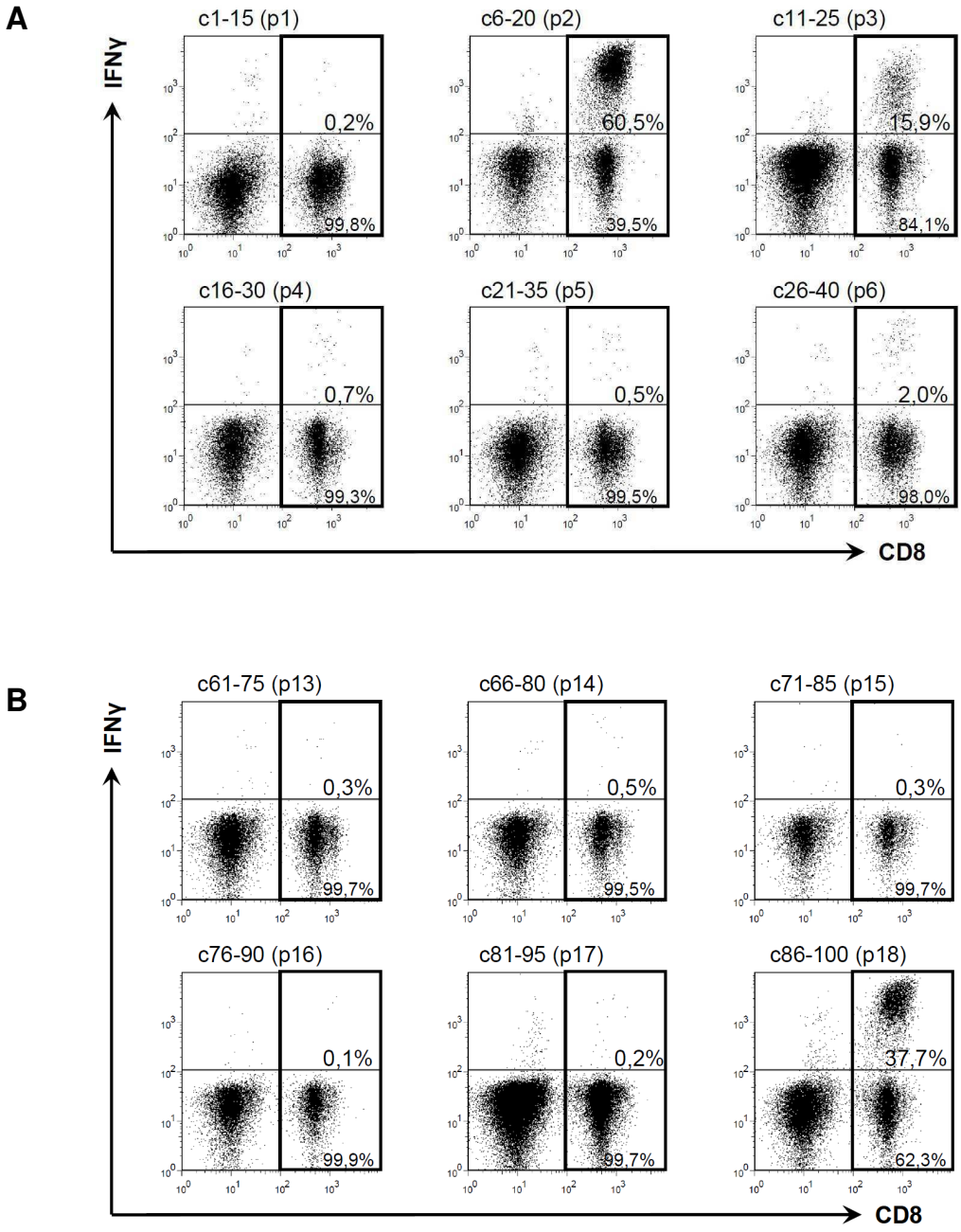

Fig. 5.3 Representative dotplots of mouse splenocytes after stimulation with individual peptides from WHcAg – derived pools 1 and 3

Splenocytes were expanded *in vitro* for 7 days in the presence of 12 individual peptides from positive WHcAg-derived pools 1 and 3. $CD8^+$ T cell response was evaluated by intracellular IFNγ staining. Presented values indicate the percentage of $IFN\gamma^+$ $CD8^+$ T cells in the $CD8^+$ T cell population.

A. Representative dotplots of splenocytes stimulated with individual peptides 1 to 6 (p1-p6) from pool 1 (c1-15 to c26-40).

B. Representative dotplots of splenocytes stimulated with individual peptides 13 to 18 (p13-p18) from pool 3 (c61-75 to c86-100).

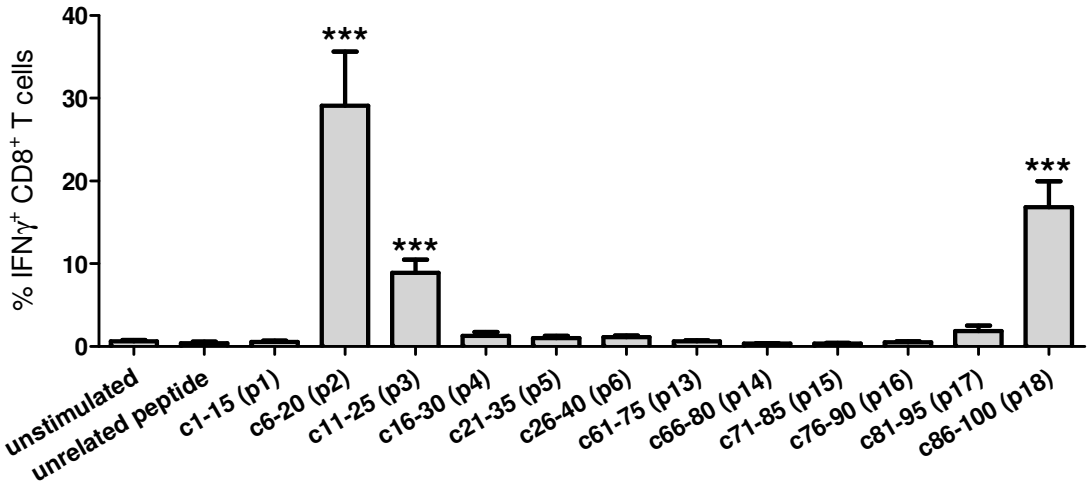

Fig. 5.4 CD8⁺ T cell response in mouse splenocytes after stimulation with individual peptides from WHcAg – derived pools 1 and 3

Splenocytes from C57BL/6 mice immunized with DNA plasmid expressing WHcAg were expanded *in vitro* for 7 days in the presence of 12 individual peptides from positive WHcAg-derived pools 1 and 3. Unstimulated cells and cells stimulated with unrelated CMV-derived peptide served as negative controls. The bars represent the mean value obtained from ten DNA-immunized mice including SEM. The statistical analysis was performed using the unpaired Student *t* test. Asterisks mark the significant difference (*** < 0,0005).

Restimulation of splenocytes with 9-mer peptides covering the sequence of WHcAg from aa 7 to 22, previously expanded for 7 days *in vitro* in the presence of peptide 2, allowed to identify H-2^b-restricted epitope (Fig. 5.5A). All ten analysed mice showed a robust IFNγ response after restimulation with peptide c13-21 (aa sequence: YQLLNFLPL), ranging from 14,5% to 57,5% (mean: 33%) of IFNγ⁺ CD8⁺ T cells. This result is significantly higher than the background of 0,2% - 1,5% detected in not-restimulated controls ($P < 0,0005$). Restimulation of the splenocytes with other tested 9-mer peptides (c7-15 to c12-20 and c14-22) induced no IFNγ response (Fig. 5.5B). Screening with 9-mer peptides covering the sequence of WHcAg from aa 86 to 100, after culturing of splenocytes with p18, pointed out the peptide c86-100 (aa sequence: VNHVNDTWG) to be the second CD8⁺ T cell epitope within WHcAg (Fig. 5.6A). The percentages of IFNγ⁺ CD8⁺ T cells detected in seven responding mice after stimulation with c86-94 ranged between 10,0% - 74,3% (mean: 28%). As Fig. 5.6B shows, there was an increased background of IFNγ⁺ CD8⁺ T cells in the not-restimulated control (mean 3,9%), as well as in other 9-mer peptides (mean 3,6% - 4,4%). Nevertheless, CD8⁺ T cell response detected against c86-94 was significantly higher than the background values ($P < 0,005$).

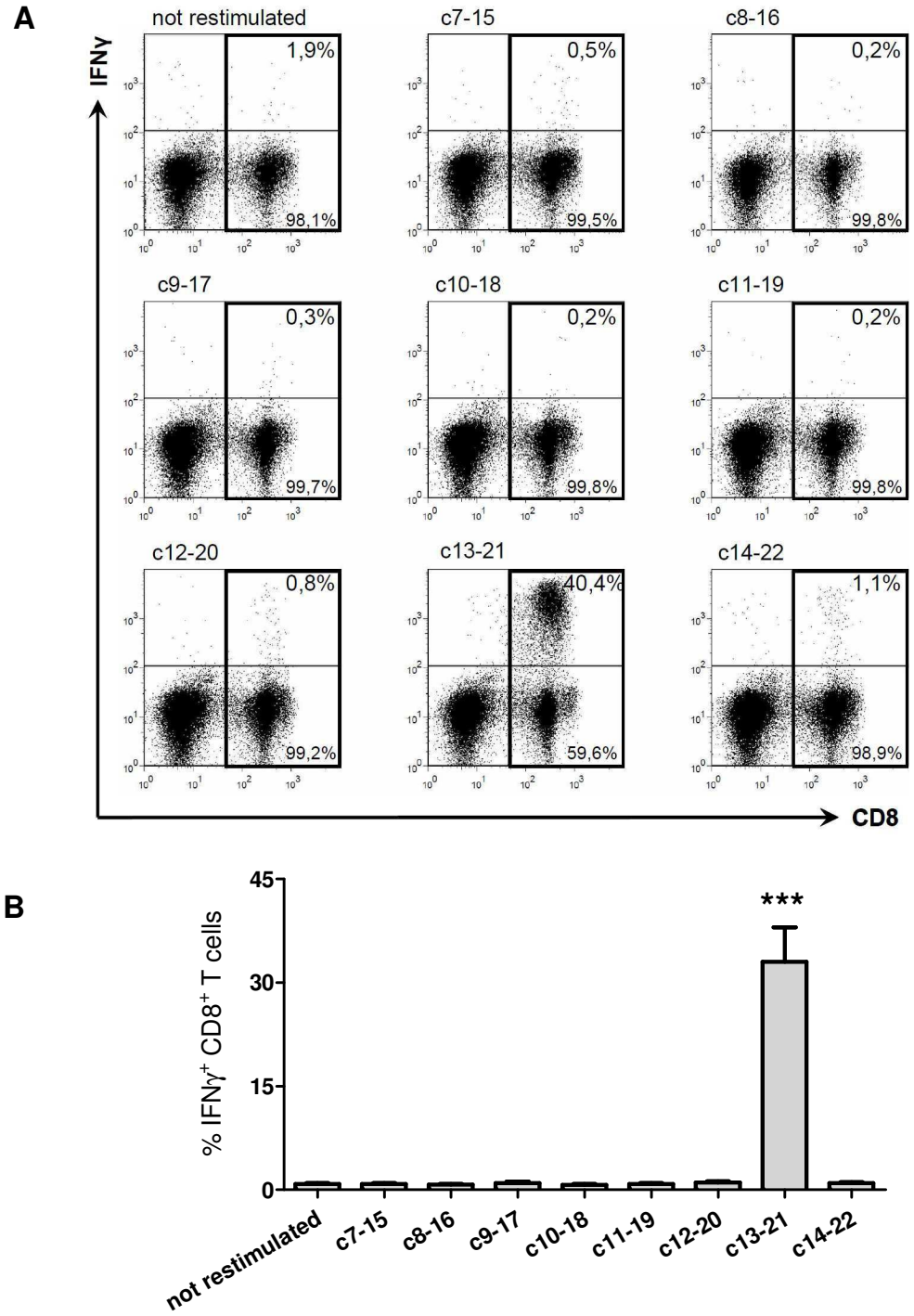

Fig. 5.5 Finemapping of CD8$^+$ T cell epitope within WHcAg sequence aa 7-22

A. Representative dotplots of splenocytes from C57BL/6 mouse immunized with DNA plasmid expressing WHcAg. Cells were expanded *in vitro* for 7 days in the presence of peptide 2 and then restimulated for 6h with eight overlapping 9-mer peptides covering the sequence of WHcAg from aa 7 to 22. CD8$^+$ T cell response was evaluated by intracellular IFNγ staining. Presented values indicate the percentage of IFNγ$^+$ CD8$^+$ T cells in the CD8$^+$ T cell population. Not-restimulated cells served as a negative control.

B. CD8$^+$ T cell response in murine splenocytes restimulated with 9-mers covering the sequence of WHcAg from aa 7 to 22. Bars represent the mean value obtained from ten DNA-immunized C57BL/6 mice including SEM. The statistical analysis between the groups was performed using the unpaired Student *t* test. Asterisks mark the significant difference (*** < 0,0005).

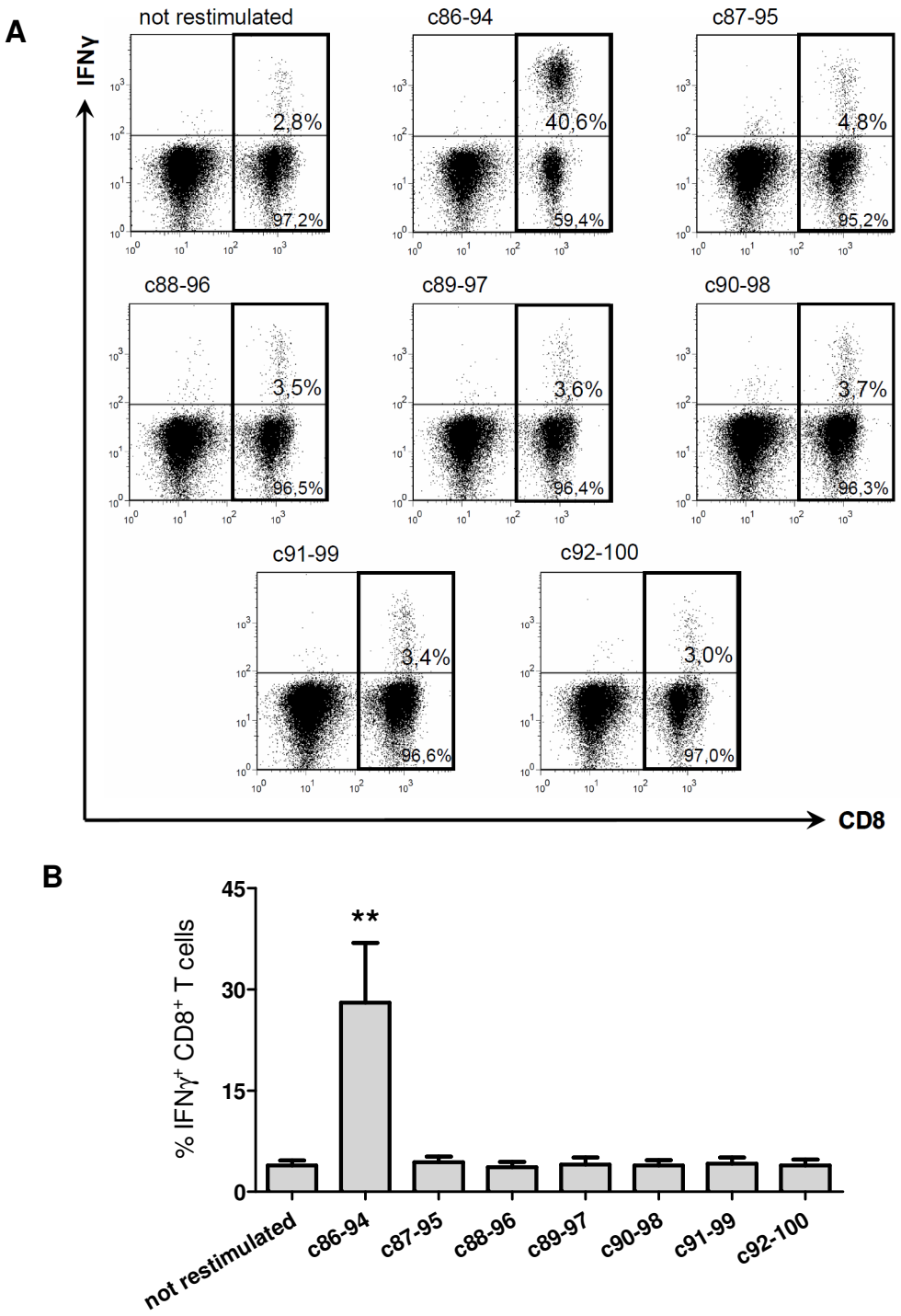

Fig. 5.6 Finemapping of CD8⁺ T cell epitope within WHcAg sequence aa 86-100

A. Representative dotplots of splenocytes from C57BL/6 mouse immunized with DNA plasmid expressing WHcAg. Cells were expanded *in vitro* for 7 days in the presence of peptide 18 and then restimulated for 6h with seven overlapping 9-mer peptides covering the sequence of WHcAg from aa 86 to 100. $CD8^+$ T cell response was evaluated by intracellular IFNγ staining. Presented values indicate the percentage of $IFN\gamma^+$ $CD8^+$ T cells in the $CD8^+$ T cell population. Not-restimulated cells served as a negative control.

B. $CD8^+$ T cell response in murine splenocytes restimulated with 9-mers covering WHcAg sequence from aa 86 to 100. Bars represent the mean value obtained from seven responding DNA-immunized mice including SEM. The statistical analysis between the groups was performed using the unpaired Student *t* test. Asterisks mark the significant difference (** < 0,005).

The position of the identified CD8$^+$ T cell epitopes in C57BL/6 mice (haplotype H-2^b) within WHcAg sequence is schematically illustrated in Fig. 5.7.

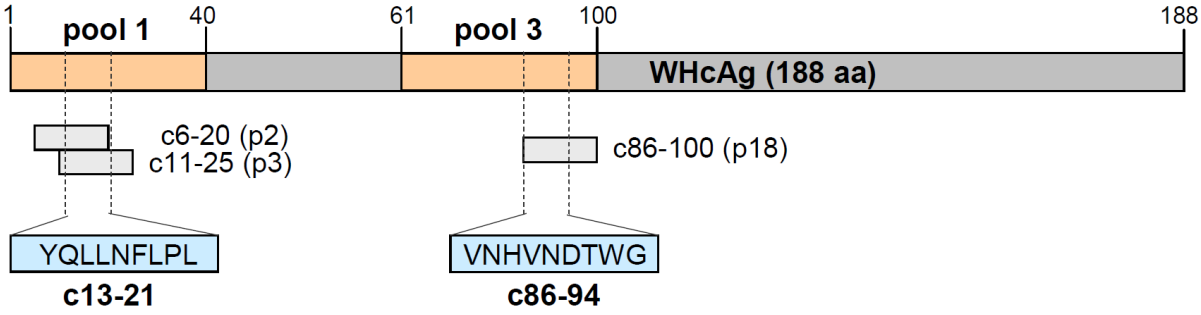

Fig. 5.7 The position of H-2^b restricted CD8$^+$ T cell epitopes within WHcAg
C57BL/6 mice were immunized with WHcAg-expressing plasmid. Two weeks after the last immunization CD8$^+$ T cell response was evaluated by intracellular IFNγ staining. At the beginning, the splenocytes were stimulated *in vitro* for 7 days with 6 pools containing 6 overlapping 15-mer peptides covering the sequence of the whole WHcAg. The positions of positive pools 1 (aa 1-40) and 3 (aa 61-100) are marked schematically as orange boxes on the WHcAg sequence. Stimulation of the splenocytes with individual peptides from pool 1 and 3 determined the 15-mer epitopes' sequences: peptides c6-20 and c11-25 within pool 1 and peptide c86-94 within pool 3 (marked as grey boxes). Finemapping with overlapping 9-mer peptides pointed out the exact epitopes' positions: c13-21 and c86-94 (aa sequences are given in blue boxes). Amino acid sequences of all peptides which were used for splenocytes stimulation are presented in the Appendix (Tab. 10.1 and Tab. 10.2).

In silico prediction of MHC class I-restricted epitopes of WHcAg for D and K loci of the mouse haplotype H-2^b was performed by using two independent algorithms: SYFPEITHI [*Rammensee et al., 1999;* http://www.syfpeithi.de/] and Bioinformatics and Molecular Analysis Section (BIMAS) MHC peptide binding prediction programme [*Parker et al., 1994*; http://bimas.cit.nih.gov/molbio/hla_bind/].

The list of the 8-10 aa in length peptides that obtained the highest scores is presented in table 5.1. Both algorithms assigned the best score for H2-D^b–restricted nonamer c13-21. This outcome correlated with the results of *in vivo* studies, as the peptide c13-21 was identified as the CD8$^+$ epitope within the WHcAg in C57BL/6 mice. The second *in vivo* identified peptide c86-94 obtained the best score as H2-D^b–restricted decamer (c86-95) by SYFPEITHI algorithm. On the contrary, the BIMAS programme indicated peptide c23-32 as the second best H2-D^b–restricted decamer (after c12-21) and assigned the c86-95 a low score. The prediction of H2-K^b–restricted peptides typed a CD8$^+$ H2-K^b–restricted epitope sequence between 7th and 16th aminoacid of WHcAg. However, *in vivo* experiments with nonamers c7-15 or c8-16 did not result in the detection of the WHcAg-specific CD8$^+$ T cell response in

murine splenocytes after stimulation with those peptides. Correlation between the results obtained in mice and *in silico* confirm the usefulness of MHC class I epitope prediction softwares in the identification of epitopes.

Tab. 5.1 The list of WHcAg predicted CD8$^+$ epitopes for C57BL/6 mice (haplotype H-2^b) using SYFPEITHI and BIMAS algorithms with scores

Position	Length	Sequence	Score	H-2^b restriction	Programme
13-21	9	Y Q L L N F L P L	24	D^b	
86-95	10	V N H V N D T W G L	23	D^b	SYFPEITHI
9-16	8	F G S S Y Q L L	21	K^b	
13-21	9	Y Q L L N F L P L	720.000	D^b	
23-32	10	F F P D I N A L V D	33.000	D^b	
86-95	10	V N H V N D T W G L	2.640	D^b	BIMAS
8-16	9	E F G S S Y Q L L	24.000	K^b	
7-16	10	K E F G S S Y Q L L	48.000	K^b	

5.2 Construction of a DNA vaccine with optimized expression of WHcAg

Several studies indicate that protein expression levels can be increased by the insertion of an intron sequences into the expression vectors [*Hermering et al., 2004; Sakurai et al., 2004; Li et al., 2005*]. The presence of an intron sequence protects mRNA molecules from degradation and facilitates their export into the cytoplasm [*Kurachi et al., 1995; Luo et al., 1999*]. Those factors result in a more efficient translation process and, as a consequence, increased gene expression. The improvement in the antigen expression may lead to a better presentation of the antigen and induction of a more robust and multifunctional immune response *in vivo*. To test this hypothesis a novel DNA plasmid (pCGWHc), encoding a β-globin intron sequence between the CMV promoter and WHcAg gene was constructed. The WHV strain 8 core protein gene was obtained from WHcAg-encoding pWHcIm plasmid. The pWHcIm plasmid was previously used as a DNA vaccine and proved to induce anti-WHc antibodies in mice [*Lu et al., 1999*]. Moreover, it provided protection against

infection after WHV challenge in woodchucks [*Lu et al., 1999*] and was investigated as a therapeutic vaccine in WHV chronic carriers [*Lu et al., 2008*].

WHcAg insert was cut out of the pWHclm plasmid by using *BamHI* and *XbaI* restriction enzymes and then introduced into *BamHI/XbaI* site of pCG vector (Fig. 5.8A). The successful insertion of WHcAg into pCG plasmid was proved by *BamHI/XbaI* restriction digestion. The characteristic band of 675 bp, corresponding to WHcAg insert, was visualized on the agarose gel (Fig. 5.8B). Additionally, the sequence of pCGWHc plasmid was verified by DNA sequencing. The map of the pCGWHc plasmid is attached in the Appendix section (Fig. 10.2).

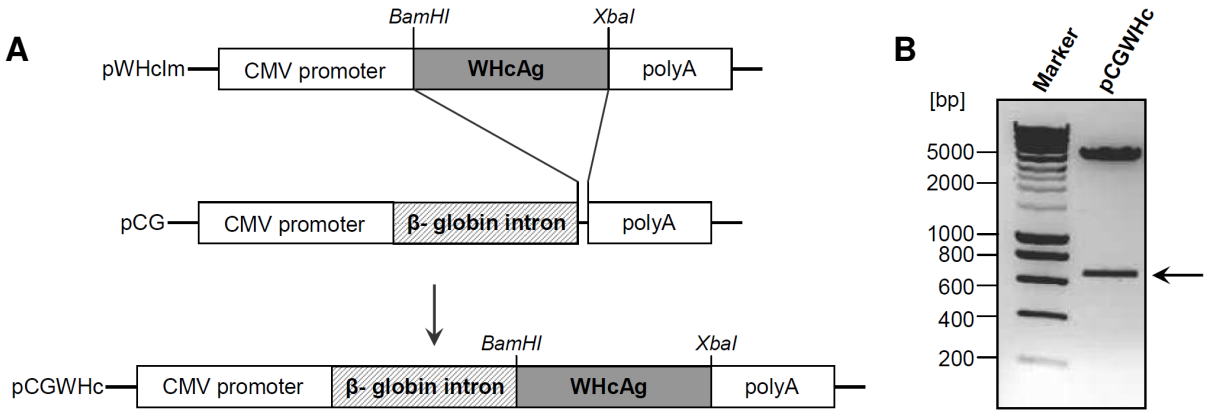

Fig. 5.8 Scheme of the cloning strategy of pCGWHc plasmid (A). Control restriction digestion of pCGWHc (B)

1 µg of DNA was digested with *BamHI* and *XbaI* restriction enzymes for 1h in 37°C and visualized on 1,5% agarose gel containing 0.5 µg/ml ethidium bromide. The arrow indicates a band of 675 bp corresponding to WHcAg insert.

To confirm the expression of WHcAg by the pCGWHc plasmid, BHK cells were transiently transfected with pCGWHc and pWHclm, that lacks the β-globin intron sequence, as a control. The levels of the protein expression were compared by indirect immunofluorescence staining and Western blot analysis, using WHcAg-specific antibodies 24h after transfection, as mentioned in the Methods section (4.3.1). To estimate the variation in the total protein content of the cell lysates, the control β-actin immunoblotting was performed.

In vitro transfection studies confirmed an increased WHcAg expression by the novel pCGWHc plasmid, containing the β-globin intron in the expression cassette. The indirect immunofluorescence staining demonstrated a strong WHcAg-specific signal in BHK cells transfected with pCGWHc, in comparison to a poor level of the protein in

pWHcIm-transfected cells (Fig. 5.9A). No WHcAg-specific immunofluorescence staining was observed in mock cells treated with the transfection reagent only. Comparable results were obtained by the Western blot analysis. The level of WHcAg in cells transfected with pCGWHc was significantly higher, than in those transfected with pWHcIm. No significant difference in β-actin levels between the lysates was observed (Fig. 5.9B).

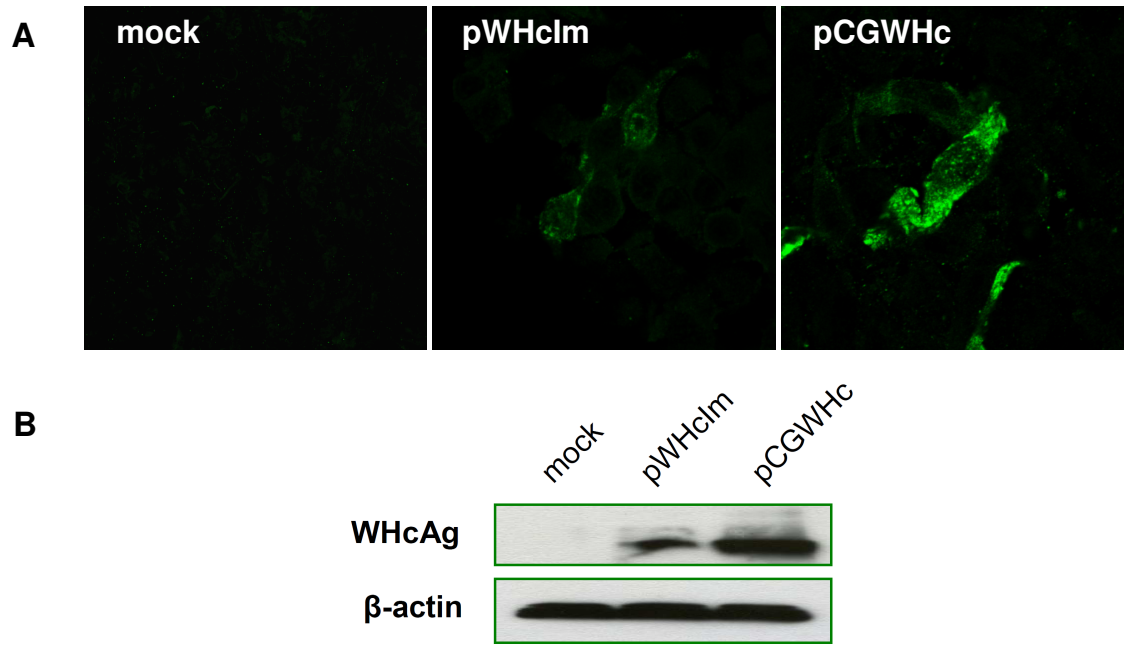

Fig. 5.9 Expression of WHcAg in BHK cells 24 h after transfection with pWHcIm and pCGWHc

A. BHK cells were transfected with 0,5 µg of plasmids using Effectene reagent. Cells were fixed with methanol and WHcAg was detected by indirect immunofluorescence staining with WHcAg-specific polyclonal rabbit antibody and a secondary FITC-coupled antibody.
B. BHK cells were transfected with 1 µg of plasmids using Lipofectamine reagent. Cell lysates were separated by SDS-PAGE and transferred to a PVDF-membrane. Detection was done with the WHcAg-specific mouse monoclonal antibody 6C5C8E4 or β-actin-specifc antibody and a secondary antibody coupled to peroxidase.

5.3 Improved WHcAg expression from pCGWHc plasmid induces stronger immune response in vivo

The expression level of WHcAg from novel pCGWHc plasmid proved to be significantly higher in comparison to pWHcIm plasmid that does not contain β-globin intron. To determine whether the improvement in the antigen expression may induce a more vigorous T cell response *in vivo*, a series of immunization with both plasmids were performed in mice (as described in detail in the Methods section 4.4.3.1). As

shown in Fig. 5.10, C57BL/6 mice were pretreated with cardiotoxin and one week later subsequently immunized for three times with pCGWHc or pWHcIm plasmids. Mice injected intramuscularly with PBS served as controls. Immunizations were performed in two week intervals. Two weeks after the last immunization the mice were sacrificed and splenectomy was performed.

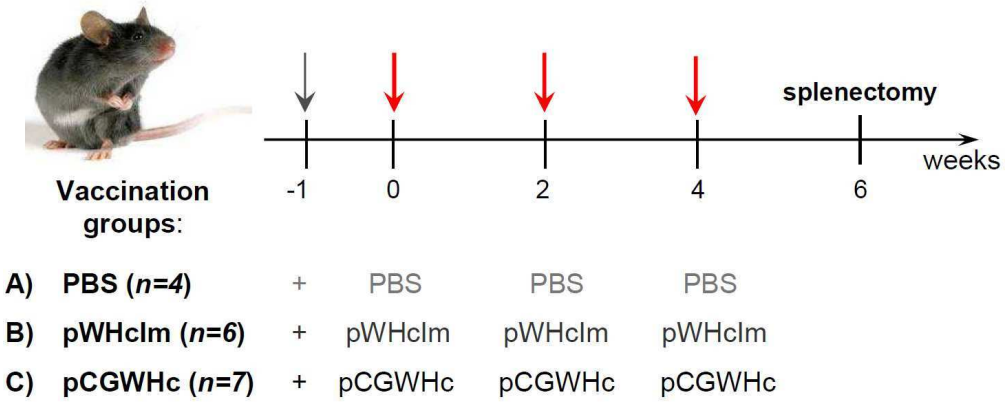

Fig. 5.10 Schedule of pCGWHc and pWHcIm immunization of C57BL/6 mice
Ten weeks old female C57BL/6 mice were pretreated with cardiotoxin (grey arrow) and one week later immunized subsequently 3 times with 100µg WHcAg-expressing plasmids intramuscularly in two weeks intervals (week 0, 2 and 4; indicated by red arrows). Six mice received pWHcIm plasmid, seven – pCGWHc plasmid and four mice were injected intramuscularly with 100µl of PBS and served as controls. Blood withdrawing was performed two weeks after each immunization (week 2, 4 and 6). Two weeks after the last immunization the mice were sacrificed and splenectomy was performed.

5.3.1 Evaluation of the humoral immune response

The improvement of immunization using the new construct was evaluated by detection of WHcAg-specific IgG antibodies (anti-WHc) in the serum of mice two weeks after each immunization by ELISA, as described in the Methods section (4.12). Evaluation of humoral immune response in mice showed that immunization with pCGWHc plasmid (high WHcAg expression) had induced significantly higher levels of anti-WHc than immunization with pWHcIm (low WHcAg expression). As shown in Fig. 5.11, single immunization with WHcAg-expressing DNA vaccines induced detectable amounts of WHcAg-specific IgG antibodies. The levels of anti-WHc increased significantly with the subsequent administration of the plasmids in both groups of mice ($P < 0{,}0005$). As expected, sera from mice injected with PBS solution as a control remained anti-WHc negative. Comparison of the antibodies levels between the groups of mice vaccinated with high-level expression plasmid pCGWHc and pWHcIm, just after one immunization, showed that pCGWHc

vaccination was able to induce anti-WHc more efficiently *in vivo*. The magnitude of humoral response induced by immunization with the pCGWHc plasmid was significantly higher ($P < 0,0005$) at every analysed time point, as compared to pWHcIm-vaccinated mice.

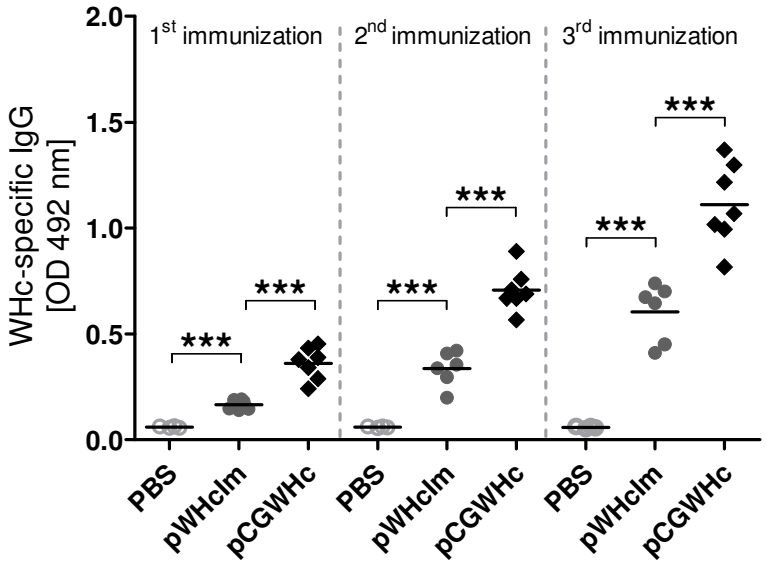

Fig. 5.11 Detection of WHcAg-specifc IgG antibodies in the sera of C57BL/6 mice after pCGWHc and pWHcIm immunization

Ten weeks old female C57BL/6 mice were immunized 3 times intramuscularly with 100µg of pWHcIm or pCGWHc plasmid at two week intervals. Four mice were injected intramuscularly with 100µl of PBS and served as controls. Sera of mice were obtained from blood samples collected two weeks after each immunization and diluted 1:1000 in PBS. WHcAg-specific ELISA was peformed using anti-mouse IgG antibody coupled to peroxidase. The statistical analysis between the groups was performed using the unpaired Student *t* test. Asterisks mark the significant difference (*** < 0,0005).

Isotype of IgG antibodies secreted by antigen-specific B cells can be regulated by subsets of $CD4^+$ helper T cells (T_H). Antigen-specific T_{H1} cells that produce IFNγ, TNFα and IL-2 enhance the secretion of IgG_{2a}, whereas IL-4-producing T_{H2} cells induce B cells to secrete IgG_1 [*Stevens et al., 1988*]. It is known, that intramuscular immunization with DNA plasmids predominantly induce T_{H1} type of immune response [*Siegel et al., 2001*]. To examine the breadth of the immune response induced by immunization with the novel pCGWHc and pWHcIm plasmids, the IgG_1 and IgG_{2a} isotypes of WHcAg-specific antibodies were analyzed in murine sera by ELISA.

As shown in Fig. 5.12, vaccinations with both plasmids expressing WHcAg induced predominantly IgG_{2a} isotype of anti-WHc from antigen-specific B cells. Already one immunization with pCGWHc induced detectable amounts of IgG_{2a} ($P < 0,0005$). By

contrast, the sera of mice immunized once with pWHcIm remained IgG_{2a} negative, demonstrating a similar quantity of WHcAg-specific IgG_{2a} as the PBS control group (Fig. 5.12A). The levels of IgG_{2a} was significantly higher in the group of mice immunized with pCGWHc as compared to the pWHcIm group after each immunization ($P < 0{,}0005$).

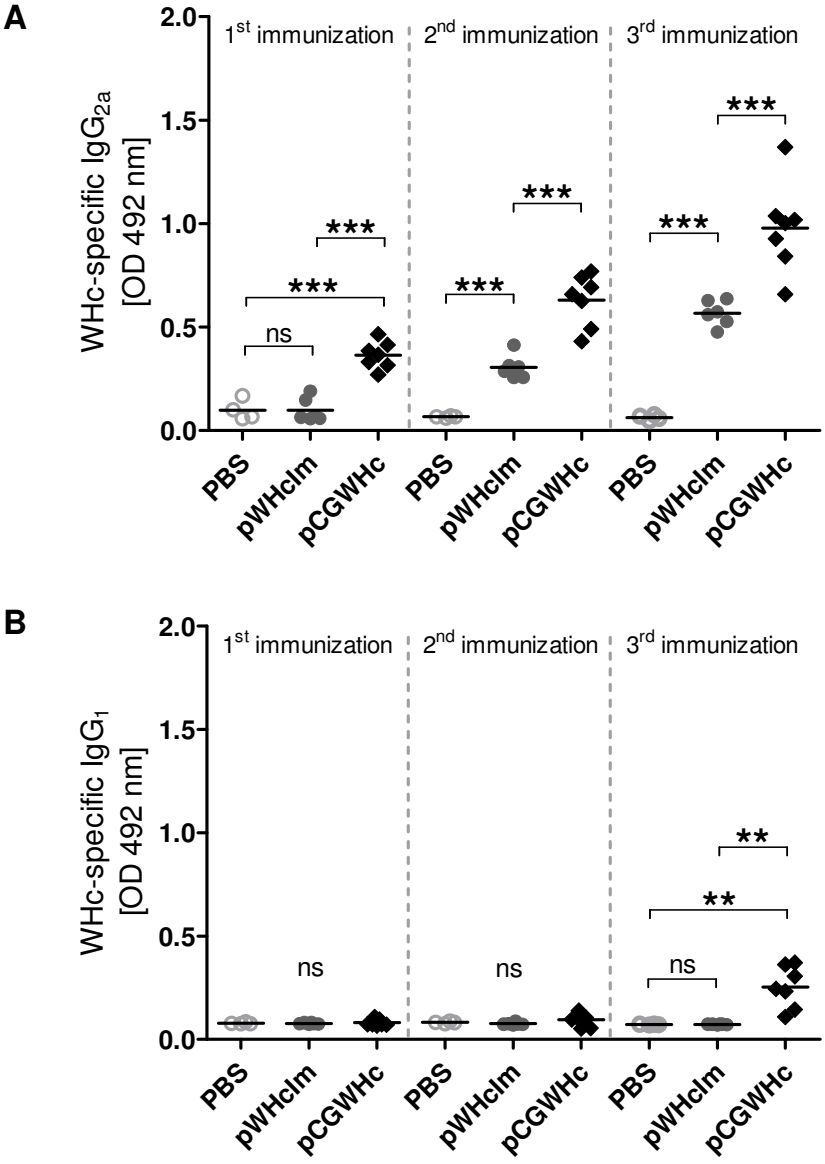

Fig. 5.12 Detection of WHcAg-specifc IgG isotypes: IgG2a (A) and IgG1 (B), in the sera of C57BL/6 mice after pCGWHc and pWHcIm immunization

Sera of mice were obtained from blood samples collected two weeks after each immunization and diluted 1:1000 in PBS. WHcAg-specific ELISA was performed using IgG isotype-specific (IgG_{2a} or IgG_1) anti-mouse antibodies coupled to peroxidase. The statistical analysis between the groups was performed using the unpaired Student *t* test. Asterisks mark the significant difference (** < 0,005; *** < 0,0005).

Detection of IgG_1 demonstrated that vaccination with pCGWHc is able to induce IgG_1 isotype of anti-WHc, however only at a low level (Fig. 5.12B). This result indicates that pCGWHc immunization induces a very strong and broad T_{H1} type of response. The levels of IgG_1 detected in the sera of mice after three immunizations with pCGWHc were significantly higher than background levels detectable in the sera from pWHcIm-immunized mice and PBS-injected mice ($P < 0,005$).

Detection of low level of IgG_1 accompanied by a high level of IgG_{2a} antibodies indicates that pCGWHc immunization induces a robust T_{H1} type of response, more vigorous than immunization with the pWHcIm plasmid.

5.3.2 Evaluation of the $CD8^+$ T cell response

Evaluation of WHcAg-specific $CD8^+$ T cell response induced in C57BL/6 mice by vaccination with pCGWHc or pWHcIm plasmid, was performed by intracellular IFNγ staining of splenocytes isolated two weeks after the third immunization. Splenocytes were stimulated *in vitro* in the presence of two previously identified $CD8^+$ T cell epitopes: c6-20 and c86-100. After 7 days of culturing, cells were restimulated for 6h with corresponding peptides and stained for IFNγ as mentioned in the Methods section (4.9.1). Splenocytes obtained from mice injected with PBS served as controls.

The percentages of $IFN\gamma^+$ $CD8^+$ T cells detected in the spleens of mice vaccinated with pCGWHc plasmid were considerably higher compared to those detected in the pWHcIm-immunized group (Fig. 5.13). IFNγ response after stimulation of splenocytes with WHcAg-derived 15-mer peptide c6-20 ranged between 43,4% – 74,2% (mean 57,4%) of $IFN\gamma^+$ $CD8^+$ T cells and 9,5% – 65,1% (mean 29,5%) in the pWHcIm group (Fig. 5.13B). The difference in the detected responses was statistically significant ($P < 0,005$). In addition, the mean percentage of $IFN\gamma^+$ $CD8^+$ T cells directed against peptide c86-100 in the pCGWHc-immunized group of mice was significantly higher (37,7%) than the value of 10,8% assessed for the pWHcIm group ($P < 0,0005$). Stimulation of splenocytes obtained from PBS-injected mice with the peptides c6-20 and c86-100 induced no IFNγ response. The responses to stimulation with WHcAg-derived epitopes measured in both plasmid-immunized groups of mice were significantly higher than the background values of 0,1% - 1,2% of $IFN\gamma^+$ $CD8^+$ T cells detected in PBS group ($P < 0,05$). No statistically significant difference between all

analysed groups of mice was demonstrated in unstimulated and unrelated peptide controls, proving that the detected positive IFNγ responses were WHcAg-specific.

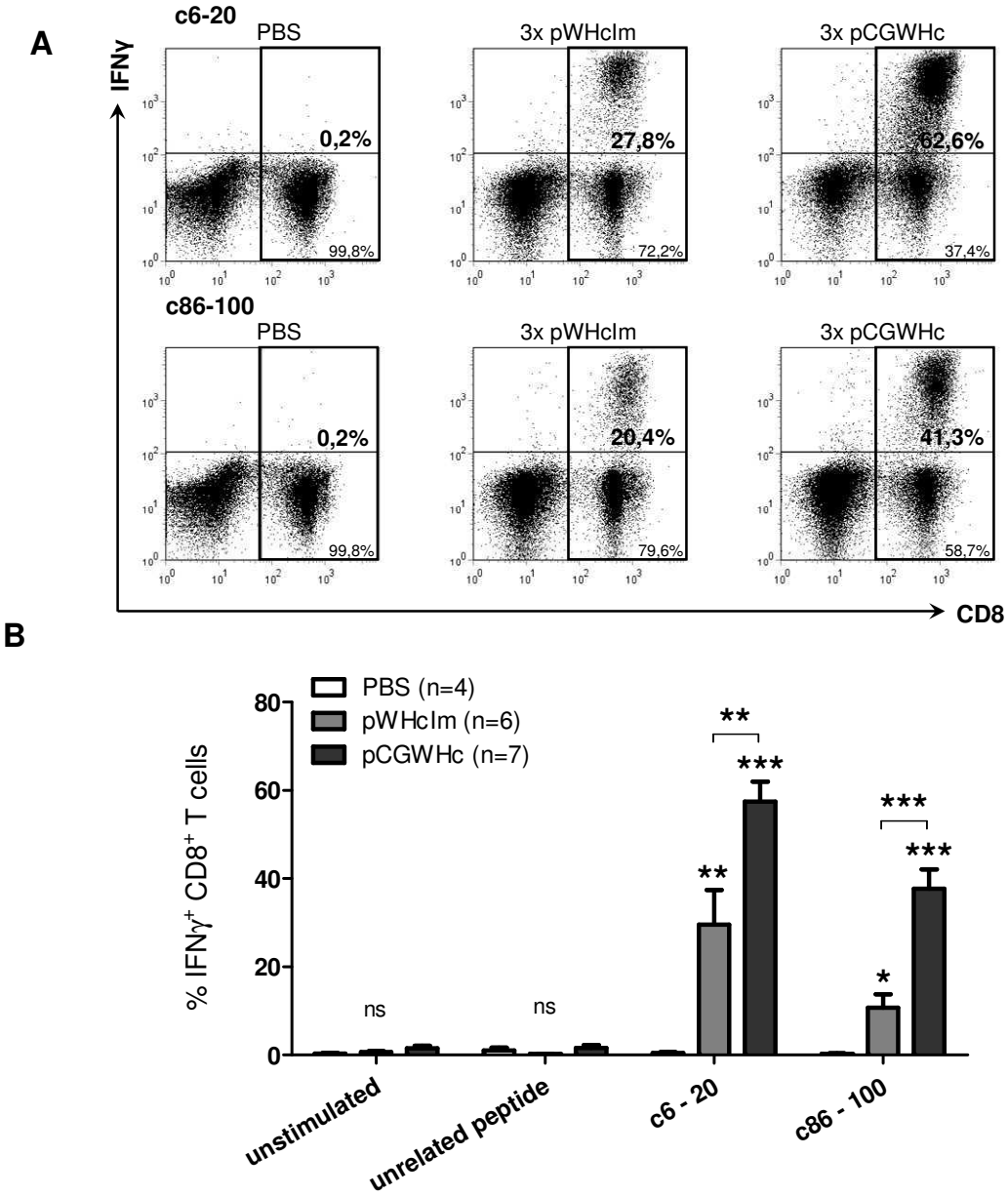

Fig. 5.13 Comparison of the magnitude of CD8⁺ T cell responses induced by immunization with the novel pCGWHc and pWHcIm plasmids

Splenocytes were expanded *in vitro* for 7 days in the presence of two identified CD8⁺ T cell epitopes: c13-21 and c86-94 and stained for intracellular IFNγ.

A. Dotplots of splenocytes stimulated with c6-20 (upper panel) and c86-100 (lower panel) of representative mouse from the pCGWHc, pWHcIm, and PBS control groups. Presented values indicate the percentage of IFNγ⁺ CD8⁺ T cells in the CD8⁺ T cell population.

B. CD8⁺ T cell response in murine splenocytes with c6-20 and c86-100. Unstimulated cells and cells stimulated with unrelated CMV-derived peptide served as controls. The bars represent the mean value obtained for each group of mice including SEM. The statistical analysis between the groups was performed using the unpaired Student *t* test. The asterisks shown directly above the bars mark the statistically significant difference between plasmid-vaccinated groups and control group: PBS-injected mice (* < 0,05;** < 0,005; *** < 0,0005; ns – not significant).

This experiment clearly demonstrates, that improved WHcAg expression from the novel pCGWHc plasmid results in the induction of a more vigorous humoral and cellular immune responses *in vivo*.

5.4 Generation of recombinant adenoviral vectors serotype 5 (Ad5) and chimeric Ad5F35 (Ad35) with improved expression of WHcAg

Vaccines based on recombinant adenoviruses are known to elicit vigorous and sustained humoral and cellular responses to the incorporated antigen [*Tatsis et al., 2004; Shiver et al., 2002; Zakhartchouk et al., 2005*]. Nevertheless, recombinant adenoviruses are very immunogenic. Even single immunization may induce neutralizing antibodies to the vector and prevent the beneficial effect of additional administration of the vaccine. Thus, recombinant adenoviruses serotype 5 and chimeric Ad5 in which the fiber knob and shaft are replaced with those of Ad35 (Ad5F35; named shortly Ad35) expressing WHcAg, were constructed. It is known, that the adenoviral hexon and the fiber protein contain most of the epitopes recognized by neutalizing antibodies. Apart from serotype-specific epitopes the hexon protein contains domains which are cross-reactive with all human serotypes [*Norrby et al., 1970*]. The epitopes localized on fiber proteins are predominantly group- and serotype-specific [*Mei et al., 1993*]. Therefore, subseqent immunization with chimeric Ad5, displaying the fiber from a distinct serotype Ad35, may partially overcome the presence of vector-specific immunity after vaccination with Ad5.

Previous experiments demonstrated that the introduction of a β-globin intron sequence between the CMV promoter and the WHcAg gene results in improved antigen expression and leads to the induction of a more vigorous immune response *in vivo* (section 5.3). Therefore, the same strategy was used in the generation of the recombinant adenoviral vectors expressing WHcAg.

The first step was to clone the gene of interest into a shuttle plasmid containing two “arms” of viral sequence for homologous recombination with the adenoviral backbone vectors. Generation of the AdV pShuttle plasmid expressing WHcAg was divided into two parts. First, the expression cassette containing the CMV immediate-early (CMV-IE) promoter, β-globin intron and polyadenylation signal was introduced into the multi cloning site (MCS) of pShuttle plasmid (Fig. 5.14A), and the DNA fragment encoding WHcAg was subcloned into the site between the β-globin intron and

polyadenylation signal (Fig. 5.14B), according to the protocols described in the Methods section. The expression cassette insert was amplified by PCR using pCG plasmid as a template and specific primers introducing *Kpn*I/*Bg*lII restriction sites. The amplified fragment after restriction digestion with corresponding enzymes was cloned into MCS of pShuttle. The successful insertion of the expression cassette into pShuttle was proved by *Kpn*I/*Bg*lII restriction digestion. The corresponding band of 1815 bp was visualized on the agarose gel (Fig. 5.15A). The insert's sequence of pCGWHc plasmid was verified by DNA sequencing. Secondly, the WHcAg sequence was amplified by PCR using the pWHcIm plasmid as a template. The specific primers used in the reaction included the sequence of *Xba*I and *Sbf*I restriction enzymes. The insert was digested using *Xba*I and *Sbf*I and then introduced into the *Xba*I/*Sbf*I site located between the β-globin intron and polyadenylation signal of the expression cassette. The successful insertion of WHcAg into pShuttle/CG plasmid was proved by *Xba*I/*Sbf*I restriction digestion. The characteristic band of 599 bp corresponding to the WHcAg insert was visualized on the agarose gel (Fig. 5.15B). The sequence of pShuttle/WHc plasmid was verified by DNA sequencing. The map of the pShuttle/WHc plasmid is attached in the Appendix section (Fig. 10.3).

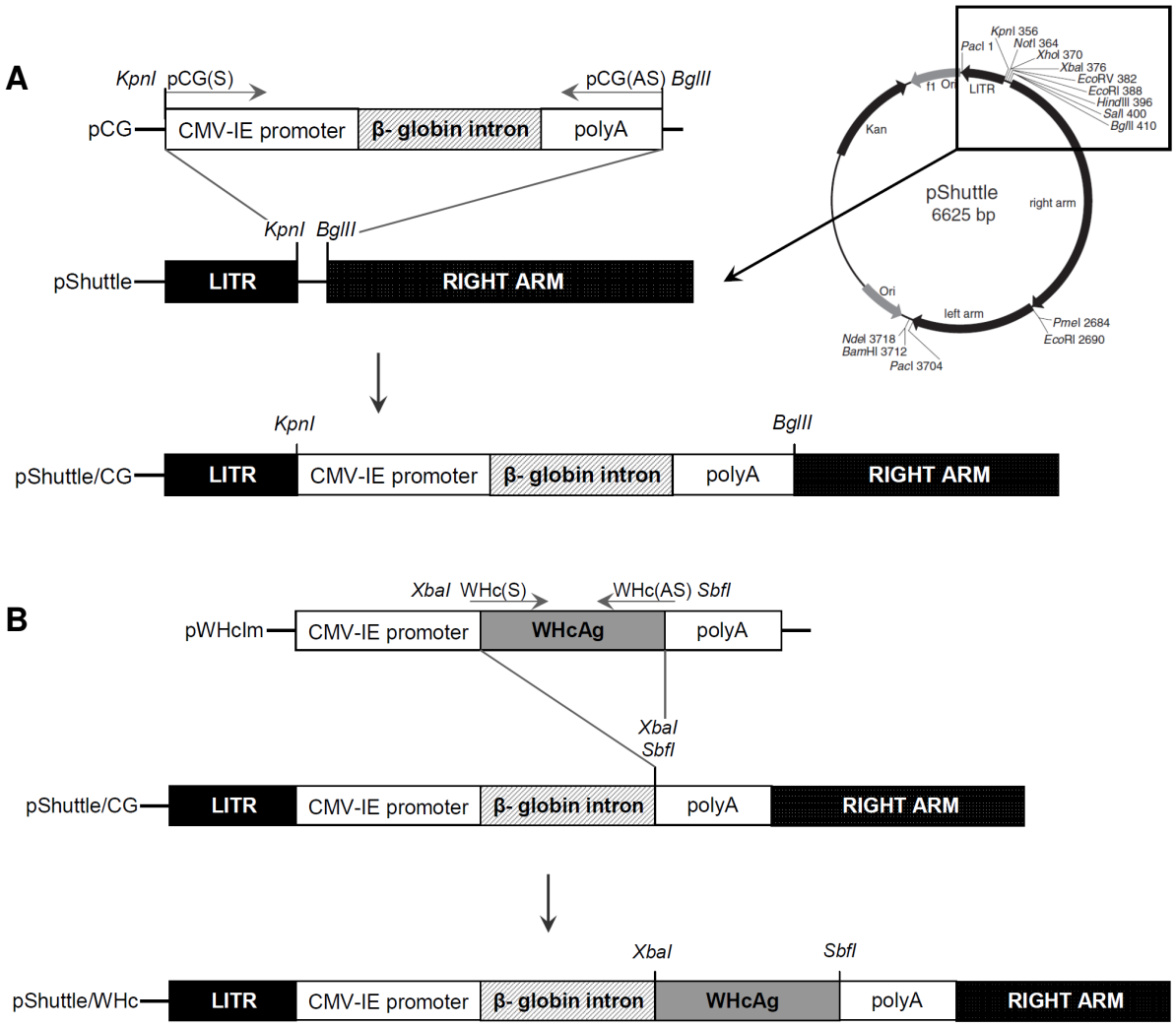

Fig. 5.14 Scheme of the cloning strategy of AdV pShuttle plasmid encoding WHcAg

A. Insertion of the expression cassette into pShuttle MCS. Insert was amplified by PCR using pCG plasmid as template and specific primers introducing *KpnI/Bgl*II restriction sites. The amplified fragment after restriction digestion with the corresponding enzymes was cloned into the MCS of pShuttle. *LITR:* left inverted terminal repeats.

B. Subcloning of the WHcAg insert. WHcAg sequence was amplified by PCR using the pWHclm plasmid as template and specific primers introducing the *XbaI/SbfI* restriction sites. The amplified fragment after restriction digestion with corresponding enzymes was cloned into the *XbaI/SbfI* site located between the β-globin intron and polyadenylation signal of the expression cassette. *LITR:* left inverted terminal repeats.

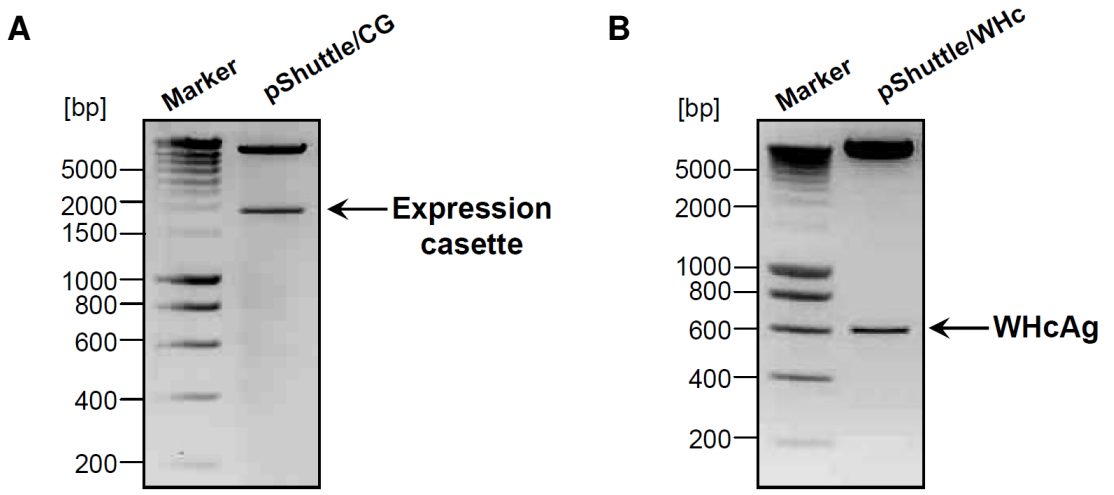

Fig. 5.15 Control restriction digestion of AdV pShuttle/WHc plasmid

A. After insertion of expression cassette containing CMV-IE promoter, β-globin intron and polyadenylation signal. 1 µg of DNA was digested with *KpnI* and *BglII* restriction enzymes for 2h in 37°C and visualized on 1,0% agarose gel containing 0.5 µg/ml ethidium bromide. The arrow indicates a band of 1815 bp corresponding to expression casette insert.

B. After insertion of the WHcAg sequence. 1 µg of DNA was digested with *XbaI* and *SbfI* restriction enzymes for 1h in 37°C and visualized on 1,5% agarose gel containing 0.5 µg/ml ethidium bromide. The arrow indicates a band of 599 bp corresponding to the WHcAg insert.

To show the expression of WHcAg from the pShuttle/WHc plasmid, BHK cells were transiently transfected with pShuttle/WHc containing the β-globin intron sequence and pShuttle that lacks β-globin intron as a control. The protein expression was detected 24 h after transfection by indirect immunofluorescence staining and Western blot analysis, using WHcAg-specific antibodies, as mentioned in the Methods section (4.3.1). To estimate the variation in the total protein content of the cell lysates, the control β-actin immunoblotting was performed.

In vitro transfection studies demonstrated the successful cloning procedure – the WHcAg was expressed correctly by the AdV pShuttle/WHc plasmid. Moreover, the novel pShuttle plasmid containing the β-globin intron in the expression cassette, exhibited an increased WHcAg expression in comparison to the pShuttle plasmid that lacked the β-globin intron sequence. Both the indirect immunofluorescence staining (Fig. 5.16A) and Western blot analysis (Fig. 5.16B) of BHK cells transfected with pShuttle plasmids confirmed that result. No WHcAg-specific staining was observed in mock cells treated with the transfection reagent only.

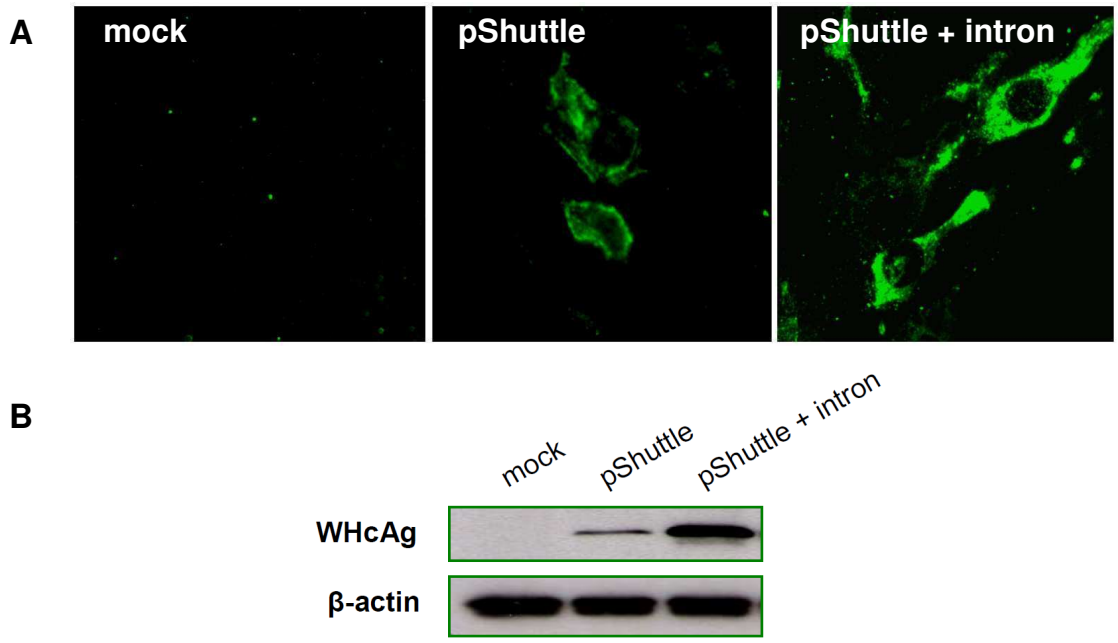

Fig. 5.16 Expression of WHcAg in BHK cells 24 h after transfection with the pShuttle/WHc and the pShuttle that does not contain an intron

BHK cells were transfected with 1 µg of plasmids, using Effectene reagent.
A. Cells were fixed with methanol and WHcAg was detected by indirect immunofluorescence staining with WHcAg-specific polyclonal rabbit antibody and a secondary FITC-coupled antibody.
B. Cell lysates were separated by SDS-PAGE and transferred to a PVDF-membrane. Detection was done with the WHcAg-specific mouse monoclonal antibody 6C5C8E4 or β-actin-specifc antibody and a secondary antibody coupled to peroxidase.

In the next step, recombinant adenoviral plasmids were generated by homologous recombination of *Pme*I-linerized pShuttle/WHc plasmid with E1 and E3-deleted pAdEasy-1 or pAdEasy-1/F35 backbone vectors in BJ5183 bacterial cells. The strategy of generating recombinant adenoviruses is described in the Methods section (1.2.7-1.2.9). Correct recombinants, containing pShuttle/WHc in the backbone, were propagated in the DH5α bacteria strain, purified and linerized with *PacI*. The maps of recombinant adenoviral plasmids expressing WHcAg: pAd5WHc and pAd5F35WHc are attached in the Appendix section (Fig. 10.4). Finally, recombinant adenoviral DNA was transfected into 293A cells that constitutively express E1 and E3 gene products. The vectors were amplified, purified and titrated by adenovirus plaque assay.

Expression of WHcAg from recombinant adenoviral vectors was confirmed by Western Blot analysis of HEK-293A cell lysates 36 h post infection with Ad5WHc and Ad35WHc (Fig. 5.17).

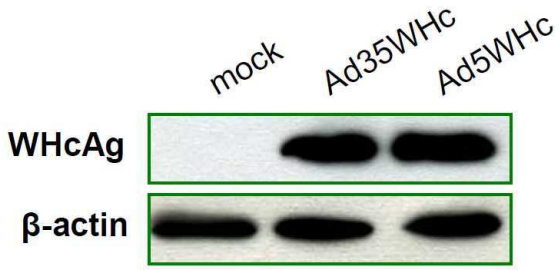

Fig. 5.17 Expression of WHcAg in HEK-293A cells 36 h after infection with the recombinant adenoviral vectors: Ad5WHc and Ad35WHc

HEK-293A cells were infected with 5×10^7 PFU of recombinant adenoviral vectors (MOI 10). Cell lysates were separated by SDS-PAGE and transferred to a PVDF-membrane. Detection was done with the WHcAg-specific mouse monoclonal antibody 10E11 or β-actin-specifc antibody and a secondary antibody coupled to peroxidase.

5.5 DNA prime – AdV boost immunization elicits more robust and functional WHV-specific immune response than DNA immunization alone

To investigate the potency of adenovirus-based vaccines to elicit a vigorous and multifunctional T cell response against WHcAg, immunization experiments in C57BL/6 mice were performed. It is widely known that recombinant adenoviruses are very immunogenic, inducing high levels of anti-AdV neutralizing antibodies. Even single immunization may induce neutralizing antibodies to the vector and thus prevent the beneficial effect of additional administration of the vaccine. To overcome this problem, mice were immunized in heterologous prime-boost regimen, using the plasmid DNA vaccine to prime the immune response. As shown in Fig. 5.18, C57BL/6 mice were pretreated with cardiotoxin. One week later they were subsequently immunized twice in a two-week interval with pCGWHc plasmid. Four weeks after the second DNA immunization, groups of mice were immunized with Ad5WHc or Ad35WHc or pCGWHc as a reference. As control, mice were immunized two times with “empty” pCG plasmid and boosted with Ad5 expressing green fluorescent protein (GFP). Two weeks after the last immunization the mice were sacrificed and splenectomy was performed.

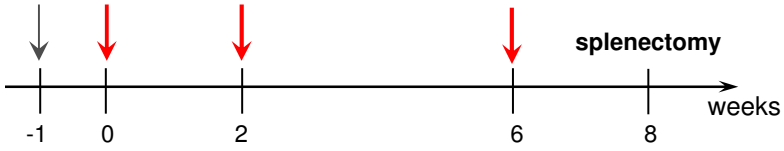

Vaccination groups:	-1	0	2	6	8
A) 2xpCG-Ad5GFP (*n=5*)	+	+ (pCG)	+ (pCG)		+ (Ad5GFP)
B) 2xpCGWHc-pCGWHc (*n=7*)	+	+	+		+
C) 2xpCGWHc-Ad5WHc (*n=7*)	+	+	+		+ (Ad5WHc)
D) 2xpCGWHc-Ad35WHc (*n=7*)	+	+	+		+ (Ad35WHc)

Fig. 5.18 Schedule of heterologous prime-boost immunization in C57BL/6 mice
Ten weeks old female C57BL/6 mice were pretreated with cardiotoxin (grey arrow) and one week later subsequently immunized 2 times with 100µg of pCGWHc plasmid intramuscularly in a two-week interval. At week 6 post first immunization, groups of seven mice were immunized with 2×10^9 PFU of Ad5WHc or Ad35WHc or 100µg pCGWHc. Immunization time points are indicated by red arrows. Five mice immunized with 100µg of "empty" pCG plasmid and 2×10^9 PFU Ad5 expressing GFP served as controls. Blood withdrawing was performed at the time point of each immunization (week 2, 6 and 8). Two weeks after the last round of immunization the mice were sacrificed and splenectomy was performed.

5.5.1 Evaluation of the humoral immune response

Evaluation of humoral immune response was performed by detection of WHcAg-specific IgG antibodies in the serum of mice after each immunization by ELISA (Methods, section 4.12). As shown in Fig. 5.19, the levels of anti-WHc antibodies were comparable in all mice immunized with pCGWHc plasmids either once or twice. The levels of anti-WHc were significantly higher in comparison to the background values obtained from mice vaccinated with "empty" pCG plasmid: $P < 0{,}05$ and $P < 0{,}0005$ after one and two immunizations, respectively. The boosting immunization with both adenoviral vectors (Ad5WHc and Ad35WHc) led to the induction of higher levels of anti-WHc in comparison to the group of mice immunized just with pCGWHc plasmid ($P < 0{,}05$). There was no statistically significant difference between the levels of anti-WHc in the mice boosted with Ad5WHc or Ad35WHc. As expected, the immunization of control mice with Ad5GFP did not induce any anti-WHc.

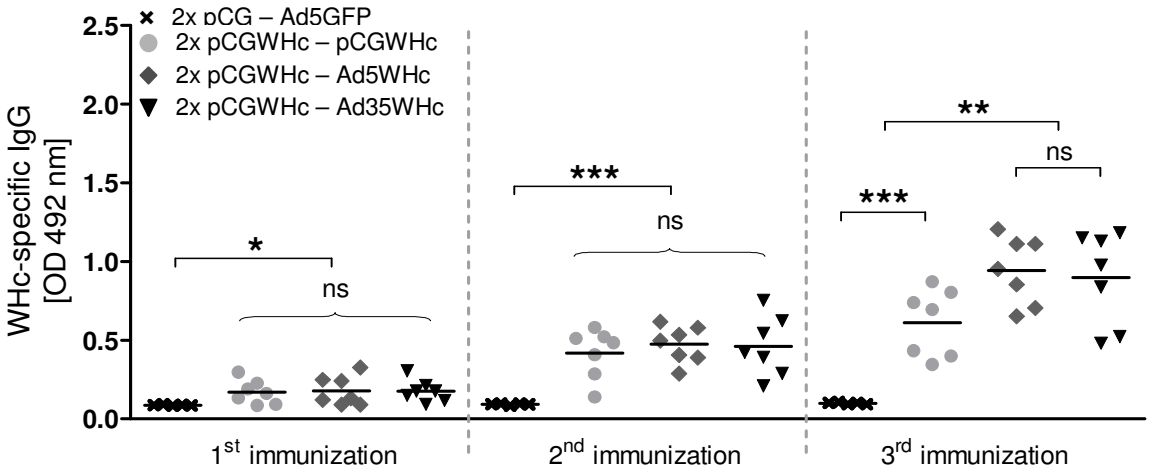

Fig. 5.19 Detection of WHcAg-specifc IgG antibodies in the sera of C57BL/6 mice immunized in heterologous prime-boost regimen, using pCGWHc plasmid and recombinant adenoviral vectors expressing WHcAg

Mice were primed two times by immunization with the pCGWHc plasmid. Four weeks later, boosting immunization with Ad5WHc or Ad35WHc or pCGWHc for reference was performed. Mice immunized with "empty" pCG and Ad5GFP served as controls. The sera of mice were obtained from blood samples collected after each immunization and diluted 1:5000 in PBS. WHcAg-specific ELISA was peformed using an anti-mouse IgG antibody coupled to peroxidase. The statistical analysis between the groups was performed using the unpaired Student *t* test. Asterisks mark the significant difference (* < 0,05; ** < 0,005; *** < 0,0005).

To evaluate the breadth of the immune response induced by the heterologous prime-boost regimen, the IgG_1 and IgG_{2a} isotypes of WHcAg-specific antibodies were analyzed in murine sera by ELISA. Detection of IgG isotypes demonstrated that all tested immunization protocols induced predominantly IgG_{2a} antibodies (Fig. 5.20A). Nevertheless, the levels of IgG_{2a} were significantly higher in those groups of mice boosted with recombinant adenoviral vectors than in those immunized with the DNA vaccine pCGWHc plasmid ($P < 0,005$). The presence of WHcAg-specifc IgG_1 antibodies in murine sera detected after the last immunization was confirmed in DNA prime – AdV boost as well as in DNA only – vaccinated groups. The levels of IgG_1 were statistically significant in comparison to background values obtained from control mice: $P < 0,05$ and $P < 0,005$ for DNA only and DNA-AdV groups respectively (Fig. 5.20B).

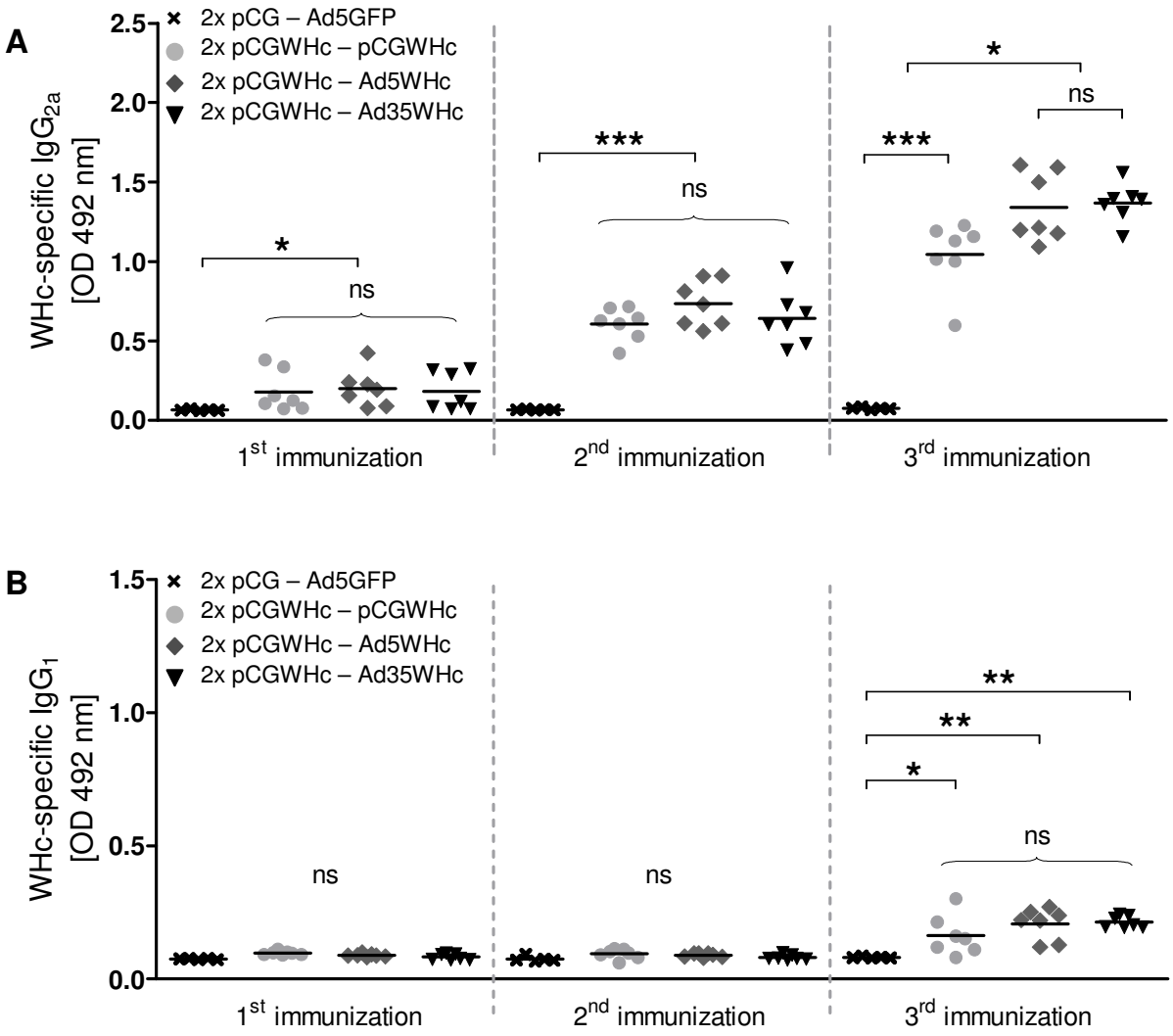

Fig. 5.20 Detection of WHcAg-specifc IgG isotypes: IgG2a (A) and IgG1 (B), in the sera of C57BL/6 mice immunized in the heterologous prime-boost regimen, using pCGWHc plasmid and recombinant adenoviral vectors expressing WHcAg

The sera of mice were obtained from blood samples collected two weeks after each immunization and diluted 1:5000 in PBS. WHcAg-specific ELISA was peformed using IgG isotype-specific (IgG_{2a} or IgG_1) anti-mouse antibodies coupled to peroxidase. The statistical analysis between the groups was performed using the unpaired Student *t* test. Asterisks mark the significant difference (* < 0,05; ** < 0,005; *** < 0,0005).

5.5.2 Evaluation of the $CD8^+$ T cell response

Comparison of WHcAg-specific $CD8^+$ T cell responses induced by the heterologous DNA–Ad5WHc or DNA–Ad35WHc with DNA only immunization regimen was performed by the intracellular IFNγ staining of splenocytes isolated two weeks after the last immunization. Splenocytes were stimulated *in vitro* in the presence of two previously identified $CD8^+$ T cell 9-mer epitopes: c13-21 and c86-94. After 7 days of

culturing, cells were restimulated for 6h with corresponding peptides and stained for IFNγ as mentioned in the Methods section 4.9.1. Splenocytes obtained from mice immunized with “empty” pCG plasmid and Ad5GFP served as controls.

The percentages of IFNγ$^+$ CD8$^+$ T cells determined in the spleens of mice vaccinated in the DNA prime – AdV boost manner were considerably higher compared to those detected in the group of mice immunized only with DNA (Fig. 5.21). The mean IFNγ response after the stimulation of splenocytes with WHcAg-derived epitope c13-21 were 21,9% for pCGWHc – immunized mice, 65,7% and 47% for pCGWHc-Ad5WHc and pCGWHc-Ad35WHc groups, respectively (Fig. 5.21B). Three-fold and over 2-fold increases in IFNγ producing CD8$^+$ T cells were detected in the groups of mice immunized in DNA-AdV manner compared to the DNA only – immunized group ($P < 0,0005$). The mean percentages of IFNγ$^+$ CD8$^+$ T cells directed against the peptide c86-94 were approximately 11,3% in pCGWHc - immunized group of mice and were significantly lower than the values 37,4% and 21,2% assessed for the pCGWHc-Ad5WHc and pCGWHc-Ad35WHc groups, respectively ($P < 0,005$). No statistically significant difference in IFNγ responses was obtained in comparison to the boosting effect of recombinant adenoviral vector serotype 5 to the chimeric Ad5F35 vector. Stimulation of splenocytes obtained from mice immunized with “empty” pCG plasmid and Ad5GFP with the peptides c13-21 and c86-94 induced no IFNγ response (0,1% to 0,3% of IFNγ$^+$ CD8$^+$ T cells). Comparison of the responses to stimulation with WHcAg-derived epitopes measured for groups immunized with WHcAg-expressing vaccines were significantly higher than those detected in control group ($P < 0,0005$). No statistically significant difference between all the analysed groups of mice was demonstrated in unstimulated and unrelated peptide controls.

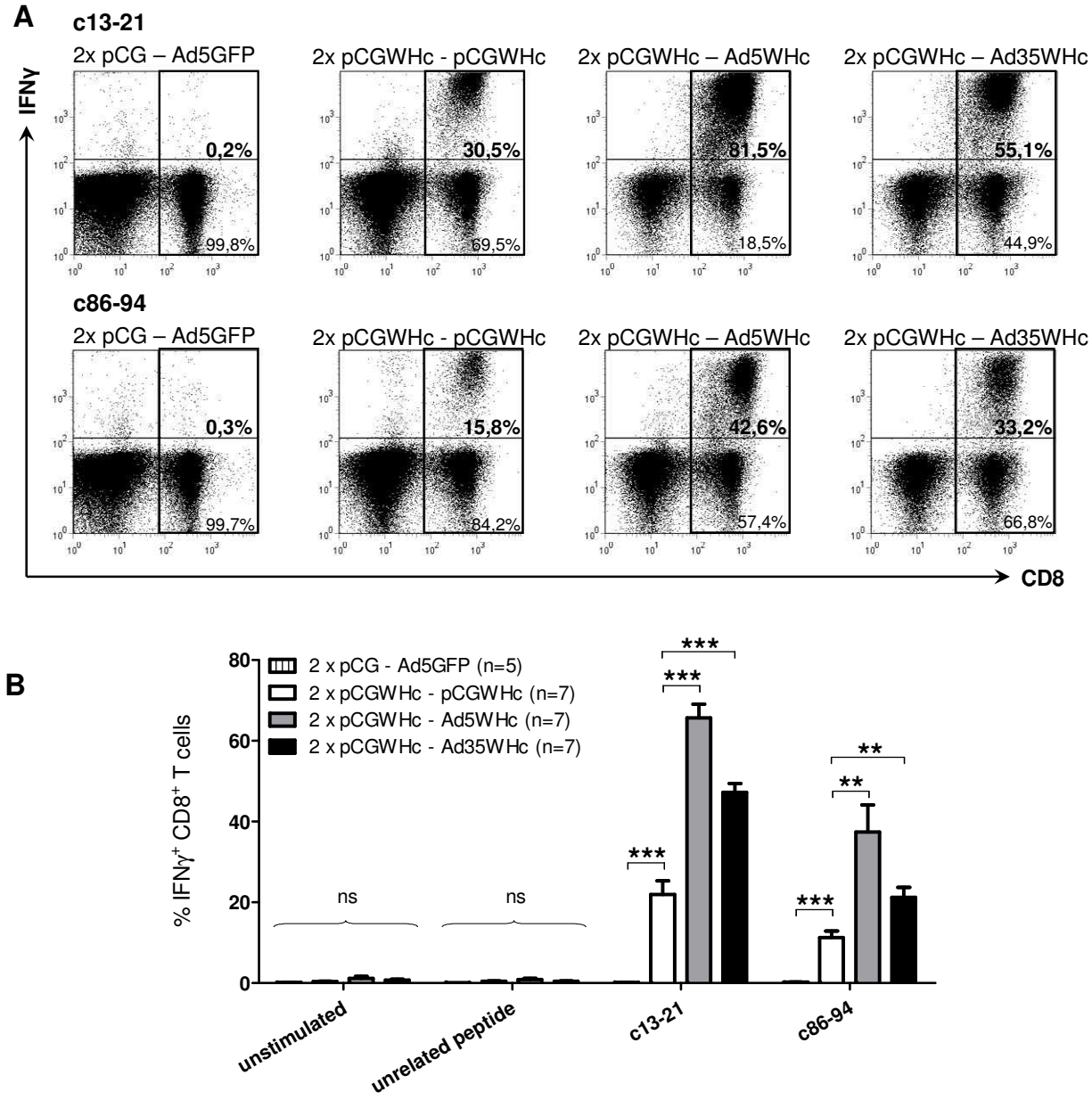

Fig. 5.21 Comparison of the magnitude of CD8⁺ T cell responses induced by pCGWHc plasmid immunization and heterologous prime-boost regimen, using recombinant adenoviral vectors expressing WHcAg

Splenocytes were expanded *in vitro* for 7 days in the presence of two identified CD8⁺ T cell epitopes: c13-21 and c86-94 and stained for intracellular IFNγ.

A. Dotplots of the splenocytes stimulated with c13-21 (upper panel) and c86-94 (lower panel) of a representative mouse from each immunization group.

B. CD8⁺ T cell response in murine splenocytes with c13-21 and c86-94. Unstimulated cells and cells stimulated with an unrelated CMV-derived peptide served as controls. The bars represent the mean value obtained for the analyzed group of mice including SEM. The statistical analysis between the groups was performed using the unpaired Student *t* test (** < 0,005; *** < 0,0005; ns – not significant).

To further study the effector functions of the $CD8^+$ T cells induced by the heterologous prime-boost regimen their degranulation capacity was evaluated. As mentioned in the Introduction (section 1.6.1), CD107a is a suitable marker for detection of degranulating antigen-specific cytotoxic T lymphocytes [*Betts et al., 2003; Rubio et al., 2003*]. CD107a protein is present in the membrane of T cell cytolytic granules. Recognition of the infected cells by CTLs results in releasing their content and the exposure of the CD107a molecule on the CTL surface, where it can be easily detected by flow cytometric analysis.

The ability of the $CD8^+$ T cells to degranulate was compared to IFNγ production in the splenocytes of mice immunized in the pCGWHc prime - Ad5WHc or Ad35WHc manner and three times only with the pCGWHc plasmid for reference, as mentioned in the Methods section (4.4.3.2). As a control, the splenocytes of mice primed two times with “empty” pCG plasmid and boosted with Ad5GFP were used. As presented in Fig. 5.22, the significant proportion of total $IFN\gamma^+$ $CD8^+$ T cells from splenocytes of all groups of mice immunized with WHcAg-expressing vaccines was positive for the CD107a degranulation marker (over 90%). However, the percentages of double-positive $CD107a^+$ $IFN\gamma^+$ $CD8^+$ T cells were significantly higher in the groups of mice boosted with Ad5WHc and Ad35WHc (mean values: 58,7% and 49,9%, respectively), than in the pCGWHc only immunized mice (mean value: 17,5%) [Fig. 5.22B]. Approximately a 3-fold increase in the number of $CD107a^+$ $IFN\gamma^+$ $CD8^+$ T cells between the heterologous prime-boost regimen groups and the group vaccinated with DNA was statistically significant ($P < 0,005$). No $CD107a^+$ $IFN\gamma^+$ $CD8^+$ T cells were detected in the spleens of mice immunized with “empty” pCG plasmid and Ad5GFP. Similar to $CD8^+$ T cells co-expressing $CD107^+$ and $IFN\gamma^+$, the percentages of IFNγ-producing cells were significantly elevated in both groups immunized in the DNA prime – AdV boost manner as compared to only DNA–vaccinated mice (mean: 4,6% vs 1,3%; $P < 0,005$ for group of mice boosted with Ad5WHc and 4,7% vs 1,3%; $P < 0,0005$ for group immunized with Ad35WHc). No significant difference in the amount of $CD107a^+$ $CD8^+$ T cells was detected between the groups immunized with pCGWHc plasmid and the heterologous prime-boost regimen. The mean percentage values of $CD8^+$ T cells expressing the CD107a degranulation marker in those groups ranging between 2,3% and 2,4% were significantly higher than the background value of 0,4% detected in splenocytes of control mice ($P < 0,0005$).

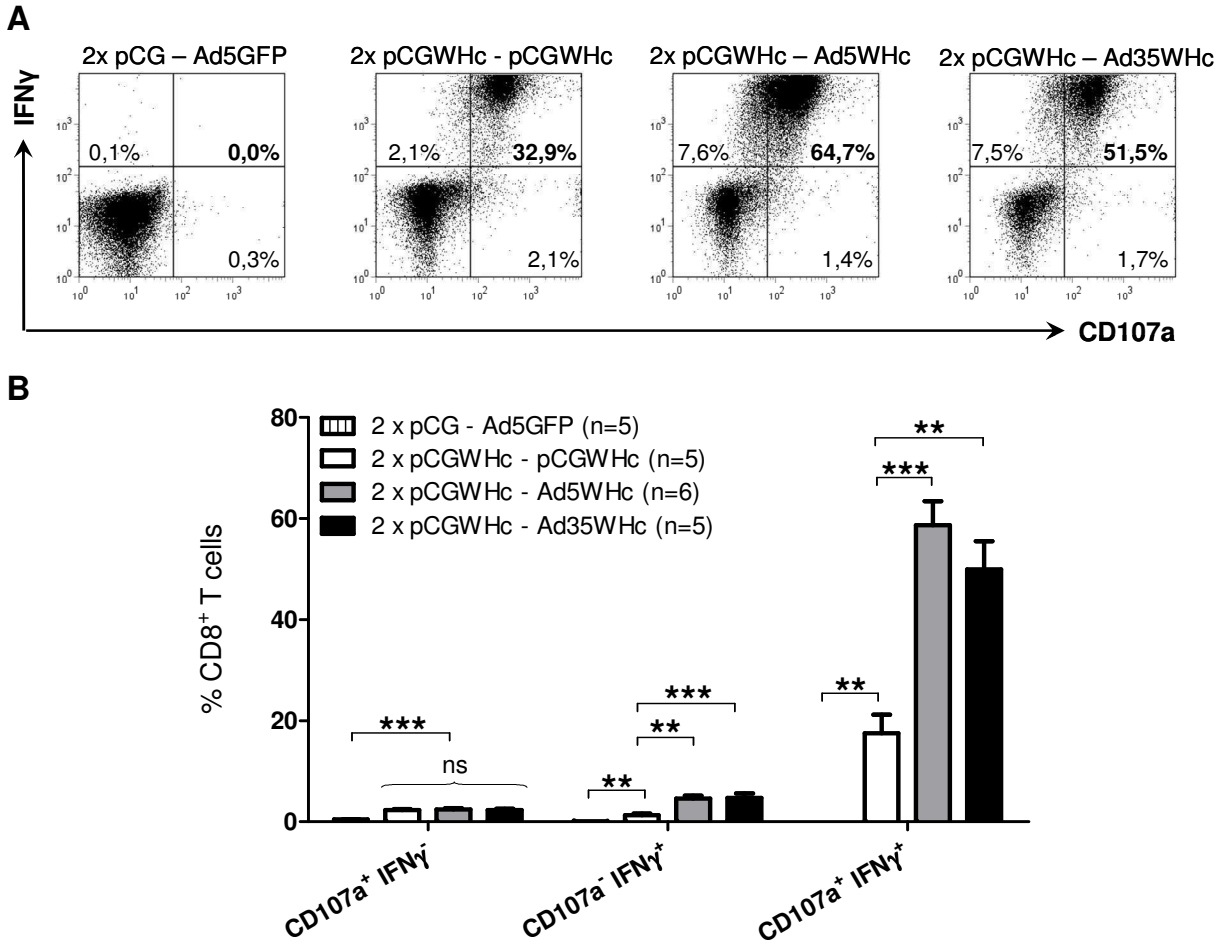

Fig. 5.22 Evaluation of degranulation activity of IFNγ$^+$ CD8$^+$ T cells induced by pCGWHc immunization and heterologous prime-boost regimen

Splenocytes were expanded *in vitro* for 7 days with the epitope c13-21 and subsequently restimulated for 5h in the presence of the CD107a antibody. Afterwards cells were stained for CD8 T cell marker and intracellularly for IFNγ.

A. Dotplots of the splenocytes of a representative mouse from each immunization group. Presented values indicate the percentage of CD107a$^+$ or/and IFNγ$^+$ CD8$^+$ T cells in the CD8$^+$ T cell population.

B. Degranulation capacity of IFNγ$^+$ CD8$^+$ T cells. The bars represent the mean value obtained for the analyzed group of mice including SEM. The statistical analysis between the groups was performed using the unpaired Student *t* test (** < 0,005; *** < 0,0005; ns – not significant).

Apart from the direct cytotoxic activities, CD8$^+$ T cells are able to produce cytokines that exhibit an antiviral activity. The secretion of IFNγ and TNFα by antigen-specific CD8$^+$ T cells proved to suppress viral replication [*Guidotti et al., 1994*]. Moreover, multifunctional T cells, which are able to secrete simultaneously more than one cytokine, demonstrated a stronger protective potential and higher capacity to clear viral, bacterial or parasitic infections [*Seder et al., 2008; Darrahet al., 2007*]. To investigate the influence of the heterologous DNA prime – AdV boost regimen on the

production of T_{H1} type cytokines by $CD8^+$ T cells, the expression of IFNγ, TNFα and IL-2 was measured in splenocytes stimulated *in vitro* for 6h with the peptide c13-21 (Methods, section 4.9.1).

As presented in Fig. 5.23A, the cytokine that had the strongest expression within the $CD8^+$ T cell population in all immunized groups was IFNγ. TNFα was produced in slightly lower levels and the less abundant cytokine was IL-2 (approximately 4-fold lower expression than IFNγ). Splenocytes from the control mice demonstrated background levels of tested cytokines. Group of mice primed with pGCWHc and boosted with Ad5WHc exhibited the highest percentages of IFNγ, TNFα and IL-2 (the mean values: 5,3%, 4,2% and 1,2% respectively). The expression of all analysed cytokines in this group was significantly higher compared to the DNA only - immunized group ($P < 0,05$). The boosting immunization with Ad35WHc also led to the increased secretion of IFNγ and TNFα in comparison to the group of mice vaccinated only with plasmid DNA ($P < 0,05$). The difference in IL-2 production between those groups was not statistically significant, even though it was elevated for the mice immunized with pCGWHc – Ad35WHc.

Determination of single, double and triple positive cells that produce IFNγ, TNFα and IL-2 within the $CD8^+$ T cell population was performed. First, the absolute number of single, double and triple cytokine producing cells was quantified for every mouse in the group and the mean value was calculated. Second, percentages of cells secreting one, two or all cytokines were evaluated. As Fig. 5.23B shows, there was no difference in the "quality" of cytokines secreting $CD8^+$ T cells between the heterologous prime – boost regimen groups, using recombinant adenoviral vectors expressing WHcAg, and in mice immunized only with WHcAg – expressing plasmid. The average values of single, double and triple cytokine producers were approximately 18%, 62% and 20% respectively. The highest proportion of the double producers was the $CD8^+$ T cell group co-expressing IFNγ and TNFα – the cytokines with the highest antiviral activity (approximately 97%, *data not shown*).

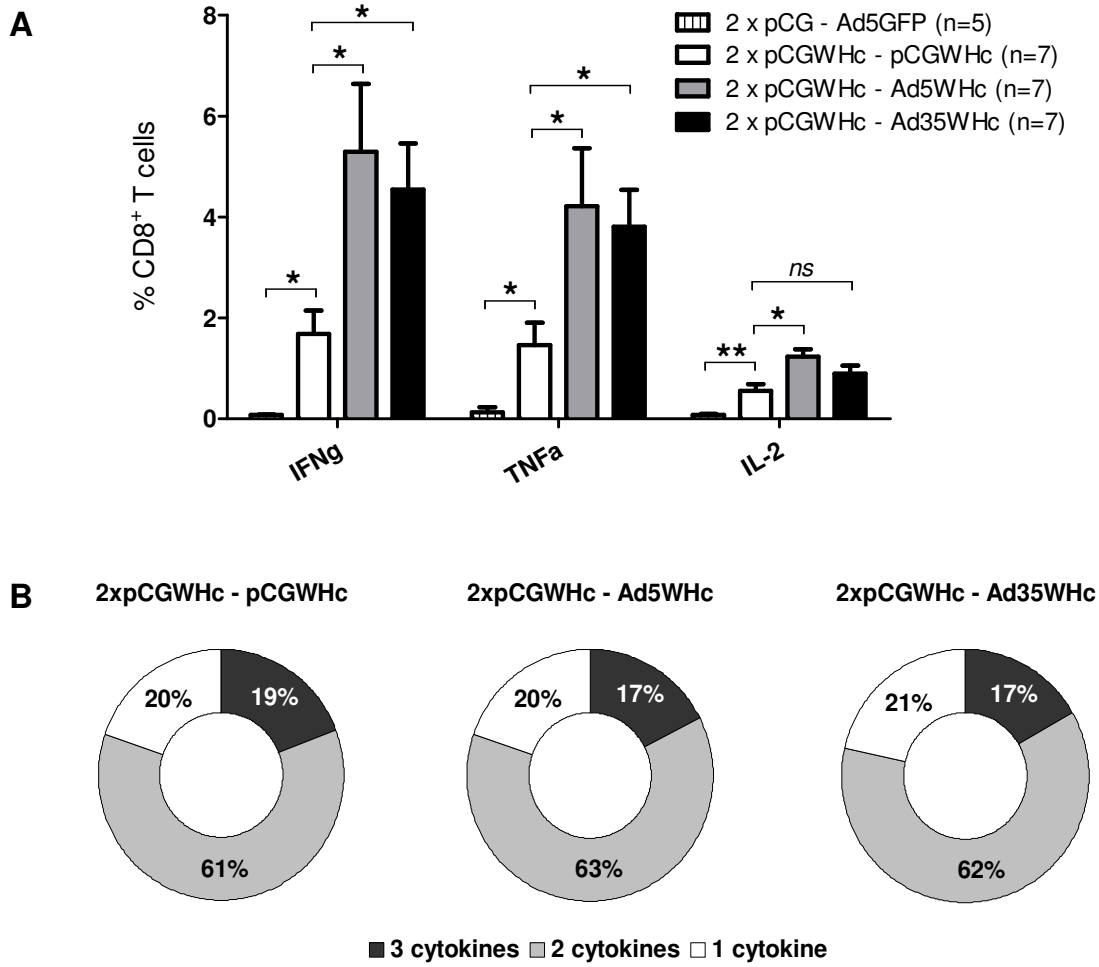

Fig. 5.23 Evaluation of multiple cytokine production by CD8$^+$ T cells induced by pCGWHc immunization and the heterologous prime-boost regimen

Splenocytes were stimulated *in vitro* for 6h with the epitope: c13-21 and stained intracellularly for IFNγ, TNFα and IL-2.

A. The expression profile of T_{H1} type cytokines IFNγ, TNFα and IL-2. The bars represent the mean value obtained for the analyzed group of mice including SEM. The statistical analysis between the groups was performed using the unpaired Student *t* test (* < 0,05; ** < 0,005; ns - not significant).

B. Evaluation of multifunctional CD8$^+$ T cells. The percentage of single, double and triple producers in cytokine-positive CD8$^+$ T cell population. The percentage values represent the mean value obtained for the analyzed group of mice.

In vitro experiments proved that heterologous priming with the pCGWHc plasmid and boosting with recombinant AdV expressing WHcAg induces significantly stronger CTL response than immunization with the pCGWHc plasmid alone. Nevertheless, the "quality" of CD8$^+$ T cells is comparable to those induced by the DNA vaccine alone. To address the question whether the more vigorous CD8$^+$ T cell response induced by DNA prime - AdV boost immunization have a stronger cytotoxic potential than those induced by the DNA vaccination alone *in vivo*, an *in vivo* cytotoxicity assay was

performed. This assay allows to *in vivo* evaluate the CTL's effector ability to eliminate cells mimicking virus-infected cells ('target cells') [*Barber et al., 2003*; *Zelinskyy et al., 2009; Dietze et al., 2011*]. *In vivo* cytotoxicity assay proved its usefulness in evaluating the antiviral therapies [*Gibbert et al., 2010*] and most recently the immunization strategies [*Rigato et al., 2011*]. The *in vivo* cytoxicity assay is described in detail in the Methods section (4.11). Briefly, three groups of mice were examined in the experiment: 6 mice were immunized three times with pCGWHc, 6 mice primed with pCGWHc were immunized two times and then boosted with Ad5WHc and 4 control mice immunized with "empty" pCG plasmid in combination with Ad5GFP. The immunization schedule is presented in Fig. 5.18 (page 87). Eight days after the last immunization the mice were intravenously injected with the same number of lymphocytes loaded with $CD8^+$ T cell epitope peptide c13-21 ("target cells") and non-loaded cells for the reference. The populations were labelled with different concentrations of CFSE dye. After 8 hours, immunized mice were sacrificed and the killing of the target cells was evaluated in the spleen.

The mice immunized in the DNA prime – Ad5WHc manner showed an improved killing of the c13-21 loaded target cells, and mimicking WHV-infected cells were found in the spleen (Fig. 5.24). The mean percentage of killing determined for 6 mice in that group was 43,8% and was significantly higher than the 20,2% obtained for mice immunized only with the pCGWHc plasmid ($P < 0,05$) [Fig. 5.24B]. The background obtained in mice immunized with vaccines that do not express WHcAg was 1,9%. The percentages of eliminated cells in groups of mice immunized either with DNA alone or in combination with Ad5WHc were significantly higher in comparison to control mice ($P < 0,05$ and $P < 0,005$, respectively).

Those data confirm that immunization in heterologous prime-boost regimen, using the recombinant AdVs not only induces CTL secreting more IFNγ, TNFα and IL-2, but it is also more effective in the elimination of cells loaded with the WHV epitope.

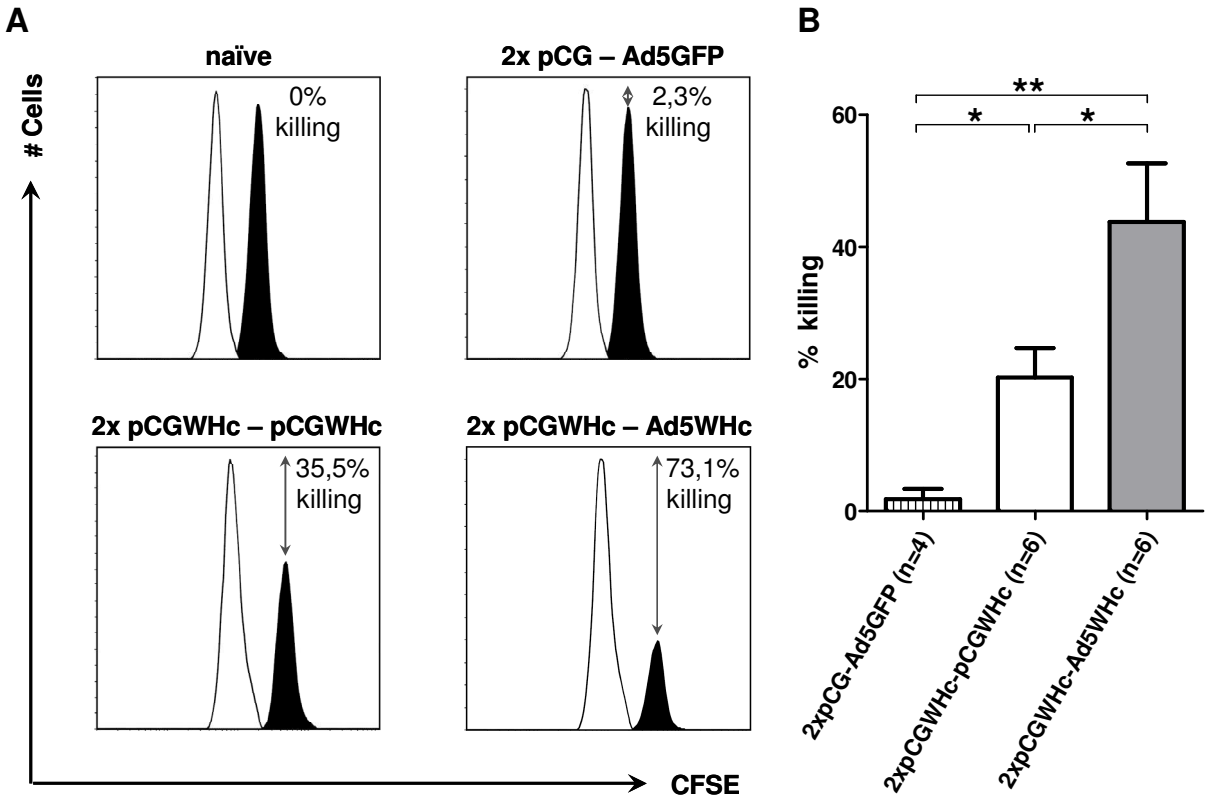

Fig. 5.24 Elimination of cells loaded with the WHcAg-derived peptide c13-21 in mice immunized with the pCGWHc plasmid and the heterologous prime-boost regimen

Mice were immunized two times with pCGWHc and boosted with Ad5WHc or pCGWHc. Mice immunized with "empty" pCG and Ad5GFP served as control. At day 8 after the last immunization, mice were intravenously injected with the same number of lymphocytes loaded with the $CD8^+$ T cell epitope c13-21 ("target cells") and non-loaded cells for the reference. To distinguish between the two populations, they were labelled with different concentrations of CFSE dye. After 8 hours the mice were sacrificed and the killing of the target cells was evaluated in the spleen. To assess the difference in the number of cells between the populations naïve mice were used as a reference.

A. Representative histograms of a $CFSE^{high}$ population of target cells (black peak) and $CFSE^{low}$ reference cells (white peak) in the spleens from each immunization group exhibiting the highest killing activity. The difference in the cell numbers between the peaks was calculated and presented as the percentage of killing (marked by grey arrows).

B. The bars represent the mean value obtained from groups of six mice immunized with WHcAg-expressing vaccines and four control mice immunized with "empty" pCG plasmid in combination with Ad5GFP including SEM. The statistical analysis between the groups was performed using the unpaired Student *t* test (* < 0,05; ** < 0,005).

5.6 DNA prime – AdV boost immunization elicits WHV-specific immune response in WHV transgenic mice

The WHV transgenic mouse strain 1217 (1217 WHV Tg mice) is a promising new animal model for studies on hepadnaviral infection, especially for the development of

new antiviral strategies. 1217 WHV Tg mice that carry the wild-type WHV transgene were generated using C57BL/6 mice. Those mice are characterized by WHV replication in the liver and the secretion of the WHV particles into the bloodstream. Moreover, they do not show WHV-specific immune responses. Therefore, WHV Tg mice exhibit at least partial immune tolerance against WHV proteins.

To investigate the potency of adenovirus-based vaccines to break the WHV-specific immune tolerance and reduce the WHV replication in WHV transgenic mice, heterologous prime-boost immunization trials were performed. As shown in Fig. 5.25, 1217 WHV Tg mice were pretreated with cardiotoxin. One week later mice were subsequently immunized two times in a two-week interval with the pCGWHc plasmid. Four weeks after the second DNA immunization, the groups of mice were immunized with either Ad5WHc or pCGWHc as reference. As controls, mice were immunized two times with "empty" pCG plasmid and were boosted with Ad5 expressing GFP. Two weeks after the third immunization mice were sacrificed and splenectomy was performed. The group of mice immunized in the heterologous DNA-Ad5WHc regimen received a second boost immunization with Ad35WHc. The vaccination was performed four weeks after Ad5WHc immunization and the mice were sacrificed two weeks later.

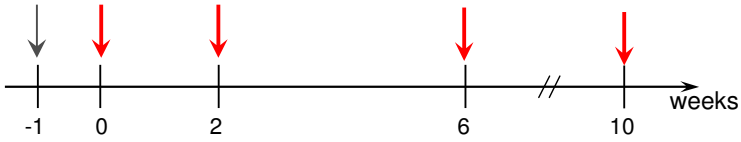

Vaccination groups:					
A) 2xpCG-Ad5GFP (*n=4*)	+	+(pCG)	+ (pCG)	+ (Ad5GFP)	
B) 2xpCGWHc-pCGWHc (*n=7*)	+	+	+	+	
C) 2xpCGWHc-Ad5WHc (*n=12*)	+	+	+	+ (Ad5WHc)	
D) 2xpCGWHc-Ad5-Ad35WHc (*n=5*)	+	+	+	+ (Ad5WHc)	+(Ad35WHc)

Fig. 5.25 Schedule of heterologous prime-boost immunization of WHV Tg mice
Ten to twelve weeks old 1217 WHV Tg mice were pretreated with cardiotoxin (grey arrow, marked as "+"). One week later they were subsequently i.m. immunized 2 times with 100µg of pCGWHc plasmid in a two-week interval (marked as "+"). At week 6, groups of seven mice were immunized with 2×10^9 PFU of Ad5WHc or 100µg pCGWHc. Immunization time points are indicated by red arrows. Four mice immunized with 100µg of "empty" pCG plasmid and 2×10^9 PFU Ad5 expressing GFP served as controls. Mice were sacrificed at week 8 and splenectomy was performed. The group of mice that received a second boost immunization with 2×10^9 PFU Ad35WHc was sacrificed at week 12. Blood withdrawing was performed at the time point of each immunization (week 2, 6, 8 and 12).

5.6.1 Evaluation of the humoral immune response

To evaluate whether immunizations with the new DNA plasmid and recombinant adenoviral vectors expressing WHcAg were able to induce an antibody response not only against the WHcAg but also WHsAg, the detection of anti-WHc and anti-WHs in the sera of 1217 WHV Tg mice was performed by ELISA (Methods, section 4.12).

As Fig. 5.26 shows, all groups of mice had undetectable levels of anti-WHc antibodies after the first DNA immunization. The levels of anti-WHc increased in all mice immunized twice with pCGWHc plasmid and were significantly higher in comparison to the background values obtained for mice vaccinated with the "empty" pCG plasmid (P < 0,05). The boosting immunization with Ad5WHc led to the induction of higher levels of anti-WHc antibodies in comparison to the group of mice immunized a third time with pCGWHc plasmid (P < 0,005). As expected, the immunization of control mice with Ad5GFP did not induce any anti-WHc. The level of anti-WHc increased additionally in the group of mice after the 4th (second boost) immunization with Ad35WHc (P < 0,005).

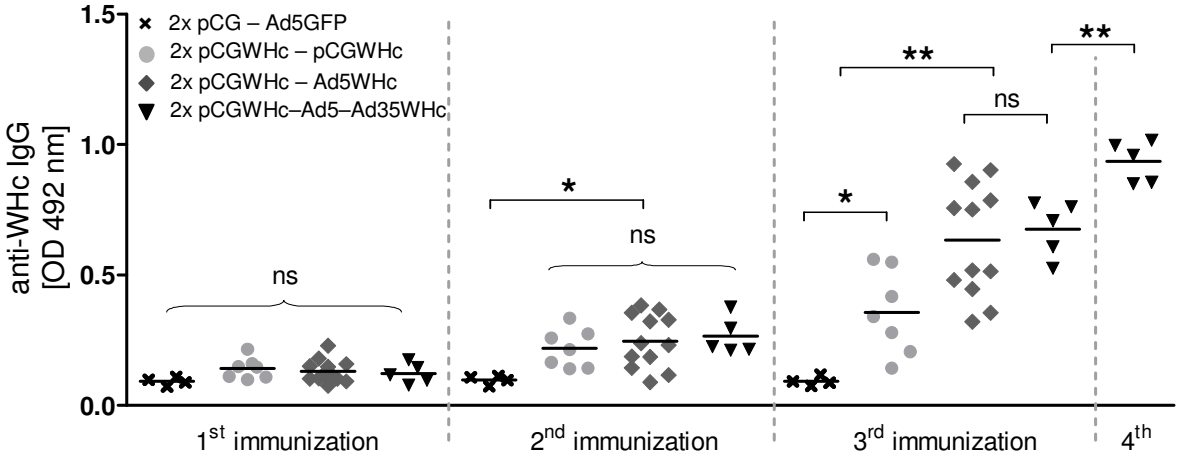

Fig. 5.26 Detection of anti-WHc IgG antibodies in the sera of 1217 WHV Tg mice immunized in the heterologous prime-boost regimen using recombinant adenoviral vectors expressing WHcAg

Mice were primed two times by immunization with the pCGWHc plasmid. Four weeks later, boosting immunization with Ad5WHc or pCGWHc was performed. The group of mice immunized 2x pCGWHc-Ad5WHc received a second boost immunization with Ad35WHc. Mice immunized with "empty" pCG and Ad5GFP served as controls. The sera of mice were obtained from blood samples collected after each immunization and diluted 1:250 in PBS. WHcAg-specific ELISA was peformed using anti-mouse IgG antibody coupled to peroxidase. The statistical analysis between the groups was performed using the unpaired Student *t* test. Asterisks mark the significant difference (* < 0,05; ** < 0,005; ns – not significant).

To evaluate the breadth of the immune response induced by the heterologous prime-boost regimen, the IgG_1 and IgG_{2a} isotypes of anti-WHc antibodies were analyzed in murine sera by ELISA. Detection of IgG isotypes demonstrated that all tested immunization protocols induce predominantly IgG_{2a} antibodies indicating a T_{H1} type of immune response (Fig. 5.27A). Nevertheless, the levels of IgG_{2a} were significantly higher in the groups of mice boosted with Ad5WHc than in those immunized with the DNA vaccine pCGWHc plasmid ($P < 0,005$). WHcAg-specifc IgG_1 antibodies were only present in the sera of mice that received the second boost immunization with Ad35WHc (Fig. 5.27B). Three out of five mice from this group demonstrated a very high levels of IgG_1 antibodies (mean $OD_{492\ nm}$: 0,89).

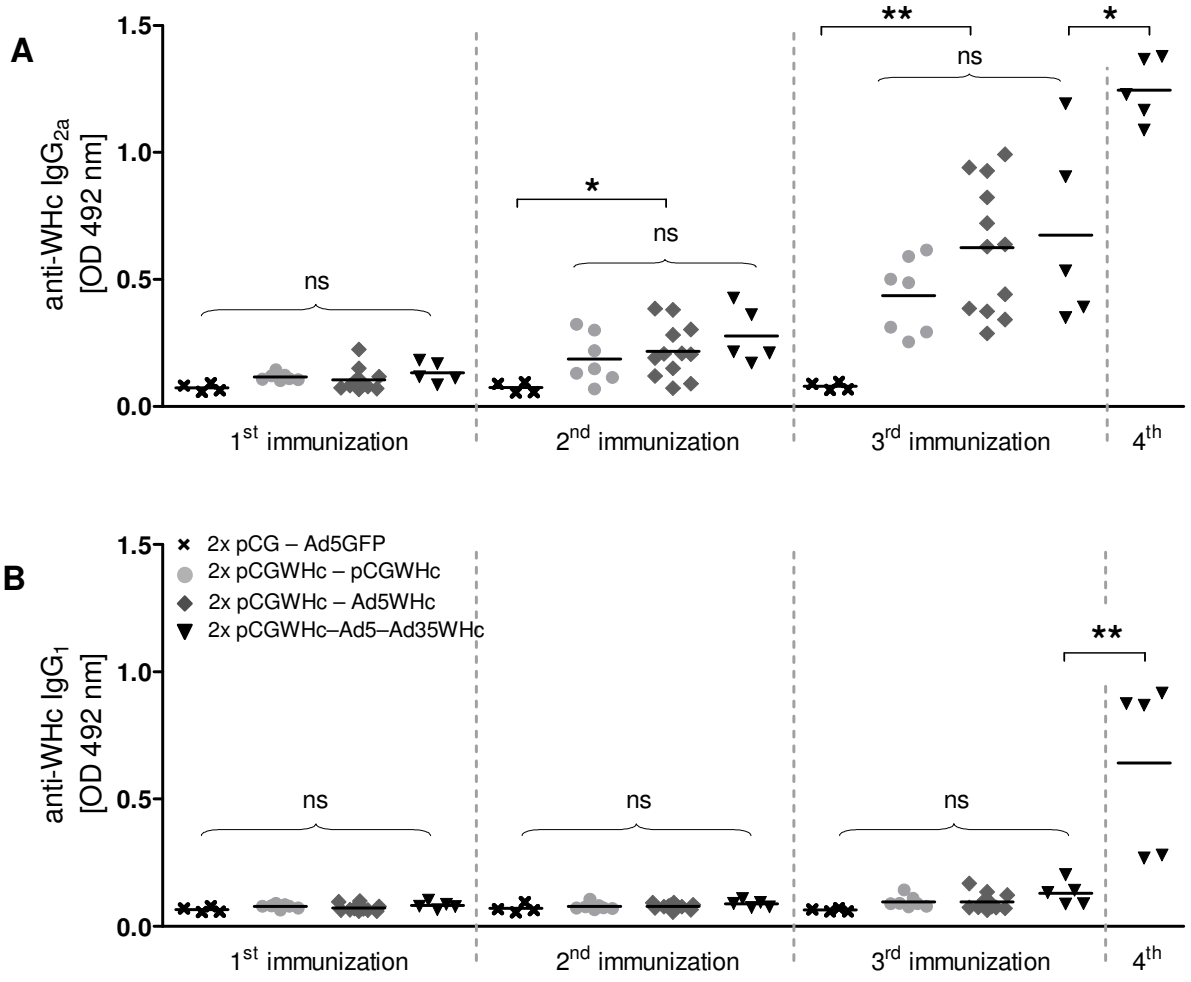

Fig. 5.27 Detection of anti-WHc IgG isotypes: IgG2a (A) and IgG1 (B), in the sera of 1217 WHV Tg mice immunized in the heterologous prime-boost regimen using recombinant adenoviral vectors expressing WHcAg

The sera of mice were obtained from blood samples collected two weeks after each immunization and diluted 1:250 in PBS. WHcAg-specific ELISA was peformed using IgG isotype-specific (IgG_{2a} or IgG_1) anti-mouse antibodies coupled to peroxidase. The statistical analysis between the groups was performed using the unpaired Student *t* test. Asterisks mark the significant difference (* < 0,05; ** < 0,005; ns – not significant).

Anti-WHs antibody-specific ELISA demonstrated that DNA immunization alone is not able to induce anti-WHs (Fig. 5.28). No anti-WHs antibodies were seen in mice immunized one, two and three times with pCGWHc. The levels of anti-WHs were comparable to the background values obtained from mice vaccinated with "empty" pCG plasmid. The anti-WHs antibodies were found in the sera of 13 out of 17 mice immunized in the heterologous DNA prime - AdV boost manner, after the boosting immunization with Ad5WHc. The level of anti-WHs in those mice was significantly higher in comparison to the control mice and mice immunized only with DNA ($P < 0{,}005$). The levels of anti-WHs increased additionally after the 4th (second boost) immunization with Ad35WHc. This result was statistically significant in comparison to mice boosted with adenoviral vector only once ($P < 0{,}005$).

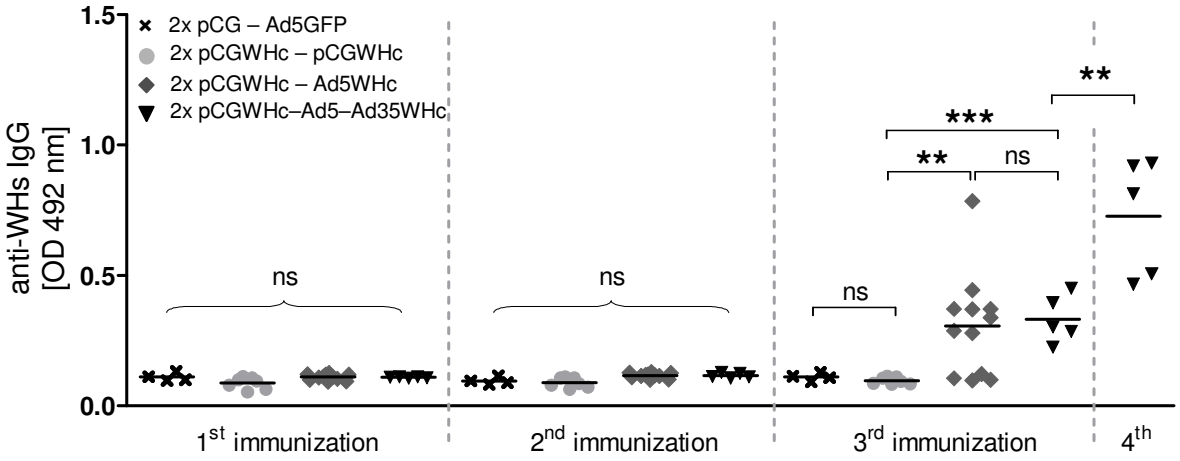

Fig. 5.28 Detection of anti-WHs IgG antibodies in the sera of 1217 WHV Tg mice immunized in the heterologous prime-boost regimen using recombinant adenoviral vectors expressing WHcAg

The sera of mice were obtained from blood samples collected after each immunization and diluted 1:250 in PBS. WHsAg-specific ELISA was performed using anti-mouse IgG antibody coupled to peroxidase. The statistical analysis between the groups was performed using the unpaired Student *t* test. Asterisks mark the significant difference (** < 0,005; *** < 0,0005; ns – not significant).

5.6.2 Evaluation of the CD8$^+$ T cell response

To evaluate whether heterologous DNA-AdV immunization was able to break the tolerance against WHcAg, the evaluation of the CD8$^+$ T cell response was performed in the immunized mice. The comparison of the WHcAg-specific CD8$^+$ T cell responses induced by DNA–Ad5WHc or DNA–Ad5WHc-Ad35WHc with DNA only immunization regimen was performed by intracellular IFNγ staining of splenocytes.

Splenocytes were isolated two weeks after the last immunization and were stimulated *in vitro* with the $CD8^+$ T cell epitope c13-21. After 7 days of culturing, the cells were restimulated for 6h with c13-21 and stained for IFNγ as mentioned in the Methods section (4.9.1). Splenocytes obtained from mice immunized with "empty" pCG plasmid and Ad5GFP served as controls.

The percentages of $IFN\gamma^+$ $CD8^+$ T cells determined in the spleens of mice vaccinated in the DNA prime – Ad5WHc boost manner were higher in comparison to the only DNA-immunized group (Fig. 5.29A-B). The IFNγ response after the stimulation of splenocytes with c13-21 was ranging from 0,2% to 2,2% (mean 1,0%) for pCGWHc – immunized mice and 0,7% to 11,4% (mean 5,0%) for pCGWHc-Ad5WHc (Fig. 5.29B). A five-fold increase in IFNγ producing $CD8^+$ T cells was found in mice immunized in DNA-Ad5WHc manner as compared to the DNA only – immunized mice ($P < 0,005$). Unexpectedly, the magnitude of IFNγ response did not increase in the group of mice that received the second boosting immunization with Ad35WHc. The mean percentages of $IFN\gamma^+$ $CD8^+$ T cells directed against c13-21 in this group were 3,8% and were slightly lower than in the DNA-Ad5WHc group. The stimulation of splenocytes with peptide c13-21 obtained from mice immunized with "empty" pCG plasmid and Ad5GFP induced no IFNγ response (0,1% to 0,3% of $IFN\gamma^+$ $CD8^+$ T cells). The comparison of the responses to stimulation with WHcAg-derived epitope measured for groups immunized with WHcAg-expressing vaccines was significantly higher than those detected for the control group ($P < 0,05$). No statistically significant difference between all analysed groups of mice was demonstrated in the unstimulated and unrelated peptide controls.

To evaluate the magnitude of the WHcAg-specific $CD8^+$ T cell response elicited in 1217 WHV Tg mice, the comparison of the results with those obtained from C57BL/6 mice was performed. As expected, the percentages of IFNγ-producing $CD8^+$ T cells detected in the splenocytes of 1217 WHV Tg mice were significantly lower compared to those in C57BL/6 mice (Fig. 5.29C). The mean percentages of $IFN\gamma^+$ $CD8^+$ T cells directed against c13-21 in the group of mice immunized only with DNA vaccine were 1% in 1217 WHV Tg mice and 21,9% in C57BL/6 mice. In the groups of mice immunized in the heterologous pCGWHc-Ad5WHc manner the mean percentages of $IFN\gamma^+$ $CD8^+$ T cells directed against c13-21 were 5% in 1217 WHV Tg mice and 65,7% in C57BL/6 mice. Those results were statistically significant ($P < 0,0005$). No

difference in the number of IFNγ producing cells between WHV Tg mice and C57BL/6 mice was observed in the control groups immunized with vaccines that do not express WHcAg.

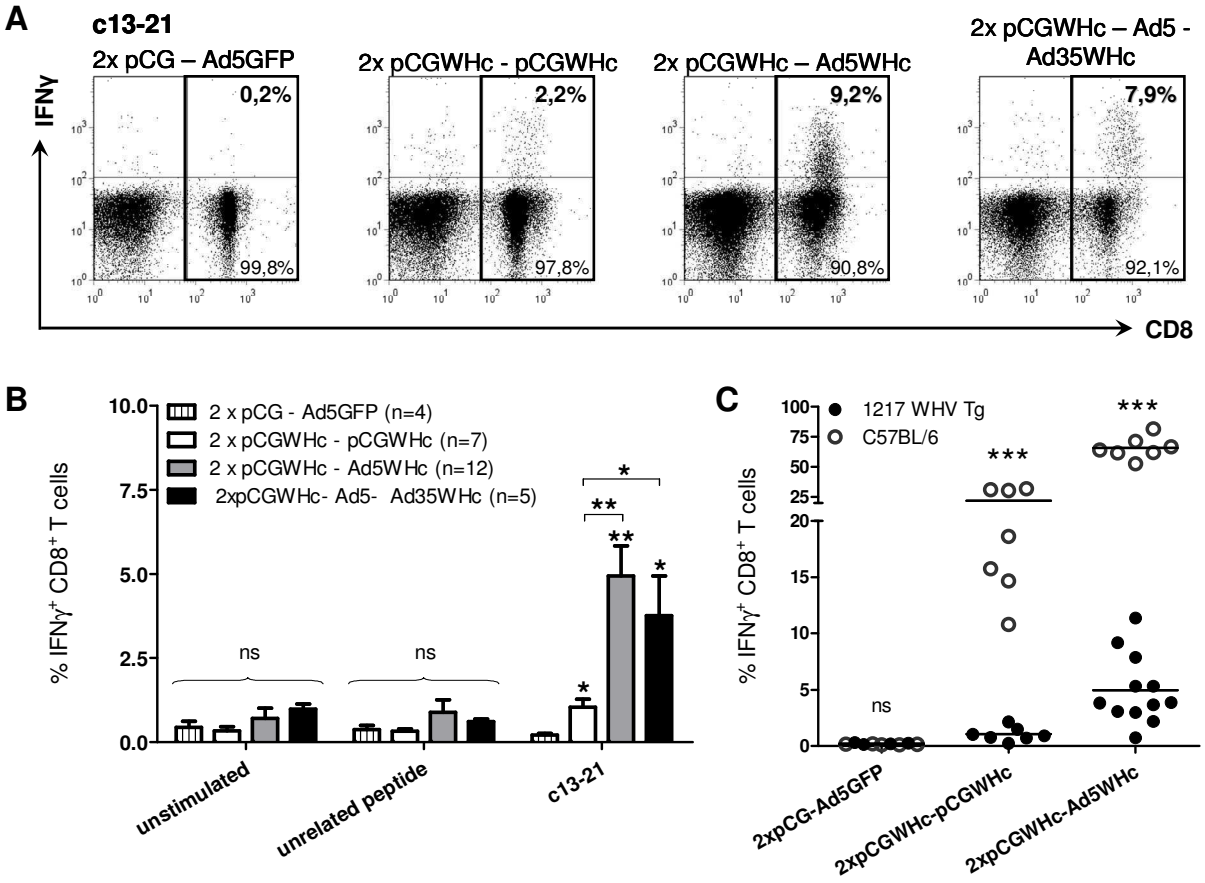

Fig. 5.29 Evaluation of CD8⁺ T cell responses induced by the heterologous prime-boost regimen using recombinant adenoviral vectors expressing WHcAg in 1217 WHV Tg mice

Splenocytes were expanded *in vitro* for 7 days in the presence of CD8⁺ T cell epitope c13-21 and stained for intracellular IFNγ.

A. Dotplots of the splenocytes of a representative mouse from each immunization group. Presented values indicate the percentage of IFNγ⁺ CD8⁺ T cells in the CD8⁺ T cell population.

B. CD8⁺ T cell response in murine splenocytes with c13-21. The bars represent the mean value obtained for the analyzed group of mice including SEM. Unstimulated cells and cells stimulated with unrelated CMV-derived peptide served as controls. The statistical analysis between the groups was performed using the unpaired Student *t* test (* < 0,05; ** < 0,005; ns – not significant).

C. Comparison of the magnitude of IFNγ responses obtained for 1217 WHV Tg and C57BL/6 mice after stimulation with c13-21. The statistical analysis between the groups was performed using the unpaired Student *t* test (*** < 0,0005; ns – not significant).

To further study the effector functions of the $CD8^+$ T cells induced by the heterologous prime-boost regimen in 1217 WHV Tg mice, the capacity of $CD8^+$ T cells to degranulate was evaluated. The expression of CD107a degranulation marker was compared to the IFNγ production in splenocytes of mice immunized in pCGWHc prime – AdV boost manner and only with pCGWHc plasmid. As controls the splenocytes of mice primed two times with "empty" pCG plasmid and boosted with Ad5GFP were used.

As presented in Fig. 5.30, the percentages of the double-positive $CD107a^+$ $IFN\gamma^+$ $CD8^+$ T cells were significantly higher in groups of mice boosted one time with Ad5WHc or two times with Ad5WHc/Ad35WHc (mean values for both groups: 2,8%), than in pCGWHc only immunized mice (mean value: 0,5%; $P < 0,05$). The percentages of cells co-expressing CD107a, IFNγ and CD8 detected in the DNA only immunized group were elevated in comparison to the control group immunized with "empty" pCG plasmid and Ad5GFP (mean values 0,5% vs 0,1%). However, this difference was not statistically significant. In addition, no statistically significant difference in the percentages of only IFNγ-producing cells was detected between the immunized groups and control mice, even though the values were elevated in pCGWHc-Ad5WHc immunized mice (mean values: 0,3% vs 1,7%). The mean percentage values of $CD8^+$ T cells expressing the CD107a degranulation marker in both DNA prime–AdV boost groups (mean: 2,3%) were significantly higher than the background value of 0,8% detected in the splenocytes of control mice ($P < 0,05$). No significant difference in the amount of $CD107a^+$ $CD8^+$ T cells was detected between the DNA only immunized mice and control group (mean values: 0,8% vs 1,2%).

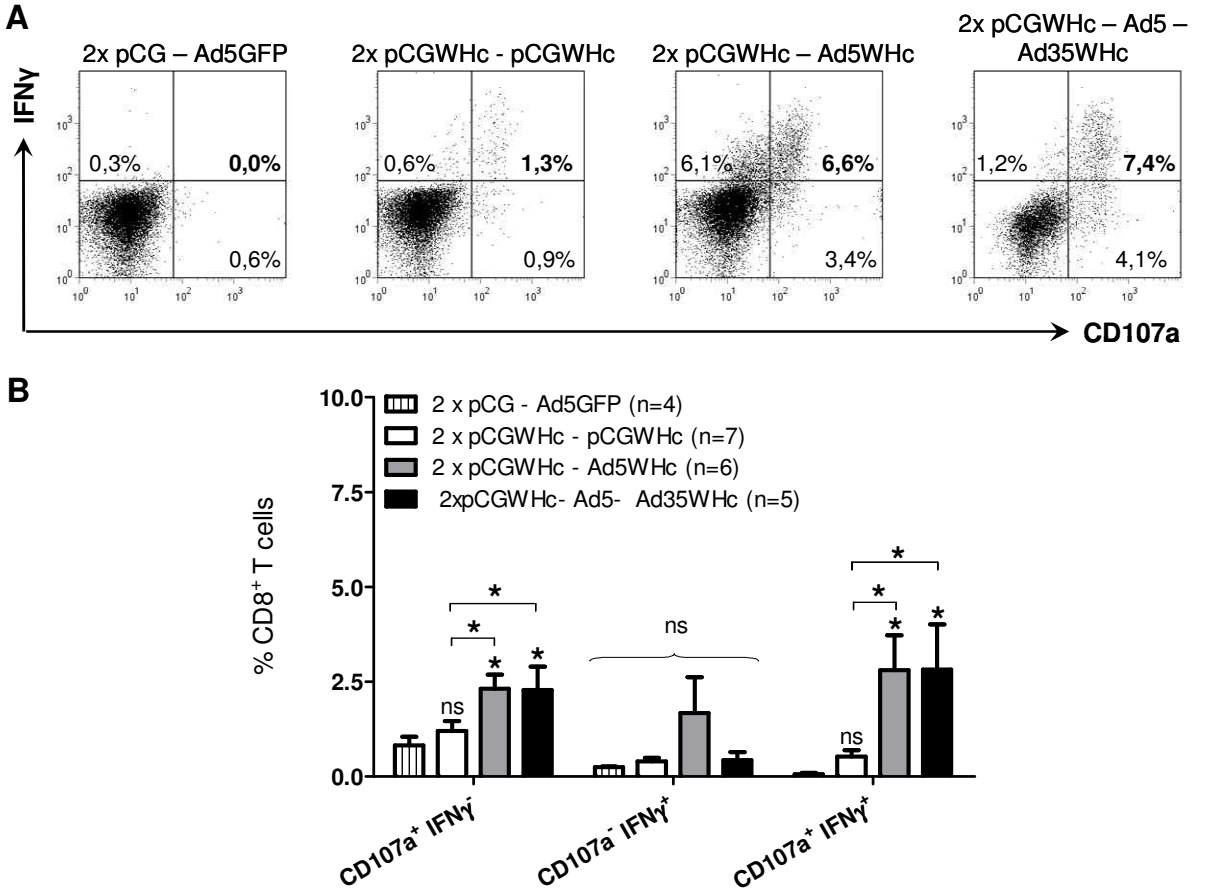

Fig. 5.30 Evaluation of degranulation activity of IFNγ$^+$ CD8$^+$ T cells induced by the heterologous prime-boost regimen in 1217 WHV Tg mice

Splenocytes were expanded *in vitro* for 7 days with the epitope c13-21 and subsequently restimulated for 5h in the presence of the CD107a antibody. Afterwards the cells were stained for the CD8 T cell marker and intracellularly for IFNγ.

A. Dotplots of the splenocytes of a representative mouse from each immunization group. The presented values indicate the percentage of CD107a$^+$ or/and IFNγ$^+$ CD8$^+$ T cells in the CD8$^+$ T cell population.

B. Degranulation capacity of IFNγ$^+$ CD8$^+$ T cells. The bars represent the mean value obtained for the analyzed group of mice including SEM. The statistical analysis between the groups was performed using the unpaired Student *t* test (* < 0,05; ns – not significant).

To further investigate the influence of the heterologous DNA prime – AdV boost regimen on multiple T_{H1} type cytokine production, the expression of IFNγ, TNFα and IL-2 was measured in splenocytes of WHV Tg mice stimulated *in vitro* for 6h with peptide c13-21 (Methods, section 4.9.1).

As presented in Fig. 5.31A, the immune response detectable after 6h stimulation was quite low in the splenocytes of WHV Tg mice. The background percentages of the T_{H1} type cytokine producing CD8$^+$ T cells obtained for most of the tested mice made the analysis impossible for the whole group of mice. Therefore, one mouse

demonstrating a positive percentage of the cytokines producers was chosen from each immunization group for the analysis (indicated by the arrows). The determination of single, double and triple positive cells that produce IFNγ, TNFα and IL-2 within the $CD8^+$ T cell population was performed. The absolute number of single, double and triple cytokine producing cells was quantified for one mouse in the group and the percentages of cells secreting one, two or all cytokines was evaluated.

Mouse number 58 which was immunized twice with pCGWHc plasmid and boosted with Ad5WHc demonstrated the highest percentages of IFNγ and TNFα expressing $CD8^+$ T cells of all analysed mice (3,5% and 2,4% respectively). The percentage of IL-2 secreting $CD8^+$ T cells detected for mouse 58 was 0,9% (Fig. 5.31A). Moreover, mouse 58 showed the highest proportion of triple and double cytokine producers: 12% and 53% respectively. The highest proportion of double cytokine producers (75,1%) were the $CD8^+$ T cells co-expressing cytokines with the strongest antiviral activity IFNγ and TNFα (Fig. 5.31C), and the most abundant cytokine in the single producers group was IFNγ (74,1%; Fig. 5.31D). Mouse number 56 which was immunized three times with the plasmid DNA vaccine and mouse number 52 from DNA-Ad5WHc-Ad35WHc group exhibited comparable results. The percentages of IFNγ, TNFα and IL-2 secreting $CD8^+$ T cells were around 1,4%; 0,6%; 0,8% for mouse number 56 and 1,1%; 0,7%; 1,5% for mouse number 52, respectively (Fig. 5.31A). Approximately, 10% of triple cytokine producers and 38% of double cytokine producers were detected for mouse 56. The percentages of $CD8^+$ T cells that simultaneously express two or three cytokines as detected in mouse 52 were 7% and 35% (Fig. 5.31B). The highest proportion of the double producers detected for both mice was found in the $CD8^+$ T cells co-expressing IFNγ and IL-2 (approximately 60%). The $IFN\gamma^+$ $TNF\alpha^+$ $CD8^+$ T cells were detectable in a frequency of 36% (Fig. 5.31C). As Fig. 5.31D shows, the most common cytokine detected in the single cytokine producer population for mouse 56 was IFNγ (55,4%). Mouse 52 showed comparable percentages of IFNγ and TNFα in the single producers group (41,9% and 38,7%, respectively).

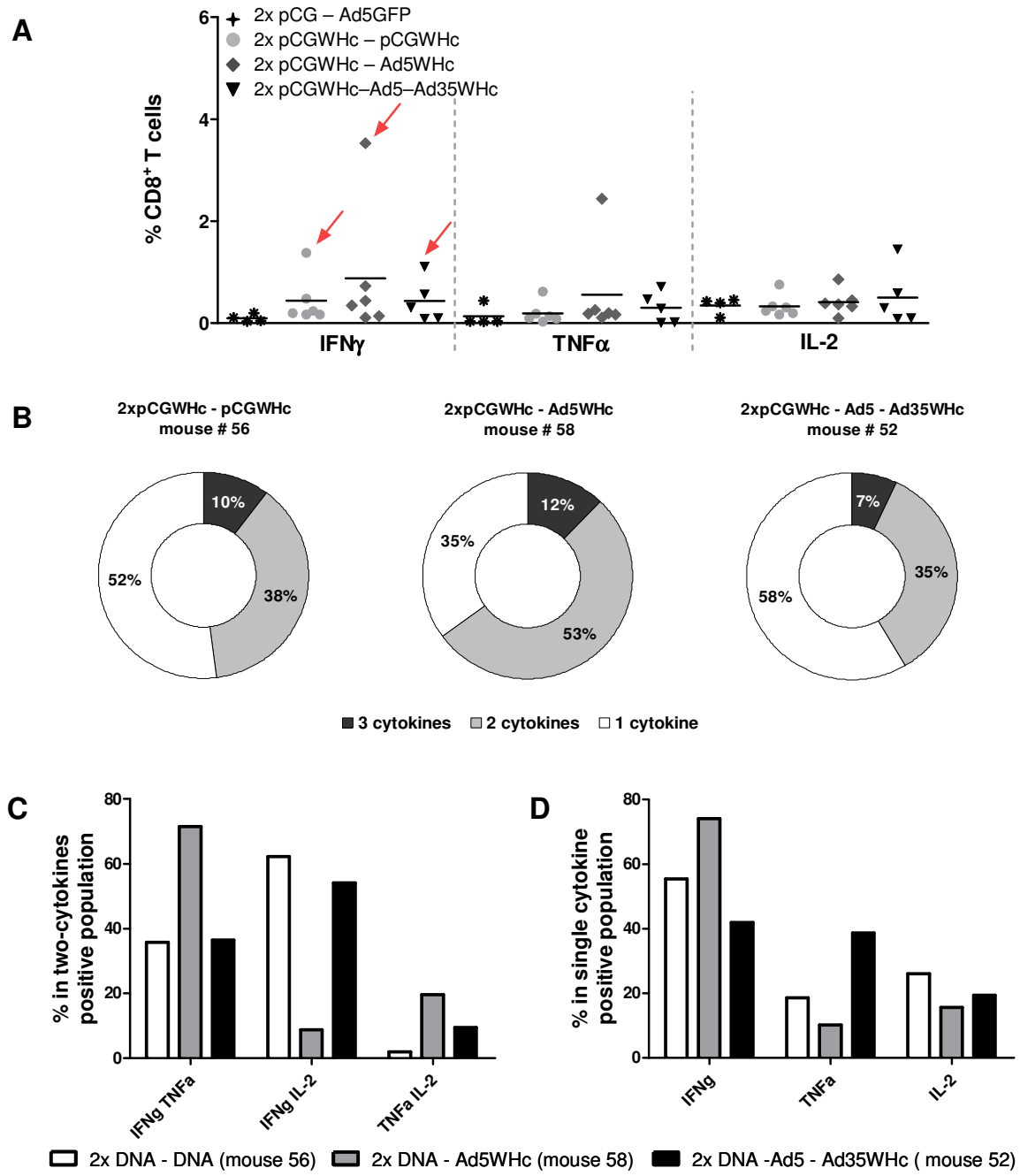

Fig. 5.31 Evaluation of multiple cytokine production by CD8$^+$ T cells induced by the pCGWHc and heterologous prime-boost immunization in 1217 WHV Tg mice

Splenocytes were stimulated *in vitro* for 6h with the epitope c13-21 and stained intracellularly for IFNγ, TNFα and IL-2.

A. The expression profile of T_{H1} type cytokines: IFNγ, TNFα and IL-2. The arrows indicate the mice from each immunization group used for detailed analysis.

B. Evaluation of multifunctional CD8$^+$ T cells. The percentage of single, double and triple producers in cytokine-positive CD8$^+$ T cell population as detected in chosen mice from each immunization group.

C. The percentages of double cytokine producers as detected in chosen mice from each immunization group.

D. The percentages of single cytokine producers as detected in chosen mice from each immunization group.

Those results indicate that the immunization of 1217 WHV Tg mice with heterologous DNA-AdV regimen breaks the immune tolerance and induces humoral and cellular immune responses against WHV proteins. Moreover, the immunizations with WHcAg-expressing vaccines were able to partially restore the multifunctionality of the $CD8^+$ T cells in the 1217 WHV Tg mouse model.

5.6.3 Impact of the immunizations on WHV replication

To examine the impact of the WHcAg-based immunizations on the WHV replication in 1217 WHV Tg mice, the viral loads were monitored in the serum of mice before the immunizations were performed (time point of cardiotoxin pretreatment) and afterwards, at the time point of sacrifice (Fig. 5.32). The quantification of WHV DNA was performed using real-time PCR analysis as described in the Methods section (4.13.3). As expected, in the control group of mice immunized with unrelated vectors that did not express WHcAg, no difference in the viral loads in serum at the beginning and at the end of the experiment was observed (Fig. 5.32A). In the group immunized three times with plasmid DNA only vaccine – pCGWHc, two out of seven mice (29%) had undetectable viral loads at the end of the experiment (Fig. 5.32B). All the other mice except one, showed a statistically significant 1 to 2 log decrease in viral load after the immunizations ($P < 0,05$). As showed in Fig. 5.32C, mice immunized three times in the heterologous prime – boost manner using Ad5WHc demonstrated the most significant reduction in viral loads ($P < 0,0005$). At the end time point, the WHV DNA was undetectable in 10 out of 12 mice of this group (83%). In the group of mice that received the fourth immunization with Ad35WHc, all the mice showed a more than 2 log decrease in viral loads. Three out of five mice (60%) exhibited the WHV viremia below the detection limit at the end of the experiment (Fig. 5.32D).

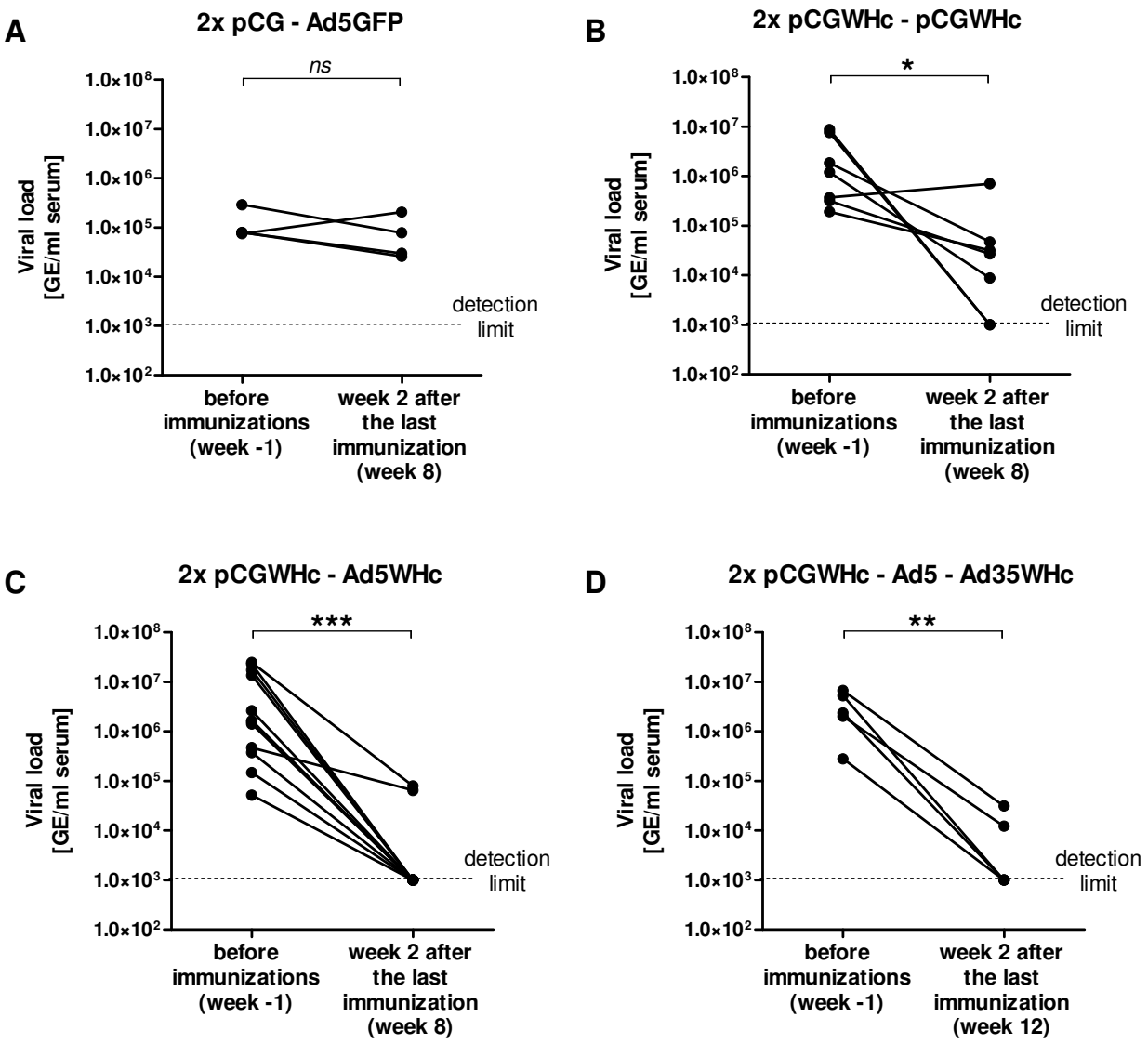

Fig. 5.32 Quantification of the viral loads in the serum of 1217 WHV Tg mice before and after the immunization trials

The viral load was evaluated by quantitative real-time PCR on DNA samples obtained from the serum of mice. The single pair of dots connected with the line represents values obtained from one mouse before and after the immunization trials (week 2 after the last immunization). The statistical analysis between the groups was performed using the Wilcoxon signed rank test (* < 0,05; ** < 0,005; *** < 0,0005; ns – not significant). *GE* – genome equivalents.

The data obtained in the WHV Tg mouse model confirm that immunization in the heterologous prime-boost regimen, using the recombinant AdVs induces stronger humoral and cellular immune responses and suppresses the WHV replication more efficiently.

5.7 Heterologous Ad5WHc – Ad35WHc immunization in naïve woodchucks protects against infection with WHV

It was demonstrated that DNA immunization of naïve woodchucks with plasmid encoding WHcAg protects the animals against infection after challenge with WHV [*Lu et al., 1999*]. Therefore, to determine the potency of recombinant adenoviral vectors to induce humoral and cellular immune responses and their protective efficacy in the challenge experiment in the woodchuck model, the animals were immunized in heterologous Ad5WHc – Ad35WHc regimen.

As shown in Fig. 5.33, two naïve woodchucks (number: 46949 and 46957) were intramuscularly immunized with Ad5WHc and four weeks later boosted with Ad35WHc. Three woodchucks (number 58059, 58063 and 70096) were immunized three times with the pCGWHc plasmid and served as a reference. Both groups of woodchucks were intravenously challenged with 1×10^7 genome equivalents (GE) of WHV strain 8. As the controls, two naïve woodchucks (number: 58055 and 58056) were inoculated with WHV, without vaccination, and served as controls.

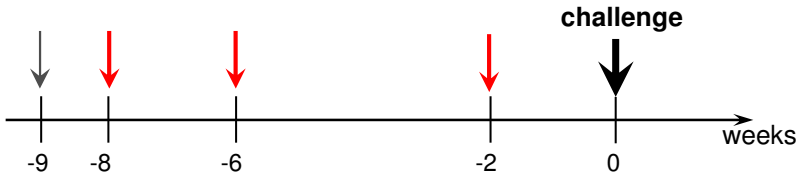

Vaccination groups:	-9	-8	-6	-2	0
A) 3x pCGWHc (*n=3*)	+	+	+	+	
B) Ad5WHc – Ad35WHc (*n=2*)	-	-	+ (Ad5WHc)	+ (Ad35WHc)	
C) naïve (*n=2*)	-	-	-	-	

Fig. 5.33 Schedule of DNA or recombinant adenoviral vectors immunization of naïve woodchucks

Three naïve woodchucks (58059, 58063 and 70096) were pretreated with cardiotoxin (grey arrow) and one week later subsequently immunized for 3 times with 1mg of pCGWHc plasmid intramuscularly in two to four weeks intervals. Two woodchucks (46949 and 46957) were intramuscularly immunized with 5×10^9 PFU Ad5WHc and four weeks later boosted with 1×10^{10} PFU of Ad35WHc. Two weeks after the last immunizations woodchucks were intravenously challenged with 1×10^7 GE of WHV, together with two naïve woodchucks (58055 and 58056) which served as controls.

5.7.1 Evaluation of the CTL response after immunizations

The T cell response in woodchucks was evaluated by flow cytometric analysis of CD107a expression on woodchucks PBMCs, as described in Methods section (4.9.1). Isolated PBMCs were stimulated *in vitro* for 3 days with WHcAg-derived epitope c96-110 or WHsAg-derived epitope s220-234 [*Frank et al., 2007*]. As controls unstimulated PBMCs and cells stimulated with unrelated CMV-derived peptide were used. Detection of degranulating cells was performed using cross-reactive anti-mouse CD107a antibody incubated with PBMCs for 5h. As the cross-reactive antibody that recognizes woodchuck CD8 molecule is yet not available, the population of $CD3^+$ $CD4^-$ lymphocytes was considered to be the cytotoxic $CD8^+$ T cells.

Vaccination with pCGWHc plasmid of the naïve woodchucks 58059 and 58063 induced significant degranulation response directed against WHcAg epitope c96-110 in woodchuck 58063 (Fig. 5.34). The WHcAg-specific CTL were detectable after two immunizations and the magnitude of response increased after the third plasmid injection. The percentage of 2,7% $CD107a^+$ T cells in $CD3^+$ $CD4^-$ population was 4-fold higher than the background values of 0,7% and 0,6% in negative controls. The woodchuck number 58059 demonstrated slightly elevated percentage of WHcAg-specific degranulating T cells: 0,9% (after three pCGWHc immunizations) in comparison to the controls (0,5%). Nevertheless, this result can be hardly considered as positive. Therefore, the experiment was repeated in woodchuck 70096. Three immunizations with WHcAg-expressing DNA vaccine induced the degranulation response directed against peptide c96-110. Nearly 5-fold increase in the percentage of $CD107a^+$ $CD3^+$ $CD4^-$ T cells detected after stimulation with WHcAg peptide (2,5%) was significantly higher than those detected for unstimulated and unrelated peptide controls (0,5% and 0,6%, respectively).

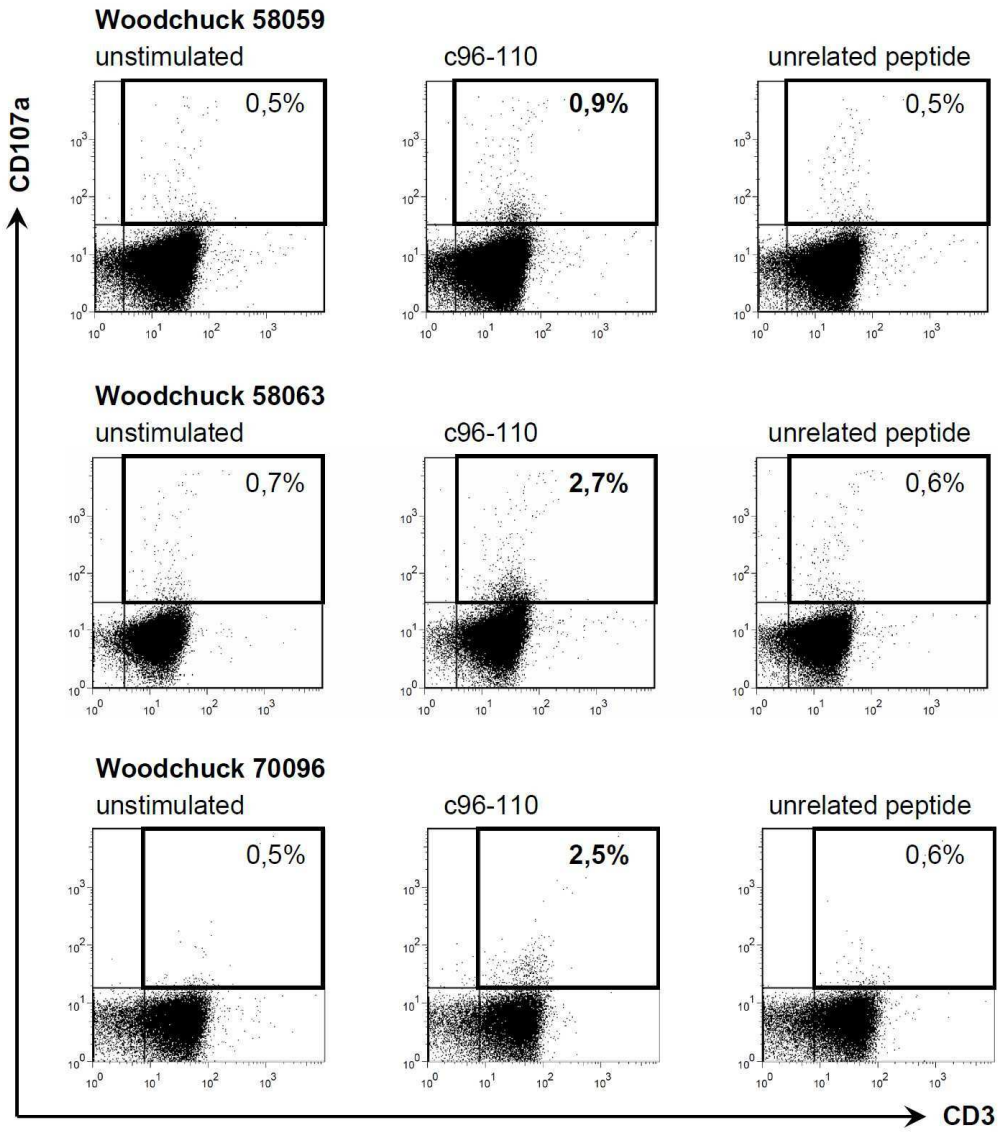

Fig. 5.34 Dotplots of PBMCs from woodchucks after three immunizations with pCGWHc plasmid

PBMCs were expanded *in vitro* for 3 days with WHcAg-derived epitope c96-110. Unstimulated cells and cells stimulated with unrelated CMV-derived peptide served as negative controls. The T cell response was evaluated by CD107a degranulation assay. The cells were gated on lymphocyte population, $7AAD^-$ and $CD4^-$ cells. Presented values show the percentage of $CD107a^+$ $CD3^+$ $CD4^-$ T cells in the $CD3^+$ $CD4^-$ T cell population.

Immunization of woodchucks 46949 and 46957 with newly constructed recombinant adenoviral vectors, expressing WHcAg, proved their potency to elicit a robust T cell response (Fig. 5.35). Just one immunization with Ad5WHc induced a comparable magnitude of WHcAg-specific degranulation responses as three plasmid DNA immunizations. The percentage of 2,8% WHcAg-specific CTLs were detected for woodchuck 46949 and 3,6% for 46957 (Fig. 5.35A). Those percentages were 5,6-fold

higher than the background value of 0,5% for woodchuck 46949 and 4,5-fold higher than the background value of 0,8% for woodchuck 46957. After immunization with Ad35WHc the induced WHcAg-specific CTL response was significantly boosted in both animals (Fig. 5.35B). Over 4-fold increase in the percentage of WHcAg-specific $CD107a^{+}$ $CD3^{+}$ $CD4^{-}$ T cells after boosting immunization (13,3%) was shown in woodchuck 46949. Woodchuck 46957 demonstrated a 2-fold increase in WHcAg-specific CTLs (7,4%).

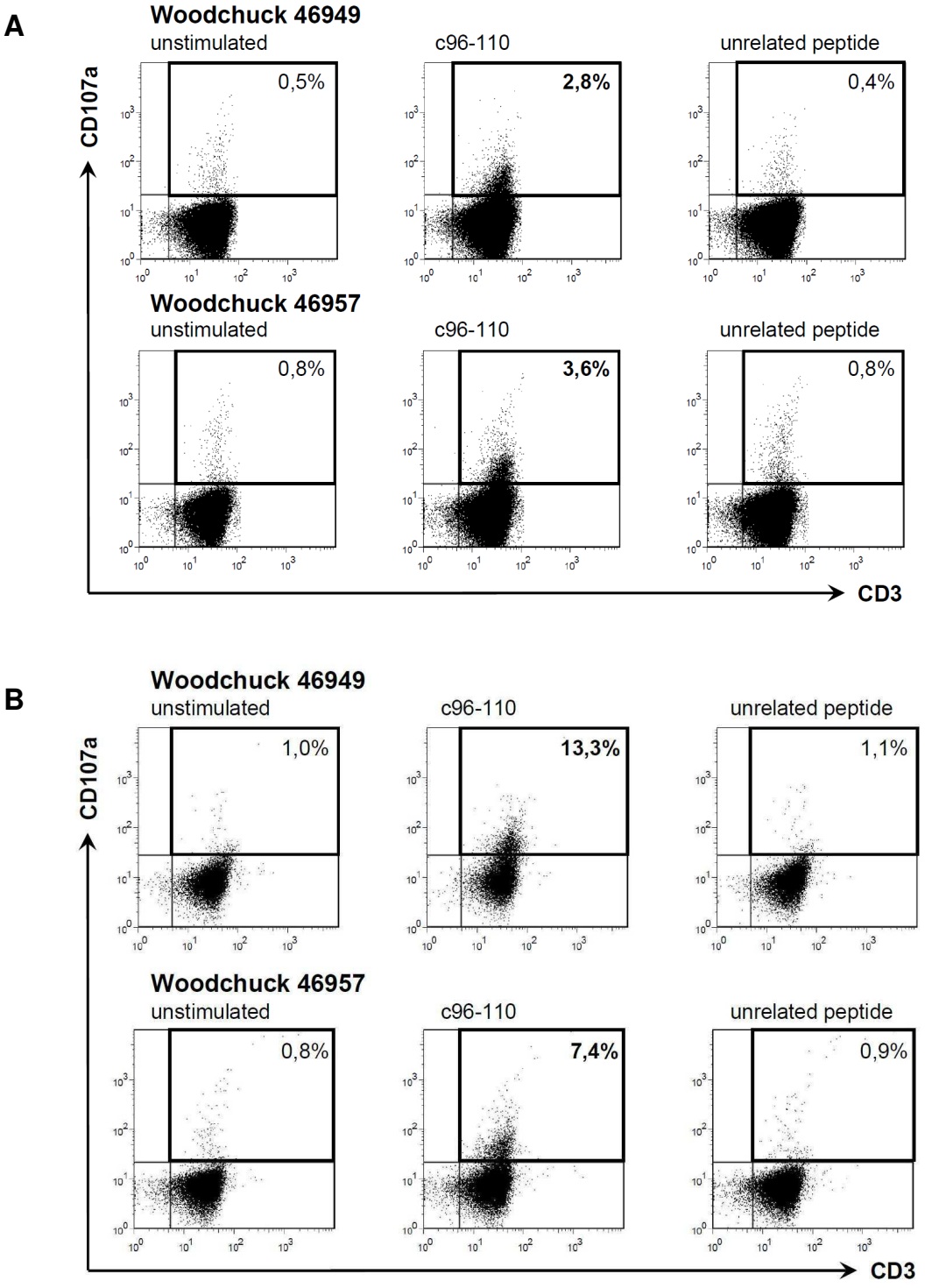

Fig. 5.35 Dotplots of PBMCs from woodchucks immunized with recombinant AdV: Degranulation response after immunization with Ad5WHc (A) and after booster immunization with Ad35WHc (B)

PBMCs were expanded *in vitro* for 3 days with WHcAg-derived epitope c96-110. Unstimulated cells and cells stimulated with unrelated CMV-derived peptide served as negative controls. The T cell response was evaluated by CD107a degranulation assay. The cells were gated on lymphocyte population, $7AAD^-$ and $CD4^-$ cells. Presented values show the percentage of $CD107a^+$ $CD3^+$ $CD4^-$ T cells in the $CD3^+$ $CD4^-$ T cell population.

5.7.2 Monitoring of WHV infection after challenge

All immunized woodchucks were intravenously inoculated with WHV (1×10^7 GE) and monitored weekly for markers of infection (Methods, section 4.4.4). Two naïve woodchucks 58055 and 58056 served as controls in the experiment. The infection of WHV in woodchucks was monitored by WHV PCR (detection limit approximately 1×10^3 WHV GE per ml of serum) and the golden standard dot-blot hybridization (limit 5×10^7 WHV GE per ml of serum), as described in Methods section (4.13.2 and 4.13.4, respectively) Detection of WHV was correlated with WHcAg- and WHsAg-specific CTL responses measured by CD107a degranulation assay and the level of the serum glutamic oxaloacetic transaminase (GOT) [Methods, section 4.15]. As WHV is a non-cythopatic virus, the elevation of GOT (value above 50 international units per l; IU/l) in the serum of the animals is a good indicator of CTL-mediated liver damage.

The immunization of woodchuck 58063 with plasmid DNA vaccine: pCGWHc induced the WHcAg-specific T cell response. As shown in Fig. 5.36A, WHV DNA was detected in the serum at week 2 and 3 post-infection (pi). Detection of WHV DNA using dot-blot hybridization did not lead to any positive result. At week 4 and 12 pi, the WHcAg-specific CTLs were detected in the peripheral blood (2,3% and 1,8%, respectively). No WHsAg-specific T cell response and no elevation in GOT levels was observed. Monitoring the infection course of the woodchuck 70096, which also demonstrated WHcAg-specific T cell response after pCGWHc vaccination, showed similar results. The graph is presented in the Appendix section (Fig. 10.5).

The woodchuck 58059, in which induction of WHcAg-specific CTLs by DNA immunizations was borderline, demonstrated viremia from week 2 to week 9 pi (Fig. 5.36B). The peak of viremia was detected by dot-blot hybridization at week 6 pi. At week 3 pi, the peak of WHcAg- and WHsAg-specific degranulation responses was detected in PBMCs (6,4% of WHcAg-specific CTLs and 1,9% of WHsAg-specific CTLs). In addition, the WHcAg-specific CTLs were detected at week 8, 11 and 12 pi. The elevation of GOT level in the serum at week 1 and week 6 to 13 pi indicated a massive influx of T cells into the liver and their increased cytotoxic activity. The peak of serum GOT level (117 IU/l) at week 10 pi correlated with WHV clearance from the blood stream.

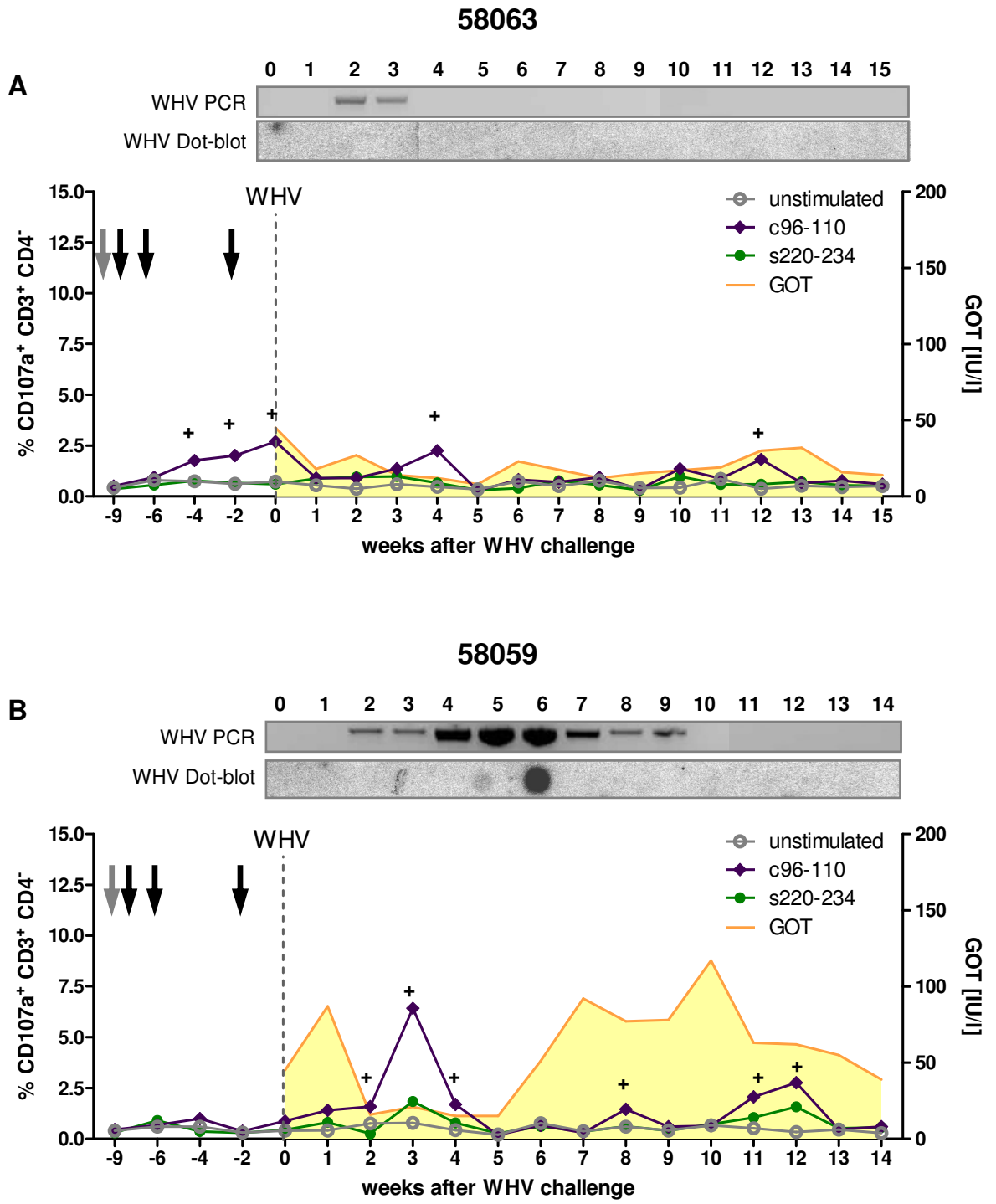

Fig. 5.36 Correlation of WHcAg- and WHsAg-specific CTL responses with WHV presence and GOT levels in pCGWHc immunized woodchucks: 58063 (A) and 58059 (B)

Woodchucks were pretreated with cardiotoxin (grey arrow) and immunized intramuscularly three times with pCGWHc plasmid (black arrows). WHcAg- and WHsAg-specific T cell response was measured by CD107a degranulation assay of woodchuck PBMCs expanded *in vitro* for 3 days with epitope c96-110 and s220-234. Unstimulated cells served as negative controls. The values show the percentage of $CD107a^+$ $CD3^+$ $CD4^-$ T cells in the $CD3^+$ $CD4^-$ T cell population. The "+" sign marks the positive responses. The T cell responses were correlated with the presence of WHV DNA and GOT levels in the serum.

Heterologous immunization of the two naïve woodchucks, 46949 and 46957, with Ad5WHc/Ad35WHc induced the robust WHcAg-specific cellular immune response detectable at the time of the WHV inoculation (Fig. 5.37). After WHV challenge, woodchuck 46949 showed short-time low-level viremia at week 2 and 3 pi (Fig. 5.37A). The presence of WHV DNA in the blood was correlating with detectable WHcAg-specific T cell response (2,8% at week 2 and 2,1% at week 3 pi). At week 3 pi, the low percentage of WHsAg-specific CTLs (1,9%) was detected in the peripheral blood of the animal.

As shown in Fig 5.38B, WHV DNA was present in serum of woodchuck 46957 longer than in woodchuck 46949 (Fig. 5.37B). The viremia was detectable from week 2 and reached its peak at week 4 pi. At week 2 pi 6,7% of WHcAg-specific and 3,0% of WHsAg-specific $CD107a^{+}$ $CD3^{+}$ $CD4^{-}$ T cells were detected. The WHcAg-specifc CTLs were also present in the peripheral blood of woodchuck 46957 at week 3 pi (4,0%). At week 7 pi, a brief break-through of the infection was observed, followed by WHcAg-specific CTL detection at week 8 pi (3,1%), what resulted in the resolution of the infection.

At week 4 pi, only a slight elevation of GOT levels in both woodchucks was detected: 56 IU/l in serum of 46949 and 54 IU/l in serum of 46957, indicating a mild cytotoxic activity in the liver.

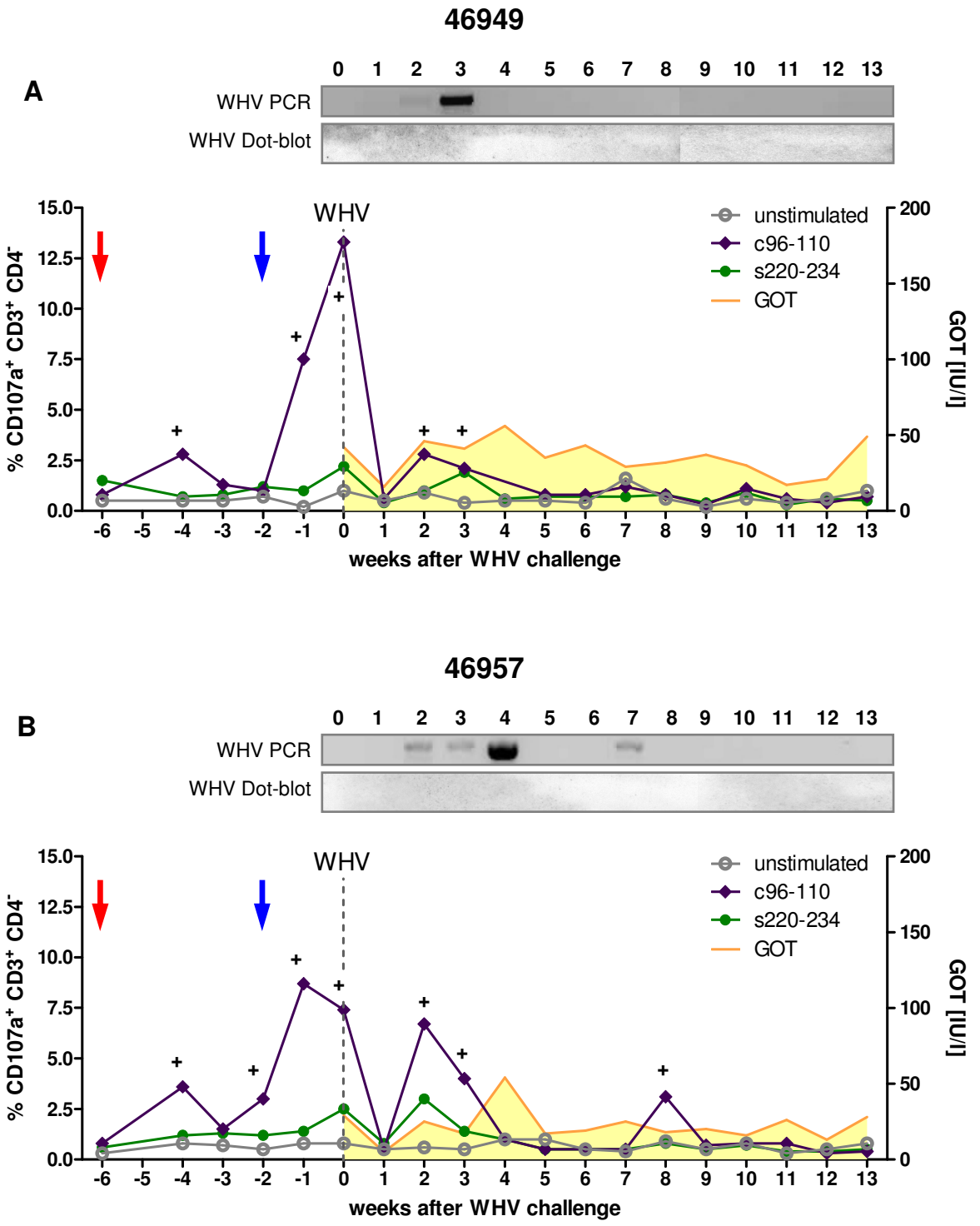

Fig. 5.37 Correlation of WHcAg- and WHsAg-specific CTL responses with WHV presence and GOT levels in Ad5WHc/Ad35WHc immunized woodchucks: 46949 (A) and 46957 (B)

Woodchucks were immunized with Ad5WHc (red arrow) and four weeks later boosted with Ad35WHc (blue arrow). WHcAg- and WHsAg-specific T cell response was measured by CD107a degranulation assay of woodchuck PBMCs expanded *in vitro* for 3 days with epitope c96-110 and s220-234. Unstimulated cells served as negative controls. The values show the percentage of $CD107a^+$ $CD3^+$ $CD4^-$ T cells in the $CD3^+$ $CD4^-$ T cell population. The "+" sign marks the positive responses. The T cell responses were correlated with the presence of WHV DNA and GOT levels in the serum.

Monitoring of WHV infection in the control woodchucks 58055 and 58056 revealed prolonged high-level viremia after the challenge in sera of both animals. As Fig. 5.38A shows, WHV DNA detected by WHV PCR was present between week 3 and 20 pi in the peripheral blood of woodchuck 58055. The high viral load was confirmed by dot-blot hybridization with WHV-specific probe. The positive signal was observed from week 6 to 15 pi. The low percentage of WHcAg-specific CTLs (2,6%) was detected at the beginning of infection at week 3. Afterwards, WHV-specific cytotoxic response was not measurable in the peripheral blood before the week 12 pi. The significant elevation of serum GOT level (100 IU/l) at week 20 pi and absence of WHV DNA in the blood at week 22 pi suggests the presence of effector WHV-specific T cells in the liver of 58055, that led to the resolution of WHV infection.

The other control woodchuck 58056 did not resolve the infection after WHV challenge. The WHV DNA evaluated by PCR was detected from week 3 pi and by dot-blot hybridization from week 5 pi (Fig. 5.38B). Both assays were positive through the whole monitoring period till week 24 pi. The WHV-specific T cell responses were generally not detectable in the peripheral blood during the examined 13 weeks pi. Only a slight elevation in the percentage of WHcAg-specific $CD107a^+$ $CD3^+$ $CD4^-$ T cells (1,8%) was detected at week 3 pi and WHsAg-specific CTLs (2,0%) at week 4 pi. No elevation of GOT levels above 50 IU/l was observed in the serum of the woodchuck 58056. Those results indicate lack of WHV-specific T cells activity in the liver, due to very high viral replication.

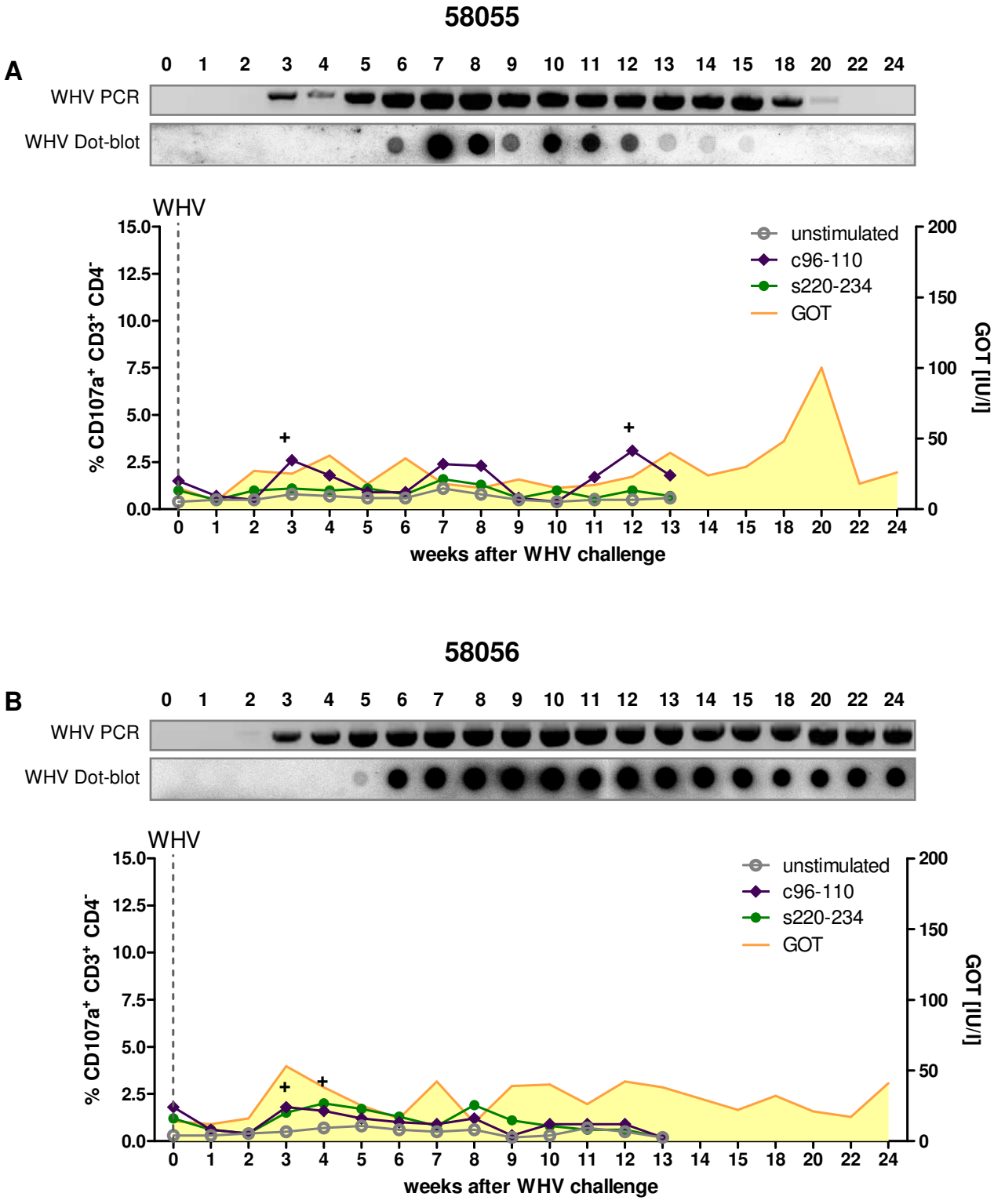

Fig. 5.38 Correlation of WHcAg- and WHsAg-specific CTL responses with WHV presence and GOT levels in control woodchucks: 58055 (A) and 58056 (B)

The woodchucks were intravenously inoculated with WHV. WHcAg- and WHsAg-specific T cell response was measured for 13 weeks by CD107a degranulation assay of woodchuck PBMCs expanded *in vitro* for 3 days with epitope c96-110 and s220-234. Unstimulated cells served as negative controls. The values show the percentage of $CD107a^+$ $CD3^+$ $CD4^-$ T cells in the $CD3^+$ $CD4^-$ T cell population. The "+" sign marks the positive responses. The T cell responses were correlated with the presence of WHV DNA and GOT levels in the serum.

5.7.3 Monitoring of the viral load after infection with WHV

The comparison of the viral loads between pCGWHc and Ad5WHc/Ad35WHc vaccinated woodchucks and control animals after WHV inoculation was performed by quantitative real-time PCR analysis (Methods, section 4.13.3).

As shown in Fig. 5.39, the immunized animals demonstrated not only a shorter WHV viremia period and lower viral load as compared to the control group (3 to 4 logs). Woodchucks 58063, 70096, 46949 and 46957 that developed WHcAg-specific CTL responses after three immunizations with pCGWHc plasmid or Ad5WHc/Ad35WHc were WHV positive in the blood for 2 to 4 weeks after the challenge. The quantified viral loads in those animals were ranging between $7,3\times10^4$ and $2,5\times10^6$ WHV GE/ml of serum (Fig. 5.39A-B). The pCGWHc-immunized woodchuck 58059, which did not develop significant WHcAg-specific T cell response, was WHV positive for 8 weeks, from week 2 to 9 pi. The peak of WHV viremia was detected at week 6 pi ($2,5\times10^9$ WHV GE/ml of serum). Afterwards, the viral load decreased and remained at the range of 1×10^6 WHV GE/ml of serum, until the resolution of infection at week 10. All animals that received immunizations remained WHV negative until the end of the monitoring period (week 22 pi, woodchucks 46949, 46957 and 70096) or week 25 pi; woodchucks 58059 and 58063).

The control woodchuck 58055 was WHV positive in the blood for 17 weeks after WHV infection (Fig. 5.39C). The peak of viral loads was detected at week 7 pi ($4,4\times10^9$ WHV GE/ml of serum). The high-level viremia, ranging between $6,3\times10^7$ and $1,3\times10^9$ WHV GE/ml of serum was observed until week 15 pi. At week 18 pi viral loads decreased and reached the value of $1,2\times10^6$ WHV GE/ml of serum. The woodchuck 58055 had undetectable viral loads (below 1×10^3 WHV GE/ml of serum) from week 22 to week 40 pi, the end of the monitoring period. The second control animal 58055 developed a chronic WHV infection. The viral loads reached the level of $1,4\times10^8$ WHV GE/ml of serum at week 5 pi and remained at a very high level: between $3,0\times10^9$ and $3,4\times10^{10}$ WHV GE/ml of serum until the end of the monitoring period (week 40 pi).

Those results indicate that the induction of a vigorous T cell response against WHcAg leads to the control of WHV and the rapid resolution of the infection.

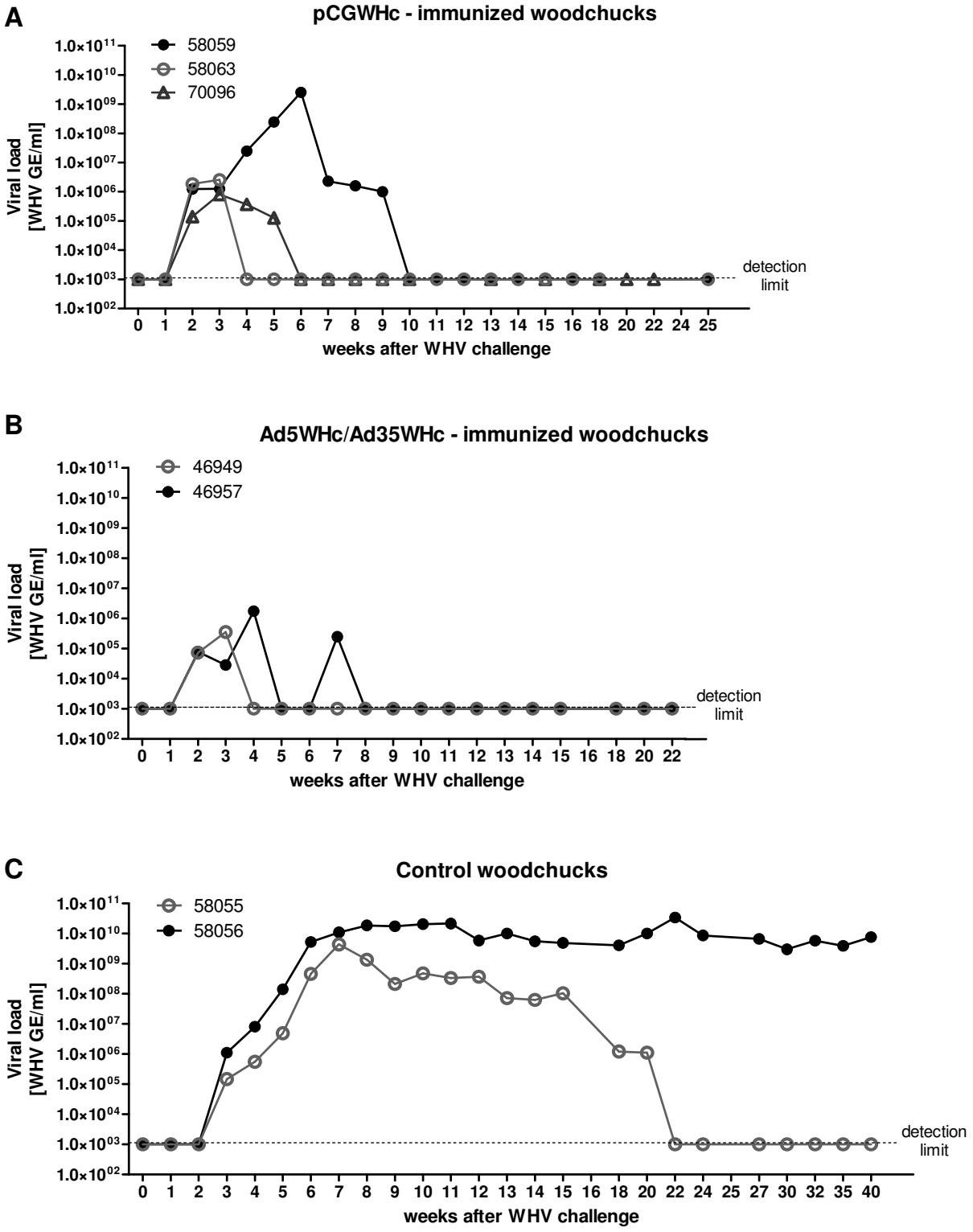

Fig. 5.39 Viral loads after WHV challenge experiment in naïve woodchucks: immunized with plasmid DNA vaccine (A), immunized with Ad5WHc/Ad35WHc (B), control animals (C)

The woodchucks were intravenously inoculated with 1×10^7 WHV GE (week 0). The viral DNA was extracted from woodchucks sera and the viral loads were quantified per ml of serum, using real-time PCR analysis.

5.7.4 Evaluation of the humoral immune response

Immunization with WHcAg-based vaccines induces the anti-WHc antibodies that do not possess the ability to neutralize the WHV virions [*Roos et al., 1989; Schodel et al., 1993*]. Induction of the neutralizing anti-WHs antibodies is crucial for the final clearance of the WHV infection [*Cote et al., 1986; Lu et al., 1999*]. To examine the impact of WHcAg-specific T cell response, elicited by pCGWHc or Ad5WHc/Ad35WHc immunization, on the induction of anti-WHs antibodies, the detection of anti-WHs antibodies was performed in the sera of woodchucks by ELISA (as described in Methods section 4.12). The effectiveness of the immunizations was evaluated by detection of anti-WHc antibodies by ELISA.

As shown in Fig. 5.40, anti-WHc antibodies were detectable in the serum of pCGWHc and Ad5WHc/Ad35WHc immunized woodchucks already after one immunization. The woodchuck 58059 (Fig. 5.40C) developed detectable WHcAg-specific antibodies after three pCGWHc immunizations, indicating that the immune response after vaccinations was insufficient, maybe due to incorrect vaccination. The anti-WHc levels were comparable in all immunized woodchucks after the infection with WHV and the antibodies were present until the end of the monitoring period.

The woodchucks 46949, 46957, 58063 and 70096, which were immunized in the proper way, anti-WHs antibodies were induced at week 2 pi. However, the levels of anti-WHs antibodies were higher in woodchucks vaccinated with recombinant adenoviral vectors, which demonstrated stronger WHcAg-specific T cell response after immunization. At the peak of anti-WHs antibodies level in the serum (week 3 pi), the OD_{492nm} value detected for representative woodchuck 46949 from Ad5WHc/Ad35WHc immunization group was 2,175 (Fig. 5.40A). As Fig. 5.40B shows, representative woodchuck 58063 immunized for three times with pCGWHc plasmid showed over 2-fold lower anti-WHs antibodies level (OD_{492nm} value 0,949) at the same time point. The amount of anti-WHs decreased in the animals from week 6 to 10 pi, as the WHV infection was not longer present. Comparable results were obtained from woodchuck 46957 and 70096, as shown in Fig. 10.6A-B (Appendix section). The woodchuck 58059 became anti-WHs positive later than the other immunized animals, at week 9 pi (Fig. 5.40C). The low level of anti-WHs antibodies was still detectable at the end of the monitoring period (week 25). The appearance of

anti-WHs antibodies in the serum of woodchuck 58059 correlated with the clearance of WHV DNA in the blood.

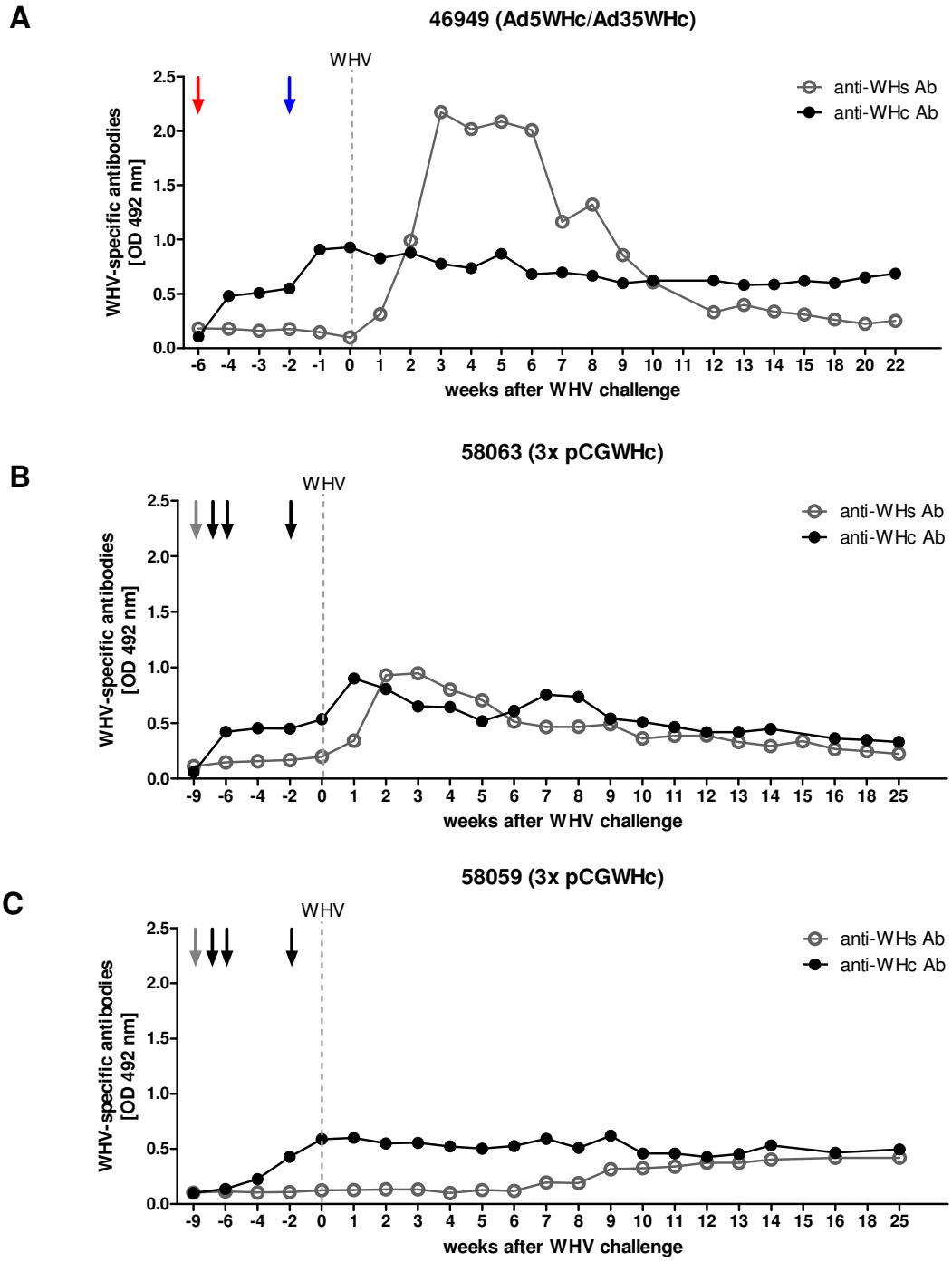

Fig. 5.40 Detection of anti-WHc and anti-WHs antibodies in the sera of woodchucks immunized with pCGWHc (B and C) plasmid or using recombinant adenoviral vectors expressing WHcAg (A)

Woodchuck 46949 was intramuscularly immunized with Ad5WHc (red arrow) and boosted with Ad35WHc (blue arrow). Woodchucks 58063 and 58059 were pretreated with cardiotoxin (grey arrow) and subsequently immunized for three times with pCGWHc plasmid (black arrows). The woodchucks were intravenously inoculated with 1×10^7 WHV GE (week 0). Woodchucks sera were diluted 1:10 in PBS. WHcAg- and WHsAg-specific ELISA was peformed using protein G coupled to peroxidase.

The control woodchuck 58055 (Fig. 5.41), which was intravenously infected with WHV, showed detectable anti-WHc antibodies at week 7 pi. Starting from week 9 pi the WHcAg-specific antibody level became comparable to those reached by immunized woodchucks. The antibodies were still present at the last screened time point: week 35 pi. The monitoring of anti-WHc antibodies of the second control woodchuck 58056 showed similar results (Appendix section, Fig. 10.6C). The anti-WHs antibodies were detected from week 18 to 24 pi. The appearance of WHsAg-specific antibodies correlated with WHV clearance from the peripheral blood at week 22 pi. The other control woodchuck, 58056, did not develop anti-WHc antibodies. Lack of anti-WHs correlates with WHV persistence through the monitoring period.

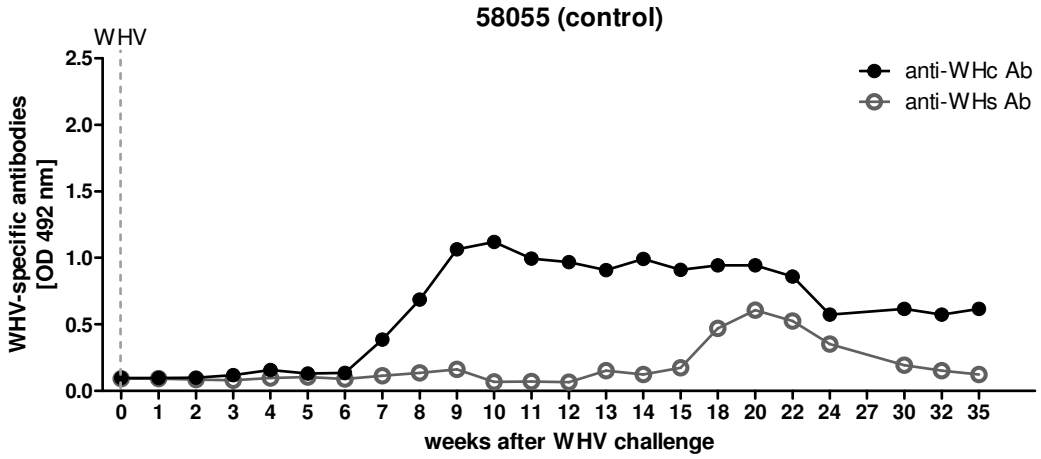

Fig. 5.41 Detection of anti-WHc and anti-WHs antibodies in the sera of control woodchuck 58055

The woodchuck was intravenously inoculated with 1×10^7 WHV GE (week 0). Woodchucks sera were diluted 1:10 in PBS. WHcAg- and WHsAg-specific ELISA was performed using protein G coupled to peroxidase.

Taken together, immunization of naïve woodchucks with heterologous Ad5WHc/Ad35WHc regimen induced stronger WHcAg-specific T cell response than immunization for three times with pCGWHc plasmid. The WHcAg-specific T cell response in immunized woodchucks led to early induction of anti-WHs antibodies and resolution of WHV infection. Those results emphasize the role of T cell response against WHcAg in control of hepadnaviral infections. WHcAg-specific T_H cells help in rapid and more robust secretion of anti-WHs as compared to the natural infection [*Millich et al., 1987*].

5.8 Evaluation of DNA prime – AdV boost immunization in combination with entecavir treatment of chronically WHV-infected woodchucks

To evaluate the effectiveness of heterologous DNA prime – AdV boost immunization regimen as the therapeutic vaccine in chronic hepadnaviral infections, the experiment based on the combination of antiviral treatment (entecavir, ETV) with immunizations of chronically WHV-infected woodchucks was performed.

Seven WHV chronic carriers were treated for 23 weeks with the guanosine nucleoside analogue ETV. For the first 12 weeks of therapy, the drug was administered in the dose of 0,2 mg per day by using osmotic pumps (Durect). From week 8 to 23 of the therapy, subcutaneous injections of 1mg of ETV were performed twice a week. At week 7, five of the seven ETV-treated animals were injected intramuscularly with cardiotoxin. Starting from week 8, the animals received subsequently 9 intramuscular immunizations with DNA plasmids, expressing WHcAg and WHsAg, Ad5WHc, and Ad35WHc as shown in Fig. 5.42. Two animals, treated only with ETV, served as a control in the experiment.

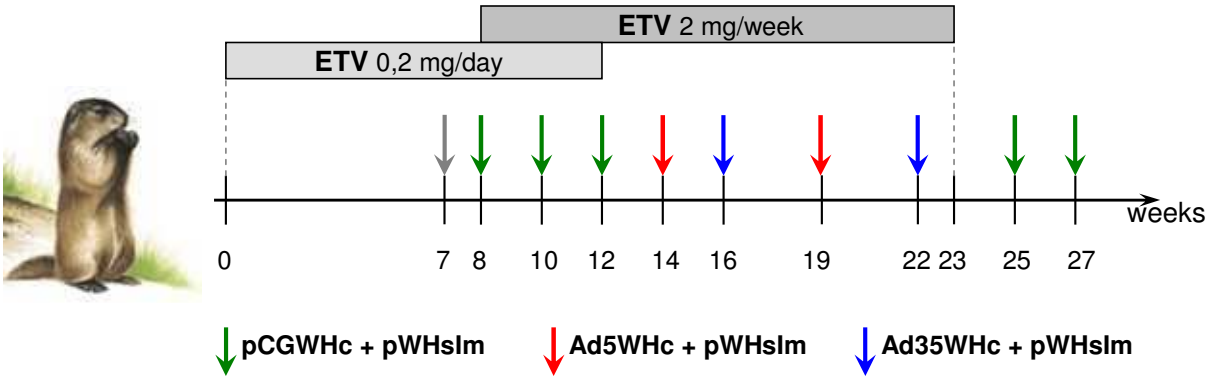

Fig. 5.42 Schedule of therapeutic DNA prime – AdV boost immunization in combination with entecavir treatment in chronic WHV carriers

Seven chronically WHV-infected woodchucks (number: 61786, 61787, 61789, 61791, 61792, 61793 and 61795) were treated with entecavir for 23 weeks. Initially, the drug was administered for 12 weeks in dose of 0,2 mg ETV per day, by mean of the osmotic pumps (Durect) implanted surgically under the skin of the animals. From week 8 to 23 of the therapy, subcutaneous injections of 1 mg ETV were performed twice a week. At week 7, five of the seven ETV-treated animals (number: 61786, 61787, 61789, 61792 and 61793) were pretreated with cardiotoxin (grey arrow) and one week later the animals received subsequently 9 intramuscular immunizations with 0,5 mg of pCGWHc together with 0,5 mg of pWHsIm (time points of immunization marked by the green arrows; weeks 8, 10, 12, 25 and 27), 1×10^{10} PFU of Ad5WHc together with 0,5 mg of pWHsIm (red arrows; weeks 14 and 19) or 1×10^{10} PFU of Ad35WHc together with 0,5 mg of pWHsIm (blue arrows; weeks 16 and 22). Two animals (number 61791 and 61795) were treated only with ETV and served as controls.

The WHV chronic carrier number 61787 that received the therapeutic immunizations survived till week 25 of the therapy (development of HCC). Since the bleeding of the animal was not possible at week 25, the last examined time point for most of the experiments for this woodchuck was week 22 of the therapy. The other woodchucks were monitored untill week 31 or 33 of treatment.

5.8.1 Evaluation of the T_H response

The WHV-specific proliferative responses were detected in woodchuck PBMCs using 2[^{3}H]-adenine labelling as described in Methods (section 4.10). Results of triplicate cultures are presented as a mean stimulation index (SI) indicating the mean total absorption for peptide stimulated PBMCs divided by the mean total absorption for unstimulated control.

As Fig. 5.43A shows, the WHV-specific proliferative responses were detectable in PBMCs of chronically WHV-infected woodchucks that received the combination therapy (ETV and DNA/Ad5WHc/Ad35WHc vaccinations) already after two immunizations with plasmid DNA vaccine (week 12 of therapy). Three out of 5 woodchucks from this group (number 61787, 61792 and 61793) showed significant proliferative responses characterized by a stimulation index above 2,7. The detected responses were mostly directed against WHsAg-derived peptides: s224-239, s252-263 or s420-431 (SI ranging from 2,94 to 22,4). Moreover, one WHV chronic carrier (61787) demonstrated WHcAg-specific proliferative responses after stimulation with c64-79 and c109-124 (SI equal 3,06 and 3,15 respectively). After three DNA injections (week 14 of therapy), all five immunized woodchucks showed significant proliferative responses (SI ranging from 3,21 to 6,25) against the WHsAg-derived peptide s252-267 (Fig. 5.43B). In addition, 3 out of 5 woodchucks demonstrated WHcAg-specific T_H responses. Woodchuck 61787 responded to stimulation with peptide c109-124 (SI = 3,01), woodchuck 61789 to peptide c78-94 (SI = 3,16) and woodchuck 61793 to peptide c117-132 (SI = 3,37).

Overall, the positive proliferative responses were present in those woodchucks that received the combination therapy (ETV + vaccinations) until week 25. Two weeks after the last ETV treatment and 3 weeks after the second Ad35WHc/pWHsIm immunization all three tested animals (61786, 61789 and 61792) had detectable WHV-specific T_H responses (Fig. 5.43C). The woodchucks 61789 and 61792

demonstrated positive responses after stimulation with WHsAg-derived peptides s224-239 and s392-407 (SI ranging from 2,7 to 4,68). Woodchuck 61786 showed WHcAg-specific proliferative responses against c117-132 (SI = 3,72).

The WHV chronic carriers number 61791 and 61795 treated only with entecavir did not show any significant WHV-specific proliferative responses during the monitoring period.

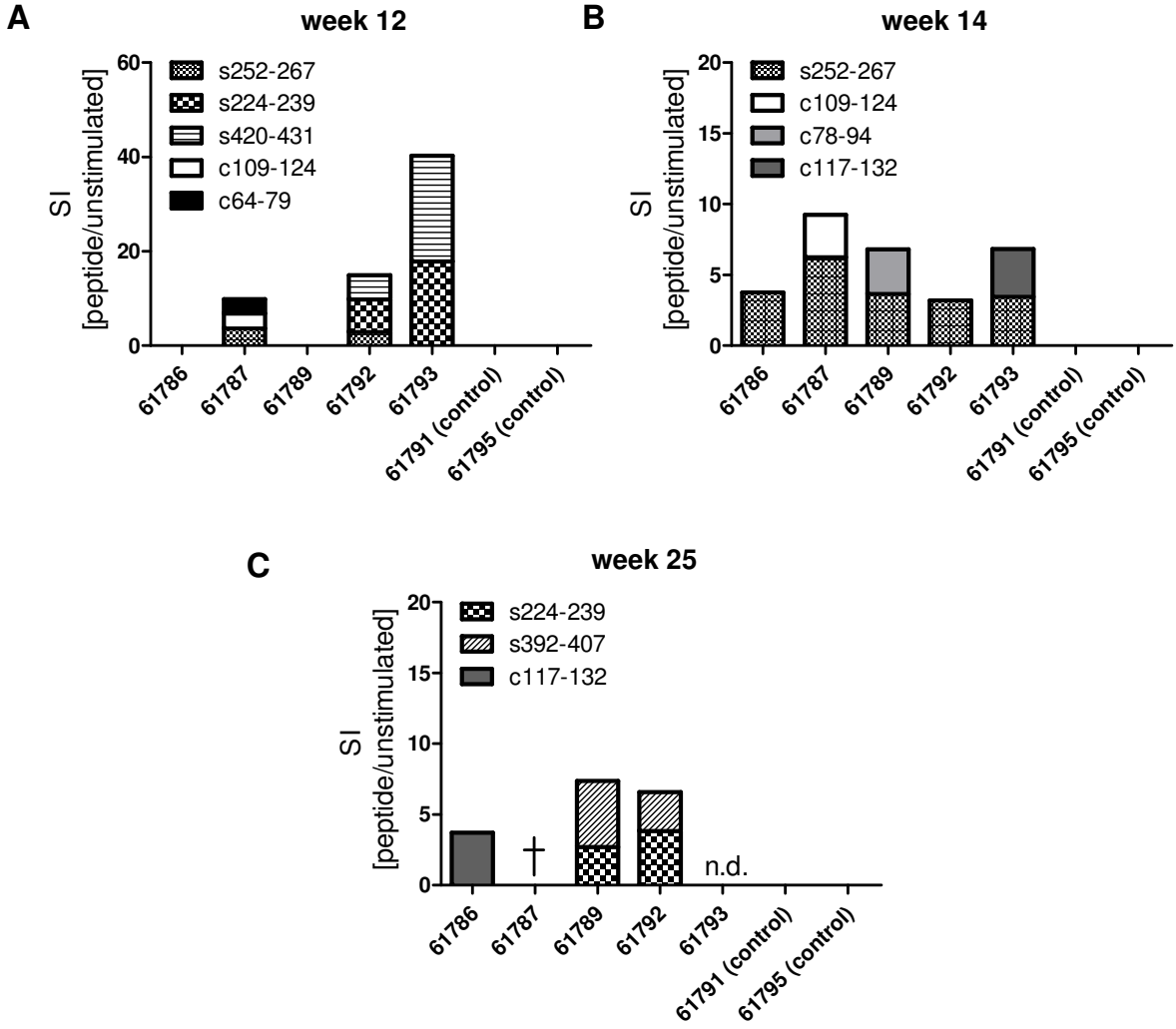

Fig. 5.43 WHcAg-specific and WHsAg-specific proliferative responses in chronic WHV carriers at the representative time points of therapy: week 12 (A), week 14 (B) and week 25 (C)

Seven chronically WHV-infected woodchucks (number: 61786, 61787, 61789, 61791, 61792, 61793 and 61795) were treated with ETV for 23 weeks. Five of the seven ETV-treated woodchucks (number: 61786, 61787, 61789, 61792 and 61793) received subsequently 9 intramuscular immunizations with DNA plasmids, expressing WHcAg and WHsAg, Ad5WHc, and Ad35WHc. The animals number 61791 and number 61795 were treated only with ETV and served as controls. The PBMCs were separated from the blood of the animals at every examined time point and stimulated with panel of 10 WHcAg-specific and 16 WHsAg-specific peptides in triplicates. After 5 days of stimulation, cells were pulsed with 2[^{3}H]adenine for 16h and the incorporation of 2[^{3}H]adenine was measured. Results for triplicate cultures are presented as a mean stimulation index (SI); *n.d.* – not done, † - dead.

The detailed data of evaluation of WHcAg- and WHsAg-specific proliferative responses in chronically WHV-infected woodchucks that received combination therapy during the monitoring period are attached in the Appendix section (Fig. 10.7A-E).

5.8.2 Evaluation of the CTL response

The evaluation of cytotoxic T cell response was performed by WHcAg- and WHsAg-specific CD107a degranulation assay until week 29 (2 weeks after the last immunization) as described in Methods (section 4.9.1).

The WHV-specific degranulation responses in $CD3^+$ $CD4^-$ T cell population were not detectable in most of the animals before week 22 of the treatment. At week 4 of ETV therapy, only a brief elevation in percentages of WHcAg- and WHsAg-specific CTLs were observed in three WHV chronic carriers (woodchucks 61786, 61791, and 61795), as shown in Fig. 5.44 (data from time points 10 to 19 is not shown, as there was no WHV-specific CTL response detectable). This result indicates that the treatment with ETV that leads to a decrease of WHV replication can transiently restore functions of virus-specific CTLs. All woodchucks from the combination therapy group and control animals had comparable background percentages of WHcAg- and WHsAg-specific CTLs at the beginning of the immunization phase (week 8) [Fig. 5.44A]. The WHcAg-specific T cell responses appeared in two immunized woodchucks 61787 and 61792 at week 22. The percentages of 1,43% and 1,51% of WHcAg-specific CTLs detected for woodchuck 61787 and 61792, were three fold higher than the mean background value of 0,43% calculated for the negative controls of all woodchucks at all time points. The WHcAg-specific degranulation response was present in all 4 woodchucks from combination therapy group that survived the end of ETV treatment until the last monitored time point week 29. The peak of WHcAg-specific CTLs detected in peripheral blood of the immunized woodchucks was detected at week 27 of treatment; the percentages of $CD107a^+$ $CD3^+$ $CD4^-$ T cells were ranging between 1,2% - 2,1% (mean: 1,7%). The control animals that were treated only with ETV did not show any significant WHcAg-specific T cell response. The mean percentages of WHcAg-specific CTLs detected from week 22 to 29 were ranging between 0,29% and 0,55% and were comparable with the mean background value (0,43%).

The impact of the therapeutic immunization on the induction of WHsAg-specific cytotoxic response is more difficult to assess. The WHsAg-specific CTL responses were not so prominent as the responses directed against WHcAg and appeared only transiently (Fig. 5.44B). Nevertheless, woodchucks that received the combination therapy demonstrated higher percentages of WHsAg-specific CTLs in comparison to background values detected for only ETV treated animals. The mean percentages of WHsAg-specific CTLs detected from week 25 to 29 of therapy were ranging between 0,88% - 1,03% in immunized woodchucks and 0,31% - 0,44% in the controls. The peak of WHsAg-specific degranulation response detected in peripheral blood of WHV chronic carriers that received immunization differed in time. At week 22 the highest percentages of WHsAg-specific CTLs were detected for 61792 (1,38%), at week 25 for 61789 (1,49%), at week 29 for 61786 and 61793 (1,63 and 1,34% respectively). Woodchuck 61787 did not show any significant WHsAg-specific degranulation response (the last examined time point was week 22 of treatment).

The detailed data of evaluation of WHcAg- and WHsAg-specific $CD107a^+$ degranulation responses detected in $CD3^+$ $CD4^-$ T cell population for each single examined chronically WHV-infected woodchuck are attached in the Appendix section (Fig. 10.8A-G).

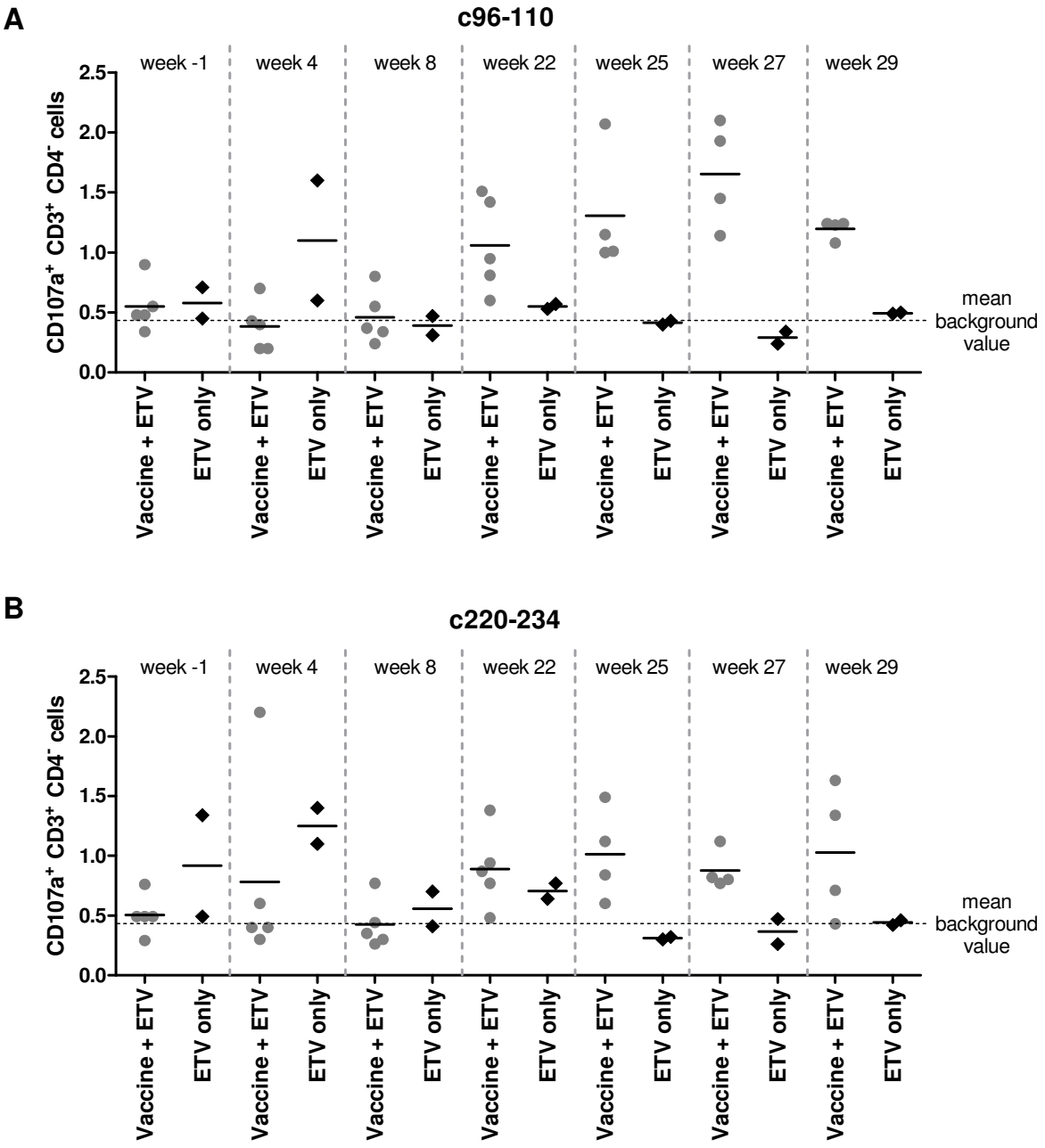

Fig. 5.44 Determination of degranulation responses in WHV chronic carriers at the representative time points of therapy: WHcAg-specific CTLs (A), WHsAg-specific CTLs (B)

Seven chronically WHV-infected woodchucks were treated with ETV for 23 weeks. Five of the seven ETV-treated woodchucks received subsequently 9 intramuscular immunizations with DNA plasmids, expressing WHcAg and WHsAg, Ad5WHc, and Ad35WHc. Two animals were treated only with ETV and served as controls. PBMCs were expanded *in vitro* for 3 days with WHcAg-derived epitope c96-110 or WHsAg-derived epitope s220-234. Unstimulated cells and cells stimulated with unrelated CMV-derived peptide served as negative controls. The background value was calculated as a mean of all values detected for negative controls in all woodchucks at all time points. The T cell response was evaluated by CD107a degranulation assay. Presented values show the percentage of $CD107a^+$ $CD3^+$ $CD4^-$ T cells in the $CD3^+$ $CD4^-$ T cell population.

5.8.3 Evaluation of the viral loads kinetics

To investigate the effect of the combination therapy on WHV replication, the sera of chronically WHV-infected woodchucks were quantified by real-time PCR analysis (Methods, section 4.13.3).

As Fig. 5.45 shows, the basal level of the viral loads prior to ETV therapy (at week 0) in WHV chronic carriers enrolled in the experiment was ranging from $3{,}1\times10^{9}$ to $1{,}2\times10^{11}$ WHV GE/ml of serum. Approximately a 5-log decrease in the viral loads was observed during the first 8 weeks of the ETV pre-treatment period in all examined woodchucks. At the time of the first immunization (week 8), no significant difference in the viral loads between the groups of woodchucks was observed. The chronic carrier number 61792 had already undetectable WHV viremia below $1{,}0\times10^{3}$ WHV GE/ml of serum. Between weeks 12 to 19 of therapy all woodchucks remained WHV negative in the blood. The rebound of viremia in ETV-only treated woodchucks was observed at week 22 of treatment. At week 25 the two control chronic carriers (61791 and 61795) showed viral loads around $5{,}4\times10^{4}$ and $2{,}4\times10^{7}$ WHV GE/ml of serum, whereas the woodchucks that were treated with the combination therapy were still WHV negative. Two out of four woodchucks (61786 and 61789) that survived through the whole monitoring period demonstrated a detectable viral load at week 27 and 29, respectively. Woodchucks number 61786 and 61789 reached the basal level of the WHV viremia ten weeks after the end of ETV treatment (week 33). The viral loads were $5{,}3\times10^{10}$ and $2{,}9\times10^{10}$ WHV GE/ml of serum, respectively and were comparable to the level of WHV GE in the control animals. The other two woodchucks from the combination therapy group were WHV negative until the end of the monitoring period. Woodchuck 61792 had an undetectable viral load at week 33 and still remained WHV negative at week 43 (*data not shown*). Woodchuck 61793 had an undetectable viral load until week 31. At this time point, the animal had to be sacrificed due to serious health problems not related to WHV infection (paralysis of the hind limbs).

The detailed data of the viral loads monitoring for all examined chronically WHV-infected woodchucks are attached in the Appendix section (Fig. 10.9A-G).

Those results demonstrate that immunization of chronically WHV-infected woodchucks with heterologous DNA prime – AdV boost regimen leads to prolonged suppression of viremia after the end of the ETV treatment. During the follow-up the

rebound of viremia in those woodchucks was observed up to 21 weeks later (end of the study) as compared to ETV-only treated controls.

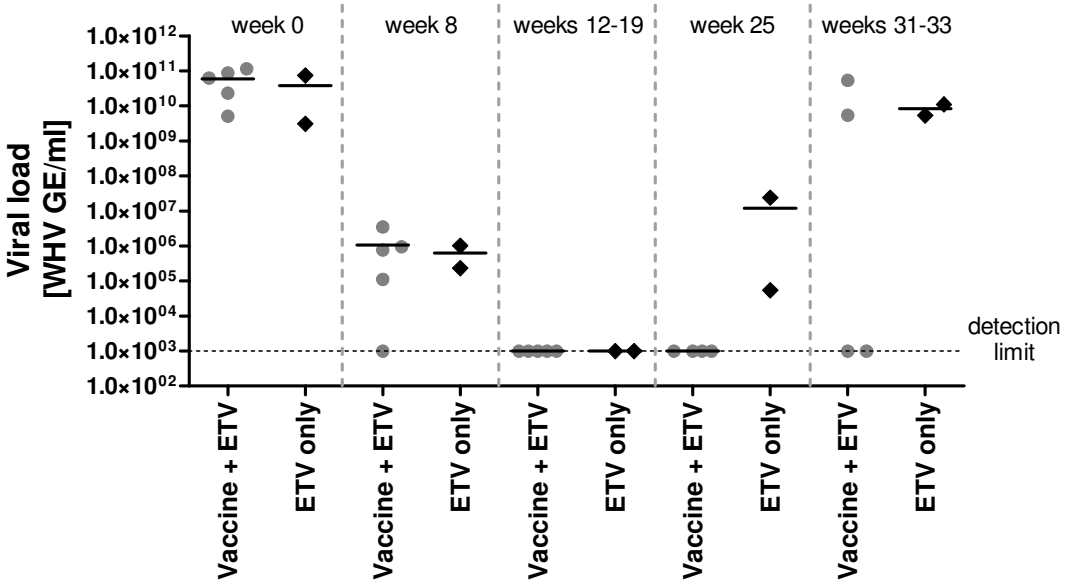

Fig. 5.45 Determination of the viral loads in WHV chronic carriers at the representative time points of therapy

Seven chronically WHV-infected woodchucks were treated with ETV for 23 weeks. Starting from week 8, five of the seven ETV-treated woodchucks received subsequently 9 intramuscular immunizations with DNA plasmids, expressing WHcAg and WHsAg, Ad5WHc, and Ad35WHc. Two animals were treated only with ETV and served as controls. The viral DNA was extracted from woodchuck sera and the viral loads were quantified per ml of serum, using real-time PCR analysis.

5.8.4 Seroconversion to anti-WHs

Apart from undetectable viral loads, the seroconversion of HBsAg to anti-HBs is the most important criterion of the resolution of HBV infection in humans [*Chisari et al., 1995*]. To check whether the examined chronic WHV carriers developed anti-WHs antibodies, the woodchuck sera were tested by ELISA (Methods, section 4.12).

As presented in table 5.2, only woodchucks 61792 and 61793 that demonstrated an undetectable viral load at the end of the monitoring period became αWHs positive. Woodchuck 61793 developed anti-WHsAg specific antibodies at week 19 of therapy and woodchuck 61792 at week 22. The other woodchucks that were treated with a combination of immunization and ETV treatment remained anti-WHs positive, as well as the control woodchucks treated only with ETV.

Tab. 5.2 Presence of anti-WHsAg specific antibodies in the sera of WHV chronic carriers

	weeks	0	2	4	6	8	10	12	14	16	19	22	25	27	29	31	33
ETV + vaccine	61786	-	-	-	-	-	-	-	-	-	-	-	-	-	-	n.d.	-
	61787	-	-	-	-	-	-	-	-	-	-	-	†				
	61789	-	-	-	-	-	-	-	-	-	-	-	-	-	-	n.d.	-
	61792	-	-	-	-	-	-	-	-	-	-	+	+	+	+	+	+
	61793	-	-	-	-	-	-	-	-	-	+	+	+	+	+	+	†
ETV	61791	-	-	-	-	-	-	-	-	-	-	-	-	-	-	n.d.	-
	61795	-	-	-	-	-	-	-	-	-	-	-	-	-	-	n.d.	-

n.d. – not done; † - dead

5.8.5 Evaluation of WHV replication in the liver

To evaluate the replication of WHV (replicative intermediates) in the liver of chronically WHV-infected woodchucks, the Southern blot analysis of DNA obtained from the liver samples collected post-mortem or through liver biopsy was performed. As a probe [^{32}P]-labelled plasmid containing the entire WHV strain 8 genome was used (Methods, section 4.14.2).

As shown in Fig. 5.46, Southern blotting showed WHV replicative intermediates, corresponding to the single-stranded DNA (ssDNA) and relaxed circular DNA (RC DNA). The WHV chronic carrier number 61787 died at week 25 shortly after the last ETV treatment. The low replication of WHV in the liver of this animal demonstrates the successful inhibition of the WHV replication by antiviral treatment. Only ssDNA replicative intermediates were detected in the liver of 61787. The woodchucks 61792 and 61793 had undetectable WHV in the blood at the end of the monitoring period (week 43 and 31, respectively) and developed anti-WHsAg antibodies. Nevertheless, only woodchuck 61792 was WHV negative in the liver at week 43. Woodchuck 61793 demonstrated a low level of WHV replication confirmed by detection of WHV ssDNA. The formation of RC DNA was still impaired in the liver of this animal at week 31 (8 weeks after the end of ETV therapy). This result shows that woodchuck 61793 did not completely clear the WHV replication. The other WHV chronic carriers treated with the combination therapy (61786 and 61789) and the control woodchucks (61791 and 61795) showed comparable levels of WHV

replication at the time points of sacrifice. All WHV replicative intermediates were detected in the livers of those animals from week 35 to week 38.

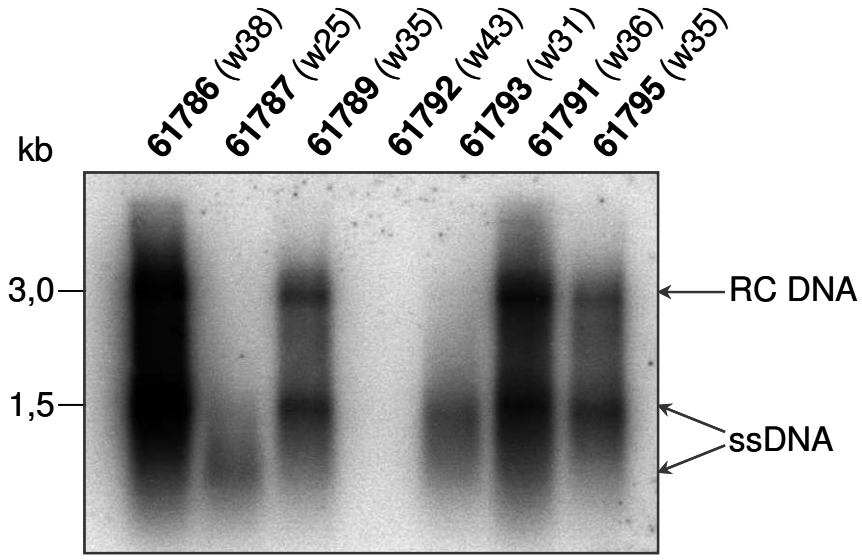

Fig. 5.46 Determination of WHV replication in the livers of WHV chronic carriers
Southern blot analysis was performed on the DNA obtained from the liver samples collected post-mortem or by liver biopsy from chronically WHV-infected woodchucks at given time points. Woodchucks number 61786, 61787, 61789, 61792 and 61793 were treated with combination therapy. Woodchucks 61791 and 61795 were treated only with ETV and served as controls. WHV replicative intermediates were detected by hybridization with [^{32}P] labelled plasmid containing the entire WHV strain 8 genome as a probe. The arrows indicate the relaxed circular WHV DNA (RC DNA; 3,0 kbp) and single-stranded WHV DNA (ssDNA; approximately 1,5 kbp).

5.8.6 Monitoring of serum transaminases levels

The high values of liver transaminases in the serum of chronically HBV-infected patients or chronically WHV-infected woodchucks may indicate not only the T cell activity in the liver but also the damage induced by the development of hepatocellular carcinoma (HCC) [*Chisari et al., 1995; Cote et al., 2000; Wang et al., 2004; Rehermann et al., 2005*]. Therefore, the monitoring of the GOT levels in the sera of the WHV chronic carriers during the experiment was performed (Methods, section 4.15).

As shown in Fig. 5.47, two animals from the combination therapy group (61786 and 61787) and one control animal (61795) demonstrated elevated GOT level in the serum at the beginning of ETV treatment (67, 87 and 150 IU/l, respectively). During the ETV treatment the serum GOT reached levels below 50 IU/l and fluctuated

around slightly elevated values in the sera of all examined woodchucks. Starting from week 23, correlating with the end of ETV treatment, the serum GOT levels significantly increased in both control chronic carriers treated only with entecavir and reached the values 106 IU/l in woodchuck 61791 and 845 IU/l in woodchuck 61795 at the end of monitoring period (week 33). At the same time point, the GOT values in woodchucks treated with ETV and additionally immunized, the elevated GOT levels were detected only in woodchuck 61789 (71 IU/l). The other woodchucks from this group demonstrated GOT levels within the "normal" range (from 12 to 21 IU/l).

The detailed data of GOT levels in the sera of all examined chronically WHV-infected woodchucks are presented in the Appendix section (Fig. 10.9A-G).

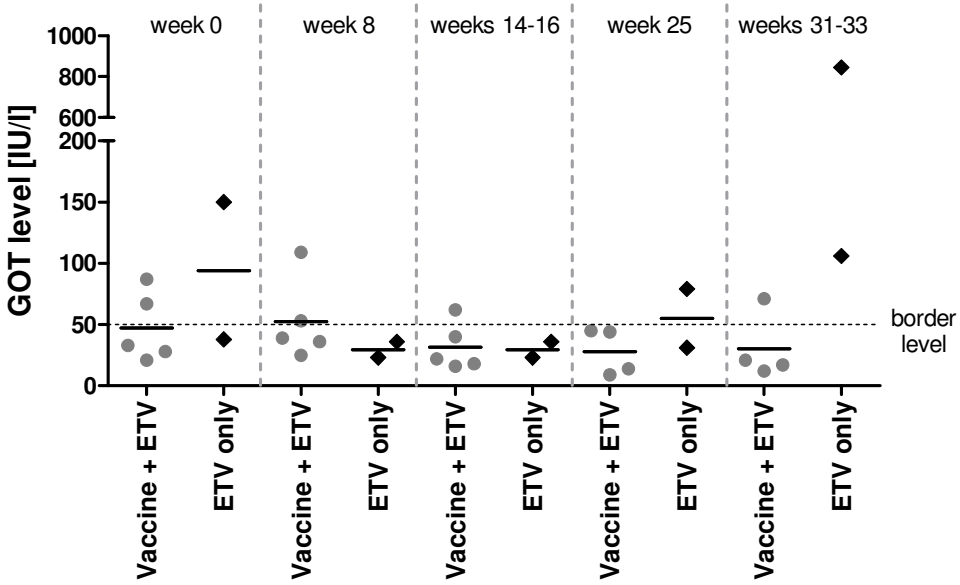

Fig. 5.47 Determination of GOT levels in the sera of WHV chronic carriers at the representative time points of therapy

Seven chronically WHV-infected woodchucks were treated with ETV for 23 weeks. Starting from week 8, five of the seven ETV-treated woodchucks received subsequently 9 intramuscular immunizations with DNA plasmids, expressing WHcAg and WHsAg, Ad5WHc, and Ad35WHc. Two animals were treated only with ETV and served as controls. The GOT levels in woodchuck sera were quantified using the standard diagnostic methods. Elevation of GOT level is assumed above 50 IU/l (border level).

5.8.7 Development of HCC

The chronic WHV infection is nearly always associated with the development of HCC in the woodchucks. The tumours appear usually in the third year of life [*Popper et al.,1987; Tennant et al., 2004*]. As wild-trapped WHV chronic carriers were used in

the study, the determination of their age is not possible. The presence of HCC was confirmed in the livers of woodchucks post-mortem or through liver biopsy procedure.

The only chronically WHV-infected woodchucks that did not develop HCC were 61792 and 61793 from the group of animals that were treated with ETV and additionally received therapeutic vaccine. At week 43 and 31, respectively, the liver tissue of those animals were indistinguishable from the 'healthy' liver. The other WHV chronic carriers in this group showed the tumours at the time of sacrifice. Woodchuck 61787 that died shortly after the end of ETV treatment showed one HCC nodule approximately 3,5 cm in diameter. The early occurrence of the tumour together with very low WHV replication detected in the liver of this woodchuck (Fig. 5.46; page 135) at the time point of death suggests the presence of HCC already at the beginning of the experiment. At week 35, in the liver of woodchuck 61789 one HCC nodule approximately 4 cm in diameter and two smaller ones (0,5 - 1 cm in diameter) were present. The representative woodchuck 61786 sacrificed at week 38 showed two small nodules approximately 3,5 cm in diameter presented in the Fig. 5.48A. The tumours in the combination therapy group were significantly smaller than the HCC detected in the ETV control group. As shown in Fig. 5.48B, the woodchuck 61791 had one big HCC nodule approximately 6,5 cm in diameter and two smaller ones (2,5 cm in diameter) at week 36. The largest tumour was detected for the control woodchuck 61795. At week 35, the woodchuck demonstrated two large nodules around 6 cm in diameter and three smaller ones ranging from 4 to 2 cm in diameter distributed all over the liver (*data not shown*).

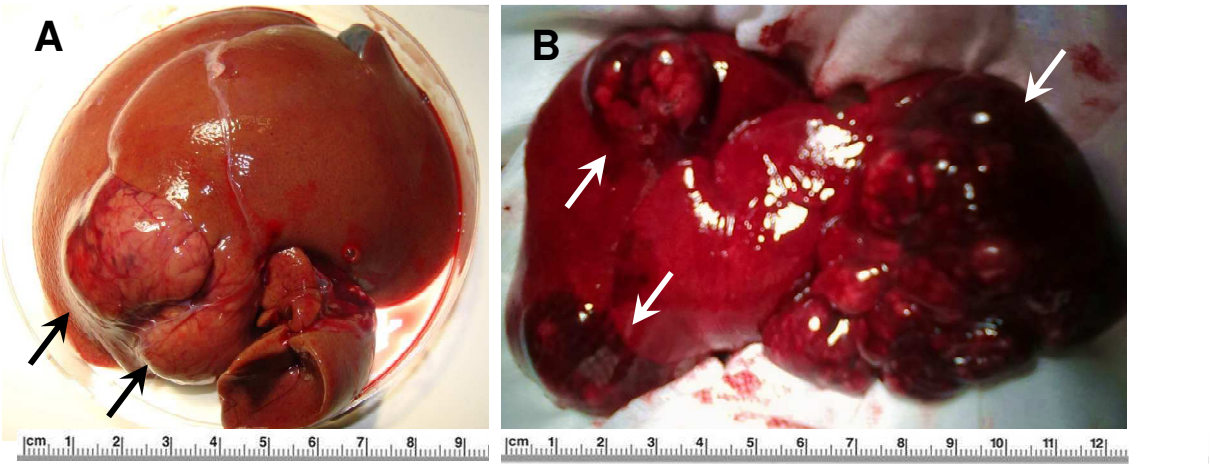

Fig. 5.48 The demonstration of the HCC in the livers of WHV chronic carriers
The representative photography for woodchuck 61786 treated with combination therapy at week 38 (A). The representative photography of the ETV control woodchuck 61791 at week 36 (B). The arrows indicate HCC nodules.

Taken together, the data clearly demonstrates that the combination therapy of chronically WHV-infected woodchucks based on ETV and heterologous DNA prime – AdV boost immunizations leads to induction of a robust WHcAg- and WHsAg-specific T cell response, prolonged suppression of WHV replication, and delay of HCC development in comparison to ETV only treated controls. Moreover, two WHV chronic carriers number 61792 and 61793 developed the sustained antiviral response, which was confirmed by the detection of anti-WHs antibodies and the absence of WHV DNA in the blood. Woodchuck number 61792 completely cleared WHV infection also in the liver.

6 Discussion

Since the introduction of preventive vaccination programmes against hepatitis B in over 170 countries, the number of new infections has been continuously decreasing. Despite the success of the prophylactic vaccines, chronic HBV infection is still a global health problem. The WHO estimates that over 360 million people are persistently infected with HBV, of whom 1 million die each year from HBV associated liver cirrhosis or hepatocellular carcinoma.

Currently, two types of antiviral therapies of chronic hepatitis B are approved: treatment with pegylated interferon alpha 2a (PEG-IFNα) or nucleoside analogues, such as adefovir, entecavir, lamivudine, telbivudine and tenofovir [*Conjeevaram et al., 2003; Janssen et al., 2005; Lau et al., 2005; Dienstag, 2008*]. Nevertheless, the efficacy of those therapies is still limited. On the one hand, treatment with PEG-IFNα leads to a sustained antiviral response in only one third of the patients. On the other hand, treatment with nucleoside analogues can significantly suppress HBV replication, but cannot completely eradicate the virus. After withdrawal of the drug, the rebound of viremia is observed in the majority of patients. Furthermore, the long-term treatment is subsequently associated with the appearance of drug-resistant HBV strains [*Raney et al., 2003; Locarnini et al., 2006*]. Therefore, the new approaches in treating chronic hepatitis B are urgently needed.

It is well documented that an appropriate adaptive immune response is required to efficiently control the HBV infection. Humoral immune response, especially neutralizing anti-HBs antibodies, play a key role in preventing HBV spread to non-infected hepatocytes [*Chisari et al., 1995; Rehermann et al., 2005*]. Nevertheless, an early, vigorous, polyclonal and multi-specific T cell immune response directed against hepatitis B virus antigens, is crucial for the resolution of the infection [*Ferrari et al., 1990; Penna et al., 1996; 1997; Guidotti et al., 1999; Maini et al., 2000; Thimme et al., 2003*]. In contrast, chronic HBV carriers demonstrate weak, transient or often undetectable $CD8^+$ T cell response that correlates with HBV persistence [*Jung et al., 1991; Penna et al., 1991; Rehermann et al., 2005; Yang et al., 2010*]. Therefore, the therapeutic vaccination approaches able to boost a functional antiviral T cell response may be a promising strategy to overcome the viral persistence.

Numerous clinical trials of therapeutic immunization exploited the conventional HBsAg-based protein vaccines. However, the anti-viral effect was only transient and did not lead to an effective control of the HBV [*Pol et al., 1994; 2001; Couillin et al., 1999; Jung et al., 2002; Dikici et al., 2003; Ren et al., 2003; Safadi et al., 2003; Yalcin et al., 2003*]. The strategies designed to specifically stimulate HBV-specific T cell response were also not successful. The DNA vaccine expressing small and middle envelope proteins resulted just in a transient induction of the HBV-specific T cell response in chronic HBV carriers [*Mancini-Bourgine et al., 2004*]. It was shown that high-level viremia negatively influences the virus-specific T cell response [*Webster et al., 2004*]. Therefore, the reduction of HBV replication by the antiviral treatment may be a rational strategy to enhance the effect of therapeutic immunization. Nevertheless, the combination of the HBsAg-based vaccines with antiviral treatment using lamivudine did not lead to a satisfactory improvement of the therapies either [*Dahmen et al., 2002; Horiike et al. 2005; Vandepapelière et al., 2007*]. Those findings clearly imply that new concepts of therapeutic vaccination are needed.

The woodchuck (*Marmota monax*) is a useful preclinical model for developing new therapeutic approaches in chronic hepadnaviral infections. Recently described advancements in the characterization and monitoring of the woodchuck T cell response and the natural occurrence of chronic WHV infection allow to evaluate potentially new therapeutic strategies in this model. Even though several innovative approaches combining antiviral treatment with nucleoside analogues, DNA vaccines, and protein vaccines were tested in chronically infected woodchucks, the effectiveness of those strategies was very limited [*Roggendorf et al., 1995; Hervas-Stubbs et al, 1997; 2001; Menne et al., 2000; 2002; Lu et al., 2003; 2008*]. However, the application of DNA vaccine expressing WHcAg in combination with antivirals in chronic WHV carriers led to a prolonged control of viral replication [*Lu et al., unpublished results*]. This result clearly shows that the induction of WHcAg-specific T cells using more potent vaccines, such as recombinant viral vectors, may be a way to achieve a sustained antiviral response. Therefore, in the presented study the novel therapeutic vaccination approach based on improved DNA vaccine and recombinant adenoviral vectors expressing WHcAg was evaluated in the preclinical model - woodchucks.

Considering the limited number of woodchucks that can be used in the experimental group, as well as the still limited number of markers and techniques available for this model, the preliminary experiments were performed in mice. Usage of mouse models for evaluation and optimization of the vaccination regimens is a common and rational approach. It allows the measurement of multiple parameters, providing sufficient number of animals to obtain statistically significant results. To take advantage of the mouse models for the evaluation of the various immunization strategies in the presented study, the WHcAg-specific $CD8^+$ T cell response was characterized in mice.

6.1 Characterization of the WHcAg-specific $CD8^+$ T cell response after DNA and DNA-AdV immunization in mice

The H-2^b-restricted epitopes within the WHcAg sequence were identified, to efficiently evaluate the $CD8^+$ T cell response elicited by vaccination in C57BL/6 and WHV transgenic mice. The strategy for the epitope finemapping was based on *in vitro* expansion of WHcAg-specific $CD8^+$ T cells subsequently with peptide pools, 15-mer peptides and finally with 9-mer peptides. This approach allowed identification of two H-2^b-restricted epitopes within the WHcAg sequence (Fig. 5.5 and Fig. 5.6; pages 70-71). The first epitope c13-21 is located within the N-terminus and the second c86-94 - within the central region of the WHcAg sequence (Fig. 5.7; page 72). The epitope c13-21 was more frequently recognized in mice immunized with plasmid DNA vaccine. Moreover, the IFNγ response detected in the splenocytes of mice after stimulation with c13-21 was stronger than with c86-94. Therefore, it can be considered as an immunodominant epitope. Many characterized woodchuck T_H epitopes and the dominant CTL epitope c96-110 are located in the N-terminal or central region of WHcAg [*Menne et al., 1998; Frank et al., 2007*]. Interestingly, the human immunidominant HLA-A2-restricted epitope c11-27 is also located within the N-terminus of HBcAg [*Bertoletti et al., 1997*]. The structure of the core protein is highly conserved among hepadnaviruses and the amino acid homology between WHcAg and HBcAg accounts for approximately 70% [*Ganem et al., 2001*]. The co-localization of the mouse, human, and, woodchuck epitopes on the N-terminal or central α-helix of the core protein indicates that these regions are highly immunogenic *in vivo* and may be preferentially presented in the context of various MHC class I molecules.

In silico prediction of MHC class I epitopes has been exploited for their identification in humans and in mice. Therefore, the question was raised whether the results of epitope finemapping correlate with the computational prediction. Indeed, the results of $CD8^+$ T cell epitope finemapping in mice confirmed the prediction determined by MHC class I epitope prediction algorithms (SYFPEITHI and BIMAS). Both softwares assigned the best score for identified H2-D^b–restricted nonamer c13-21. The algorithms also typed the other peptide c86-94, although with variable scores (Tab. 5.1; page 73). A recently published study, described the epitopes of WHcAg in BALB/c mice (genetic background H-2^d) basing on the computational prediction. This strategy resulted in the identification of two $CD8^+$ T cell H-2^d -restricted epitopes c19-27 and c61-69 [*Ochoa-Callejero et al., 2010*].

These findings imply that *in silico* prediction may be a more rational approach in the characterization of the epitopes for MHC molecules of known genetic background.

6.1.1 Immunization with vaccines demonstrating improved WHcAg expression induces a more vigorous immune response in mice

Previously described reports clearly imply that available therapeutic vaccines need further improvement. Therefore, the following issues were addressed in the presented study. Firstly, whether optimization of the WHcAg expression can be achieved by a simple genetic modification of the vaccine vectors. Secondly, whether this improvement may influence the magnitude of the elicited immune response after immunization *in vivo*. Thus, the strategy based on insertion of the intron sequences into the expression vectors was evaluated.

The presence of intron sequences protects mRNA molecules from degradation and facilitates their export into the cytoplasm [*Kurachi et al., 1995; Luo et al., 1999*]. Those factors result in a more efficient translation process and, as a consequence, increased gene expression. The construction of the novel DNA plasmid (pCGWHc) and recombinant adenoviral vectors (Ad5 and Ad5F35) containing a β-globin intron sequence between the CMV promoter and WHcAg gene proved that the raised hypothesis was true. The presence of a β-globin intron in the expression cassette of the vectors indeed resulted in a significant increase of WHcAg expression in comparison to the constructs that lacked the intron sequences (Fig. 5.9; page 75 and Fig. 5.16; page 85).

As the improvement in the antigen expression may lead to a better presentation of the antigen and the induction of a more robust immune response *in vivo,* the immunization of mice with the improved DNA vaccine (pCGWHc) and DNA vaccine that shows low expression of WHcAg (pWHcIm) was performed. The aim of the study was to develop the vaccines that are able to elicit potent cellular immune response in chronically WHV-infected woodchucks. Therefore, the appropriate delivery of the DNA vaccines needed to be taken into consideration. It was shown that intramuscular delivery of the DNA vaccines results in an induction of T_{H1}-dominant type of immune response [*Siegel et al., 2001*], whereas intradermal application, e.g. by gene gun, preferentially primes T_{H2} type of response [*Feltquate et al., 1997*]. Therefore, the intramuscular route of immunization was chosen to preferentially induce a vigorous $CD8^+$ T cell response *in vivo* (T_{H1}).

The results of the presented study clearly showed that the improved WHcAg expression by the novel DNA vaccine (pCGWHc) resulted in a very strong humoral and cellular immune responses in mice, as compared to the plasmid that showed low antigen expression. As expected, both plasmids induced a T_{H1} type of response confirmed by IgG_{2a} subtype of anti-WHc (Fig. 5.12A; page 78) and a secretion of IFNγ by $CD8^+$ T cells (Fig. 5.13A; page 80). The broader immune response induced by the novel DNA vaccine was proven by the detection of low level IgG_1 (IgG_{2a}: IgG_1 ratio = 4:1) [Fig. 5.12B; page 78]. The antibodies of IgG_1 subtype are predominantly detected during T_{H2} type of response [*Stevens et al., 1988*]. Nevertheless, it was shown that the appearance of low level of IgG_1 accompanied with high level of IgG_{2a} indicates a very strong T_{H1} type of response. In addition, the optimized plasmid elicited approximately 3-fold higher percentages of $IFN\gamma^+$ $CD8^+$ T cells detected in splenocytes expanded *in vitro* with both previously characterized WHcAg epitopes (Fig. 5.13B; page 80). These results confirm that the high antigen expression provided by the optimized DNA vaccine induces more vigorous humoral and cellular immune responses. Moreover, the results are consistent with previous findings, which show that an improved antigen expression may be also achieved by using the codon optimization strategy, inclusion of a consensus Kozak sequence or more potent hybrid promoters in construction of adenoviral-based vaccines. In those studies the immunization of mice with optimized adenoviral vectors led to the induction of a more vigorous antibody and T cell responses and provided an

enhanced protection against infection with Ebola virus and venezuelan equine encephalitis virus (VEEV) [*Richardson et al., 2009; Williams et al., 2009*]. The strategy based on the insertion of intron used in the presented study suggested that this approach can also be successfully used for the optimization of the vaccines.

As the generation of the vaccines that demonstrate better efficacy *in vivo* was accomplished, the question was raised whether the further optimization of the vaccination regimen may lead to an additional improvement of the induced immune response.

6.1.2 Optimization of the vaccination regimen by usage of AdVs leads to induction of the increased magnitude of response in mice

Vaccines based on recombinant viruses have gained a great interest because of their ability to stimulate robust humoral and cellular immune responses. The successful generation of the optimized adenoviral vectors raised the question whether their application may be beneficial for the improvement of the DNA vaccination protocol. Taking into consideration that the induction of an effective immune response in the chronic WHV carriers would definitely require multiple vaccinations, the benefits of using AdVs displaying the fibers from distinct serotypes was also evaluated.

The levels of anti-WHc antibodies were significantly higher in groups of mice boosted with Ad5WHc or Ad35WHc than in those boosted with pCGWHc (Fig. 5.19; page 88). Those results support the findings of Yang et al., who demonstrated higher antibodies titer against Ebola virus glycoprotein (GP) in mice immunized in DNA-Ad5 manner than in mice immunized only with DNA vaccine [*Yang et al., 2003*]. The strong antibody response correlated with significantly higher frequencies of $IFN\gamma^+$ $CD8^+$ T cells detected in both AdV-boosted groups than in DNA-only immunized mice (Fig. 5.21; page 91). Similar results were obtained in mice and non-human primates during the evaluation of several immunization strategies in the development of prophylactic vaccines against HIV and Ebola virus [*Casimiro et al., 2003; Yang et al., 2003*]. A slightly lower percentage of $IFN\gamma^+$ $CD8^+$ T cells detected in mice immunized with DNA-Ad35WHc than with DNA-Ad5WHc may be due to the fact that those vectors use different receptors to be internalized into the cells. The recombinant adenoviral vector serotype 5 interacts with CAR receptor and the chimeric Ad35 fiber binds to CD46 [*Bergelson, 1999*]. Concordant with the presented

results, a slightly less effective performance of Ad5F35 than Ad5 immunization in mouse model was shown previously [*Bayer et al., 2008*].

The obtained results clearly indicate that the addition of recombinant adenoviral vectors to the DNA vaccination regimen further improved the magnitude of the induced $CD8^+$ T cell response. Therefore, the question whether the DNA-AdV immunization induces the T cells of a different phenotype as the DNA immunization alone was addressed.

6.1.3 DNA-AdV immunization induces the same phenotype of $CD8^+$ T cells as DNA immunization

Recent developments in the multicolor flow cytometry technology have made it possible to simultaneously examine several functionality markers on a cellular level. Antigen-specific $CD8^+$ T cells that concurrently display multiple functions, e.g. degranulation and various cytokine production, have been associated with non-progressive HIV infection [*Betts et al., 2006*] and protective immunity against vaccinia virus vaccination [*Precopio et al., 2007*]. Defects in the cytokine production by $CD8^+$ T cells during chronic HBV and progressive HIV infection have been recently reported [*Zimmerli et al., 2005; Das et al., 2008*]. Therefore, induction of a potent multifunctional $CD8^+$ T cell response is highly desirable. The immunization of healthy individuals with DNA and Ad5, expressing HIV-1 gag protein, induced a distinct $CD8^+$ T cell response profile in comparison to Ad5-Ad5 immunization. The DNA-Ad5 regimen elicited a more diverse sets of phenotypes, particularly those which displayed the multiple markers, in a higher proportion of the vaccinees [*Cox et al., 2008*]. Those findings show that heterologous DNA prime – AdV boost might be more effective in inducing the multifunctional $CD8^+$ T cell response. To address this hypothesis the $CD8^+$ T cell response induced by DNA-AdV and only DNA vaccination regimens was examined in two functionality assays. The first assay combined the evaluation of the $CD8^+$ T cell degranulation functions (detected by CD107a degranulation marker) with the production of most potent anti-viral cytokine IFNγ. The percentages of the $CD8^+$ T cells that co-expressed both markers were significantly higher (approximately 3-fold) in splenocytes of mice immunized in heterologous DNA-Ad5WHc or DNA-Ad35WHc than in mice immunized only with DNA (Fig. 5.22; page 93). Nevertheless, the “quality” of induced cells was comparable. More than 90% of all $IFN\gamma^+$ $CD8^+$ T cells were also $CD107a^+$ in splenocytes of mice from all vaccinated

groups. The second analysis evaluated simultaneous secretion of T_{H1} type cytokines such as IFNγ, TNFα, and IL-2 by $CD8^+$ T cells. Mice immunized with DNA-Ad5WHc or DNA-Ad35WHc exhibited significantly higher percentages of $IFN\gamma^+$, $TNF\alpha^+$ and IL-2 $CD8^+$ T cells, compared to the group only immunized with DNA (Fig. 5.23A; page 95). Determination of single, double and triple positive cells that produce IFNγ, TNFα and IL-2 within the $CD8^+$ T cell population, demonstrated that there was no difference in "quality" of cytokines secreting $CD8^+$ T cells between the groups (Fig. 5.23B; page 95).

These results clearly demonstrate that heterologous DNA prime – recombinant adenovirus boost immunization induced an extremely robust immune response in comparison to DNA vaccination alone. Even though the magnitude of immune response was significantly higher, there was no apparent difference in the phenotype of the $CD8^+$ T cells induced by DNA or DNA-AdV regimen. This finding can be a result of using the same priming strategy for all immunization regimens. The DNA vaccines proved to be a very potent tool in priming the T cell response [*Barouch et al., 2001*]. In absence of the protein content of the viral vector, DNA immunization facilitates the development of the T cell response specific against the antigen of interest. The DNA immunization effectively induces a long-term memory T cell response [*Michel et al., 2001*]. Though the response might be at a relative low level, it may select the T cells with receptors of increased affinity [*Busch et al., 1999*]. The immunization with a very immunogenic recombinant adenoviral vector results in a robust boosting of the primary antigen-specific response. Those findings provide a possible explanation of the difference in the quantity but not in the "quality" of $CD8^+$ T cell response between the DNA and DNA-AdV vaccination regimens. The efficacy of the heterologous DNA-AdV immunization was further evaluated by the characterization of $CD8^+$ T cell functions *in vivo.*

6.1.4 DNA-AdV immunization induces $CD8^+$ T cells with stronger cytotoxic potential *in vivo* than DNA immunization

The evaluation of the CTL's effector functions after DNA -AdV immunization directly *in vivo*, gives an insight whether this regimen elicits more $CD8^+$ T cells with stronger cytotoxic potential than DNA vaccination alone. The results of *in vivo* cytoxicity assay showed that, indeed, the mice immunized in DNA-Ad5WHc manner showed significantly improved killing of the c13-21 loaded 'target cells' than mice immunized

only with DNA (Fig. 5.24; page 97). This result proves that the $CD8^+$ T cells, induced by DNA prime-Ad5WHc boost immunization, show a stronger cytotoxic activity *in vivo*.

Taken together, these findings led to the conclusion that improvement of the vaccines and optimization of the vaccination regimen by addition of AdV brought an synergistic effect. The innovative heterologous prime-boost regimen does not only result in an induction of the extremely robust $CD8^+$ T cell response, but also seems to be potentially more effective in killing WHV-infected cells than only DNA regimen.

6.2 The DNA prime – AdV boost breaks the immune tolerance against WHV antigens in WHV transgenic mice

The preliminary results obtained from C57BL/6 mice showed that the utility of improved vaccines and optimization of the immunization protocol induces a more potent WHcAg-specific response than previously investigated strategies. Therefore, the question whether the improved DNA-AdV immunization is able to overcome the immune tolerance to WHV-antigens in 1217 WHV Tg mice was raised. As 1217 WHV Tg mice show an undetectable T cell response to the WHV antigens, they can model chronic hepadnaviral infection. Therefore, the issue whether improved vaccination is able to induce anti-WHc antibodies was addressed.

It was shown previously that immunization of 1217 WHV Tg mice with pWHcIm plasmid, expressing WHcAg, induces significant levels of IgG_{2a} subtype of anti-WHc antibodies [*Meng et al., manuscript in preparation*]. In the presented study similar results were obtained after immunization of mice with optimized pCGWHc plasmid. Mice immunized in DNA-Ad5WHc manner developed significantly higher levels of anti-WHc in comparison to the group of immunized only with DNA, as it was shown in C57BL/6 mice. All mice immunized with DNA vaccine or DNA-Ad5WHc demonstrated only IgG_{2a} subtype of anti-WHc antibodies (Fig. 5.27; page 100). Interestingly, the additional increase in anti-WHc levels after second boosting immunization with Ad35WHc (DNA-Ad5-Ad35WHc) correlated with the development of high levels of IgG_1 in several mice (Fig. 5.27B; page 100). Almost the same levels of IgG_{2a} and IgG_1 antibodies detected in three out of five mice (IgG_{2a}:IgG_1 ratio = 4:3) may indicate the development of a mixed T_{H1}/T_{H2} responses. As the robust humoral immune response could be elicited by the improved DNA-Ad5WHc or DNA-Ad5-Ad35WHc,

next, the impact of vaccination on induction of WHcAg-specific $CD8^+$ T cell response was evaluated.

The immunization experiments of 1217 WHV Tg mice showed that WHcAg $CD8^+$ T cell response can be elicited upon pWHcIm immunization. Nevertheless, the magnitude of the response was significantly lower than in normal mice [*Meng et al., manuscript in preparation*]. The results obtained in the study reveal the same tendency. Immunization with optimized pCGWHc vaccine induced a low IFNγ response, that was significantly higher in the splenocytes of mice immunized with heterologous DNA-AdV regimen (Fig. 5.29A-B, page 103). The $CD8^+$ T cell response obtained for groups of 1217 WHV Tg mice immunized with DNA or DNA-Ad5 was significantly lower than this being induced in respective groups of C57BL/6 mice (Fig. 5.29C; page 103). These results indicate that there is only a partial immune tolerance to the WHV antigens in 1217 WHV Tg mice. This tolerance suppresses the induction of the vigorous T cell response, which may also be the case in chronically infected woodchucks or patients.

As mentioned previously, there was no apparent change in the “quality” of the $CD8^+$ T cells induced by DNA or DNA-AdV regimen in C57BL/6 mice. Nevertheless, in the tolerogenic host, in which the magnitude of the induced immune response is lower, the different immunization protocols might induce $CD8^+$ T cells of different phenotype. Moreover, the phenotype of the cells may vary from those elicited in the wild-type mice. Indeed, the multifunctional analysis of the $CD8^+$ T cells induced in 1217 WHV Tg and C57BL/6 mice showed the difference in the phenotype of the $CD8^+$ T cells. The evaluation of the CD107a and IFNγ co-expression, showed that there is significantly smaller proportions of the double-positive cells ($CD107a^+$ $IFN\gamma^+$) in 1217 WHV Tg mice in comparison to C57BL/6 mice. It was shown that approximately 90% of total $IFN\gamma^+$ or $CD107a^+$ $CD8^+$ T cells co-express both markers in C57BL/6 mice in response to stimulation with c13-21 (Fig. 5.22; page 93). In 1217 WHV Tg mice this frequency was merely 41% (Fig.5.30; page 105). Moreover, in mice boosted twice with Ad5WHc and Ad35WHc the proportion of IFNγ-secreting cells was lower than in mice which were boosted with Ad5WHc only once. The obtained results show that there is impaired IFNγ production correlating with comparable CD107a expression after the second booster vaccination. Those findings together with the change of anti-WHc antibody profiles, might suggest that immunization with Ad35WHc changes the

phenotype of the elicited $CD8^+$ T cells. In order to fully explain and understand those findings, a more detailed phenotypic study needs to be performed to confirm the change of the T cell response profile in those mice.

The evaluation of the T_{H1} cytokine secretion (IFNγ, TNFα and IL-2) was not possible for the whole experimental group of mice because of a very low $CD8^+$ T cell response detected after 6h stimulation with c13-21 (Fig. 5.31A; page 107). Unfortunately, expansion of splenocytes of mice in culture for 7 days resulted in a complete loss of IL-2 production [*data not shown*]. This outcome seems to be related to the addition of recombinant IL-2 into the cell culture in quite high concentration to maintain the growth of the cells. Nevertheless, the strategy based on choosing one mouse from every vaccination group that exhibited the significant $CD8^+$ T cell response allowed for a very limited insight in the phenotype of the cells. Apparently, the highest proportion of cells producing all three cytokines was shown for mouse from the DNA-Ad5 group (Fig. 5.31B; page 107). This mouse also showed the highest proportion of $IFN\gamma^+$ $TNF\alpha^+$ $CD8^+$ T cells in the double cytokine producing cells. Interestingly, the mice from DNA-Ad5-Ad35WHc group demonstrated the highest proportion of $IFN\gamma^+$ $IL\text{-}2^+$ $CD8^+$ T cells (Fig. 5.31D; page 107). Recent data reported the defects in the IL-2 production by $CD8^+$ T cells during chronic HBV infection [*Das et al., 2008*]. Moreover, the high proportion of $IFN\gamma^+$ $IL\text{-}2^+$ $CD8^+$ T cells correlates with the non-progressive HIV infection [*Zimmerli et al., 2005*]. Those findings, suggest that the possible change in phenotype of the $CD8^+$ T cells in 1217 WHV Tg mice that received the double AdV boost might be beneficial for controlling persistent viral infections. However, the results need further investigation on the bigger cohort of mice in order to obtain the statistical significance.

6.2.1 Heterologous DNA-AdV immunization induces anti-WHs antibodies.

To address the question whether the potent WHcAg-specific T cell response is able to brake the immune tolerance against the WHsAg, the detection of anti-WHs was performed. Surprisingly, 76% of mice immunized by combinating plasmid DNA and Ad5 or Ad5-Ad35 expressing WHcAg developed anti-WHs antibodies (Fig. 5.28; page 101). It was shown previously that mice immunized with primed with HBcAg-specific T_H epitope can induce anti-HBs antibodies after “challenge” with HBV particles in contrast to mice that were not immunized [*Millich et al., 1987*]. This experiment shows that core-specific helper response is able to prime WHsAg-specific

B cells. In the presented study the development of anti-WHs was restricted to groups of mice immunized in DNA-AdV manner that exhibited the strongest WHcAg-specific $CD8^+$ T cell response. It can be assumed that stronger $CD8^+$ T cell response is also correlated with potent $CD4^+$ T cell response in those mice. This T cell response, induced by heterologous prime-boost immunization, was able to brake the tolerance against WHsAg. It was previously shown that 1217 WHV Tg mice may develop low levels of anti-WHc with increasing age. However, the development of anti-WHs antibodies was never demonstrated [*Meng et al., manuscript in preparation*]. Nevertheless, it could be speculated that 1217 WHV Tg mice may develop a very low level of anti-WHs, not detectable by routinely used techniques. In that case, induction of a potent WHcAg-specific T cell response would easily facilitate anti-WHs development.

The induction of anti-WHs antibodies in 1217 WHV Tg mice upon DNA-AdV immunization is of great impact as the chronic hepadnaviral infections correlate with a lack of antibodies against the surface proteins. Consequently, this result implies that the novel immunization strategy may be more effective in control of chronic WHV infection in woodchucks and possibly in patients.

6.2.2 The immunization of 1217 WHV Tg mice in DNA-AdV manner leads to a significant reduction in the viral loads

The 1217 WHV Tg mouse model gave the possibility to examine the impact of the vaccination on WHV replication. As the previous experiments, based on immunization with pWHcIm plasmid did not lead to reduction of WHV replication [*Meng et al., manuscript in preparation*]. Therefore, the question whether the newly developed optimized immunization strategy may result in significant reductions in the viral loads in 1217 WHV Tg mice was addressed. The results of the presented study showed that the immunization with optimized vaccines is able to significantly reduce WHV replication, as all tested vaccination protocols resulted in the significant reduction in WHV viral load (Fig. 5.32; page 109). However, the pronounced suppression in WHV replication was observed in DNA-Ad5WHc or DNA-Ad5-Ad35WHc vaccination group, in which 83% and 60% of the mice respectively had undetectable viral loads at the end of the experiment (Fig. 5.32C-D; page 109). These results prove that immunization of WHV transgenic mice with the optimized DNA and AdV-based vaccines is able to effectively suppress WHV replication.

The promising results, using the optimized heterologous DNA prime-AdV boost immunization regimen in C57BL/6 and 1217 WHV Tg mouse models, raised the important question whether the improved vaccines would also be effective in the woodchuck model.

6.3 Heterologous Ad5WHc–Ad35WHc or improved DNA immunization protects naïve woodchucks against WHV infection

The vaccination trial with improved DNA vaccine or recombinant adenoviral vectors (Ad5WHc/Ad35WHc) in naïve woodchucks allowed to address the following questions: do the optimized constructs induce a potent CTL response in woodchucks and does this response provide a protection against the WHV infection?

The results clearly show that immunization of woodchucks with the new pCGWHc plasmid or Ad5WHc/Ad35WHc expressing WHcAg induced WHcAg-specific immune response that indeed resulted in the control of a subsequent WHV infection. Previously described study already demonstrated that immunization of woodchucks with plasmid expressing WHcAg (pWHcIm) protected woodchucks from WHV infection. Three vaccinations with pWHcIm induced anti-WHc antibodies, but a very low T cell response, evaluated by 2[^{3}H]-adenine-based proliferation assay detectable only in several woodchucks [*Lu et al., 1999*]. Recently established CD107a degranulation assay [*Frank et al., 2007*] allowed, for the first time, the detection of WHcAg-specific CTLs, elicited by vaccination in the peripheral blood of woodchucks. Vaccination with pCGWHc plasmid of the naïve woodchucks induced significant degranulation responses directed against WHcAg epitope c96-110 in two out of three woodchucks (Fig. 5.34; page 112). As the successful DNA vaccination depends on a very precise delivery of the plasmid, the borderline T cell response, detected in the third woodchuck (58059), might have been a result of incorrect immunization (Fig. 5.34A; page 112). The percentages of WHcAg-specific CD107a$^+$ CD3$^+$ CD4$^-$ T cells detected in two responder woodchucks after three immunizations with pCGWHc plasmid were comparable to those induced just by one immunization with recombinant adenoviral vector (Ad5WHc) [Fig. 5.35A; page 114]. The magnitude of WHcAg-specific degranulation responses significantly increased after boosting immunization with Ad35WHc in both woodchucks immunized in heterologous Ad5WHc/Ad35WHc manner. This observation confirms that usage of the chimeric

Ad5F35 vector avoids the vector-specific immunity after immunization with Ad5 (Fig. 5.35B; page 114). The high percentages of 13,3% and 7,4% of WHcAg-specific CTLs after Ad35WHc immunization are comparable to those detected during the acute phase of WHV infection [*Frank et al., 2007*]. These results clearly demonstrate the potency of adenoviral vectors to the induce vigorous CTL response in woodchucks. The elicited WHcAg-directed CTL response was significantly higher than the "classical" DNA vaccination. Similar results were obtained in rhesus macaques immunized three times with plasmid DNA or twice with Ad5 expressing HIV-1 *gag* gene. The T cell response against HIV-1 gag antigen, induced by homologous Ad5 immunization, was stronger in magnitude than this induced by DNA vaccination alone or with addition of the adjuvant [*Casimiro et al., 2003*]. Moreover, Ad5 immunization elicited protective immunity against the infection with simian immunodeficiency virus (SIV) or HIV-SIV hybrid virus [*Shiver et al., 2002; Casimiro et al., 2005*], as well as Ebola virus [*Sullivan et al., 2006*] in nonhuman primates. In addition, heterologous Ad5/Ad5F35 immunization of mice resulted in an improved immune protection against Friend retrovirus infection in comparison to homologous Ad5 immunization [*Bayer et al., 2008*]. The results of this study imply the usefulness of Ad5WHc/Ad35WHc immunization against hepadnaviral infections in the woodchuck model.

The levels of anti-WHc antibodies, induced by plasmid or by heterologous Ad5WHc/Ad35WHc immunizations, were comparable in all animals. Anti-WHc antibodies are not able to neutralize the virions of WHV and are not able to prevent the infection of the hepatocytes [*Roos et al., 1989; Schodel et al., 1993*]. Therefore, a limited infection of hepatocytes occurred in vaccinated woodchucks after challenge. In all successfully immunized woodchucks only a short-time viremia (2 to 4 weeks) was observed, compared to the control woodchucks that were just infected with WHV. Moreover, the viral loads detected in immunized woodchucks were 3 to 4 logs lower than those reached in the control woodchucks (Fig. 5.39; page 122). The short-time low level viremia was accompanied by the appearance of WHV-specific CTLs in the blood and no or low level elevation of GOT, indicating that only a small number of hepatocytes was eliminated by cytotoxic T cells (Fig. 5.36A; page 116 and Fig. 5.37; page 118). Altogether, the data confirm the small-scale infection of hepatocytes in those woodchucks. Woodchuck 58059, which partially responded to vaccination,

showed a prolonged viremia concurrent with high elevation in GOT level, compared to all the other responder woodchucks (Fig. 5.36B; page 116). Those data demonstrate a bigger-scale WHV infection that correlates with increased number of lysed WHV-infected hepatocytes. A similar course of infection was shown for one of the control woodchucks (58055) [Fig. 5.38A; page 120]. Nevertheless, the WHV viral load in the partially responder woodchuck was significantly shorter (12 weeks) than in the control animal. This finding shows that even the partial response, induced by immunization, is able to clear the WHV more efficiently. The other control woodchuck developed a persistent WHV infection after WHV inoculation. In adult woodchucks infection with WHV usually leads to chronic infection in about 5-10% of the animals [*Cotte et al., 2000*]. The control woodchuck that established chronic WHV infection did not show any WHV-specific T cell responses over the monitoring period (Fig. 38B; page 120). Those findings correlate with the previously described reports showing that WHV chronic carriers demonstrate weak or no virus-specific T cell responses [*Menne et al., 1998; Frank et al., 2007*].

The development of neutralizing antibodies directed against the surface antigen epitopes, is crucial for the resolution of the HBV infection in humans [*Hoofnagle, 1981; Chisari et al., 1995*], as well as, for the resolution of WHV infection in woodchucks [*Cote et al., 1986; Lu et al., 1999*]. The appearance of anti-WHs antibodies correlated with the time of the WHV clearance in all examined woodchucks. The presence of anti-WHs antibodies in the woodchucks, which responded to vaccination already at week 2 after WHV challenge, shows, that priming of WHsAg-specific B cell response occurred as a result of the immunization. Those results are consistent with Lu et al. where it is shown that immunization of woodchucks with plasmid expressing WHcAg led to an early induction of high levels of anti-WHs antibodies and a limited WHV infection [*Lu et al., 1999*]. Levels of anti-WHs correlated with the magnitude of the WHcAg-specific T cell response after vaccination. The most prominent anti-WHs response, as well as the WHcAg-specific T cell response, was detected in woodchucks immunized in heterologous Ad5WHc/Ad35WHc manner (Fig. 5.40A; page 124). The intermediate levels of anti-WHs were detected in two woodchucks which responded to pCGWHc immunization. As mentioned above, one of the two control woodchucks established a chronic WHV infection after WHV and as expected did not develop anti-WHs (Fig. 10.6C; page

184). The other one, developed low-level anti-WHs at a later stage of the infection (week 18 pi) than the immunized woodchucks did (Fig. 5.41; page 125). Those observations show that WHcAg-specific T cells, elicited by the vaccination provided help to the WHsAg-specific B cells. The intermolecular help results in a rapid and more robust production of anti-WHs, compared to the natural infection [*Millich et al., 1987*].

In contrast to anti-WHc, the levels of anti-WHs decreased in time. This finding reflects the observations in humans. It is known, that anti-HBs antibodies become undetectable over time after acute HBV infection in humans, whereas anti-HBc antibodies persist life-long [*Shepard et al., 2006*].

6.4 Heterologous prime-boost immunization in combination with entecavir treatment may lead to control of chronic WHV infection

The results obtained in mice and naïve woodchucks clearly showed, that the novel vaccines induce a more potent WHV-specific immune response than previously investigated strategies. Therefore, the final evaluation of the DNA-AdV regimen was performed in chronic WHV carriers.

The reduction of viral load by the nucleoside analogues pre-treatment is necessary to enhance the effect of therapeutic immunization. The results from the previous studies clearly confirm the poor efficacy of the lamivudine treatment in woodchucks [*Mason et al., 1998; Hervas-Stubbs et al., 2001; Lu et al., 2008*]. Lamivudine treatment of chronic HBV infection is associated with a frequent resistance to the therapy found in approximately 70% of the patients after 4 years of treatment [*Chang et al., 2004*]. Moreover, lamivudine-resistant strains were isolated from chronically WHV-infected woodchucks treated with lamivudine [*Jacob et al., 2004*]. The evaluation of various nucleoside analogues in woodchucks revealed also potent antivirals suitable for this model, such as clevudine [*Menne et al., 2002*] and telbivudine [*Bryant et al., 2001*].

In the presented study, WHV chronic carriers were treated with guanosine nucleoside analogue entecavir. Entecavir proved to efficiently suppress the viral replication during chronic HBV infection in patients [*Karino et al., 2010; Yuen et al., 2011*], as well as chronic WHV infection in woodchucks [*Genovesi et al., 1998; Colonno et al., 2001; Lu et al.,* unpublished data]. As expected, the rapid decrease in the viral load in chronically WHV-infected woodchucks was observed during the first weeks of ETV

therapy. WHV became undetectable in the blood of all animals by week 12 of the treatment (Fig. 10.9A-G; page 192). It was assumed that the WHV suppression by antiviral treatment may be also beneficial during the first stage of the immunization phase [*Lu et al., personal communication*]. Therefore, the immunizations were performed together with a continuous entecavir treatment until week 23.

6.4.1 Heterologous prime-boost immunization in combination with ETV leads to induction of WHV-specific T cell response in all treated chronic carriers

Previous reports indicate that combination therapy (antivirals + vaccine) of chronic WHV infection may restore WHV-specific T cell responses. The first study was based on lamivudine treatment combined with immunization with plasmid DNA vaccine (expressing WHsAg, WHcAg and woodchuck IFNγ) and antigen-antibody WHsAg/anti-WHs IC vaccines together. The study demonstrated significant lymphoproliferative responses only in one out of 8 woodchucks after the last immunization [*Lu et al., 2008*]. The second study examined clevudine therapy in combination with protein WHsAg vaccine. The treatment led to the induction of rapid and sustained proliferative responses against WHsAg approximately in 70% of the woodchucks [*Menne et al., 2002*]. Therefore, the question whether the novel prime-boost strategy inducing a very potent T cell response in the previous models can lead to the improved T_H and CTL responses in chronic WHV carriers.

In this study, WHV-specific T helper responses were detected in PBMCs of all chronically WHV-infected woodchucks that received therapeutic vaccine combined with ETV, but not in controls treated only with ETV. The woodchucks from the combination therapy group developed early and sustained WHsAg- and WHcAg-specific proliferative responses (Fig. 5.43; page 128). The responses were detected in some woodchucks already after two DNA immunizations. All woodchucks that received the combination therapy had significant proliferative responses after three DNA immunizations, that were detectable until week 25 (two weeks after the end of the ETV treatment and 3 weeks after the second Ad35WHc/pWHsIm immunization).

The proliferative responses were predominantly directed against the two WHsAg-derived T_H peptides s224-239 and s252-267. The position of the epitope s224-239 overlapped with the peptide s226-245 preferentially recognized in WHV chronic

carriers after clevudine/WHsAg combination therapy [*Menne et al., 2002*]. Those findings indicate that amino acid sequences at the N-terminus of WHsAg are a preferable target for T cell response. Moreover, several WHcAg-derived T_H epitopes identified in woodchucks with acute self-limited WHV infection [*Menne et al., 1998*] were recognized in WHV carriers. The WHcAg-specific proliferative responses were most frequently directed against the peptides c64-79, c109-124 and c117-132.

Following the appearance of T helper cells, WHcAg- and WHsAg-specific CTLs were detectable in all woodchucks that received combination therapy, but not in ETV treated controls. Only brief CTL responses were detected shortly after the beginning of ETV treatment at week 4. The 3 to 4 logs decrease of the viral load led to induction of WHsAg-specific CTLs in one of seven ETV treated woodchucks (61795; Fig. 10.8G; page 189) and WHcAg-specific CTLs in two chronic carriers (61786 and 61791; Fig. 10.8A,F; page 189). Those findings are consistent with the data obtained from chronic HBV patients treated with nucleoside analogues. The treatment with lamivudine could transiently restore HBV-specific T cell immune response in some of the patients [*Boni et al., 2001; 2003*]. The appearance of sustained WHcAg-specific CTL response after the vaccinations correlated with the phase of Ad5WHc and Ad35WHc administration. The WHcAg-specific degranulation response was present in the woodchucks from combination therapy from week 22 until the last monitored time point week 29 (Fig. 5.44A; page 131). In addition, all four woodchucks treated with combination therapy that survived the end of ETV treatment demonstrated prominent WHsAg-specific CTL responses. The WHsAg-specific CTL responses were not so prominent as responses directed against WHcAg and appeared only transiently (Fig. 5.44B; page 131).

The data obtained from HBV infection in patients underline the role of core-specific T cell responses as a factor leading to the virus clearance [*Ferrari et al., 1990; Penna et al., 1997; Guidotti et al., 1999; Maini et al., 2000; Thimme et al., 2003*]. The immunotherapy examined in the presented work demonstrated that sustained WHcAg-specific T helper response and CTL response could be induced in WHV-chronically infected woodchucks. The novel prime-boost immunization induced a more potent WHV-specific immune response than previously investigated strategies also in chronically WHV-infected woodchucks. Significant WHV-specific T_H

and CTL responses were elicited for the first time in all chronic carriers from combination therapy group. Since ETV-only treatment did not induce significant T cell responses in the control animals, this outcome was an effect of the therapeutic DNA prime–recombinant adenovirus boost immunization. Those results also prove that high WHV replication during the chronic infection correlates with hyporesponsiveness of the T cells, as it was shown in chronically HBV-infected patients [*Webster et al., 2004*]. Potent antiviral drugs such as ETV are crucial to enhance the therapeutic effect of the vaccination.

6.4.2 Heterologous prime-boost immunization in combination with ETV leads to sustained antiviral response in treated chronic carriers

All four woodchucks from the combination therapy group that survived the whole monitoring period demonstrated a prolonged suppression of WHV replication, compared to ETV-only treated controls. Two woodchucks (61786 and 61789) became WHV positive 5 and 7 weeks later than ETV-only treated controls. The other two (61792 and 61793) were WHV negative until the end of the monitoring period, suggesting that those animals might clear the chronic WHV infection (Fig. 5.45; page 133).

To confirm this finding, the detection of anti-WHs antibodies was evaluated, as the seroconversion of HBsAg and the presence of anti-HBsAg specific antibodies is the most important criterion in the resolution of HBV infection in humans [*Chisari et al., 1995*]. Indeed, both woodchucks that demonstrated undetectable viral loads at the end of the monitoring period (61792 and 61793) developed anti-WHs antibodies what prove that the sustained antiviral response was developed in those animals (Tab. 5.2; page 134). Nevertheless, only woodchuck 61792 was WHV negative in the liver. Woodchuck 61793 demonstrated low level of WHV replication confirmed by the detection of WHV ssDNA replicative intermediate (Fig. 5.46; page 135).

The data obtained from woodchuck 61792 clearly demonstrate that the novel combination strategy (ETV + prime-boost vaccination) led to the complete clearance of WHV infection in one of four woodchucks. Premature euthanasia of the woodchuck 61793 did not allow to interpret the results fully. The fact that WHV ssDNA replicative intermediate was present in the liver of this woodchuck shows that woodchuck 61793 was not able to completely clear the WHV infection in the liver. This might imply that

the WHV replication could be restored in this animal. Nevertheless, the formation of RC DNA that indicates the assembly of progeny virions was still impaired. This finding correlates with the fact that the patients who recovered from acute hepatitis B may show residual HBV replication in the liver. However, those patients are not viremic due to the high neutralizing anti-HBs antibody concentration, which prevent the spread of the infection [*Rehermann et al., 1996; Yuki et al., 2003*]. As woodchuck 61793 had an undetectable WHV load and developed anti-WHs (in contrast to other woodchucks which showed full WHV replication in the liver), it can also be assumed that a long-term control of WHV infection was achieved in this animal.

The previously described study based on ETV treatment in combination with DNA (plasmids encoding WHcAg and WHsAg) together with protein (WHcAg and WHsAg) immunization resulted in the clearance of WHV infection in 2 out of 6 WHV chronic carriers [*Lu et al., unpublished results*]. Nevertheless, the period of ETV treatment was much longer (1 year) and animals received 12 immunizations. In the presented study, the ETV treated period was shortened from 52 to 23 weeks and the number of immunizations was reduced from 12 to 9. Nevertheless, the efficacy of the presented therapy was similar, which proves that the immunization with optimized plasmids and recombinant adenoviral vectors shows a great potential. The utility of optimized WHsAg expressing plasmids and recombinant viral vectors encoding WHsAg could bring additional benefit in the treatment of chronic WHV infection.

It was shown that the high values of liver transaminases in the serum of chronic hepatitis B patients or woodchucks may indicate the progression of the liver disease [*Chisari et al., 1995; Cote et al., 2000; Wang et al., 2004; Rehermann et al., 2005*]. Therefore, the question was addressed whether the novel therapeutic strategy may prevent the liver damage by the HCC development and, as a consequence, may lead to a normalization of the liver enzymes.

During ETV treatment, the serum GOT levels returned to normal levels in the sera of all examined woodchucks. However, the GOT levels remained low in the group that received a combinatory treatment, but not in ETV-only treated controls. It is known that the inhibition of the viral replication by antiviral treatment suppresses the progression of liver disease. The treatment of WHV chronic carriers with potent antiviral drugs as clevudine leads to a sustained decrease of liver enzymes levels in the serum [*Menne et al., 2002*]. Similar results were obtained in chronically HBV-

infected patients who demonstrated normalization of ALT levels during ETV treatment [*Karino et al., 2010; Yuen et al., 2011*]. Nevertheless, in the presented study the effect was more pronounced in the woodchucks that were additionally vaccinated (Fig. 5.47; page 136). The prolonged suppression of WHV replication achieved by heterologous DNA prime – AdV boost immunization also resulted in delaying the onset of HCC development (Fig. 5. 48; page 138).

6.5 Conclusion

It can be concluded that by improved vectors for vaccination, by the optimization of the vaccination protocol, and by the addition of a potent antiviral treatment a novel and potent strategy in treatment of chronic hepadnaviral infections was obtained. The results of this study proved that the combination of DNA vaccine and recombinant adenoviral vectors led to the induction of improved T_H and CTL WHV-specific responses for the first time in all treated chronic WHV carriers. Moreover, the long-term control of WHV was achieved in 2 out of 4 carriers. These findings indicate that the therapeutic approach evaluated in this study induces a potent T cell response and seems to be an effective strategy to achieve a sustained control of chronic hepadnaviral infections. In addition, this new approach may have an impact on clinical trials of the therapeutic vaccination in chronically HBV-infected patients. A latest study of a French group from the Pasteur Institute in Paris reported that the combination of antiviral treatment with DNA vaccine expressing HBsAg failed completely in eliminating the HBV infection in chronic HBV carriers [*Stanislas Pol, personal communication*]. Therefore, the results obtained in this study using a preclinical model present a promising alternative strategy. The combination of potent antivirals with the therapeutic vaccines which are focusing on the induction of a strong anti-core T cell response may be a more beneficial immunotherapy of chronic hepatitis B.

7 Summary

More than 360 million people worldwide are persistently infected with the hepatitis B virus (HBV). The recommended treatment of chronic hepatitis B with interferon-α and/or nucleoside analogues does not lead to satisfactory results. It is well documented that the viral persistence is caused by an absence of the effective virus-specific T cell response. Therefore, the induction of HBV-specific T cells by therapeutic vaccination may be an innovative strategy to overcome virus persistence. Vaccination with commercially available HBV vaccines and DNA vaccines in patients did not result in an induction of the immune response, which would effectively control the HBV infection. Due to this, a more potent therapeutic vaccines are needed. The woodchuck (*Marmota monax*) is a useful preclinical model for developing new therapeutic approaches in chronic hepadnaviral infections. Several approaches using classical protein and DNA vaccines were tested previously in the woodchuck model without success. The high viral load observed in chronic hepadnaviral infections may have impaired the induction of an effective virus-specific T cell response. Therefore, the application of more potent vaccines, e.g. recombinant viral vectors in combination with antiviral treatment, may be required to achieve sustained antiviral response.

In the presented study, an innovative therapeutic strategy, combining vaccination with optimized DNA and recombinant adenoviral vectors (AdV), as well as potent antiviral treatment with entecavir (ETV), was evaluated in the woodchuck model. It was hypothesized that this approach may be an effective strategy to improve WHV-specific immune responses and as a result lead to the resolution of chronic WHV infection.

For that purpose, an improved DNA vaccine (pCGWHc), adenoviral vector serotype 5 (Ad5WHc) and chimeric Ad5 displaying Ad35 fiber (Ad35WHc) expressing high levels of woodchuck hepatitis core antigen (WHcAg) were constructed. The efficacy of the improved vaccines was tested first in mice and in naïve woodchucks. The improved WHcAg expression by pCGWHc caused a detection of significantly stronger $CD8^+$ T cell response (interferon-γ production) and higher anti-WHc levels in C57BL/6 mice, compared to the previously used DNA plasmid vaccine. Immunization of mice by pCGWHc prime-AdV boost regimen enhanced $CD8^+$ T cell response even more, compared to immunization with DNA alone. Moreover, the vigorous cytotoxic activity

of these WHcAg-specific $CD8^+$ T cells could be demonstrated *in vivo*. To further evaluate the efficacy of the new prime-boost regimen the vaccination of WHV transgenic mice (1217 WHV Tg) was performed. The immunizations elicited an unexpected anti-WHc and anti-WHs antibodies and WHcAg-specific $CD8^+$ T cell response which led to a significant suppression of WHV replication in those mice. Next, the heterologous Ad5WHc/Ad35WHc immunization was performed in naïve woodchucks. The immunization resulted in the induction of a strong cellular immune response in woodchucks and protected them from WHV infection after the challenge. Altogether, these results clearly showed, that heterologous DNA-AdV immunization induces a more potent WHV-specific immune response than previously investigated strategies in mice and woodchucks. Therefore, this novel DNA prime-AdV boost regimen was used to treat chronically WHV-infected woodchucks in combination with entecavir (ETV) to induce a proper CTL response. Seven animals were treated with ETV for 23 weeks. Starting from week 8, five of them received additional 9 immunizations with DNA plasmids, expressing WHcAg and WHsAg, Ad5WHc and Ad35WHc. For the first time, the significant WHsAg- and WHcAg-specific proliferative responses (CD4) and degranulation responses (CD8) were detected in all chronic carriers that received immunizations in combination with ETV treatment. Moreover, 2 of 4 immunized woodchucks, which completed the ETV and vaccination treatment, demonstrated sustained antiviral response (undetectable viral load and development of anti-WHs).

These findings indicate that the therapeutic approach evaluated in this study induces a potent T cell response and seems to be an effective strategy to achieve sustained control of chronic hepadnaviral infections. These results obtained in a preclinical model might be the base for the clinical trials of therapeutic vaccines which induce strong anti-core T cell response in combination with antivirals as a possible immunotherapy in chronically HBV-infected patients.

8 Zusammenfassung

Weltweit sind derzeit mehr als 360 Millionen Menschen mit dem Hepatitis B Virus (HBV) chronisch infiziert. Die empfohlenen Behandlungsstategien bei chronischer Hepatitis B, bestehend aus Interferon-α und/oder Nukleosid-Analoga, zeigen keine zufriedenstellenden Erfolge. In der Literatur ist beschrieben, dass die Viruspersistenz durch das Fehlen einer effektiven virus-spezifischen T-Zellantwort mitunter verursacht wird. Daher stellt die Induktion einer HBV-spezifischen T-Zellantwort durch eine therapeutische Vakzinierung eine innovative Strategie zur Behandlung dar, um die Viruspersistenz zu überwinden. Die Schutzimpfung mit kommerziell erhältlichen HBV-Impfstoffen und DNA-Vakzinen in Patienten führt zu keiner ausreichenden Immunantwort, die HBV effektiv kontrolliert. Infolgedessen werden neue wirksame therapeutische Impfstoffe dringend benötigt. Das nordamerikanische Waldmurmeltier (*Marmota monax; engl*. woodchuck) ist ein nützliches, prä-klinisches Modell zur Entwicklung neuer therapeutischer Ansätze in chronischen hepadnaviralen Infektionen. Bisherige Therapieansätze im Murmeltier Model, unter Verwendung von klassischen Protein- und DNA-Vakzinen waren ohne Erfolg. Die hohe Viruslast, die in chronischen hepadnaviralen Infektionen beobachtet wird, kann die effektive, virus-spezifische T-Zellantwort beeinträchtigen. Aus diesem Grund werden wirksamere Impfstoffe, wie zum Beispiel eine Kombination aus rekombinanten viralen Vektoren und antivirale Behandlung benötigt, um eine andauernde antivirale Antwort zu erzielen.

In der vorliegenden Arbeit wurde eine innovative therapeutische Strategie im Murmeltier-Model verfolgt, die in einer kombinierten Vakzinierungsstrategie aus optimierten DNA- und rekombinanten Adenoviralen Vektoren (AdV) sowie aus einer wirksamen, antiviralen Behandlung mit Entecavir (ETV) bestand. Es wurde angenommen, dass dieser Ansatz eine effektive Immunisierungsstrategie darstellt, um eine spezifische Immunantwort gegen das Murmeltier Hepatitis Virus (WHV) zu verbessern und als Ergebnis zu einer Eliminierung der chronischen WHV-Infektion führt.

Zu diesem Zweck wurden Vektoren konstruiert, die das Murmeltier Hepatitis Core Antigen (WHcAg) stark exprimieren: ein verbesserter DNA-Impfstoff (pCGWHc), ein Adenoviraler Vektor des Serotyps 5 (Ad5WHc) und einen chimären Ad5 mit

präsentierenden Ad35 Fibern. Die Wirksamkeit dieser verbesserten Impfstoffe wurde zuerst in Mäusen und in naiven Murmeltieren getestet. Die durch pCGWHc verbesserte WHcAg Expression bewirkte eine signifikant stärkere $CD8^+$ T-Zellantwort (Interferon γ Produktion) und höhere anti-WHc Level in C57BL/6 Mäusen als in zuvor verwendeten DNA Plasmid-Vakzinen. Im Vergleich zu DNA-Immunisierung konnte eine weitere Verbesserung der $CD8^+$ T-Zellantwort erzielt werden, indem eine pCGWHc „prime-AdV boost“ Immunisierungsstrategie in Mäusen angewandt wurde. Darüber hinaus konnte gezeigt werden, dass diese WHcAg-spezifischen $CD8^+$ T-Zellen eine starke zytotoxische Aktivität *in vivo* besaßen. Zur weiteren Beurteilung der neuen „prime-boost“ Strategie wurden WHV-transgene Mäuse (1217 WHV Tg) immunisiert. Die Immunisierung rief eine unerwartete anti-WHc und anti-WHs Antikörperproduktion sowei eine WHcAg-spezifische CD8+ T-Zellantwort aus, die zu einer signifikanten Verminderung der WHV Replikation in den Mäusen führte. Im Anschluss wurde die heterologe Ad5/Ad35WHc Immunisierung in naiven Murmeltieren durchgeführt, welche eine starke zelluläre Immunantwort ausgelöste. Des Weiteren bot diese Immunisierungsstrategie effektiven Schutz vor einer WHV-Infektion. Zusammenfassend zeigen diese Ergebnisse, dass eine heterologe DNA-AdV Immunisierung eine weitaus stärkere WHV-spezifische Immunantwort induzieren kann, als die zuvor in Mäusen und Murmeltieren angewandten Immunisierungsstrategien. Zu diesem Zweck wurde diese neuartige DNA „prime-AdV boost“ Strategie dazu verwendet, chronisch WHV-infizierte Murmeltiere in Kombination mit ETV für 23 Wochen zu behandeln. Ausgehend von Woche 8 erhielten 5 der chronisch WHV-infizierten Murmeltiere 9 Immunisierungen mit den DNA-Plasmiden, welche WHcAg und WHsAg sowie Ad5WHc und Ad35WHc exprimieren. Zum ersten Mal konnte eine signifikante WHsAg- und WHcAg-spezifische Proliferationsantwort (CD4) und Degranulationsantwort (CD8) in allen chronisch infizierten Murmeltieren detektiert werden. Des Weiteren konnte gezeigt werden, dass 2 aus 4 immunisierten Murmeltieren, die die Behandlung mit ETV und Vakzine abgeschlossen hatten, eine anhaltende antivirale Immunantwort aufwiesen.

Diese Ergebnisse verdeutlichen, dass der gewählte therapeutische Ansatz eine wirksame T-Zellantwort induziert und eine effektive Behandlungsstrategie zu sein scheint, um eine anhaltende Kontrolle von chronischen hepadnaviralen Infektionen zu erzielen. Die in dieser Arbeit beschriebenen Befunde im prä-klinischen Model

könnten die Basis für eine klinische Studie zur therapeutischen Vakzinierung zur Immuntherapie chronischer HBV-infizierter Patienten darstellen, die in Kombination mit antiviralen Agentien in der Lage ist eine starke anti-Core T-Zellantwort zu erzielen.

9 References

Bangari DS and Mittal SK. Development of nonhuman adenoviruses as a vaccine vectors. *Vaccine* **2006**; 24: 849-862.

Barber DL, Wherry EJ and Ahmed R. Cutting edge: rapid in vivo killing by memory CD8 T cells. *J Immunol* **2003**; 171: 27-31.

Barouch DH, Craiu A, Santra S, *et al.* Elicitation of high-frequency cytotoxic T-lymphocyte responses against both dominant and subdominant simian-human immunodeficiency virus epitopes by DNA vaccination of rhesus monkeys. *J Virol* **2001**; 75: 2462-2467.

Barouch DH, Pau MG, Custers JH, *et al.* Immunogenicity of recombinant adenovirus serotype 35 vaccine in the presence of pre-existing anti-Ad5 immunity. *J Immunol* **2004**; 172: 6290-6297.

Bayer W, Schimmer S, Hoffmann D, *et al.* Evaluation of the Friend Virus model for the development of improved adenovirus-vectored anti-retroviral vaccination strategies. *Vaccine* **2008**; 26: 716-726.

Beasley RP, Hwang LY, Lin CC, *et al.* Hepatocellular carcinoma and hepatitis B virus: prospective study of 22,707 men in Taiwan. *Lancet* **1982**; 2: 1129-1133.

Bergelson JM. Receptors mediating adenovirus attachment and internalization. *Biochem Pharmacol* **1999**; 57: 975-979.

Berk PD and Popper H. Fulminant hepatic failure. *Am J Gastroenterol* **1978**; 69: 349–400.

Bertoletti A, Southwood S, Chesnut R, *et al.* Molecular features of the hepatitis B virus nucleocapsid T-cell epitope 18-27: interaction with HLA and T-cell receptor. *Hepatology* **1997**; 26: 1027-1034.

Bertolino P, Bowen DG, McCaughan GW, *et al.* Antigen-specific primary activation of CD8+ T cells within the liver. *J Immunol* **2001**; 166: 5430-5438.

Betts MR, Brenchley JM, Price DA, *et al.* Sensitive and viable identification of antigen-specific CD8+ T cells by a flow cytometric assay for degranulation. *J Immunol Methods* **2003**; 281: 65-78.

Betts MR, Nason MC, West SM, *et al.* HIV nonprogressors preferentially maintain highly functional HIV-specific CD8+ T cells. *Blood* **2006**; 107: 4781-4789.

Boni C, Penna A, Ogg GS, *et al.* Lamivudine treatment can overcome cytotoxic T-cell hyporesponsiveness in chronic hepatitis B. *J Hepatol* **2001**; 33: 963-971.

Boni C, Penna A, Bertoletti A, *et al.* Transient restoration of anti-viral T cell responses induced by lamivudine therapy in chronic hepatitis B. *J Hepatol* **2003**; 39: 595-605.

Boni C, Fisicrao P, Valdatta C, *et al.* Characterization of hepatitis B virus (HBV) specific T-cell dysfunction in chronic HBV infection. *J Viro.* **2007**; 81: 4215-4225

Bortolotti F, Cadrobbi P, Crivellaro C, *et al.* Long-term outcome of chronic type B hepatitis in patients who acquire hepatitis B virus infection in childhood. *Gastroenterology* **1990**; 99: 805–810.

Bosch V, Bartenschlager R, Radziwill G, *et al.* The duck hepatitis B virus P-gene codes for protein strongly associated with the 5'-end of the viral DNA minus strand. *Virology* **1988**; 166: 475–485.

Bowen DG, Zen M, Holz L, *et al.* The site of primary T cell activation is a determinant of the balance between intrahepatic tolerance and immunity. *J Clin Invest* **2004**; 114: 701-712.

Bryant ML, Bridges EG, Placidi L, *et al.* Antiviral L-nucleosides specific for hepatitis B virus infection. *Antimicrob Agents Chemother* **2001**; 45: 229-235.

Buchbinder SP, Mehrota DV, Duerr A, *et al.* Efficacy assessment of a cell-mediated immunity HIV-1 vaccine (the Step Study); a double-blind, randomized, placebo-controlled, test-of-concept trial. *Lancet* **2008**; 372: 1881-1893.

Buchen-Osmond C. Further progress in ICTVdB, a universal virus database. *Arch Virol* **1997**; 142: 1734-1739.

Busch DH and Pamer EG. T cell affinity maturation by selective expansion during infection. *J Exp Med* **1999**; 189: 701-710.

Buscher M, Reiser W, Will H, *et al.* Transcripts and the putative RNA pregenome of duck hepatitis B virus: Implications for reverse transcription. *Cell* **1985**; 40: 717–724.

Casimiro DR, Chen L, Fu TM, *et al.* Comparative immunogenicity in rhesus monkeys of DNA plasmid, recombinant vaccinia virus, and replication-defective adenovirus vectors expressing a human immunodeficiency virus type 1 gag gene. *J Virol* **2003**; 77: 6305-6313.

Casimiro DR, Wang F, Schleif WA, *et al.* Attenuation of simian immunodeficiency virus SIVmac239 infection by prophylactic immunization with DNA and recombinant adenoviral vaccine vectors expressing gag. *J Virol* **2005**; 79: 15547-15555.

Chang TT, Lai CL, Chien RN, *et al.* Four years of lamivudine treatment in Chinese patients with chronic hepatitis B. *J Gastroenterol Hepatol* **2004**; 19: 1276-1282.

Chen L, Zhang Z, Chen W, *et al.* B7-H1 up-regulation on myeloid dendritic cells significantly suppresses T cell immune function in patients with chronic hepatitis B. *J Immuno.* **2007**; 178: 6634–6641.

Chisari FV and Ferrari C. Hepatitis B virus immunopathology. *Ann Rev Immunol* **1995**; 13:29-60.

Cohen BJ. The IgM antibody responses to the core antigen of hepatitis B virus. *J Med Virol* **1978**; 3: 141-149.

Colonno RJ, Genovesi EV, Medina I, *et al.* Long-term entecavir treatment results in sustained antiviral efficacy and prolonged life span in the woodchuck model of chronic hepatitis infection. *J Infect Dis* **2001**; 184: 1236-1245.

Conjeeveram HS and Lok AS. Management of chronic hepatitis B. *J Hepatol* **2003**; 38: S90-S103.

Couillin I, Pol S, Mancini M, *et al*. Specific vaccine therapy in chronic hepatitis B: induction of T cell proliferative responses specific for envelope antigens. *J Infect Dis* **1999**; 180: 15-26

Cote PJ, Shapiro M, Engle E, *et al.* Protection of chimpanzees from type B hepatitis by immunization with woodchuck hepatitis virus surface antigen. *J Virol* **1986**; 60:895-901.

Cote PJ and Gerin JL. *In vivo* activation of woodchuck lymphocytes measured by radiopurine incorporation and interleukin-2 production: implications for modeling immunity and therapy in hepatitis B virus infection. *Hepatology* **1995**; 22: 687-699

Cote PJ, Korba BE, Miller RH, *et al.* Effects of age and viral determinants on chronicity as an outcome of experimental woodchuck hepatitis virus infection. *Hepatology* **2000**; 31: 190-200.

Cox KS, Clair JH, Prokop MT, *et al.* DNA gag/adenovirus type 5 (Ad5) gag and Ad5 gag/Ad5 gag vaccines induce distinct T-cell response profiles. *J Virol* **2008**; 82: 8161-8171.

Dahmen A, Herzog-Hauff S, Bocher WO, *et al.* Clinical and immunological efficacy of intradermal vaccine plus lamivudine with or without interleukin 2 in patients with chronic hepatitis B. *J Med Virol* **2002**; 66: 452-460.

Dane DS, Cameron CH and Briggs M. Virus-like particles in serum of patients with Australia-antigen-associated hepatitis. *Lancet* **1970**; 1: 695-698.

Danthinne X and Imperiale MJ. Production of first generation of adenovirus vectors: a review. *Gene Ther* **2000**; 7: 1707-1714.

Darrah PA, Patel DT, De Luca R, *et al.* Multifunctional TH1 cells define a correlate of vaccine-mediated protection against Leishmania major. *Nat Med* **2007**; 13: 843-850.

Das A, Hoare M, Davies N, *et al.* Functional skewing of the global CD8 T cell population in chronic hepatitis B virus infection. *J Exp Med* **2008**; 205: 2111-2124.

Davis HL, Michel ML, Mancini M, *et al.* Direct gene transfer in skeletal muscle: plasmid DNA-based immunization against the hepatitis B virus surface antigen. *Vaccine* **1994**; 12:1503-1509.

Di Q, Summers J, Burch JB, *et al.* Major differences between WHV and HBV in the regulation of transcription. *Virology* **1997**; 229: 25-35.

Dienstag JL. Hepatitis B virus infection. *N Engl J Med* **2008**; 359: 1486-1500.

Dietze KK, Zelinskyy G, Gibbert K, *et al.* Transient depletion of regulatory T cells in transgenic mice reactivates virus-specific CD8+ T cells and reduces chronic retroviral set points. *Proc Natl Acad Sci USA* **2011**; 108: 2420-2425.

Dikici B, Kalayci AG, Ozgenc F, *et al.* Therapeutic vaccination in the immunotolerant phase of children with chronic hepatitis B infection. *Pediatr Infect Dis J* **2003**; 22: 345-349.

Falk K, Rotzsche O, Stevanovic S, *et al.* Allele-specific motifs revealed by sequencing of self peptides eluted from MHC molecules. *Nature* **1991**; 351: 290-296.

Farina SF, Gao GP, Xiang ZQ, *et al.* Replication-defective vector based on a chimpanzee adenovirus. *J Virol* **2001**; 75: 11603-11613.

Feltquate DM, Heaney S, Webster RG, *et al.* Different T helper cell types and antibody isotypes generated by saline and gene gun DNA immunization. *J Immunol* **1997**; 158: 2278-2284.

Ferrari C, Penna A, Bertoletti A, *et al.* Cellular immune response to hepatitis B virus-encoded antigens in acute and chronic hepatitis B virus infection. *J Immunol* **1990**; 145: 3442-3449.

Fitzgerald JC, Gao GP, Reyes-Sandoval A, *et al.* A simian replication-defective adenoviral recombinant vaccine to HIV-1 gag. *J Immunol* **2003**; 170: 1416-1422.

Frank I, Budde C, Fiedler M, *et al.* Acute esolving woodchuck hepatitis hirus (WHV) infection is associated with a strong cytotoxic T-lymphocyte response to a single WHV core peptide. *J Virol* **2007**; 81: 7156-7163.

Galibert F, Mandart E, Fitoussi F, *et al.* Nucleotide sequence of the hepatitis B virus genome (subtype ayw) cloned in *E. coli*. *Nature* **1979**; 281: 646–650.

Galibert F, Chen TN and Mandart E. Nucleotide sequence of a cloned woodchuck hepatitis virus genome: comparison with the hepatitis B virus sequence. *J Virol* **1982**; 41: 51-65.

Ganem D. Persistent infection of humans with hepatitis B virus: mechanisms and consequences. *Rev Infect Dis* **1982**; 4:1026-1047.

Ganem D, Greenbaum L and Varmus HE. Virion DNA of ground squirrel hepatitis virus: Structural analysis and molecular cloning. *J Virol* **1982**; 44: 374–383.

Ganem D and Schneider RJ. Hepadnaviridae: the viruses and their replication. In: Knipe DM *et al.,* eds. *Fields Virology*, 4th ed. Philadelphia, Lipincott-Raven **2001**.

Gao W, Robbins PD and Gambotto A. Human adenovirus type 35: nucleotide sequence and vector development. *Gene Ther* **2003**; 10:1941-1949.

Genovesi EV, Lamb L, Medina I, *et al.* Efficacy of the carbocyclic 2'-deoxyguanosine nucleoside BMS-200475 in the woodchuck model of hepatitis B virus infection. *Antimicrob Agents Chemother* **1998**; 42: 3209-3217.

Gerin JL, Cote PJ, Korba BE, *et al.* Hepatitis B virus and liver cancer: the woodchuck as an experimental model of hepadnavirus-induced liver cancer. In: Hollinger FB *et al.,* eds. *Viral hepatitis and liver disease*. Baltimore (MD), Williams & Wilkins; **1991**.

Gerlich WH and Robinson WS. Hepatitis B virus contains protein attached to the 5' terminus of its complete DNA strand. *Cell* **1980**; 21: 801–809.

Gibbert K, Dietze KK, Zelinskyy G, *et al.* Polyinosisc-polycytidilic acid treatment of Friend retrovirus-infected mice improves functional properties of virus-specific T cells and prevents virus-induced disease. *J Immunol* **2010**; 185: 6179-6189.

Guidotti LG, Guilhot S and Chisari FV. Interleukin-2 and alpha/beta interferon down-regulate hepatitis B virus gene expression in vivo by tumor necrosis factor-dependent and –independent pathways. *J Virol* **1994**: 68: 1265-1270.

Guidotti LG, Ishikawa T, Hobbs MV, *et al.* Inracellular inactivation of the hepatitis B virus by cytotoxic T lymphocytes. *Immunity* **1996**; 4: 25-36.

Guidotti LG, Rochford R, Chung J, *et al*. Viral clearance without destruction of infected cells during acute HBV infection. *Science* **1999**; 284: 825-829.

Heathcote J, McHutschison J, Lee S, *et al.* A pilot study of the CY-1899 T-cell vaccine in subjects chronically infected with hepatitis B virus. The CY 1899 T cell vaccine Study Group. *Hepatology* **1999**; 30: 531-536.

Heermann KH, Goldmann U, Schwartz W, *et al.* Large surface proteins of hepatitis B virus containing the pre-s sequence. *J Virol* **1984**; 52: 396-402.

Hermening S, Kugler S, Bahr M, *et al.* Increased protein expression from adenoviral shuttle plasmid and vectors by insertion of a small chimeric intron sequence. *J Virol Meth* **2004**; 122: 73-77.

Hervas-Stubbs S, Lasarte JJ, Sarobe P, *et al*. Therapeutic vaccination of woodchucks against chronic woodchuck hepatitis virus infection. *J Hepatol* **1997**; 27: 726-736.

Hervas-Stubbs S, Lasarte JJ, Sarobe P, *et al*. T helper cell response to woodchuck hepatitis virus antigens after therapeutic vaccination of chronically-infected animals treated with lamivudine. *J Hepatol* **2001**; 35: 105-111.

Hollinger FB and Liang TJ. Hepatitis B virus. In: Knipe DM *et al.,* eds. *Fields Virology*, 4th ed. Philadelphia, Lipincott-Raven **2001**.

Hoofnagle JH. Serologic markers of hepatitis B virus infection. *Annu Rev Med* **1981**; 32: 1–11.

Horiike N, Fazle SM, Michitaka K, *et al*. In vivo immunization by vaccine therapy following virus suppression by lamivudine: a novel approach for treating patients with chronic hepatitis B. *J Clin Virol* **2005**; 32: 156-161.

Horwitz MS. Adenoviruses. In: Knipe DM *et al.,* eds. *Fields Virology*, 4th ed. Philadelphia, Lipincott-Raven **2001**.

Jacob JR, Korba BE, Cote PJ, *et al.* Suppression of lamivudine-resistant B-domain mutants by adefovir dipivoxil in the woodchuck hepatitis virus model. *Antiviral Res* **2004**; 63: 115-121.

Janssen HL, Van Zonneveld M, Senturk H, *et al.* Rotterdam Foundation for Liver Research. Pegylated interferon alfa-2b alone or in combination with lamivudine for HBeAg-positive chronic hepatitis B: a randomised trial. *Lancet* **2005**; 365: 123-129.

Jung MC, Spengler U, Schraut W, *et al.* Hepatitis B virus antigen-specific T-cell activation in patients with acute and chronic hepatitis B. *J Hepatol* **1991**; 13: 310-317.

Jung MC, Gruner N, Zachoval R, *et al*. Immunological monitoring during therapeutic vaccination as a prerequisite for the design of new effective therapies : induction of a vaccine-specific CD4+ T-cell proliferation response in chronic hepatitis B carriers. *Vaccine* **2002**; 20: 3598-3612.

Karino Y, Toyota J, Kumada H, *et al.* Efficacy and resistance of entecavir following 3 years of treatment of Japanese patients with lamivudine-refractory chronic hepatitis B. *Hepatol Int* **2010**; 4: 414-422.

Khalighinejad N, Hariri H, Behnamfar O, *et al.* Adenoviral gene therapy in gastric cancer. *World J Gastroenterol* **2008**; 14: 180-184.

Kibuuka H, Kimutai R, Maboko L, *et al.* A phase ½ study of a multiclade HIV-1 DNA plasmid prime and recombinant adenovirus serotype 5 boost vaccine in HIV-uninfected east Africans (RV 172). *J Infect Dis* **2009**; 201: 600-607.

Kock J, Borst EM and Schlicht HJ. Uptake of duck hepatitis B virus into hepatocytes occurs by endocytosis but does not require passage of the virus through an acidic intracellular compartment. *J Virol* **1996**; 70: 5827–5831.

Korba BE, Cote PJ and Gerin JL. Mitogen-induced replication of woodchuck hepatitis viruses in cultured peripheral blood lymphocytes. *Science* **1988**; 241: 1213-1216.

Korba BE, Cote PJ, Menne S, *et al.* Clevudine therapy with vaccine inhibits progression of chronic hepatitis and delays onset of hepatocellular carcinoma in chronic woodchuck hepatitis virus infection. *Antivir Ther* **2004**; 9: 937-952.

Krugman S, Overby LR, Mushahwar IK, *et al.* Viral hepatitis type B: studies on natural history and prevention re-examined. *N Engl J Med* **1979**; 300: 101-106.

Kuhlmann KF, Gouma DJ and Wesseling JG. Adenoviral gene therapy for pancreatic cancer: where do we stand? *Dig Surg* **2008**; 25 :278-292

Kurachi S, Hitomi Y, Furukawa M, *et al.* Role of intron I in expression of the human factor IX gene. *J Biol Chem* **1995**; 270: 5276–5281.

Lanford RE, Chavez D, Brasky KM, *et al.* Isolation of a hepadnavirus from the woolly monkey, a New World primate. *Proc Natl Acad Sci USA* **1998**; 95: 5757-5761.

Lau GK, Piratvisuth T, Luo KX, *et al.* Peginterferon alfa-2a HBeAg-positive chronic hepatitis B study group. peginterferon alfa-2a, lamivudine, and the combination for HBeAg-positive chronic hepatitis B. *N Engl J Med* **2005**; 352: 2682-2695.

Lechner RL and Kelly TJ Jr. The structure of replicating adenovirus 2 DNA molecules. *Cell* **1977**; 12: 1007-1020.

Li H, Gao Y, Raizada MK, *et al.* Intronic enhancement of angiotensin II type 2 receptor transgene expression in vitro and in vivo. *BBRC* **2005**; 336: 29-35.

Li S, Gowans EJ, Chougnet C, *et al.* Natural regulatory T cells and persistent viral infection. *J Virol* **2008**; 82: 21-30.

Liaw YF, Pao CC, Chu CM, *et al.* Changes of serum hepatitis B virus DNA in two types of clinical events preceding spontaneous hepatitis B e antigen seroconversion in chronic type B hepatitis. *Hepatology* **1987**; 7: 1–3.

Lien JM, Aldrich CE and Mason WS. Evidence that a capped oligoribonucleotide is the primer for duck hepatitis B virus plus-strand DNA synthesis. *J Virol* **1986**; 57: 229–236.

Liu CJ, Kao JH, Shau WY, *et al.* Naturally occurring hepatitis B surface gene variants in chronic hepatitis B virus infection: correlation with viral serotypes and clinical stages of liver disease. *J Med Virol* **2002**; 68 :50-59.

Locarnini S and Mason WS. Cellular and virological mechanisms of HBV drug resistance. *J Hepatol* **2006**; 44: 422-431.

Lu M, Hilken G, Kruppenbacher J, *et al.* Immunization of woodchucks with plasmids expressing woodchuck hepatitis virus (WHV) core antigen and surface antigen supresses WHV infection. *J Virol* **1999**; 73: 281-289.

Lu M, Klaes R, Menne S, *et al*. Induction of antibodies to the PreS region of surface antigens of woodchuck hepatitis virus (WHV) in chronic carrier woodchucks by immunizations with WHV surface antigens. *J Hepatol* **2003**; 39: 405-413.

Lu M, He LF, Xu Y, *et al.* Evaluation of combination therapies of chronic HBV infection with lamivudine and DNA-vaccines or antigen-antibody complexes in the woodchuck model. *J Virol* **2008**; 82: 2598-2603.

Luo MJ and Reed R. Splicing is required for rapid and efficient mRNA export in metazoans. *Proc Natl Acad Sci USA* **1999**; 96: 14937–14942.

Maier H, Isogawa M, Freeman GJ, *et al.* PD-1:PD-L1 interactions contribute to the functional suppression of virus-specific CD8+ T lymphocytes in the liver. *J Immunol* **2007**; 178: 2714-2720.

Maini MK, Boni C, Lee CK, *et al.* The role of virus-specific CD8+ cells in liver damage and viral control during persistent hepatitis B virus infection. *J Exp Med* **2000**; 191: 1269-1280.

Marion PL, Oshiro LS, Regnery DC, *et al.* A virus in Beechey ground squirrels that is related to hepatitis B virus of humans. *Proc Natl Acad Sci USA* **1980**; 77: 2941-2945.

Mancini-Bourgine M, Fontaine H, Scott-Algara D, *et al.* Induction or expansion of T-cell responses by a hepatitis B DNA vaccine administered to chronic HBV carriers. *Hepatology* **2004**; 40: 874-882.

Mason WS, Seal G and Summers J. Virus of Pekin ducks with structural and biological relatedness to human hepatitis B virus. *J Virol* **1980**; 36: 829-836.

Mason WS, Cullen J, Moraleda G, *et al.* Lamivudine therapy of WHV-infected woodchucks. *Virology* 1998; 245: 18-32.

Matthews KS, Alvarez RD and Curiel DT. Advancements in adenoviral based virotherapy for ovarian cancer. *Adv Drug Deliv Rev* **2009**; 61: 836-841.

McClary H, Koch R, Chisari FV, *et al.* Relative sensitivity of hepatitis B virus and other hepatotropic viruses to the antiviral effects of cytokines. *J Virol* **2000**; 74: 2255-2264.

McElrath MJ, De Rosa SC, Moodie Z, *et al.* HIV-1 vaccine-induced immunity in the test-of-concept Step Study; a case-cohort analysis. *Lancet* **2008**; 372:1894-1905.

McMahon BJ, Alward WL, Hall DB, *et al.* Acute hepatitis B virus infection: relation of age to clinical expression of the disease and subsequent development of the carrier state. *J Infect Dis* **1985**; 151: 599-603.

McMahon BJ, Alberts SR, Wainwright RB, *et al.* Hepatitis B-related sequelae: prospective study of 1400 hepatitis B surface antigen-positive Alaska Native carriers. *Arch Intern Med* **1990**; 150: 1051-1054.

Mei YF and Wadell G. Hemagglutination properties and nucleoside sequence analysis of the fiber gene of adenovirus genome types 11p and 11a. *Virology* **1993**; 194: 453-462.

Menne S, Maschke J, Lu M, *et al.* T-Cell response to woodchuck hepatitis virus (WHV) antigens during acute self-limited WHV infection and convalescence and after viral challenge. *J Virol* **1998**; 72: 6083-6091.

Menne S, Roneker CA, Korba BE, *et al*. Breaking T cell tolerance in chronic WHV infection by vaccination with WHsAg alone and in combination with the antiviral drug L-FMAU. *Antiviral Ther* **2000**; 5: B58.

Menne S, Roneker CA, Tennant BC, *et al*. Immunogenic effects of woodchuck hepatitis virus surface antigen vaccine in combination with antiviral therapy: breaking of humoral and cellular immune tolerance in chronic woodchuck hepatitis virus infection. *Intervirology* **2002**; 45: 237-250.

Menne S and Cote PJ. The woodchuck as an animal model for pathogenesis and therapy of chronic hepatitis B virus infection. *World J Gastroenterol* **2007**; 13: 104-124.

Michel ML and Loirat D. DNA vaccines for prophylactic or therapeutic immunization against hepatitis B. *Intervirology* **2001**; 44: 78-87.

Miller RH, Kaneko S, Chung CT, *et al.* Compact organization of the hepatitis B virus genome. *Hepatology* **1989**; 9: 322-327.

Millich DR, McLachlan A, Thornton GB, *et al.* Antibody production to the nucleocapsid and envelope of the hepatitis B virus primed by a single synthetic T cell site. *Nature* **1987**; 329: 547.

Morelli AE, Larregina AT, Ganster RW, *et al.* Recombinant adenovirus induces maturation of dendritic cells via NF-kappaB-dependent pathway. *J Virol* **2000**; 74: 9617-9628.

Moroy T, Etiemble J, Trepo C, *et al.* Transcription of woodchuck hepatitis virus in the chronically infected liver. *EMBO J* **1985**; 4: 1507–1514.

Nemerow GR, Pache L, Reddy V, *et al.* Insights into adenovirus host-cell interactions from structural studies. *Virology* **2009**; 384: 380-388.

Ni YH, Chang MH, Hsu HY, *et al.* Mutations of T-Cell epitopes in the hepatitis B virus surface gene in children with chronic infection and hepatocellular carcinoma. *Am J Gastroenterol* **2008**; 103: 1004-1009.

Norrby E, Van der Veen and Espmark A. A new serological technique for identification of adenovirus infection. *Proc Soc Exp Biol Med* **1970**; 134: 889-895.

Ochoa-Callejero L, Otano I, Vales A, *et al.* Identification of CD4+ and CD8+ T cell epitopes of woodchuck hepatitis virus core and surface antigens in BALB/c mice. *Vaccine* **2010**; 28: 5323-5331.

Okazaki T and Honjo T. The PD-1-PD-L pathway in immunological tolerance. *Trends Immunol* **2006**; 27:195-201.

Parker KC, Bednarek MA and Coligan JE. Scheme for ranking potential HLA-A2 binding peptides based on independent binding of individual peptide side-chains. *J Immunol* **1994**; 152: 163-175.

Penna A, Chisari FV, Bertoletti A, *et al.* Cytotoxic T lymphocytes recognize an HLA-A2-restricted epitope within the hepatitis B virus nucleocapsid antigen. *J Exp Med* **1991**; 174: 1565-70.

Penna A, Artini M, Cavalli A, *et al.* Long-lasting memory T cell responses following self-limited acute hepatitis B. *J Clin Invest* **1996**; 98: 1185-1194.

Penna A, Del Prete G, Cavalli A, *et al.* Predominant T helper 1 cytokine profile of hepatitis B virus nucleocapsid-specific T cells in acute self-limited hepatitis B. *Hepatology* **1997**; 25: 1022-1027.

Pettersson U and Roberts RJ. Adenovirus gene expression and replication: a historical review. *Cancer Cells* **1986**; 4: 37-57.

Pol S, Driss F, Michel ML, *et al.* Specific vaccine therapy in chronic hepatitis B infection. *Lancet* **1994**; 344: 342.

Pol S, Nalpas B, Driss F, *et al.* Efficacy and limitations of a specific immunotherapy in chronic hepatitis B. *J Hepatol* **2001**; 34: 917-921.

Popper H, Roth L, Puecell RH, *et al.* Hepatocarcinogenicity of the woodchuck hepatitis virus. *Proc Natl Acad Sci USA* **1987**; 84: 866-870.

Precopio ML, Betts MR, Parrino J, *et al.* Immunization with vaccinia virus induces polyfunctional and phenotypically distinctive CD8(+) T cell responses. *J Exp Med* **2007**; 204: 1405-1416.

Raney AK, Hamatake RK and Hong Z. Agents in clinical development for the treatment of chronic hepatitis B. *Expert Opin Investig Drugs* **2003**; 12: 1281-1295.

Rammensee HG, Bachmann J, Emmerich NN, *et al.* SYFPEITHI: database for MHC ligands and peptide motifs. *Immunogenetics* **1999**; 50: 213-219.

Rehermann B and Nascimbeni M. Immunology of hepatitis B virus and hepatitis C virus infection. *Nat Rev Immunol* **2005**; 5: 215-229.

Rehermann B, Ferrari C, Pasquinelli C, *et al.* The hepatitis B virus persists for decades after patients' recovery from acute viral hepatitis despite active maintenance of a cytotoxic T-lymphocyte response. *Nat Med* **1996**; 2: 1104-1108.

Ren F, Hino K, Yamaguchi Y, *et al*. Cytokine-dependent anti-viral role of CD4-positive T cells in therapeutic vaccination against chronic hepatitis B viral infection. *J Med Virol* **2003**; 71: 376-384.

Richardson JS, Yao MK, Tran KN, *et al.* Enhanced protection against Ebola virus mediated by an improved adenovirus-based vaccine. *PLoS One* **2009**; 4: e5308.

Robinson WS and Lutwick LI. The virus of hepatitis, type B (first of two parts). *N Engl J Med* **1976**; 295: 1168-1175.

Roingeard P, Lu SL, Sureau C, *et al.* Immunocytochemical and electron microscopic study of hepatitis B virus antigen and complete particle production in hepatitis B virus DNA transfected HepG2 cells. *Hepatology* **1990**; 11: 277–285.

Rigato PO, de Alencar BC, Vasconcelos JR, *et al.* Heterologous plasmid DNA prime-recombinant human adenovirus 5 boost vaccination generates a stable pool of protective long-lived CD8+ T effector memory cells specific for a human parasite, Trypanosoma cruzi. *Infect Immun* **2011** (Feb 28). [online publication, ahead of print].

Rigg RJ and Schaller H. Duck hepatitis B virus infection of hepatocytes is not dependent on low pH. *J Virol* **1992**; 66: 2829–2836.

Roos S, Fuchs K and Roggendorf M. Protection of woodchucks from infection with woodchuck hepatitis virus by immunization with recombinant core protein. *J Gen Virol* **1989**; 70:2087-2095.

Roggendorf M and Tolle TK. The woodchuck: and animal model for hepatitis B virus infection in man. *Intervirology* **1995**; 38: 100-112.

Rubio V, Stuge TB, Singh N, *et al.* Ex vivo identification, isolation and analysis of tumor-cytolytic T cells. *Nat Med* **2003**; 9: 1377-1382.

Rushbrook SM, Ward SM, Unitt E, *et al.* Regulatory T cells suppress in vitro proliferation of virus-specific CD8+ T cells during persistent hepatitis C virus infection. *J Virol* **2005**; 79: 7852–7859.

Rux JJ and Burnett RM. Adenovirus structure. *Hum Gene Ther* **2004**; 15: 1167-1176.

Safadi R, Israeli E, Papo O, *et al.* Treatment of chronic hepatitis B virus infection via oral immune regulation toward hepatitis B virus proteins. *Am J Gastroenterol* **2003**; 98: 2505- 2515.

Sakurai F, Kawabata K, Yamaguchi T, *et al.* Optimization of adenovirus serotype 35 vectors for efficient transduction in human hematopoietic progenitors: comparison of promoter activities. *Gene Ther* **2005**; 12: 1424-1433.

Sattler F and Robinson WS. Hepatitis B viral DNA molecules have cohesive ends. *J Virol* **1979**; 32: 226–233.

Schodel F, Neckermann G, Peterson D, *et al.* Immunization with recombinant woodchuck hepatitis virus nucleocapsid antigen or hepatitis B nucleocapsid antigen protects woodchucks from woodchuck hepatitis infection. *Vaccine* **1993**; 11: 624-628.

Seder RA, Darrah PA and Roeder M. T-cell quality in memory and protection: implications for vaccine design. *Nat Rev Immunol* **2008**; 8: 247-258.

Seeger C, Ganem D and Varmus HE. Biochemical and genetic evidence for the hepatitis B virus replication strategy. *Science* **1986**; 232: 477–484.

Seeger C and Mason WS. Hepatitis B virus biology. *Microbiol Mol Biol Rev* **2000**; 64:51-68.

Shenk T. Adenoviridae: the viruses and their replication. In: Knipe DM *et al.*, eds. *Fields Virology*, 4th ed. Philadelphia, Lipincott-Raven **2001**.

Shepard CW, Simard EP, Finelli L, *et al.* Hepatitis B virus infection: epidemiology and vaccination. *Epidemiol Rev* **2006**; 28: 112-125.

Shiver JW, Fu TM, Chen L, *et al.* Replication-incompetent adenoviral vaccine vector elicits effective anti-immunodeficiency virus immunity. *Nature* **2002**; 415: 331-335.

Siegel F, Lu M and Roggendorf M. Coadministration of gamma interferon with DNA vaccine expressing woodchuck hepatitis virus (WHV) core antigen enhances the specific immune response and protects against WHV infection. *J Virol* **2001**; 75: 5036-5042.

Signas C, Akusjarvi G and Pettersson U. Adenovirus 3 fiber polypeptide gene: implications for the structure of the fiber protein. *J Virol* **1985**; 53: 672-678.

Sprengel R, Kaleta EF and Will H. Isolation and characterization of a hepatitis B virus endemic in herons. *J Virol* **1988**; 62: 3832-3839.

Stevens TL, Bossie A, Sanders VM, *et al.* Regulation of antibody isotype secretion by subsets of antigen-specific helper T cells. *Nature* **1988**; 334: 255-258.

Sullivan NJ, Sanchez A, Rollin PE, *et al.* Development of a preventive vaccine for Ebola virus infection in primates. *Nature* **2000**; 408: 605-609.

Sullivan NJ, Geisbert TW, Geisbert JB, *et al.* Immune protection of nonhuman primates against Ebola virus with single low-dose adenovirus vectors encoding modified GPs. *PLoS Med* **2006**; 6: e177.

Summers J, O'Connell A and Millman I. Genome of hepatitis B virus: Restriction enzyme cleavage and structure of DNA extracted from Dane particles. *Proc Natl Acad Sci USA* **1975**; 72: 4597–4601.

Summers J, Smolec JM and Snyder R. A virus similar to human hepatitis B virus associated with hepatitis and hepatoma in woodchucks. *Proc Natl Acad Sci USA* **1978**; 75: 4533-4537.

Suomalainen M, Nakano MY, Keller S, et al. Microtubule-dependent plus- and minus end-directed motilities are competing processes for nuclear targeting of adenovirus. *J Cell Biol* **1999**; 144: 657-672.

Tatsis N and Ertl HC. Adenoviruses as vaccine vectors. *Mol Ther* **2004**; 10: 616–629.

Tennant BC, Toshkov IA, Peek SF, *et al.* Hepatocellular carcinoma in the woodchuck model of hepatitis B virus infection. *Gastroenterology* **2004**; 127: S283-S293.

Testut P, Renard CA, Terradillos O, *et al.* A new hepadnavirus endemic in arctic ground squirrels in Alaska. *J Virol* **1996**; 70: 4210-4219.

Thimme R, Wieland S, Steiger C, *et al*. CD8+ T cells mediate viral clearance and disease pathogenesis during acute hepatitis B virus infection. *J Virol* **2003**; 77: 68-76.

Trapani JA and Smyth MJ. Functional significance of the perforin/granzyme cell death pathway. *Nat Rev Immunol* **2002**; 2:735-747.

Trautmann L, Janbazian L, Chomont N, *et al.* Upregulation of PD-1 expression on HIV-specific CD8+ T cells leads to reversible immune dysfunction. *Nat Med* **2006**; 12: 1198-1202.

Tuttleman JS, Pourcel C and Summers J. Formation of the pool of covalently closed circular viral DNA in hepadnavirus-infected cells. *Cell* **1986**; 47: 451-460.

Urbani S, Amadei B, Tola D, *et al.* Restoration of HCV-specific T cell functions by PD-1/PD-L1 blockade in HCV infection: effect of viremia levels and antiviral treatment. *J Hepatol* **2008**; 48: 548-558.

Van der Molen RG, Sprengers D, Binda RS, *et al.* Functional impairment of myeloid and plasmacytoid dendritic cells of patients with chronic hepatitis B. *Hepatology* **2004**; 40: 738–746.

Vandamme P and Van Herck K. A review of the long-term protection after hepatitis a and B vaccination. *Travel Med Infect Dis* **2007**; 5: 79–84.

Vandepapelière P, Lau GK, Leroux-Roels G, *et al.* Therapeutic HBV Vaccine Group of Investigators. Therapeutic vaccination of chronic hepatitis B patients with virus suppression by antiviral therapy: a randomized, controlled study of co-administration of HBsAg/AS02 candidate vaccine and lamivudine. *Vaccine* **2007**; 25: 8585-8597.

Vayda ME, Rogers AE and Flint SJ. The structure of nucleoprotein cores released from adenoviruses. *Nucleic Acids Res* **1983**; 11: 441-460.

Vitiello A, Ishioka G, Grey HM, *et al.* Development of a lipopeptide-based therapeutic vaccine to treat chronic HBV infection. I. Induction of a primary cytotoxic T lymphocyte response in humans. *J Clin Invest.* **1995**; 95: 341-349.

Wan S, Xia C and Morel L. IL-6 produced by dendritic cells from lupus-prone mice inhibits CD4+CD25+ T cell regulatory functions *J Immunol* **2007**; 178: 271–279.

Wang Y, Menne S, Baldwin BH, *et al.* Kinetics of viremia and acute liver injury in relation to outcome of neonatal woodchuck hepatitis virus infection. *J Med Virol* **2004**; 73: 406-415.

Webster GJ, Reignat S, Brown D, *et al.* Longitudinal analysis of CD8+ T cells specific for structural and nonstructural hepatitis B virus proteins in patients with chronic hepatitis B: implications for immunotherapy. *J Virol* **2004**; 78: 5707-5719.

Weiss L, Donkova-Petrini V, Caccavelli L, *et al.* Human immunodeficiency virus-driven expansion of CD4+CD25+ regulatory T cells, which suppress HIV-specific CD4 T-cell responses in HIV-infected patients. *Blood* **2004**; 104: 3249–3256.

Wen YM, Wu XH, Hu DC, *et al*. Hepatitis B vaccine and anti-HBs complex as approach for vaccine therapy. *Lancet* **1995**; 345: 1575-1576.

Wherry JE, Ha SJ, Kaech SM, *et al.* Molecular signature of CD8+ T cell exhaustion during chronic viral infection. *Immunity* **2007**; 27:670-684.

Wickham TJ, Mathias P, Cheresh DA, *et al.* Integrins alpha v beta 3 and alpha v beta 5 promote adenovirus internalization but not virus attachment. *Cell* **1993**; 73: 309-319.

Williams AJ, O'Brien LM, Phillpotts RJ, *et al.* Improved efficacy of a gene optimised adenovirus-based vaccine for venezuelan equine encephalitis virus. *Virol J* 2009; 6: 118.

Wirth T, Samaranayake H, Pikkarainen J, *et al.* Clinical trials for glioblastoma multiforme using adenoviral vectors. *Curr Opin Mol Ther* **2009**; 5: 485-492.

Xiang ZQ, Yang Y, Wilson JM, *et al.* A replication-defective human adenovirus recombinant serves as a highly efficacious vaccine carrier. *Virology* **1996**; 219: 220-227.

Xin KQ, Jounai N, Someya K, *et al.* Prime-boost vaccination with plasmid DNA and a chimeric adenovirus type 5 vector with type 35 fiber induces protective immunity against HIV. *Gene Ther* **2005**; 12: 1769-1777.

Xu D, Fu J, Jin L, *et al.* Circulating and liver resident CD4+ CD25+ regulatory T cells actively influence the antiviral immune response and disease progression in patients with hepatitis B. *J Immunol* **2006**; 177: 739-747.

Xu DZ, Zhao K, Guo LM, *et al.* A randomized controlled phase IIb trial of antigen-antibody immunogenic complex therapeutic vaccine in chronic hepatitis B patients. *PLoS One* **2008**; 3, Article ID e2565.

Yalcin K, Acar M and Degertekin H. Specific hepatitis B vaccine therapy in inactive HBsAg carriers: a randomized controlled trial. *Infection* **2003**; 31: 221-225.

Yang PL, Althage A, Chung J, et al. Immune effectors required for hepatitis B virus clearance. *Proc Natl Acad Sci USA* **2010**; 107: 798-802.

Yang SH, Lee CG, Park SH, *et al.* Correlation of antiviral T-cell responses with suppression of viral rebound in chronic hepatitis B carriers: a proof-of-concept study. *Gene Ther* **2006**; 13: 1110-1117.

Yang ZY, Wyatt LS, Kong WP, *et al.* Overcoming immunity to a viral vaccine by DNA priming before vector boosting. *J Virol* **2003**; 77: 799-803.

Yao X, Zheng B, Zhou J, *et al.* Therapeutic effect of hepatitis B surface antigen-antibody complex is associated with cytolytic and non-cytolytic immune responses in hepatitis B patients. *Vaccine* **2007**; 25: 1771-1779.

Yuen MF, Seto WK, Fung J, *et al.* Three Years of Continuous Entecavir Therapy in Treatment-Naïve Chronic Hepatitis B Patients: VIRAL Suppression, Viral Resistance, and Clinical Safety. *Am J Gastroenterol* **2011**; (Mar 1). [online publication, ahead of print].

Yuki N, Nagaoka T, Yamashiro M, *et al.* Long-term histologic and virologic outcomes of acute self-limited hepatitis B. *Hepatology* **2003**; 37: 1172-1179.

Zakhartchouk AN, Viswanathan S, Mahony JB, *et al.* Severe acute respiratory syndrome coronavirus nucleocapsid protein expressed by an adenovirus vector is phosphorylated and immunogenic in mice. *J Gen Virol* **2005**; 86: 211–215.

Zelinskyy G, Dietze KK, Huesecken YP, *et al.* The regulatory T-cell response during acute retroviral infection is locally defined and controls the magnitude and duration of the virus-specific cytotoxic T-cell response. *Blood* **2009**; 114: 3199-3207.

Zimmerli SC, Harari A, Cellerai C, *et al.* HIV-1-specific IFN-gamma/IL-2-secreting CD8 T cells support CD4-independent proliferation of HIV-1-specific CD8 T cells. *Proc Natl Acad Sci USA* **2005**; 102: 7239-7244.

10 Appendix

10.1 WHcAg and WHsAg amino acid sequences of WHV strain 8

WHcAg (188 amino acids)

MDIDPYKEFG SSYQLLNFLP LDFFPDLNAL VDTATALYEE ELTGREHCSP
HHTAIRQALV CWDELTKLIA WMSSNITSEQ VRTIIVNHVN DTWGLKVRQS
LWFHLSCLTF GQHTVQEFLV SFGVWIRTPA PYRPPNAPIL STLPEHTVIR
RRGGARASRS PRRRTPSPRR RRSQSPRRRR SQSPSANC

WHsAg (431 amino acids)

MGNNIKVTFN PDKIAAWWPA VGTYYTTTYP QNQSVFQPGI YQTTSLINPK
NQQELDSVLI NRYKQIDWNT WQGFPVDQKL PLVSRDPPLK PHINQSAQTF
EIKPGPIIVP GIRDIPRGLV PPQTPTNRDQ GRKPTPPTPP LRDTHPHLTM
KNQTFRLQGF VDGLRDLTTT ERYHNAYGDP FTTLSPVVPT VSTILSPPST
TGDPALSPEM SPSSLLGLLA GLQVVYFLWT KILTIAQNLD WWWTSLSFPG
GIPECTGQNS QFQTCKHLPT SCPPTCNGFR WMYLRRFIIY LLVLLLCLIF
LLVLLDWKGL IPVCPLQPTT ETTVNCRQCT LSVQDTYTPP YCCCLKPTAG
NCTCWPIPSS WALGNYLWEW ALARFSWLNL LVPLLQWLGG ISLIAWFLLI
WMIWFWGPAL LSILPPFIPI FVLFFLIWVY I

10.2 Sequences of peptides used for in vitro stimulation

WHcAg- and WHsAg-derived synthetic peptides used for *in vitro* stimulation of murine splenocytes and woodchuck PBMCs for flow cytometric analysis and proliferation assays are presented in tables below (Tab. 10.1- Tab. 10.4). The amino acid sequences, the position of the peptide in the protein sequence and used abbreviations are given.

Tab. 10.1 Amino acid sequence of WHcAg-derived 9-mer peptides used for *in vitro* stimulation of murine splenocytes

Abbr.	Position	Sequence	Abbr.	Position	Sequence
p2n1	c7-15	KEFGSSYQL	p18n1	c86-94	VNHVNDTWG
p2n2	c8-16	EFGSSYQLL	p18n2	c87-95	NHVNDTWGL
p2n3	c9-17	FGSSYQLLN	p18n3	c88-96	HVNDTWGLK
p2n4	c10-18	GSSYQLLNF	p18n4	c89-97	VNDTWGLKV
p2n5	c11-19	SSYQLLNFL	p18n5	c90-98	NDTWGLKVR
p2n6	c12-20	SYQLLNFLP	p18n6	c91-99	DTWGLKVRQ
p2n7	c13-21	YQLLNFLPL	p18n7	c92-100	TWGLKVRQS
p2n8	c14-22	QLLNFLPLD			

Tab. 10.2 Amino acid sequence of WHcAg-derived 15-mer peptides used for *in vitro* stimulation of murine and woodchuck lymphocytes

Abbr.	Position	Sequence	Abbr.	Position	Sequence
p1	c1-15	MDIDPYKEFGSSYQL	p19	c91-105	DTWGLKVRQSLWFHL
p2	c6-20	YKEFGSSYQLLNFLP	p20	c96-110	KVRQSLWFHLSCLTF
p3	c11-25	SSYQLLNFLPLDFFP	p21	c101-115	LWFHLSCLTFGQHTV
p4	c16-30	LNFLPLDFFPDLNAL	p22	c106-120	SCLTFGQHTVQEFLV
p5	c21-35	LDFFPDLNALVDTAT	p23	c111-125	GQHTVQEFLVSFGVW
p6	c26-40	DLNALVDTATALYEE	p24	c116-130	QEFLVSFGVWIRTPA
p7	c31-45	VDTATALYEEELTGR	p25	c121-135	SFGVWIRTPAPYRPP
p8	c36-50	ALYEEELTGREHCSP	p26	c126-140	IRTPAPYRPPNAPIL
p9	c41-55	ELTGREHCSPHHTAI	p27	c131-145	PYRPPNAPILSTLPE
p10	c46-60	EHCSPHHTAIRQALV	p28	c136-150	NAPILSTLPEHTVIR
p11	c51-65	HHTAIRQALVCWDEL	p29	c141-155	STLPEHTVIRRRGGA
p12	c56-70	RQALVCWDELTKLIA	p30	c146-160	HTVIRRRGGARASRS
p13	c61-75	CWDELTKLIAWMSSN	p31	c151-165	RRGGARASRSPRRRT
p14	c66-80	TKLIAWMSSNITSEQ	p32	c156-170	RASRSPRRRTPSPRR
p15	c71-85	WMSSNITSEQVRTII	p33	c161-175	PRRRTPSPRRRRSQS
p16	c76-90	ITSEQVRTIIVNHVN	p34	c166-180	PSPRRRRSQSPRRRR
p17	c81-95	VRTIIVNHVNDTWGL	p35	c171-185	RRSQSPRRRRSQSPS
p18	c86-100	VNHVNDTWGLKVRQS	p36	c176-188	PRRRRSQSPSANC

Tab. 10.3 Amino acid sequence of WHcAg-derived peptides used for *in vitro* stimulation of woodchuck lymphocytes (Proliferation assay)

Abbr.	Position	Sequence	Abbr.	Position	Sequence
cp1	c1-16	MDIDPYKEFGSSYQLL	cp13	c85-100	IVNHVNDTWGLKVRQS
cp2	c8-23	EFGSSYQLLNFLPLDF	cp14	c93-108	WGLKVRQSLWFHLSCL
cp10	c64-79	ELTKLIAWMSSNITSE	cp15	c101-116	LWFHLSCLTFGQHTVQ
cp11	c71-86	WMSSNITSEQVRTIIV	cp16	c109-124	TFGQHTVQEFLVSFGV
cp12	c78-93	SEQVRTIIVNHVNDTW	cp17	c117-132	EFLVSFGVWIRTPAPY

Tab. 10.4 Amino acid sequence of WHsAg-derived peptides used for *in vitro* stimulation of woodchuck lymphocytes (Proliferation assay)

Abbr.	Position	Sequence	Abbr.	Position	Sequence
sp1	s210-225	MSPSSLLGLLAGLQVV	sp17	s322-337	TTVNCRQCTLSVQDTY
sp3	s224-239	VVYFLWTKILTIAQNL	sp19	s336-351	TYTPPYCCCLKPTAGN
sp5	s238-253	NLDWWWTSLSFPGGIP	sp21	s350-365	GNCTCWPIPSSWALGN
sp7	s252-267	IPECTGQNSQFQTCKH	sp23	s364-379	GNYLWEWALARFSWLN
sp9	s266-281	KHLPTSCPPTCNGFRW	sp25	s378-393	LNLLVPLLQWLGGISL
sp11	s280-295	RWMYLRRFIIYLLVLL	sp27	s292-407	SLIAWFLLIWMIWFWG
sp13	s294-309	LLLCLIFLLVLLDWKG	sp29	s406-421	WGPALLSILPPFIPIF
sp15	s308-323	KGLIPVCPLQPTTETT	sp31	s420-431	IFVLFFLIWVYI

10.3 Vector maps

The maps of all plasmids that were generated and used during the experiments are presented below (Fig. 10.1 - Fig. 10.4).

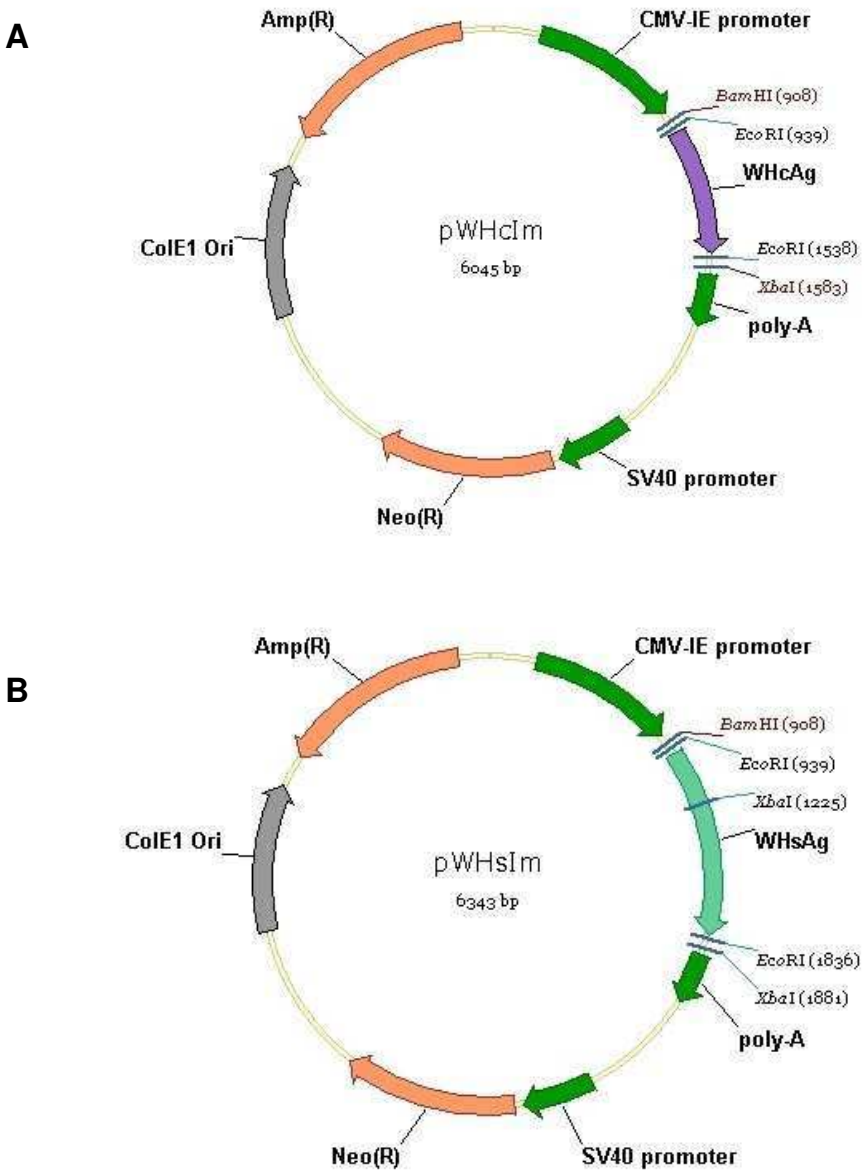

Fig. 10.1 Vector maps of pWHcIm (A) and pWHsIm (B) plasmids

Plasmids were constructed on the basis of pcDNA3 vector (Invitrogen). The inserts were amplified by PCR with specific primers and cloned into pCRII vectors (Invitrogen). Afterwards, the inserts were cloned into *EcoR*I site of the vector. The expression of WHcAg from pWHcIm plasmid and WHsAg from pWHsIm plasmid is under control of CMV-IE promoter of the vector. Plasmids were kindly provided by Prof. Mengji Lu (Institut für Virologie, Universitätsklinikum, Essen).

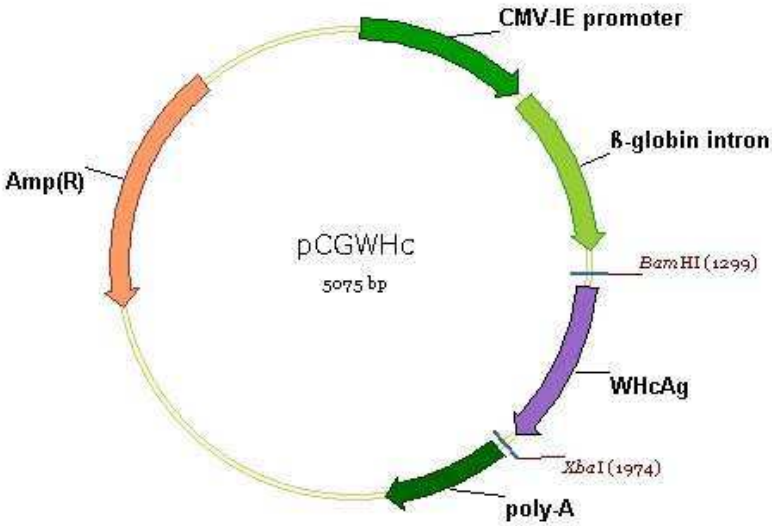

Fig. 10.2 Vector map of pCGWHc plasmid

Plasmid was constructed on the basis of pCG vector (kindly provided by Prof. Ulf Dittmer, Institut für Virologie, Universitätsklinikum, Essen). pCG contains a β-globin intron sequence between CMV-IE promoter and the polyadenylation signal and the ampicillin resistance gene: Amp(R). The WHcAg insert was obtained from pWHcIm vector, by cutting with *BamH*I and *Xba*I restriction enzymes, and then introduced into *BamH*I/*Xba*I site of pCG vector.

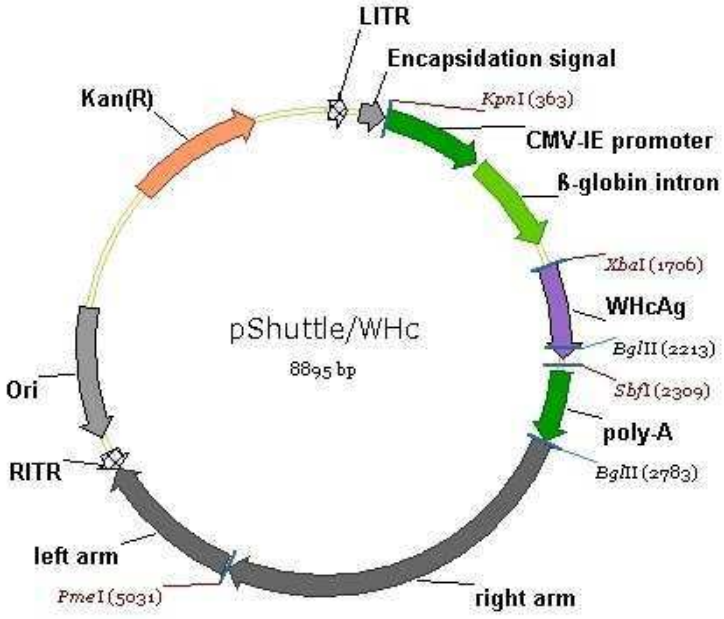

Fig. 10.3 Vector map of pShuttle/WHc plasmid

pShuttle plasmid (Qbiogene) contains two “arms” of viral sequence for homologous recombination with the adenoviral backbone vectors. Moreover, it contains adenoviral left and right inverted terminal repeats (LITR and RITR, respectively) and the kanamycin resistance gene: Kan(R). The expression cassette (CMV-IE promoter, β-globin intron and polyadenylation signal) was amplified by PCR using pCG plasmid as template and primers introducing *Kpn*I/*Bgl*II restriction sites. The amplified fragment was cloned into MCS of the pShuttle. The WHcAg sequence was obtained from pWHcIm plasmid by PCR with specific primers introducing *Xba*I/*Sbf*I restriction sites and cloned into *Xba*I/*Sbf*I site of the vector.

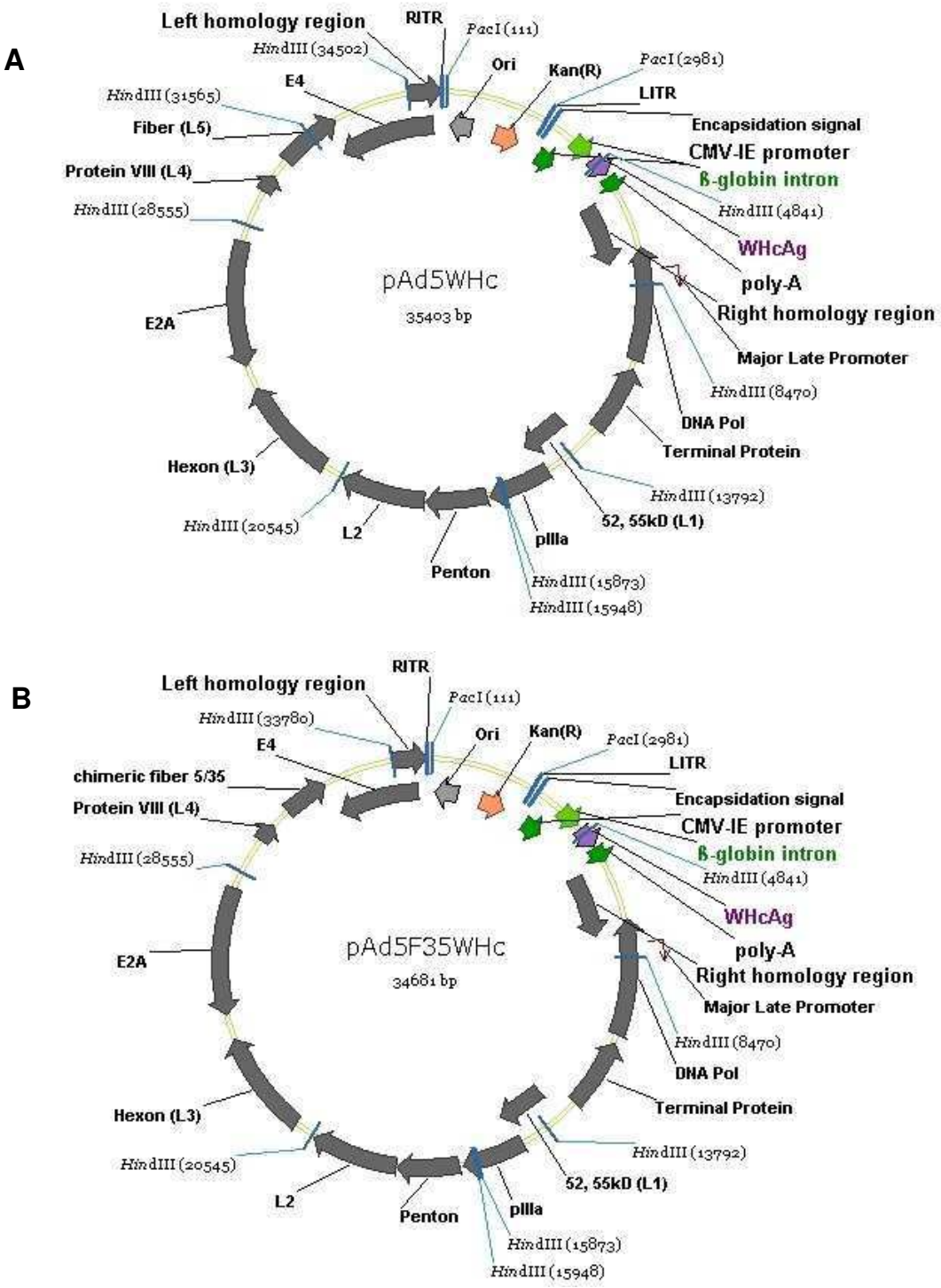

Fig. 10.4 Vector maps of pAd5WHc (A) and pAd5F35WHc (B) plasmids

The recombinant adenoviral plasmids were constructed on the basis of replication defective E1/E3-deleted pAdEasy-1 (pAd5WHc) and modified pAdEasy-1/F35 (pAd5F35WHc) backbone vectors (Qbiogene). The pShuttle/WHc plasmid, expressing WHcAg under the CMV-IE promoter, was linerized with *Pme*I and introduced in the E1 region by homologous recombination into the backbone vectors. The pAd5WHc and pAd5F35WHc contain all necessary adenoviral sequences to produce recombinant AdV particles in E1 supporting cell lines. The kanamycin resistance gene: Kan(R) originates from pShuttle plasmid. Restriction digest with *Pac*I releases the linear recombinant adenoviral genomes.

10.4 Supplementary figures

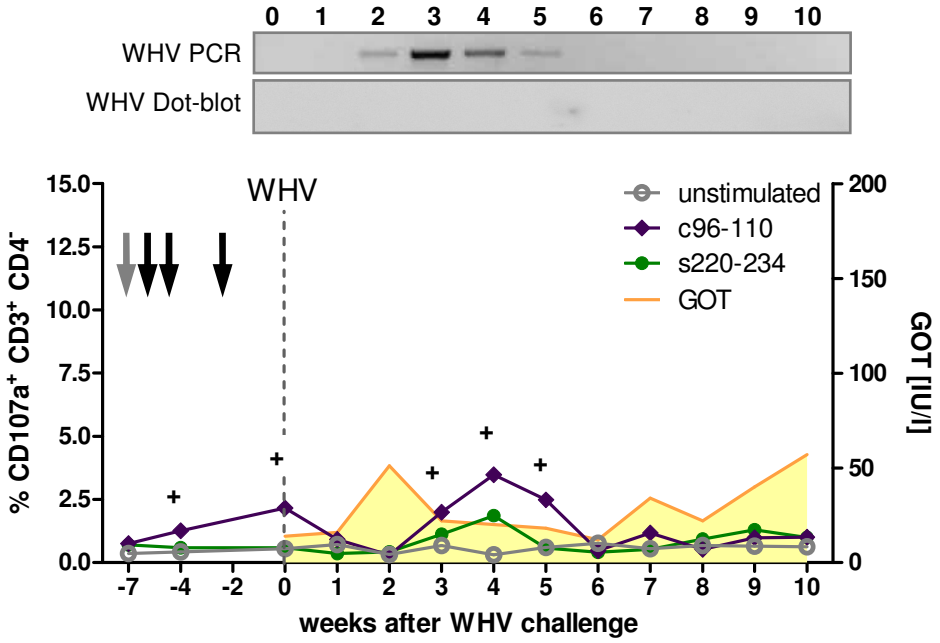

Fig. 10.5 Correlation of WHcAg- and WHsAg-specific CTL responses with WHV presence and GOT levels in pCGWHc immunized woodchuck: 70096

Woodchuck was pretreated with cardiotoxin (grey arrow) and immunized intramuscularly three times with pCGWHc plasmid (black arrows). WHcAg- and WHsAg-specific T cell response was measured by CD107a degranulation assay of woodchuck PBMCs expanded *in vitro* for 3 days with epitope c96-110 and s220-234. Unstimulated cells served as negative controls The values show the percentage of $CD107a^+$ $CD3^+$ $CD4^-$ T cells in the $CD3^+$ $CD4^-$ T cell population. The "+" sign marks the positive responses. The T cell responses were correlated with the presence of WHV (detected by WHV PCR and golden standard dot-blot hybridization) and GOT levels in the serum.

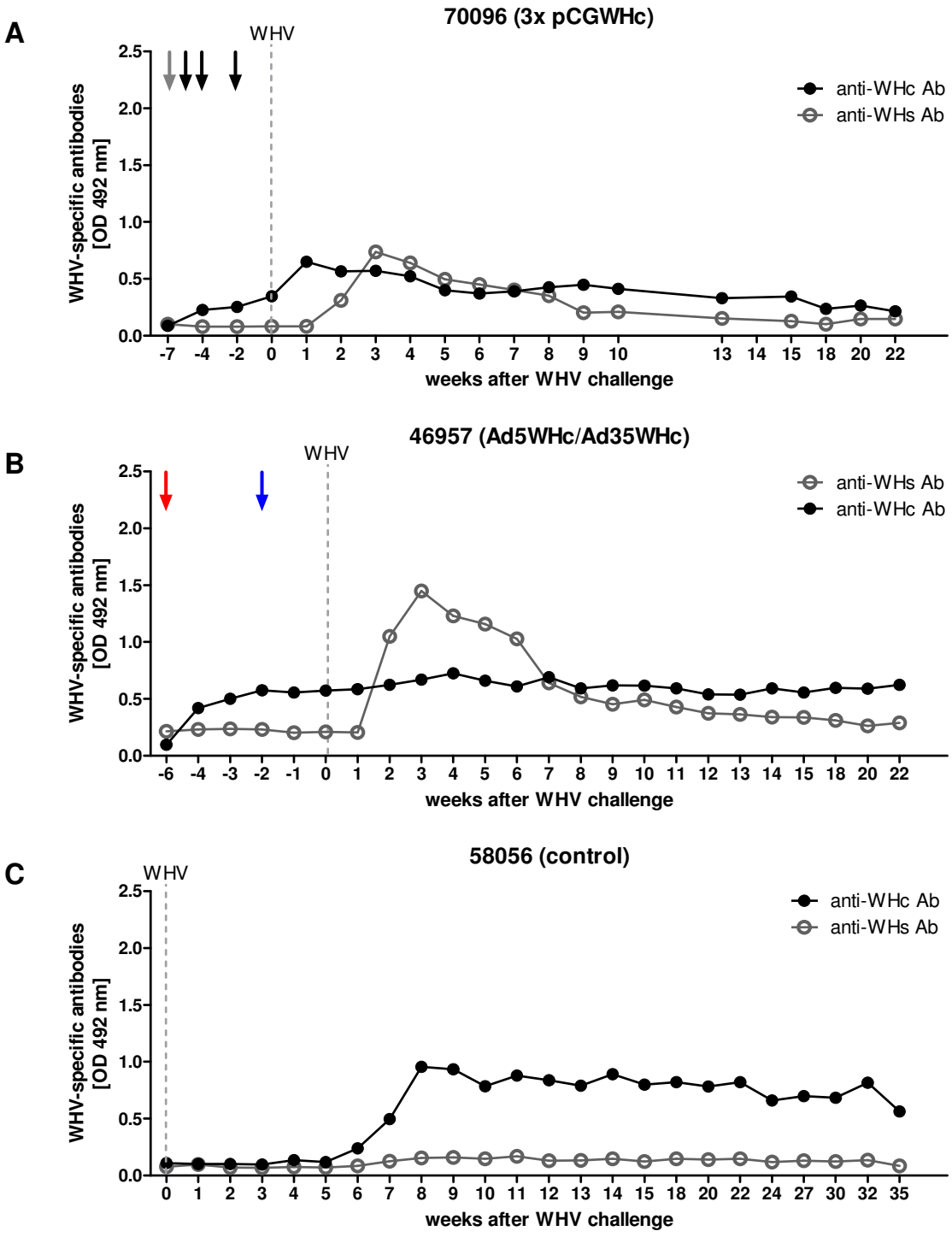

Fig. 10.6 Detection of anti-WHc and anti-WHs antibodies in the sera of woodchucks immunized with pCGWHc plasmid or Ad5WHc/Ad35WHc. Data of woodchuck 70096 (A), 46957 (B) and control 58056 (C)

Woodchuck 70096 was pretreated with cardiotoxin (grey arrow) and subsequently immunized for three times with pCGWHc plasmid (black arrows). Woodchuck 46949 was intramuscularly immunized with Ad5WHc (red arrow) and boosted with Ad35WHc (blue arrow). Immunized woodchucks and the control animal 58056 were intravenously inoculated with 1×10^7 WHV GE (week 0). Woodchucks sera were diluted 1:10 in PBS. WHcAg- and WHsAg-specific ELISA was performed using protein G coupled to peroxidase.

A

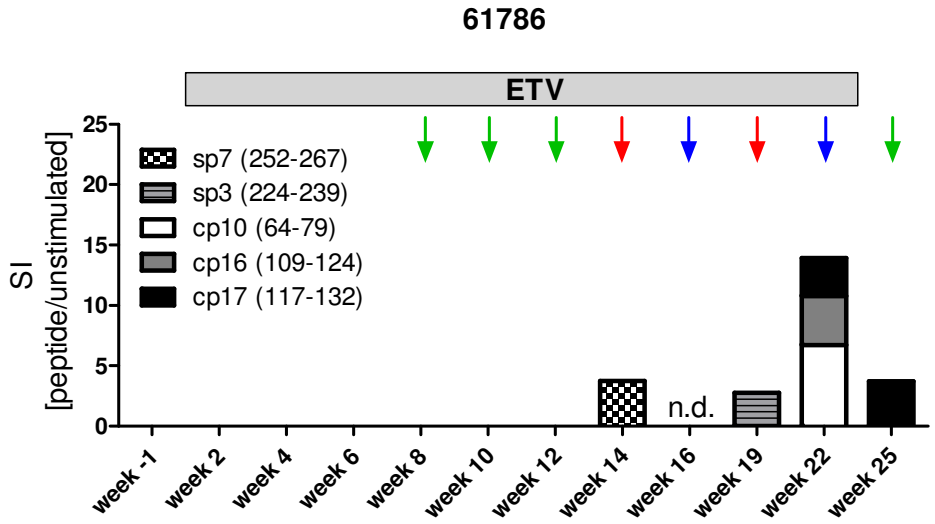
61786
ETV
SI [peptide/unstimulated]
sp7 (252-267)
sp3 (224-239)
cp10 (64-79)
cp16 (109-124)
cp17 (117-132)
n.d.
week -1
week 2
week 4
week 6
week 8
week 10
week 12
week 14
week 16
week 19
week 22
week 25

B

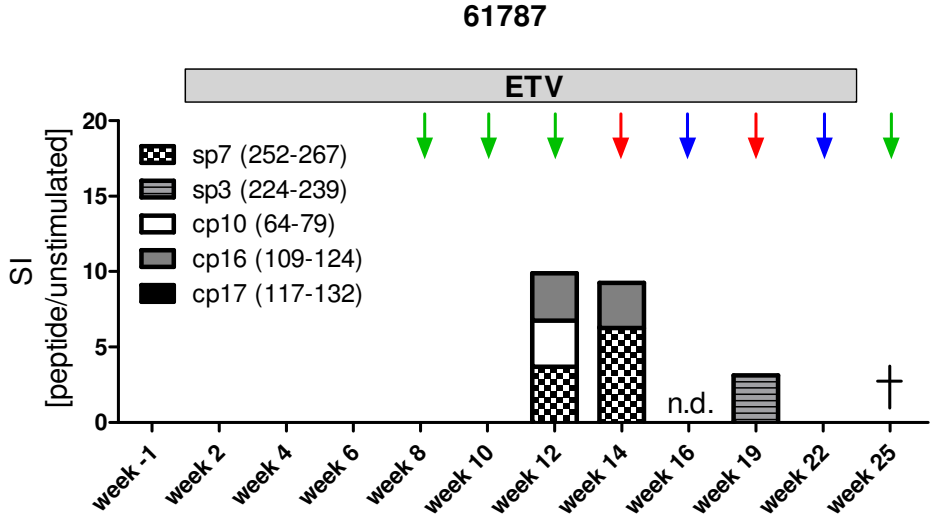
61787
ETV
SI [peptide/unstimulated]
sp7 (252-267)
sp3 (224-239)
cp10 (64-79)
cp16 (109-124)
cp17 (117-132)
n.d.
week -1
week 2
week 4
week 6
week 8
week 10
week 12
week 14
week 16
week 19
week 22
week 25

C

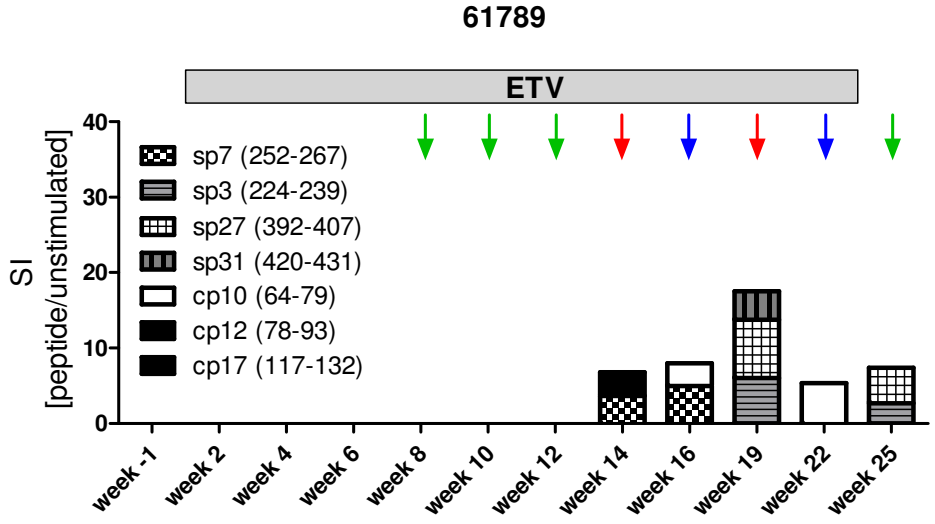
61789
ETV
SI [peptide/unstimulated]
sp7 (252-267)
sp3 (224-239)
sp27 (392-407)
sp31 (420-431)
cp10 (64-79)
cp12 (78-93)
cp17 (117-132)
week -1
week 2
week 4
week 6
week 8
week 10
week 12
week 14
week 16
week 19
week 22
week 25

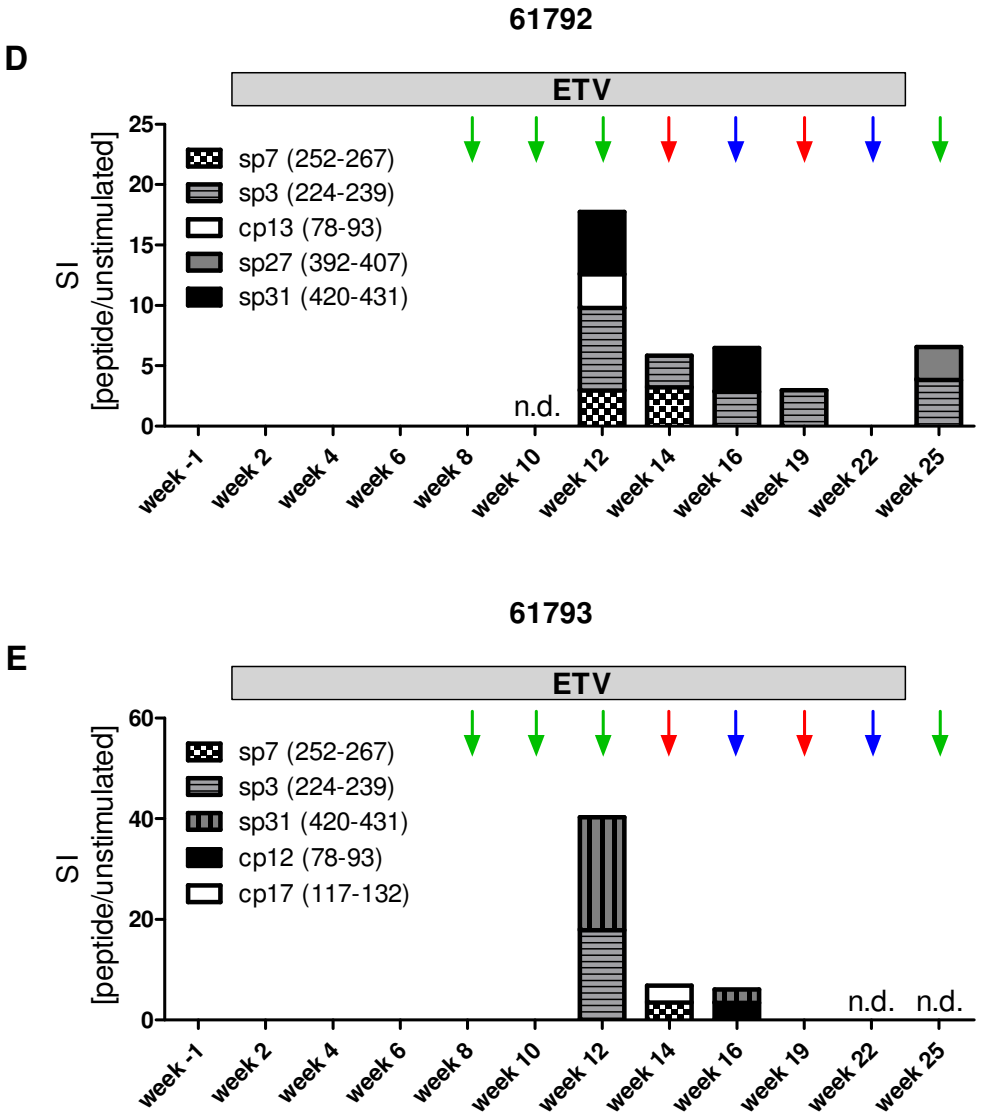

Fig. 10.7 WHcAg-specific and WHsAg-specific proliferative responses in WHV chronic carriers that were treated with combination therapy (A-E)

The WHV chronic carriers (number: 61786, 61787, 61789, 61792 and 61793) were treated with entecavir for 23 weeks. Starting from week 8 woodchucks received subsequently 9 intramuscular immunizations with pCGWHc/pWHsIm (time points of immunization marked by the green arrows), Ad5WHc/pWHsIm (red arrows) and Ad35WHc/pWHsIm (blue arrows). The PBMCs were separated from the blood of the animals at every examined time point and stimulated with panel of 10 WHcAg-specific and 16 WHsAg-specific peptides in triplicates. After 5 days of stimulation, cells were pulsed with 2[^{3}H]adenine for 16h and the incorporation of 2[^{3}H]adenine was measured. Results for triplicate cultures are presented as a mean stimulation index (SI): mean total absorbtion for peptide stimulated PBMCs divided by the mean total absorption for unstimulated control; *n.d.* – not done; † - dead.

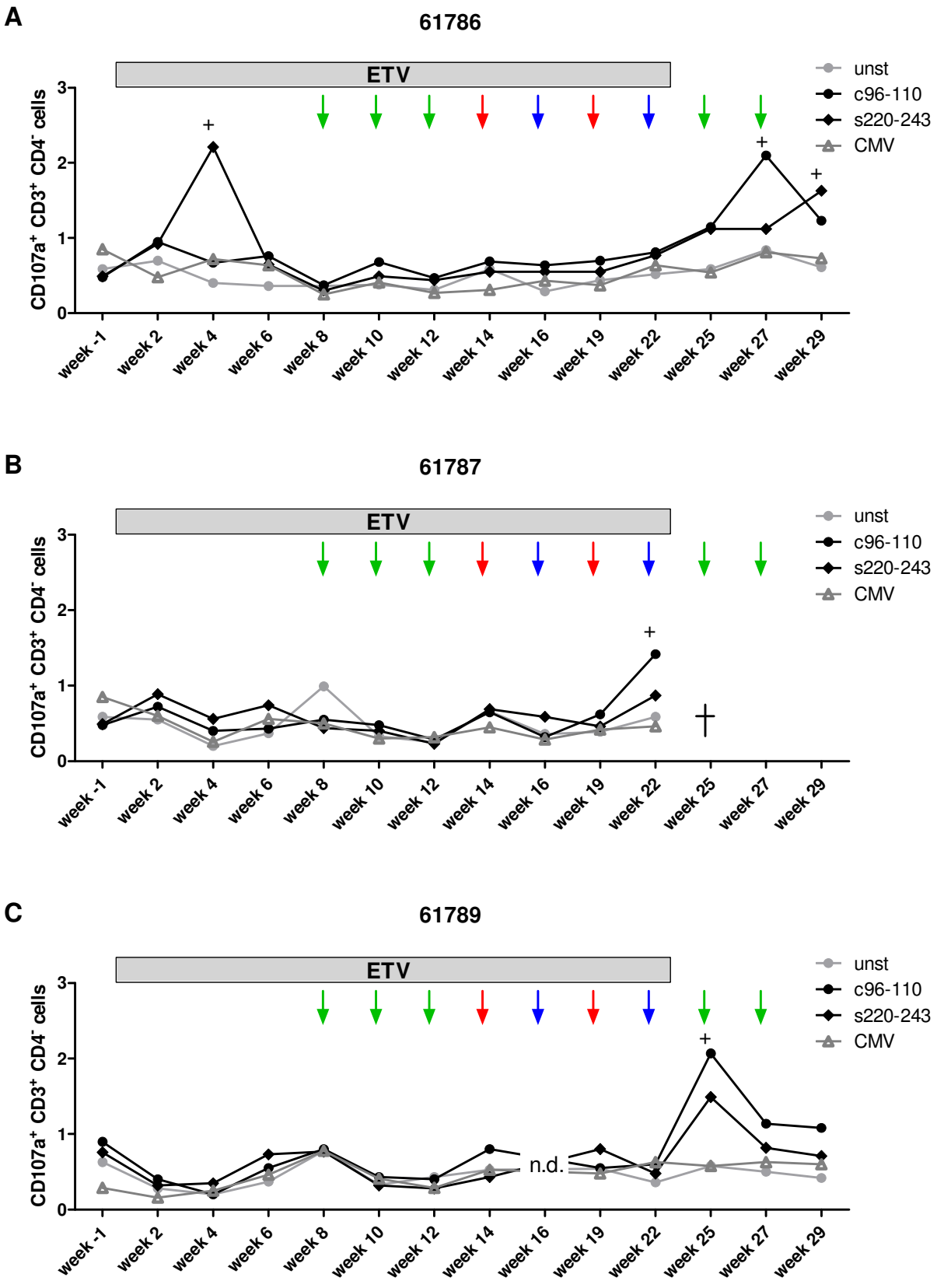
A
61786
ETV
unst
c96-110
s220-243
CMV
CD107a+ CD3+ CD4- cells
0
1
2
3
week -1
week 2
week 4
week 6
week 8
week 10
week 12
week 14
week 16
week 19
week 22
week 25
week 27
week 29
B
61787
ETV
unst
c96-110
s220-243
CMV
CD107a+ CD3+ CD4- cells
C
61789
ETV
unst
c96-110
s220-243
CMV
CD107a+ CD3+ CD4- cells
n.d.

D

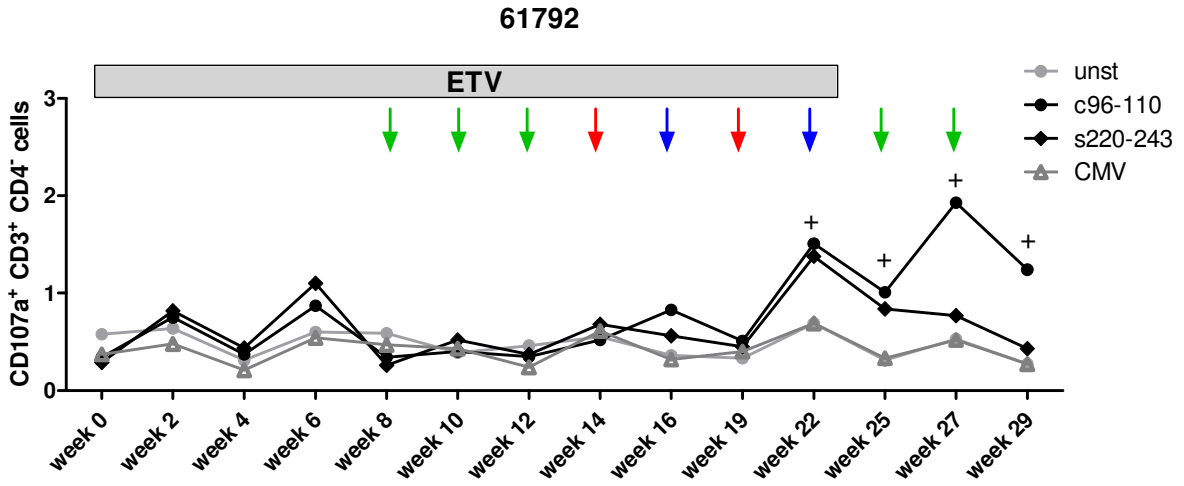
61792
ETV
unst
c96-110
s220-243
CMV
CD107a+ CD3+ CD4- cells
0
1
2
3
week 0
week 2
week 4
week 6
week 8
week 10
week 12
week 14
week 16
week 19
week 22
week 25
week 27
week 29

E

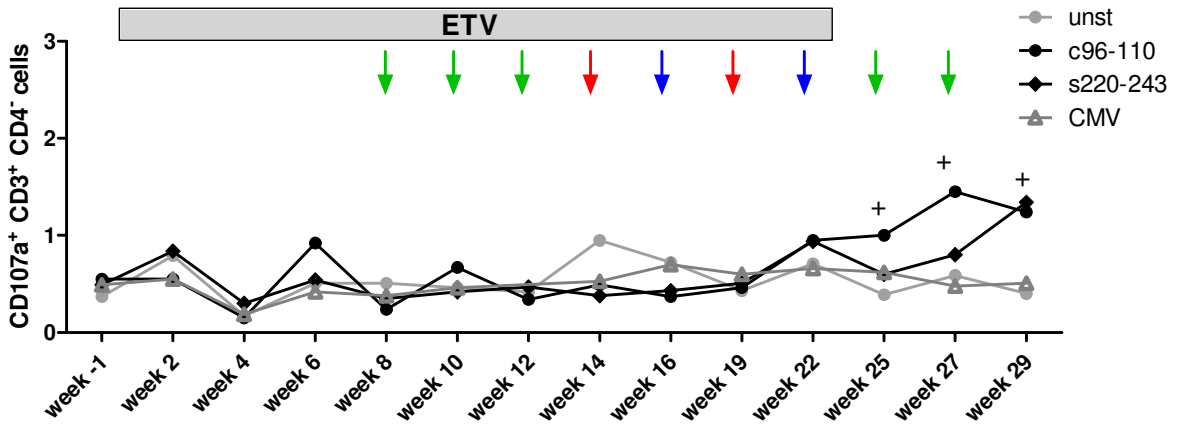
61793
ETV
unst
c96-110
s220-243
CMV
CD107a+ CD3+ CD4- cells
0
1
2
3
week -1
week 2
week 4
week 6
week 8
week 10
week 12
week 14
week 16
week 19
week 22
week 25
week 27
week 29

F

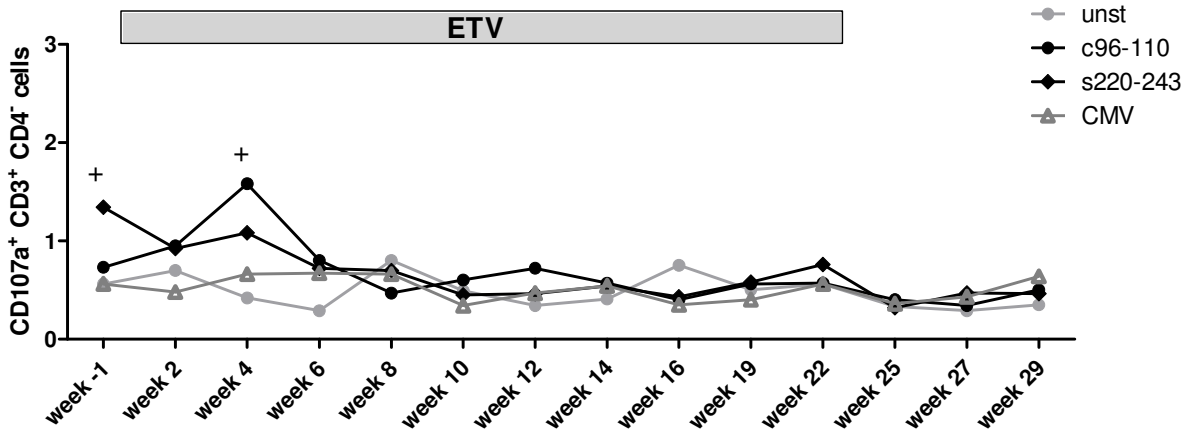
61791
ETV
unst
c96-110
s220-243
CMV
CD107a+ CD3+ CD4- cells
0
1
2
3
week -1
week 2
week 4
week 6
week 8
week 10
week 12
week 14
week 16
week 19
week 22
week 25
week 27
week 29

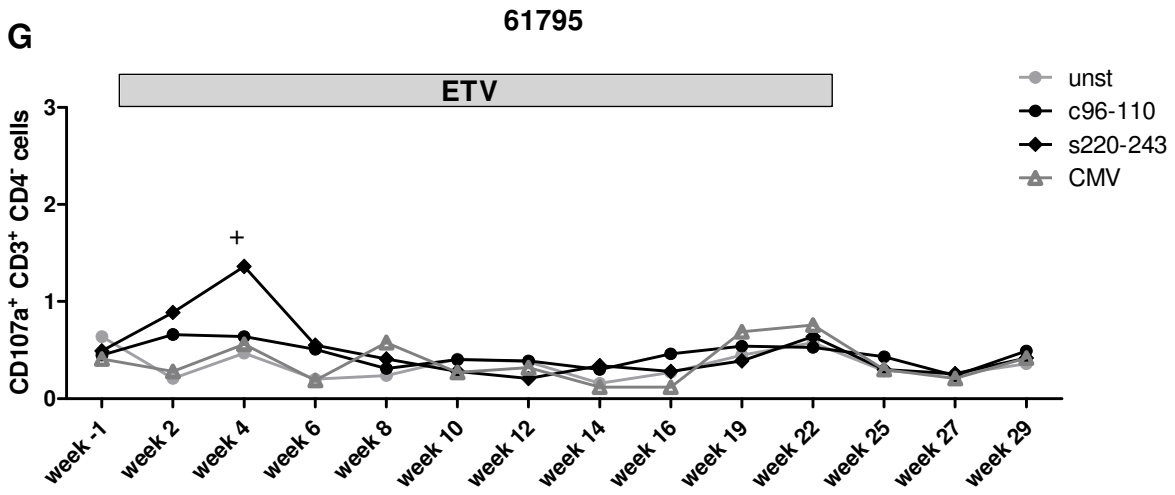

Fig. 10.8 Determination of CD107a$^+$ degranulation responses in WHV chronic carriers at all monitored time points of therapy: combination therapy group (A-E), ETV only treated controls (F-G)

Seven chronically WHV-infected woodchucks were treated with entecavir for 23 weeks. Five of the seven ETV-treated woodchucks (61786, 61787, 61789, 61792 and 61793) received subsequently 9 intramuscular immunizations with pCGWHc/pWHsIm (time points of immunization marked by the green arrows), Ad5WHc/pWHsIm (red arrows) and Ad35WHc/pWHsIm (blue arrows). Two animals (61791 and 61795) were treated only with ETV and served as controls. PBMCs were expanded *in vitro* for 3 days with WHcAg-derived epitope c96-110 or WHsAg-derived epitope s220-234. Unstimulated cells and cells stimulated with unrelated CMV-derived peptide served as a negative controls. The T cell response was evaluated by CD107a degranulation assay. Presented values shows the percentage of CD107a$^+$ CD3$^+$ CD4$^-$ T cells in the CD3$^+$ CD4$^-$ T cell population. The positive CTL responses are marked with "+" sign; *n.d.* – not done, † - dead.

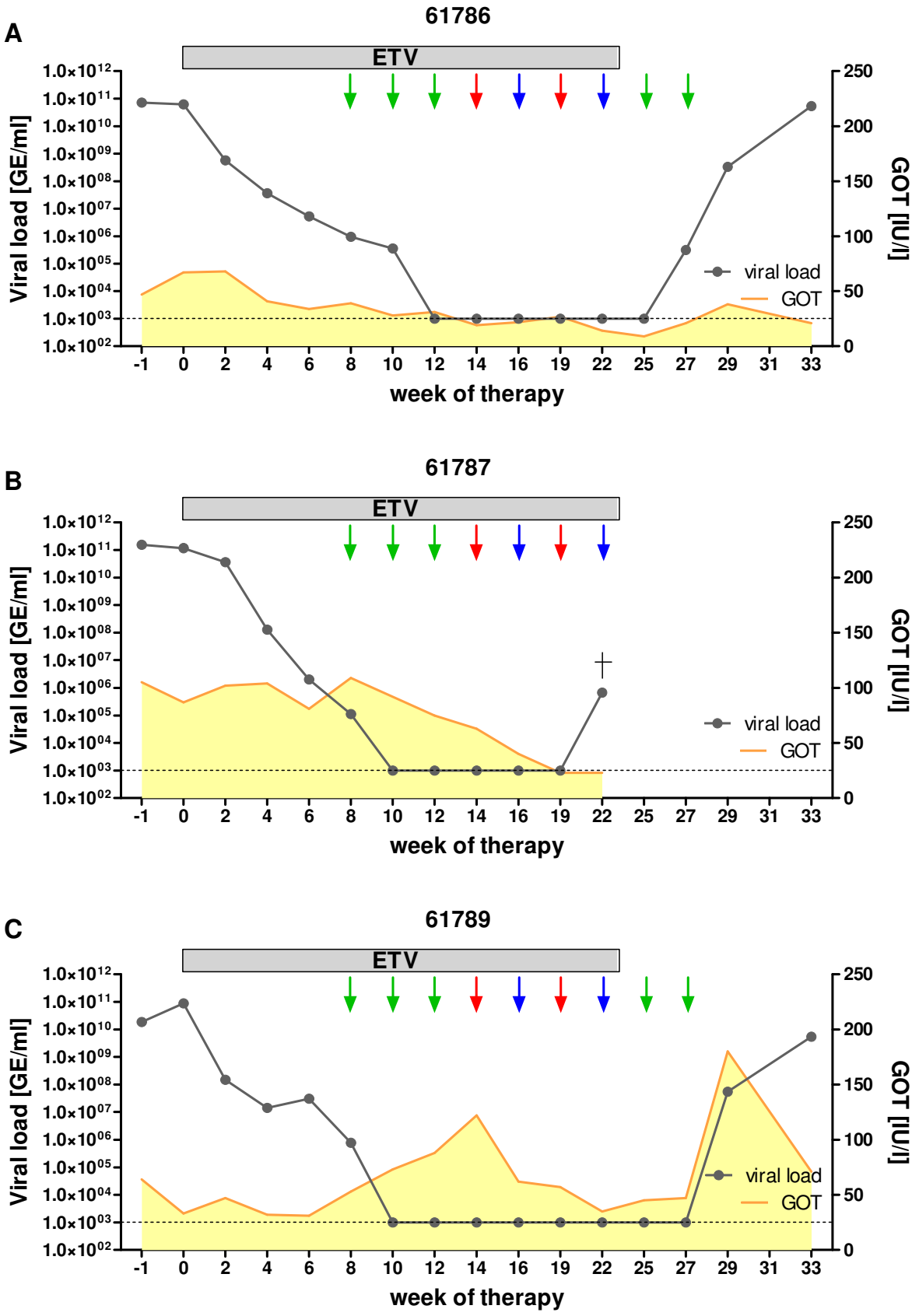
A
61786
ETV
Viral load [GE/ml]
GOT [IU/l]
viral load
GOT
week of therapy
B
61787
ETV
Viral load [GE/ml]
GOT [IU/l]
viral load
GOT
week of therapy
C
61789
ETV
Viral load [GE/ml]
GOT [IU/l]
viral load
GOT
week of therapy

D

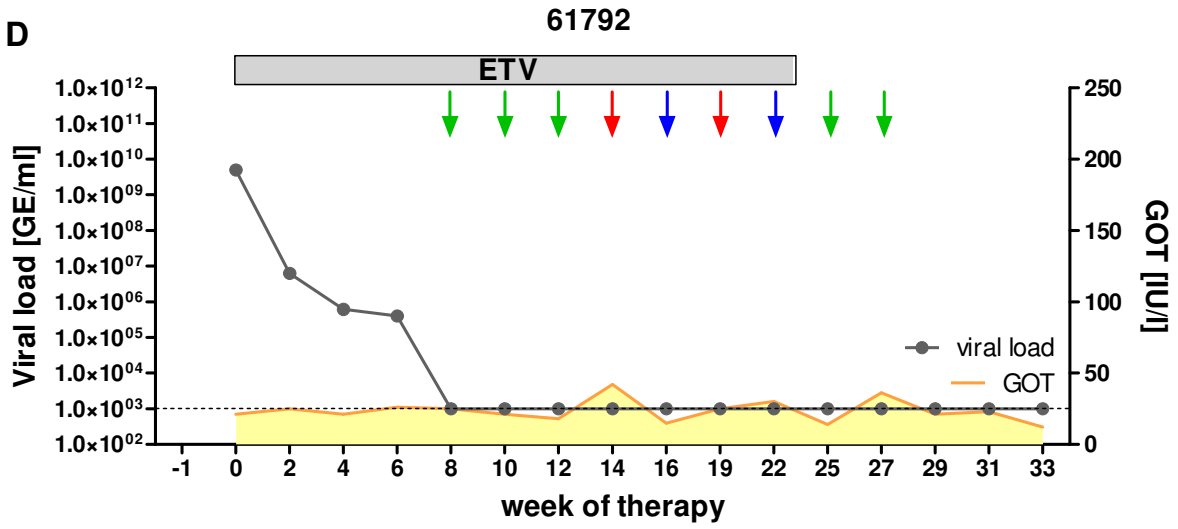
61792
ETV
Viral load [GE/ml]
GOT [IU/l]
viral load
GOT
week of therapy

E

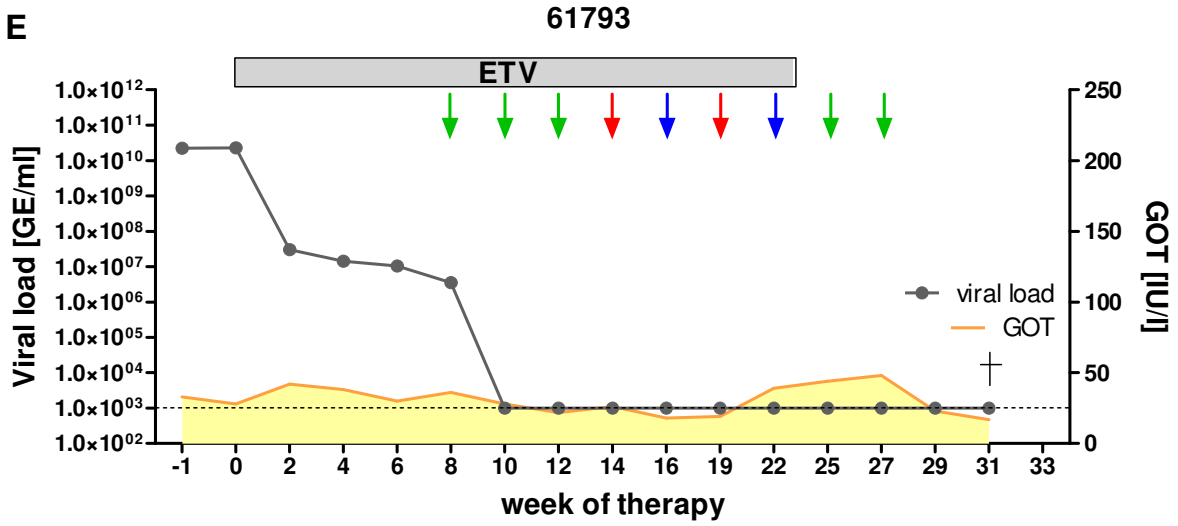
61793
ETV
Viral load [GE/ml]
GOT [IU/l]
viral load
GOT
week of therapy

F

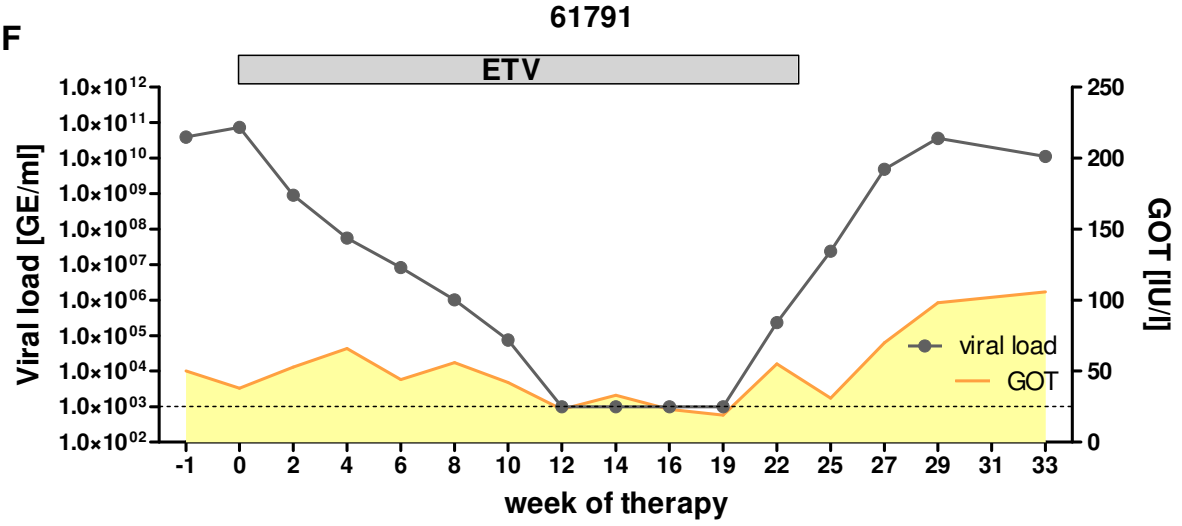
61791
ETV
Viral load [GE/ml]
GOT [IU/l]
viral load
GOT
week of therapy

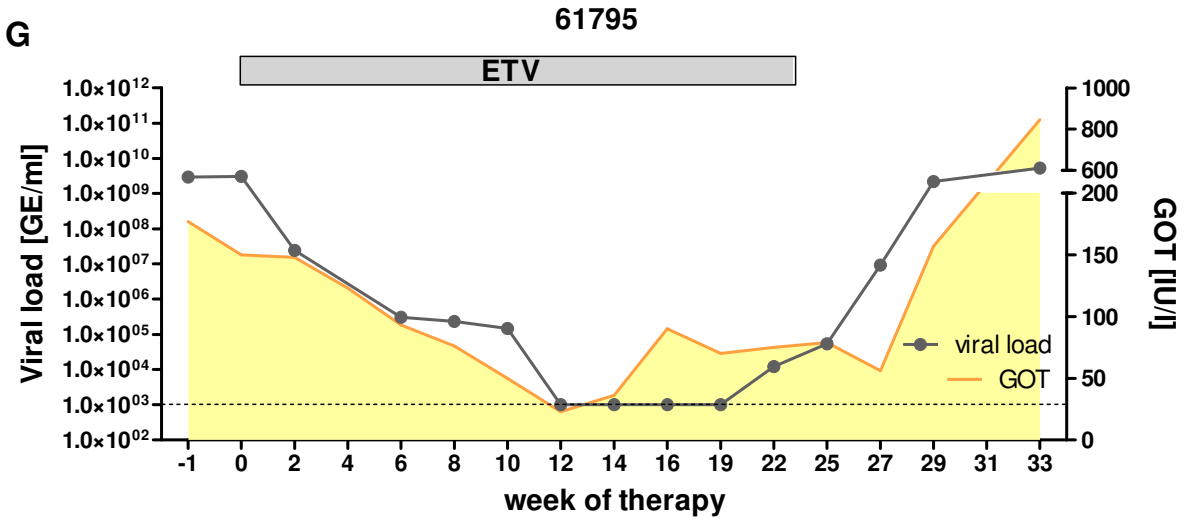

Fig. 10.9 Correlation of WHV viral load and serum GOT levels in WHV chronic carriers at all monitored time points of therapy: combination therapy group (A-E), ETV only treated controls (F-G)

Seven chronically WHV-infected woodchucks were treated with entecavir for 23 weeks. Five of the seven ETV-treated woodchucks (61786, 61787, 61789, 61792 and 61793) received subsequently 9 intramuscular immunizations with pCGWHc/pWHsIm (time points of immunization marked by the green arrows), Ad5WHc/pWHsIm (red arrows) and Ad35WHc/pWHsIm (blue arrows). Two animals (61791 and 61795) were treated only with ETV and served as controls. The viral DNA was extracted from woodchucks sera and the WHV viral load was quantified per mililiter of serum, using real-time PCR (the detection limit: 1×10^3 WHV GE/ml of serum). The GOT levels in woodchucks sera were quantified using the standard diagnostic methods. Elevation of GOT level is assumed above 50 IU/ml (border level); † - dead.

11 Abbreviations

7AAD	7-amino-actinomycin D
α ……	anti
aa	amino acid
Ab	Antibody
Abbr.	Abbreviation
AdV	Adenovirus
Ad5 ……...	Adenovirus serotype 5
Ad35 …….	Adenovirus serotype 35
Ad35F35 ……..	Chimeric Ad5 displaing Ad35 fiber
AF …….	Alexa fluor
ALT ……...	Alanine transaminase
APC ……..	Antigen presenting cell
APC ……..	Allophycocyanin
APS ……..	Ammonium persulfate
ASHV …….	Arctic squirrel hepatitis virus
AST…….	Aspartate transaminase
BFA ……..	Brefeldin A
BHK	Baby hamster kidney
bp …… ….	base pair
BSA ……..	Bovine serum albumin
^{o}C ……..	degree Celsius
CAR ……...	Coxsackie-adenovirus receptor
cccDNA ……	covalently closed circular DNA
CD	Cluster of differentiation
CFSE	Carboxyfluorescein succinimidyl ester
Ci	Curie
CMV	Cytomegalovirus
CPE ……..	Cytopathic effect
CTL ……...	Cytotoxic T cells

CTLA-4 ……. Cytotoxic T-lymphocyte antigen 4

DC ……. Dendritic T cells
dCTP …… deoxycytidine triphosphate
DHBV ……... Duck hepatitis B virus
DMEM …….. Dulbecco's Modified Eagles's Medium
DMSO …….. Dimethylsulfoxide
DNA …….. Deoxyribonucleic acid
dNTP …… deoxyribonucleotide
DR ……. Direct repeat

E.coli ……. *Escherichia coli*
EDTA …… Ethylenediaminetetraaceticacid
eF …….. eFluor
e.g. ……. for example
ELISA ……... Enzyme-linked immunosorbent assay
EN ……. Enhncer
engl. ..... English
et al. ..... and others (*lat.* et alii)
ETV ..... Entecavir
ER ..... Endoplasmic reticulum

FACS ..... Fluorescence activated cells sorting / sorter
FCS ..... Fetal calf serum
F ..... Farad
Fig. ……. Figure
FITC ……. Fluorescein isothiocyanate

g ……. gram
gag ……. Group-specific antigen
GFP …….. Green fluorescent protein
GOT …… …….. Glutamic oxaloacetic transaminase
GE ……. Genome equivalents
GSHV ……... Ground squirrel hepatitis virus

h …… hour
H-2 …… Histocompatibility-2
HBcAg …….. Hepatitis B virus core antigen
HBeAg …….. Hepatitis B virus “e” antigen
HBsAg …….. Hepatitis B virus surface antigen
HBV …….. Hepatitis B virus
HBxAg …….. Hepatitis B virus“x” antigen
HCC …….. Hepatocellular carcinoma
HCV …….. Hepatitis C virus
HEK …….. Human embronic kidney
HHBV ……... Heron hepatitis B virus
HIV …… Human Immunodeficiency Virus
HLA …….. Human leukocyte antigen
HRP …….. Horse radish peroxidase

IC …….. Immunogenic complex
IE …….. Immediate early
IFN …… Interferon
Ig ……... Immunoglobulin
IL ……... Interleukin
ITR …… Inverted terminal repeat
IU …….. International unit

J …… Joule

kb ……. kilo base pair

l …… liter
lat. ..... Latin
LITR ……. Left inverted terminal repeat
LB ……. Lurian broth

M ……... Molar
MCS ……. Multi cloning site
MEM ..... Minimum Essential Medium

MHC	Major histocompatibility complex
µ	micro
m	milli
min	minute
MOI	Multiplicity of infection
mRNA	messenger RNA
n	nano
n.d. ……	not done
n.s. ……	not significant
Ω ……...	Ohm
OD ……	Optical density
OPD ……..	o-Phenylendiamine
ORF ……..	Open reading frame
p ……..…….	peptide
PAGE ……...	Polyacrylamide gel electrophoresis
PBS ……..	Phosphate buffered saline
PBMC ……...	Peripheral blond mononuclear cell
PCR ……..	Polymerase chain reaction
PD-1 …….	Programmed cell death receptor 1
PD-L1 ……...	Programmed cell death 1 ligand 1
PE …….	Phycoerythrin
PEG ……..	Pegylated
PEI ……	Polyethyleneimine
PerCP ……..	Peridinin-chlorophyll-protein complex
PFU ……..	Plaque forming units
pgRNA …….	pregenomic RNA
pH …….	-log [H^+] (*lat.* potentia Hydrogenii)
pi ……...	post infection
PVDF	Polyvinylidene fluoride
RC DNA	Relaxed circular DNA
RITR	Right inverted terminal repeat

RNA	Ribonucleic acid
RNase ……..	Ribonuclease
s ……	second
SARS …….	severe acute respiratory syndrome
SDS ……..	Sodiumdodecylsulfate
SI ……..	Stimulation index
ssDNA ……..	single-stranded DNA
Tab. ……..	Table
TBE ……..	Tris-Borate-EDTA
$TCID_{50}$ ……..	Tissue culture infectious dose 50
TCR ……..	T cell receptor
TEMED ……	Tetramethylethylenediamine
Tg ……..	Transgenic
T_H ……...	T helper
TNF…….	Tumour necrosis factor
TP …….	Terminal protein
Tris …….	Tris-(hydroxymethyl)-aminomethane
U …….	Unit
V …….	Volt
VEEV …….	Venezuelan equine encephalitis virus
v/v …….	volume per volume
WHcAg …….	Woodchuck hepatitis virus core antigen
WHeAg …….	Woodchuck hepatitis virus “e” antigen
WHO …….	The World Health Organization
WHsAg …….	Woodchuck hepatitis virus surface antigen
WHV …….	Woodchuck hepatitis virus
WHxAg …….	Woodchuck hepatitis virus “x” antigen
WMHBV ……...	Woolly monkey hepatitis B virus
w/v ……	weight per volume

12 List of figures

13 List of tables

14 Acknowledgements

I am very grateful to my PhD project supervisor **Prof. Dr. med. Michael Roggendorf** for giving me the possibility to complete the presented study in the Institute of Virology, Essen. I am thankful for his wise guidance, advices, encouragement and support during the work on my scientific topic and the dissertation.

I am deeply thankful to **Prof. Dr. rer. nat. Mengji Lu** for his constructive ideas, inspiring discussions, time and support.

I am very thankful to **Dr. med. Melanie Fiedler** for her kind and helpful assistance during the animal experiments.

I am very grateful to **PD Dr. rer. nat. Oliver Wildner** for precious ideas in hard times.

I am very grateful to **Ms. Anja Mayer**, **Mrs. Thekla Kemper** and **Ms. Barbara Bleekmann** not only for excellent technical assistance, but also for helping me to keep my spirits up.

I would like to acknowledge my dear colleagues **Ejuan Zhang**, **Katrin Schöneweiss** and **Dr. rer. nat. Ina Schulte** that supported me greatly during the project. I am very thankful to **Dr. rer. nat. Kathrin Gibbert** and **Dr. rer. nat. Wibke Bayer** for precious, helpful advices and for editorial assistance. In addition, I am very grateful to **Lena Johrden**. Without her help I would not have accomplished this thesis.

I would like to thank **Dr. med. Xiaoyong Zhang**, **Mr. Jian Fu** and **Mr. Jing Lu** for helping me with surgeries of the woodchucks.

I highly appreciate the financial support provided by Deutsche Forschungs-gemeinschaft (DFG).

I am deeply grateful to **Ms. Delia Cosgrove**, **Ms. Daniela Catrini** and **Ms. Natalie Gehlmann** for helping me in every way during my stay in Germany, encouragement and editorial assistance.

I am truly grateful to **my parents**, **Kasia** and **Rafal,** for patience, unconditional support, love and faith in me. You were the strength that kept me going on.

And, last but not least, I specially thank my friends **Federica**, **Ilseyar**, **Kathrin**, **Katrin**, **Lena**, **Maren**, **Marina**, **Marianne**, **Milena**, **Nina**, **Olena, Savita, Silvia**, **Simone** and **Teona** for making my stay in Essen pleasant, precious and joyful. You will stay in my heart forever.

15 Curriculum vitae

Anna Dagmara Kosinska

born on the 4th of June 1983 in Lodz, Poland

certified Biotechnologist

Professional experience:

since 10/2007 **PhD thesis**

"Improvement of therapeutic vaccination for the treatment of chronic hepatitis B in a preclinical model (woodchuck)"

Institute of Virology,
University of Duisburg-Essen, Essen, Germany

10/2006 – 06/2007 **Diploma thesis**

"Utility of qualititative and quantitative PCR-based methods in predicting the risk of Epstein-Barr virus-associated lymphoproliferative disorders in haematopoietic stem cells transplant recipients"

Laboratory of Molecular Genetics and Virology,
Jagiellonian University, Krakow, Poland

07/2006 – 08/2006 **External laboratory practice**

Institute of Virology, Medical School of Hanover, Hanover, Germany

Academic education:

10/2002 - 06/2007 **Studies of Biotechnology (specialization: Biochemistry)**

Diploma

Faculty of Biochemistry Biophysics and Biotechnology,
Jagiellonian University, Krakow, Poland
Final grade: very good

Secondary education:

09/1998 – 06/2002 "*Boleslaw Prus*" Secondary School number XXI, Lodz, Poland
'A' Level: very good
Graduation with honours

Essen, 19.04.2011

Anna Kosinska

16 Declaration (Erklärungen)

Erklärung:

Hiermit erkläre ich, gem. § 6 Abs. 2, f der Promotionsordnung der Math.-Nat. Fakultäten zur Erlangung der Dr. rer. nat., dass ich das Arbeitsgebiet, dem das Thema *„Improvement of therapeutic vaccination for the treatment of chronic hepatitis B in a preclinical model (woodchuck)“* zuzuordnen ist, in Forschung und Lehre vertrete und den Antrag von Anna Kosinska befürworte.

Essen, den _____ _____

Michael Roggendorf

Erklärung:

Hiermit erkläre ich, gem. § 7 Abs. 2, c und e der Promotionsordnung der Math.-Nat. Fakultäten zur Erlangung des Dr. rer. nat., dass ich die vorliegende Dissertation selbständig verfasst und mich keiner anderen als der angegebenen Hilfsmittel bedient habe und alle wörtlich oder inhaltlich übernommenen Stellen als solche gekennzeichnet habe.

Essen, den _____ _____

Anna Kosinska

Erklärung:

Hiermit erkläre ich, gem. § 7 Abs. 2, d und f der Promotionsordnung der Math.-Nat. Fakultäten zur Erlangung des Dr. rer. nat., dass ich keine anderen Promotionen bzw. Promotionsversuche in der Vergangenheit durchgeführt habe, dass diese Arbeit von keiner anderen Fakultät abgelehnt worden ist, und dass ich die Dissertation nur in diesem Verfahren einreiche.

Essen, den _____ _____

Anna Kosinska